From a swollen granule to a suspension: shear flow behaviour of a physically modified starch

Mélinda Desse

Ecole Doctorale 364 : Sciences Fondamentales et Appliquées

N°attribué par la bibliothèque
|__|__|__|__|__|__|__|__|__|__|__|

T H E S E

pour obtenir le grade de
Docteur de l'Ecole Nationale Supérieure des Mines de Paris
Spécialité «Sciences et Génie des Matériaux»

présentée et soutenue publiquement par

Mlle Melinda Desse

Soutenue le 19 Décembre 2008

FROM A SWOLLEN GRANULE TO A SUSPENSION: SHEAR FLOW BEHAVIOUR OF A PHYSICALLY MODIFIED STARCH

Directeurs de thèse : Tatiana Budtova, John Mitchell et Bettina Wolf

Jury :

Prof. Paula Modenaers	Rapporteur
Prof. Steve Harding	Rapporteur
Prof. Volker Ribitsch	Examinateur
Dr. Tatiana Budtova	Examinateur
Dr. Bettina Wolf	Examinateur

“ What would you do if I sang out of tune,
Would you stand up and walk out on me?
Lend me your ear and I’ll sing you a song,
And I will try not to sing out of key.
Oh I get by with a little help from my friends
I get high with a little help from my friends
Oh I’m gonna try with a little help from my friends…”

With a Little Help from My Friends, the Beatles

Acknowledgments

There are many people I wish to thank… everybody who has help me getting to this day in any kind of way.

First, I would like to thank John Mitchell and Tatiana Budtova for putting together this European Ph.D and for choosing me (well I am not sure they really did but…). It has been an enriching experience scientifically and humanely speaking. However, this project could have never been possible without the perseverance of Patrick Navard who founded EPNOE and I am therefore grateful for that.

I also thank the jury for participating in this Ph.D. defence, Paula Moldeaners, Steve Harding, Volker Ribitsch, which I have to admit is a little experimental. Special thanks to Paula Moldenaers and Steve Harding who, in the end, will have to write two reports about this manuscript/thesis.

Thank you also to my supervisors, John Mitchell for his support, his kindness. He is the typical image of “the great scientist” but most important he is that great scientist! Thank you to Bettina Wolf who took the project along after a year, and who probably wondered what could be done with me. Well, thanks to her help, her extended knowledge in rheology and her good advice, I finally got there. Mostly I want to thank the one who has always followed me from beginning to end, Tatiana Budtova. You have always believed in me, supported me, and stuck with me through thick and thin, ups and downs (and there were some downs!…). Thank you also for all the good scientific advice, your rigor in the scientific approach. I have learnt a lot from you all.

I would like to thank the people who have helped me with experimental work: Shirley Ang and Gordon Morris for AUC and SEC-MALLS experiments, Madian Abu-Hardan with DSC measurements, Dorine Fraiseau for her work on single starch granules, Roland Hainault and Simon Becker for the technical support on the counter rotating shear cell.

After spending a year in half in both Sutton Bonington (Nottingham University) and Sophia Antipolis (CEMEF) there are many people I would like to thank.

From Nottingham, there is of course Val who is the person to know, always helpful (finding rooms on campus) always with a smile. Her English is fantastic! Believe me, you understand everything she says but manages to teach you a new word each time (and you want to listen, she has the best stories to tell!). Thank you to Anne-Laure and Nuno (the Carebear couple, life seems sweet and easy with them), Anne-Laure and Andreas (the glamorous couple). Thank you also to Lea who didn't stay for very long but with whom I had a great time and great Risotto (I hope to see you soon in Kenya). Line my Rheology conference friend (and our good laughs on the "sprut effect", I still don't know what it is…). Mostly I would like to thank Lydie in whom I have found a true friend.

Thank you to Celine and Emmanuelle, my first office friends (we have gone through the first and last stretch together), the PCP group and mainly Roland, Romain, Monica and Nicolas. Great thanks to my latest office collegues, Nadia, Yoann and Jean-François who have been great. Thank you for all the fun, the office dinners and moral support whenever I received corrections. Thank you to the administrative crew: Marie-Françoise Guénéguan, Sylvie Massol for their great help and good mood, Patrick Coëls, Geneviève Anseeuw. I shall not forget all of the other people who have contributed to nice times on the Côte d'azur but that I did not work with: Sabine, Raphaëlle, Marie, Christophe, Greg, Larbi, Maxime, Damien, Benoît, Mat, Antoine, Bibi, Aude, Dingue, Bad, Tom.

Thank you to the people who have offered me shelter when I didn't have a place to sleep (Roland, Yoann, Emmanuelle, Lydie. And yes it happened also in Nottingham…)

I can't forget my friends who supported me from a distance: Samy, Romie my best friends. Gerald, who has had to put up with me especially at the end and Fred, my brother and friend who one day said "Well it took her a while to realise she wasn't stupid", so thank you for believing in me.

It would not be complete without thanking my parents who have always believed in me and without whom I would not be writing these words. They have supported my choices without interfering and have never let me down. I hope that in the same way I will not let them down.

Table of Content

Abstract

It has been seen that starch that remains in a granular form when heated and used in food systems offered better flavour perception than hydrocolloid thickened products. It seems that starch that remains in the granular form has a better mixing ability in the mouth, leading to better release of the tastants to the receptor. A suggested parameter to differentiate food thickeners is droplet break-up. In this context, the flow behaviour of starch was studied in depth to better understand its properties. First, a single swollen-in-water granule was studied using the rheo-optical tool. The granule is suspended in an immiscible fluid and submitted to a simple shear. Evidence of its deformation and of the release and ejection of the solvent in the suspending matrix was shown and interpreted. The suspension of swollen-in-water starch granules was characterised rheologically and its continuous phase was analysed. The behaviour of the suspension under flow was seen to depend on the volume fraction occupied by the granules and their deformability. The analysis of the continuous phase revealed the presence of solubilised low molecular weight amylopectin. Finally a droplet of starch suspension suspended in an immiscible matrix was compared to a model droplet of a hydrocolloid solution. I was shown that starch suspension droplet breaks up more easily than the hydrocolloid droplet. An in depth study of the break-up conditions of a starch suspension droplet revealed a different mechanism than that observed for fluids. Break-up occurred due to rearrangement of the granules and the creation of thin “zones”. The yield stress of the suspension was seen to play a major role in the break-up of the starch suspension droplets.

Résumé français

Le but de ce travail de thèse est de comprendre le comportement sous écoulement de particules molles à différents niveaux : la particule seule, la suspension, et une gouttelette de cette suspension. Les particules molles étudiées dans ce travail sont les granules gonflés d'amidon. L'amidon est un des polymères naturels les plus utilisés et est présent partout dans le monde végétal. On peut citer parmi les plus connus, l'amidon de blé et de maïs (amidon de céréales), l'amidon de pomme de terre, mais il en existe bien d'autres variétés. Les applications pour l'amidon sont nombreuses et diverses : dans la fabrication de tablettes en pharmacie, comme agent de recouvrement dans la fabrication de papier et comme additif dans les matériaux utilisé dans le bâtiment ou encore comme épaississant dans les produits cosmétiques. Dernièrement, l'intérêt s'est accru pour l'utilisation de l'amidon pour fabriquer des plastiques biodégradables. Néanmoins, dû à sa grande valeur nutritionnelle, l'amidon est surtout utilisé dans l'industrie agroalimentaire.

Contexte de l'étude

Les systèmes comportant plusieurs phases, comme les émulsions et les mélanges de polymères sont utilisés dans de nombreux domaines tels que l'industrie cosmétique, agroalimentaire ou encore l'industrie plastique. Pour comprendre leur comportement sous cisaillement de nombreuses études se sont intéressées à la déformation et à la rupture d'une goutte plongée dans une matrice immiscible. Ce type d'étude permet également de connaître la morphologie des mélanges et la taille des gouttes après cisaillement.

Dernièrement, il fut suggéré que la déformation et la rupture de gouttelette pouvait servir comme paramètre physique pour comparer des systèmes alimentaires. Il a été montré que des différences étaient perçues par un panel d'analystes sensoriels selon le type d'épaississant utilisé. Il semblerait que les produits épaissi par une solution de polymère (type Hydroxypropylmethyl cellulose, HPMC) offrait un goût diminué par rapport aux produits épaissis avec de l'amidon et plus particulièrement ceux qui retenait une forme granulaire après préparation. Ces

variations de goûts semblent être liées à la capacité des épaississants à se mélanger en bouche. Avec un épaississant qui se mélange bien, les agents de flaveurs seront mieux diffusés et donc seront plus rapidement transportés aux récepteurs sensoriels. La capacité d'une goutte à se rompre semble être liée à la microstructure de l'épaississant : une solution de polymère est un mélange de macromolécules emmêlés tandis qu'une suspension d'amidon correspond à des granules, plus faciles à séparer. Un paramètre physique qui pourrait être corrélée avec la capacité à se mélanger en bouche serait la facilité d'une goutte à se rompre dans un liquide immiscible ; plus une goutte se casse facilement, plus le mélange en bouche est aisé. Il serait donc possible de prévoir si un épaississant donnera une meilleure perception en bouche que l'autre.

Problématique

Lors de cette thèse nous allons tenter de répondre à plusieurs questions qui se posent lorsque l'on compare ces systèmes alimentaires :

- Comment va se rompre une goutte de suspension comparée à une goute de solution ?
- Quel est l'effet de la microstructure sur les conditions de rupture ?
- Quels sont les mécanismes de rupture d'une goutte de suspension ?

Afin d'analyser la déformation et la rupture de goutte dans un milieu immiscible il est nécessaire de bien connaître les caractéristiques des systèmes étudiés, comme leur rhéologie ou encore leurs propriétés de surface. De plus dans le cas d'une suspension d'amidon où les granules sont déformables, connaître et comprendre le comportement d'une seule particule peut se révéler intéressant pour interpréter les résultats obtenus. Toutes ces considérations soulèvent les questions suivantes:

- Comment comparer une suspension et une solution, qui du point de vue microstructure sont très différents ?
- Comment définir les propriétés de surface d'une suspension ?

En résumé, l'objectif de cette thèse est de caractériser et d'analyser le comportement sous écoulement d'une suspension d'amidon de maïs cireux modifié en vue de comprendre les différences potentielles entre les conditions de rupture d'une goutte de suspension d'amidon et une goutte de solution d'hydrocolloïde (HPMC).

Approche Expérimentale

Afin de réaliser cette étude, nous allons procéder en trois étapes :

- Caractérisation et interprétation du comportement d'un seul granule : caractérisation au microscope optique, au microscope électronique à balayage (MEB) et caractérisation de la surface au moyen de la microscopie à force atomique (AFM). Le comportement d'un granule sec et d'un granule gonflé sera également étudié à l'aide de l'outil rhéo-optique.

- Caractérisation et analyse de la suspension : le comportement rhéologique de la suspension d'amidon est étudié et interprété à diverses concentrations. L'étude est réalisée en écoulement et en mode oscillatoire avec un rhéomètre rotationnel. La phase continue de la suspension est également analysée afin de déterminer si un peu de matière polymérique (type amylopectine) est solubilisée dans la phase continue lors de la préparation de l'échantillon. L'ultracentrifugation, la chromatographie d'exclusion stérique sont parmi les méthodes utilisées.

- La comparaison de goutte de suspension d'amidon et de solution d'HPMC se fait à l'aide de l'outil rhéo-optique. Les gouttes sont immergées dans une matrice immiscible, de l'huile de silicone(PDMS). Elles sont ensuite soumises à un cisaillement simple appliqué entre deux plateaux parallèles transparents tournant en sens inverse. Les gouttes sont comparées autant que possibles, compte tenu de leur nature, dans des conditions similaires.

Organisation de la thèse

La thèse est organisée de la façon suivante :

Chapitre I : Introduction

Le Chapitre I est consacré à l'introduction de la thèse. C'est une version anglophone abrégée du résumé en français ; il reprend de la même façon, le contexte de l'étude, l'approche expérimentale et l'organisation de la thèse.

Chapitre II : Contexte Scientifique

Le Chapitre II donne le contexte scientifique de l'étude. Afin de permettre au lecteur une bonne lecture de ce document, les différentes notions présentées dans l'introduction sont reprises dans ce chapitre. Dans une première partie, un bref rappel sur la perception du goût en bouche ainsi que l'importance du choix de l'épaississant et de sa viscosité est donné. Au-delà d'une concentration critique en épaississant la perception diminue ; ensuite selon le choix de l'épaississant, bien que leurs viscosités soient identiques la perception peut être différente. En ce sens, l'amidon sous forme de suspension offre une meilleure perception qu'une solution de polymère où les macromolécules sont entremêlées.

C'est pourquoi la deuxième partie de ce chapitre est consacrée à l'amidon. Sa composition, sa structure, ses propriétés et son comportement rhéologiques sont définie. L'amidon est en fait un mélange de deux polymères dont l'unité monomère est le glucose, l'amylose et l'amylopectine mais dont la conformation dans l'espace diffère. L'organisation de ces molécules au sein du granule est une alternance d'anneaux concentriques amorphes et semi-cristallins donnant ainsi une structure semi-cristalline à l'amidon. Selon les proportions d'amylose et d'amylopectine et leur localisation dans le granule, l'amidon aura des propriétés différentes et

notamment celles de gonflement. En effet, une des caractéristiques de l'amidon est de gonfler lorsque ce dernier est chauffé dans l'eau chaude augmentant ainsi la viscosité du milieu. Le gonflement dépend de la nature de l'amidon, de la localisation de l'amylose et de l'amylopectine dans les granules, de la présence d'impuretés et des conditions de chauffage. Le gonflement des granules d'amidon va influer sur les propriétés d'écoulement. Il sera donc nécessaire d'être précis lors de la préparation de nos échantillons. Si l'on considère la rhéologie d'une suspension d'amidon (granule + phase continue), le comportement dépendra de la concentration en amidon. Si la concentration est en dessous d'une concentration critique, la rhéologie est gouvernée par la phase continue et la fraction volumique occupée par les granules. En revanche, si la concentration est telle que les granules sont en contact, les propriétés rhéologiques dépendront de la déformabilité des granules. La caractérisation de ce système est nécessaire pour l'étude de la déformation de gouttelette.

Dans la dernière partie, on considère la déformation et la rupture de gouttelettes plongées dans une matrice immiscible. Quelques modèles et équations utilisés pour l'analyse sont donnés. Deux nombres adimensionnels sont utilisés pour caractériser ce type de système. Le rapport de viscosité p (viscosité de la goutte/viscosité de la matrice) et le nombre capillaire Ca qui est le rapport des forces qui tendent à déformer la goutte (forces visqueuses) sur les forces qui tendent à la maintenir sphérique (forces interfaciales). Les tendances observées pour les systèmes newtoniens et les systèmes viscoélastiques sont revus. Il semblerait qu'une goutte viscoélastique a tendance à moins se déformer qu'une goutte newtonienne. A l'inverse une matrice viscoélastique tendra à déformer la goutte plus qu'une matrice newtonienne.

Chapitre III : Matériaux et méthodes

Le troisième chapitre est consacré à la description des matériaux et méthodes utilisés au cours de notre travail.

En premier lieu nous avons cherché à caractériser l'amidon afin de préparer au mieux les suspensions pour la suite de l'étude. La température de gélatinisation et son degré de gonflement maximal moyen ont été déterminés à l'aide d'un microscope optique. La température de gélatinisation a été définie comme étant la température où tous le granules ont perdu leur cristallinité et dans le cas de l'amidon de maïs cireux modifié, T_{gel} = 73°C. Son degré de gonflement maximal moyen est de 12.5g/g. La concentration pour laquelle la fraction volumique est maximale, c'est-à-dire que tout le volume est occupé par les granules et où ces derniers sont gonflés à leur maximum est de 8%. Les suspensions sont ensuite préparées en ajoutant l'amidon à l'eau sous agitation ; le mélange est chauffé au bain marie à la température désirée (73°C) et laissé une minute à cette température afin de s'assurer que tout les granules sont gonflés à l'équilibre. Pour caractériser la phase continue de la suspension, cette dernière est obtenue par centrifugation ; le surnageant est récupéré et analysé et le culot est jeté.

La caractérisation des huiles de silicone est donnée et sera nécessaire pour la suite de l'étude ; des huiles de viscosité de 100mPa.s (pour le mesures de tension interfaciales), 25, 75, 170, 220, 1000Pa.s (pour les expériences de déformations de gouttes) sont utilisées.

Les principales méthodes utilisées sont la rhéo-optique dans une cellule contra rotative, la rhéologie et les mesures de tension interfaciales. Ces trois méthodes sont décrites en détail dans le chapitre III.

L'outil rhéo-optique combine une action mécanique avec une observation visuelle. Le système a été développé au CEMEF : deux plateaux parallèles et transparents sont montés sur un microscope. Les deux plateaux tournent en sens opposé ce qui permet une visualisation constante de l'objet lors de l'expérimentation. Entre ces deux plateaux, se trouve une goutte de fluide suspendue dans une matrice immiscible. En faisant tourner plateaux, la goutte est soumise à un cisaillement simple et se déforme. L'expérience est enregistrée à l'aide d'une caméra CDD, et d'un enregistreur DVD raccordés au système.

Le comportement rhéologiques est étudié en écoulement et en mode dynamique à l'aide de deux rhéomètres rotationnels (MCR 301 d'Anton Paar et C-VOR Bohlin de Malvern Instrument).

La tension interfaciale entre l'huile et les systèmes étudiés est mesurée à l'aide d'un tensiomètre (PAT-1 de Sinterface) par la méthode de la goutte pendante.

Enfin, les méthodes utilisées pour caractériser les granules (MEB et AFM) ainsi que celles mises en place pour l'analyse de la phase continue (DSC, Ultracentrifugation, SEC-MALLS) sont également décrites.

Chapitre IV : Propriétés de surfaces d'un granule d'amidon et son comportement sous cisaillement

Dans ce chapitre, les granules d'amidon de pomme de terre et de maïs cireux modifiés sont comparés. L'amidon de pomme de terre est choisi pour souligner les variations selon la source botanique. De plus, il est de très grande taille et possède une grande déformabilité ; il présente donc un intérêt dans l'étude du comportement du granule d'amidon sous cisaillement. L'étude de la forme des granules sec (par MEB) a montré la polydispersité des granules quelque soit l'origine de l'amidon mais surtout une grande variation de forme selon la source. Les grains de maïs cireux modifiés ont une forme très irrégulière, angulaire ressemblant un peu à des silex taillés. En revanche, les rains d'amidon de pomme de terre présente une forme homogène, patatoïde et une surface plus lisse. Grâce à l'AFM il a été possible de quantifier cette rugosité de surface sub-micronique non observable par MEB. Tandis que l'amidon de maïs cireux présente une rugosité de surface élevée avec la présence de pores et de cratères, l'amidon de pomme de terre possède une rugosité faible sans aspérités particulières. Les imperfections de surface de l'amidon de maïs cireux modifié sont dues aux traitements thermiques auquel il a été soumis. L'analyse AFM sur des granules gonflés a révélé que la rugosité du maïs cireux subsistait bien qu'étant plus faible. En revanche, il a été impossible de réaliser des mesures sur les granules de pomme de terre car ceux-ci présentaient une grande élasticité et la pointe de l'AFM s'enfonçait dans les granules. Une fois la pointe retirée le granule retrouvait sa forme initiale immédiatement.

L'étude rhéo-optique sur granules secs à montré que les deux systèmes se comportaient plus ou moins comme des sphères rigides, si l'on prend en compte l'erreur de l'outil. Sur des granules gonflés (à leur maximum), les expériences ont

révélé que les granules pouvaient se déformer jusqu'à deux fois leur taille initiale. Lorsque les granules sont soumis à des cisaillements suffisamment élevés, du solvant peut sortir des granules et rester attacher aux extrémités. Si le cisaillement est encore augmenté, du solvant est éjecté dans la matrice. Bien que ce phénomène ne soit pas visible lors de l'expérience, la perte de visibilité des granules due au changement de densité et surtout la perte de volume mesurée en fin d'expérience indique que du solvant sort des granules. Cette étude est surtout qualitative car il est difficile de pouvoir quantifier et comparer ce type de système. En effet, nous avons vu qu'il existait une grande diversité de taille parmi les granules d'une même population mais en plus le degré de gonflement peut varier d'une particule à l'autre. Par conséquent, entre deux amidons d'origine différente la comparaison n'est pas évidente. Néanmoins quelques constatations importantes peuvent être faites. Les deux granules sont censés être gonflés à leur maximum ; or le degré de gonflement de la pomme de terre est supérieur à celui du maïs cireux modifié. Il serait donc logique d'avoir plus de solvant éjecté de la pomme de terre que du maïs. Néanmoins, la perte de volume semble montrer le contraire. Une des hypothèses est que la présence de pores et de cratères à la surface du granule d'amidon de maïs cireux modifié permettraient une éjection plus facile du solvant. Une autre possibilité est que la présence d'amylose en périphérie du granule de pomme de terre offrirait une barrière qui ralentirait la perte de solvant. Une étude future plus poussée sur de nombreux granules suivie d'une analyse statistique des résultats serait nécessaire pour conclure sur de tels résultats.

Chapitre V : Propriétés d'une suspension d'amidon

Ce chapitre est dédié à la caractérisation d'une suspension d'amidon de maïs cireux modifié. Nous avons considéré le comportement rhéologique de la suspension ainsi que les caractéristiques de la phase continue. Il est important de connaître ces dernières car la phase continue peut avoir un impact sur la rhéologie de la suspension ; la phase continue sera en contact avec le milieu hydrophobe lors des expériences de déformation de gouttelettes et par conséquent il faut définir ses propriétés de surfaces et sa composition.

Dans un premier temps une suspension d'amidon à la concentration où la fraction volumique est 1 (pas ou peu de solvant autour) et où les granules sont gonflés au maximum est étudiée. La suspension est en régime concentré, les granules sont en contact. Nous avons montré que, dans ce cas, la suspension présentait un seuil d'écoulement. En dessous d'une certaine contrainte, les granules sont emprisonnés par les granules voisins. Il faut dépasser une certaine énergie afin que les particules puissent bouger librement. Lorsque les granules sont libres de bouger ils s'organisent et se structure ce qui confère des propriétés rhéofluidifiantes à la suspension. Ce phénomène est amplifié par la déformation des granules sous écoulement. Une certaine élasticité a pu être mesurée (première différence de force normale) au-delà de 300Pa. C'est précisément à cette contrainte que l'on observe une déformation des granules gonflés d'amidon de maïs cireux modifié. En se déformant, les granules stockent de l'énergie, ce qui est à l'origine de l'élasticité mesurée. Les mesures de viscoélasticité de suspension en mode oscillatoire montre qu'à cette concentration la suspension à un comportement de type gel avec G'>G'' et G' indépendant de la fréquence.

Lorsque l'on fait varier la concentration on peut observer l'émergence de certaines caractéristiques selon que l'on se trouve en régime dilué ou semi-dilué (les granules ne sont pas en contact) ou en régime concentré (les particules sont en contact). Cette concentration critique est de 5%, valeur de concentration pour laquelle un seuil d'écoulement est mesuré. Dans le premier cas (dilué), la rhéologie du système est gouvernée par la phase continue et la fraction volumique occupée par les granules ; plus les granules sont nombreux, par exemple, plus la viscosité sera élevée. Cette étude a également montré que des interactions entre particules qui n'étaient pas en contact (semi dilué) pouvaient se produire et augmenter la viscosité attendue. Ces interactions ont lieu entre les molécules à la surface des granules adjacents.

Dans le deuxième cas (régime concentré), la rhéologie de la suspension dépend de la déformabilité des granules. Plus la concentration augmente (tandis que la fraction volumique reste maximale à 1), moins les granules ont d'eau pour gonfler et plus ils sont rigides. Cette augmentation de la rigidité provoque une augmentation du seuil d'écoulement et de la viscosité. De plus, plus il y a de granules, plus le nombre de contacts est multiplié et plus les interactions par ancrage mécanique

(possible grâce à la rugosité de surface) sont favorisées, augmentant du même coup le seuil d'écoulement.

L'étude de la phase continue a montré que des molécules ayant une petite activité de surface étaient solubilisés dans le surnageant. La matière polymérique présente dans la phase continue est en fait de l'amylopectine de bas poids moléculaire (10^7g/mol). L'analyse quantitative indique que la concentration en amylopectine dépend de la concentration initiale de la suspension (de 0.63mg/ml à 6.67mg/ml pour des concentrations initiales d'amidon de 10mg/ml et 50mg/ml respectivement). La présence d'amylopectine dans la phase continue peut s'expliquer par deux phénomènes qui se produisent probablement en même temps :

- De petites molécules d'amylopectine suffisamment linéaires pour sortir du granule se solubilisent dans le milieu.
- Les molécules d'amlopectine en surface du granule sont arrachées lors de la préparation des échantillons d'amidon.

Chapitre VI : Déformation et rupture sous cisaillement d'une goutte de suspension d'amidon : comparaison avec une goutte de solution de polymère

L'étude comparative des gouttelettes de suspensions d'amidon et de solution d'HPMC est la finalité de cette thèse et constitue la majeure partie de ce chapitre.

Avant de pouvoir analyser le comportement des gouttelettes et de comparer les deux systèmes, la caractérisation d'une solution d'HPMC est nécessaire. L'étude a été réalisée sur diverses concentrations, ceci afin de pouvoir choisir des solutions d'HPMC ayant une viscosité équivalent à celle de la suspension aux taux de cisaillement étudiés. A 20°C, la solution d'hydrocolloïde est rhéofluidifiante, non thixotropic et possède un comportement en faible déformation entre le liquide et le gel. L'HPMC possède une grande activité de surface car il a des groupes hydrophiles (hydroxypropyl) et d'autres hydrophobes (groupe méthyl). Sa tension interfaciale dans l'huile est donc deux fois plus faible que celle de l'eau dans l'huile et est de 16,5mN/m. Cette value ne varie pas avec la concentration car on se trouve au dessus de la concentration micellaire critique.

L’observation visuelle en régime dilué et concentré des gouttes de suspension d’amidon et d’HPMC révèle des différences non seulement entre les régimes de concentration mais aussi entre les deux systèmes. En régime dilué, les granules circulent dans la suspension avant de s’agglomérer aux extrémités. Quelques granules sont éjectés avec un peu de solvant par pincement des extrémités, formant ainsi une goutte concentrée en granules. Plus on augmente le cisaillement, et donc la contrainte, plus les granules sont éjectés jusqu'à ce qu’il ne reste qu’une goutte de solvant. En régime concentré (la fraction volumique est 1), les gouttes de suspension se rompent en deux gouttes d’environ la même taille. Pour la suite de l’étude seul le cas concentré est considéré ; les contraintes appliquées sont en dessous de contraintes de début de libération de solvant d’un granule. Pour l’HPMC dilué, la goutte se casse par « tip-streaming » c'est-à-dire que de toute petites gouttelettes sortent des par les pointes de la goutte. Pour les concentrations d’HPMC (régime semi-dilué c*<c<c**) pour lesquelles la viscosité est comparable avec celui de la suspension d’amidon, la goutte d’HPMC ne se casse pas.

La comparaison des deux systèmes est difficile dû à leur microstructure : leur comportement rhéologique et leur propriété de surface sont très différents. Même en étudiant à une viscosité équivalente le nombre capillaire appliqué sera différent car la tension interfaciale est différente. Nous avons choisi des concentrations en HPMC qui donne des viscosités équivalentes à la suspension d’amidon pour des values de taux de cisaillement de 1.8 et 2.9s^{-1}. Néanmoins, comme les gouttes sont plongées dans une huile de silicone de haute viscosité, considérer le taux de cisaillement n’est pas tout à fait juste. A contraintes équivalentes, les viscosités ne le sont plus les mêmes et les rapports de viscosité sont différents. Cependant leur élasticité est la même aux contraintes appliquée. L’étude comparative est quand même réalisée aux mêmes contraintes. La comparaison de gouttes de même taille au même cisaillement a montré que la goutte de HPMC ne se casse pas tandis que celle de la suspension d’amidon se rompt. Ceci est un résultat inattendu dans ce sens que le nombre Capillaire appliqué à l’HPMC est plus élevé que celui de l‘amidon et de plus le rapport de viscosité entre l’HPMC et l’huile de silicone est également supérieur et est tel que la rupture devrait se produire plus facilement. Toutefois, la solution d’HPMC suit les prédictions faites pour les fluides viscoélastiques. Cela suggère un mode de rupture différent pour l’amidon que pour celui de fluides. C’est pourquoi une étude en profondeur sur le mécanisme et les conditions de rupture d’une goutte

de suspension d'amidon a été menée. Cette étude a montré que le seuil d'écoulement jouait un grand rôle dans la rupture de la goutte. Si la contrainte ne dépasse pas ce seuil, la goutte ne se rompt pas, elle agit comme un solide. Si la contrainte dépasse très légèrement le seuil d'écoulement, mais que la contrainte interne de la goutte n'est pas suffisante, la goutte ne se casse pas. Quand la contrainte est suffisante, la goutte casse comme les fluide Newtonien. Néanmoins le mécanisme est différent : la contrainte interne est assez grande pour provoquer une circulation interne et donc un réarrangement des granules. Ce réarrangement laisse des zones peu concentrées en granules ; la rupture ce produit à ce niveau là. Lorsque la contrainte est très élevée, les granules à l'intérieur de la goutte se déforment facilitant la circulation du solvant et des granules ; la rupture est ainsi plus aisée. Dans ce cas les nombres capillaires sont plus faibles que pour des fluides Newtonien. Néanmoins, il existe de nombreux paramètres encore inexplorés ; l'influence de la taille des particules, de leur nombre, de leur déformabilité.

Chapitre VII : Conclusions et perspectives

Les résultats principaux sont résumés dans ce chapitre et des perspectives scientifiques fondamentales ainsi que des applications industrielles potentielles sont présentées.

Chapter I: Introduction

The aim of this Ph.D. work was to understand the flow behaviour of soft matter at various levels: the soft particle, its suspension and finally a droplet of the suspension. The soft matter considered here is starch. It is one of the most widely used natural polymers and finds it sources in the plant world. The main ones are cereal starches from wheat and corn but starch can also be found in potatoes (tuber starches), rice, peas and many more and can also be genetically, physically or chemically modified to enhance their properties. It has many applications in various industries: to manufacture tablets in the pharmaceutical industry, as a coating agent in the paper-making field, as an additive in building materials and as a thickening agent in cosmetics. Lately, interest has been increasing for the use of starch to produce biodegradable plastics. However, due to its nutritional value, starch is mostly used in food products as a texturing and thickening agent.

I.1 Motivation for the study

Many studies on flavour perception and mouth feel from viscous solutions containing thickening agents have been conducted. The rheological variable considered as one of the most important in taste and flavour perception is the shear viscosity. For example Cook et al (2003) have suggested that the Kokini shear stress controls flavour perception in viscous foods.

Recently it was shown that systems with equivalent shear viscosities show large differences in taste perception (Ferry et al., 2006). For pastes thickened by starches which retain granular form, perception and mouth feel are good. On the other hand, for solutions thickened with hydroxypropyl methyl cellulose (HPMC), perception and mouth feel are poor. Moreover, the use of a non-crosslinked waxy maize starch, where the granule disrupts easily during processing, will result in a reduction in perception.

It has been suggested that the mechanisms that determines the frequently reported reduction in taste perception with increased hydrocolloid-induced viscosity is restricted in-mouth mixing with saliva (Ferry et al., 2006). Bad mixing reduces the extent to which tastants are transported to the receptors (taste buds) and unmixed material in the mouth also leads to poor mouthfeel. This restricted mixing would be due to the entanglement of the polymer chains as opposed to starch thickened systems where the granular form is maintained, hence entanglement cannot occur.

It is of interest to determine which structural and rheological properties of liquid foods correlate well with taste perception. Droplet break-up is thought to be a possible parameter to differentiate hydrocolloid thickened systems from those thickened with starch retaining granular form. The objective of this PhD study was to answer the following questions, using modified waxy maize starch:

- How will a suspension droplet break up compared to a viscoelastic model droplet?
- What is the effect of droplet microstructure on the break-up conditions?
- What are the break-up conditions for such systems? Is this a good parameter to differentiate food thickeners?

To understand and analyse the deformation and break-up of a droplet immersed in an immiscible fluid, their thorough characterisation should be carried out prior to experiments. The conditions for deformation will depend on different parameters such as the viscosity of each phase, the interfacial tension between the two phases. These issues lead to the following questions:

- How to compare a solution vs. a suspension in rheological terms?
- What should be considered when measuring the interfacial tension between a suspension and another fluid?

To summarise, the objective was to study and understand the behaviour under flow of a modified waxy maize starch at the granular and the suspension level, in view of understanding possible differences arising between the shear induced break-up of starch suspension droplets and aqueous polymer solution droplets (HPMC).

I.2. Experimental approach

In order to answer the questions listed above, experiments to characterise the starch granules, the behaviour of starch suspensions and the break-up of starch suspension droplets in an immiscible fluid were carried out. The experiments were done as follows:

First, the modified waxy maize starch granules were characterised in terms of gelatinisation temperature, swelling degree, determination of the shape and surface properties using optical microscopy, Scanning Electron Microscopy (SEM) and Atomic Force microscopy (AFM). The behaviour of dry and swollen-in-water granules was observed using the rheo-optical tool.

Secondly, the suspension of swollen-in-water starch granules was analysed. Prior to the analysis, a preparation procedure was defined in order to study the system in identical conditions. The modified waxy maize starch granules were swollen in hot water (which will be called the solvent throughout the thesis) under gentle stir at a specific temperature, the gelatinisation temperature determined previously. At this stage, all of the granules have lost their crystallinity and most of them are swollen to their maximum but retain their granular form. The rheological behaviour of the suspension was characterised using a rotational rheometer. The continuous phase of the suspension was also analysed to be used in the suspension droplet deformation study. The continuous phase was obtained through centrifugation of the suspension. Differential Scanning Calorimetry (DSC), iodine staining, Analytical Ultracentrifugation (AUC) and Size Exclusion Chromatography coupled with Multi Angle laser Light Scattering (SEC-MALLS) were used to carry out the analysis of the continuous phase. The characterisation of the granules and the suspension behaviour will allow analysis and interpretation of the droplet deformation data.

To compare the deformation of starch suspension droplets to HPMC solution droplets, the rheo-optical tool was used. The drops are immersed in an immiscible

fluid between two counter rotating transparent parallel plates. Observation is done through an optical microscope. The set-up allows in-situ monitoring of the droplets. The deformation and break-up of droplets of both types of system as a function of drop/immiscible fluid viscosity ratio and applied stress was investigated in details and compared. The criteria of starch suspension droplet break-up were determined.

I.3. Organisation of the thesis

This thesis is organised in the following way.

The second Chapter will introduce the context and scientific background of the study. First, a brief review will be given on in-mouth flavour perception and the implications of the viscosity and the choice of thickener, to guide the reader through the motivations of the study. The second part of Chapter II will be dedicated to starch as it is the main material used in this study. The composition and structure of starch granules will be described. Swelling and gelatinisation of starch in water will be given as well as the influence of structure on the process. The swelling and gelatinisation conditions have a great influence on the rheological properties of starch thickened samples as it will be seen. The last part of this literature review will summarise the different findings on droplet deformation and breakup. Relevant definitions and models will be given as well as the description of the pioneering works on the subject. Many studies have been carried out on Newtonian systems, i.e. where both the dispersed and the continuous phase are Newtonian. Hence, the global findings for such systems will be described. However, in most practical applications one or both phases are viscoelastic leading to different results. Finally, systems where the dispersed phase is a suspension droplet will be reviewed as it the closest to the systems that will be studied in this work. However, only one article related to the subject was found, evidencing the lack of research in the field and thus showing the innovative angle of this Ph.D. work.

Materials and methods used for this study are described in the third Chapter. The used starches (modified waxy maize and potato starch) are presented and

determination of the gelatinisation temperature as well as the maximum degree for both starches is given. The preparation of the samples will also be explained. Hydroxypropylmethyl cellulose (HPMC) and silicon oil were also used for the experiments and will hence be described in this section. To study the shear-induced flow behaviour starch suspensions (and also the HPMC solutions) two main methods were used: the rheo-optical counter rotating shear cell (set-up developed in CEMEF) and rotational rheometers. Both methods will be thoroughly described in this Chapter. Surface tension measurements were carried out with a tensiometer using the pendent drop method. Finally, many other methods were used to characterise the starch granules (SEM, AFM) and the continuous phase of a starch suspension (DSC, iodine staining, AUC and SEC-MALLS) and will be given in Chapter III.

The first results Chapter (Chapter IV) will be showing the characterisation of modified waxy maize and potato starch granules, i.e. their shape and surface properties as well as their behaviour under shear. The SEM pictures and AFM analysis will be given. Finally, the qualitative study of the behaviour of swollen in water starch granules under shear will be explained and interpreted along with the difficulty arising when studying such systems.

The rheological properties of a modified waxy maize starch suspension will be described in Chapter V. The first part of the chapter will be dedicated to the rheological properties of the suspension at different concentrations. Influence of volume fraction and deformability of the granule will be demonstrated. The data obtained for the continuous phase will be analysed and discussed.

Once the starch suspension is fully characterised, it is possible to study the behaviour of a droplet submitted to shear. Comparison with an HPMC solution droplet will be given in Chapter VI. First, the HPMC solution will be characterised as it is needed for the analysis of droplet deformation data. This data will be analysed and differences between the systems will be interpreted. Both systems will be compared in terms of microstructure, droplet deformation and break-up. An in depth study on the break-up conditions of suspension droplets will be carried out. Interpretation hypothesis for suspension break-up criterion will be given.

The overall results of this study will be summarised and relations between the chapters will be explained in the conclusions and perspectives Chapter (Chapter VII). Suggestions for future work and further application will also be given.

This work was done and partly funded thanks to the European Polysaccharide Network of Excellence (EPNOE).

Reference List:

Cook, D. J., Hollowood, T. A., Linforth, R. S. T., and Taylor, A. J. (2003). Oral shear stress predicts flavour perception in viscous solutions. *Chemical Senses*, 28, 11-23.

Ferry, A. L., Hort, J., Mitchell, J. R., Cook, D. J., Lagarrigue, S., and Pamies, B. V. (2006). Viscosity and flavour perception: Why is starch different from hydrocolloids? *Food Hydrocolloids*, 20, 855-862.

Résumé du chapitre II

Contexte scientifique

Notre étude porte sur les suspensions d'amidon soumis à un cisaillement et plus précisément à la déformation et la rupture d'une gouttelette de suspension d'amidon soumis à un cisaillement simple. L'origine de cette étude est la détermination d'un paramètre physique permettant de comparer divers épaississants alimentaires qui offrent des différences dans la perception du goût bien qu'ils soient à des viscosités et des concentrations en arômes équivalents. Pour que le lecteur comprenne les différents implications de ce sujet, et pour poser le contexte scientifique, trois sujets ont été abordés au cours de ce chapitre : sur les généralités de perception du goût en bouche, sur l'amidon en mettant l'accent sur la rhéologie des suspensions d'amidon et enfin sur le comportement sous cisaillement de gouttes liquides dans une matrice immiscible.

Dans une première partie, une brève récapitulation a été présentée. Tout d'abord quelques aspects généraux sur les arômes et leur perception ont été donnés pour situer le contexte. La perception du goût est influencée par la viscosité du produit : au-delà d'une concentration critique, c*, la perception est largement diminuée. Il semblerait que cela soit dû à un transport réduit des agents de flaveur vers les récepteurs sensoriels. De plus ce transport serait conditionné par le type d'épaississant utilisé : une solution de polymère (type hydrocolloide) ne permet pas une aussi bonne perception du goût que les suspensions d'amidon (les granules ont gardé une forme de particules).

Pour mieux comprendre les spécificités de l'amidon, la seconde partie est dédiée à expliquer sa composition, sa structure, ses propriétés et son comportement rhéologique. Grâce à une grande valeur nutritionnelle et ses capacités de gonflement dans l'eau, l'amidon est un ingrédient de premier choix dans l'industrie alimentaire. Ce biopolymère a des origines diverses conférant ainsi une large palette de

propriétés selon la source utilisée. L'amidon est composé d'amylose et d'amylopectine, deux polymères dont l'unité monomère est le glucose mais dont l'arrangement dans l'espace diffère. L'organisation de ces molécules au sein du granule est une alternance d'anneaux concentriques amorphes et semi-cristallins donnant ainsi une structure semi cristalline à l'amidon. Les granules chauffés dans l'eau gonflent et augmentent ainsi la viscosité. Selon les conditions de préparation, la concentration et la composition en amylose et amylopectine, l'échantillon aura différentes propriétés d'écoulement. En dessous d'une certaine concentration appelée concentration critique (où les granules sont en contact), les propriétés rhéologiques sont gouvernées par la fraction volumique occupée par les granules. Plus les granules sont gonflés, plus ils prennent de la place et plus la viscosité sera élevée. Dans le cas où la concentration est supérieure à la concentration critique, la rhéologie dépendra essentiellement de la déformabilité des granules. Plus les granules seront gonflés, plus ils seront déformables et donc sensibles au cisaillement ; par conséquent la viscosité sera plus faible. Quand on considère la rhéologie des suspensions d'amidon il est important de connaître les conditions de préparations de l'échantillon car ils influencent le gonflement des granules. De plus, des interactions entre particules, encore largement méconnues, peuvent influencer son écoulement. Néanmoins, pour étudier la déformation d'une goutte de suspension d'amidon il est nécessaire de connaître sa rhéologie.

Dans la dernière partie, le comportement de gouttelettes plongées dans une matrice immiscible est considéré. Les modèles définis pour les systèmes purement Newtoniens (goutte Newtonienne et matrice Newtonienne) sont d'abord expliqué. Deux nombres adimensionnels sont utilisés pour décrire la majorité des systèmes étudiés : le rapport de viscosité p qui équivaut au rapport de la viscosité de la goutte sur la viscosité de la matrice et le nombre capillaire Ca qui est le rapport de forces qui tendent à déformer la goutte (forces visqueuses) sur les forces qui tendent à la maintenir sphérique (forces interfaciales). Une goutte soumise à un cisaillement se déforme ; si ce dernier est augmenté au-delà d'un certain seuil la goutte peut se rompre (lorsque les forces interfaciales sont trop faibles par rapport aux forces visqueuses). On parle dans ce cas de nombre capillaire critique. Il existe une relation entre le rapport de viscosité et le nombre capillaire critique, déterminée pour des systèmes Newtoniens. Selon la valeur du rapport de viscosité il est plus ou moins

difficile de rompre la goutte. Dans le cas ou une des deux phases est viscoélastique, la déformation ainsi que les conditions de rupture changent. Si la matrice est viscoélastique, la goutte Newtonienne aura tendance à se déformer plus et à rompre plus facilement que dans le cas analogue Newtonien. En revanche si la goutte est élastique, elle se déformera moins et cassera plus difficilement. Finalement, dans le cas ou les deux phases sont élastiques des ruptures peuvent survenir pour des rapports de viscosité très élevés contrairement aux autres cas. De plus certaines ruptures peuvent s'effectuer dans un axe différent que celui de l'écoulement.

Pour finir, une petite partie a été consacrée à l'étude de la déformation et rupture de gouttelette de suspension. Il semblerait que le comportement dépende essentiellement de la fraction volumique occupée par les particules.

Chapter II: Scientific background

Multi-phase systems such as emulsions are widely used in cosmetics, food and pharmaceutical applications and have therefore been widely studied. Through droplet break-up in simple shear flow it is possible to appreciate some of the factors determining drop size distribution in polymer mixtures and emulsions and consequently have a better understanding of the bulk rheology and overall mixture properties. Such studies could contribute to an understanding of the differences observed in the flavour perception between starch and hydrocolloid thickened products at the same shear viscosity (Mitchell et al., 2008). Because the idea of correlating flavour perception in starch systems and droplet behaviour was at the origin of this work, two main directions in the scientific background will be considered: starch as a thickening material and droplet behaviour under shear.

The specific characteristics of starch are of interest in the food industry for its great nutritional value but also for its thickening properties. Some starches allow better flavour perception and mouthfeel than others or than hydrocolloid thickened products and this is of importance as the use of these starches could allow a reduction of salt concentration in food products and thus help current health issues. Many phenomena are involved in flavour perception such as chemical interactions but also physical and structural characteristics of the product, such as the ability to efficiently mix with saliva in the mouth. The mixing ability could be estimated by studying the behaviour of a droplet of starch suspension under simple shear, i.e. its deformation and break-up conditions and comparing to the behaviour of hydrocolloid droplets under similar conditions.

All of these intertwined notions are important to clarify and in order to guide the readers through this work, previous studies on these subjects will be explained in this chapter. A first part will deal with the influence of the viscosity of food products on flavour perception; only the key conclusions will be presented here as it is not the main interest of this study. However, it seemed important that the reader understood the initial motivation for this research. As starch is present in all aspects of this study, a second section on starch structure and its rheological characteristics is

presented here. Finally the last part is fully dedicated to the theories and results obtained to this day for droplet deformation and break-up.

II.1 Flavour perception

II.1.1 General aspects of flavour and its perception

Flavour can be considered as a mixture of non volatile compounds sensed on the tongue (taste) and volatile compounds that are perceived through the sense of smell (aroma). Aroma seems altogether more important than taste; it can be easily demonstrated by the difficulties of the subject in identifying flavour with his/her nose pinched (Taylor & Linforth, 1996).

Perceived flavour during consumption is due to stimulation of three principal sensory systems (Cerf-Duscastel & Murphy, 2001): taste, olfaction and trigeminal system. The latter is a somatosensory system for the face as it provides sensory innervation to the oral cavity and motor innervation to the muscle of mastication (http://cancerweb.ncl.ac.uk/cgi-bin/omd?trigeminal+system, consulted 30/07/08). Aroma-taste interactions have been thoroughly studied; however, what is happening at the somatosensory/ taste/aroma level is not well understood (Cook et al., 2003).
Food can be consumed in many ways; different physical states of the food products may lead to many different studies. It is obvious that flavour perception in liquid beverages will not be the same as for fat based products or low moisture content products such as cereals. For example, a liquid may not be diluted by saliva since it is consumed rapidly whereas eating cereal induces chewing and mixing with saliva and will consequently stay longer times in the mouth (Taylor & Linforth, 1996). It is possible to imagine that during consumption many factors may influence the release of volatile and non-volatile components such as structure break-up during mastication and mixing with saliva. Lately, an interest has been building on the relationships that exist between flavour perception and oral viscosity, texture and structure of hydrocolloid or starch thickened products (Bayarri et al., 2007; Cook et al., 2002; De Roos, 2003; Ferry et al., 2006; Koliandris et al., 2008).

II.1.2 Influence of viscosity and texture on flavour perception

Baines & Morris (1987, 1988) studied the relation between flavour perception and viscosity of the product. They detected a reduced flavour perception above the coil overlap concentration c* in hydrocolloid solutions. When the viscosity of the solution was above this critical concentration a decrease in flavour perception was perceived. It was suggested that it was due to inefficient mixing with saliva above c*, thus reducing transport of small tastants to the receptors on the tongue. In contrast De Roos (2003) attributed this phenomenon to binding of flavour compounds to the thickener and the effect of the latter on mass transport. Although there is strong evidence of flavour binding to thickening agents, such as hydrocolloids and starches (Jouquand et al., 2004; Jouquand et al., 2006; Rutschmann & Solms, 1989), the reduction of tastant transportation to the receptors by other mechanisms such as reduced mixing efficiency is a preferred hypothesis. Indeed, studies showed that although strong binding between protein and flavour occurs, there is little or no effect on the release of the compounds during consumption (Le Guen & Vreeker, 2003; Weel et al., 2002). A further study by Cook et al. (2003) showed through analytical methods that there was no change in retronasal release of aromas during consumption for viscous hydrocolloid solutions above c* although a trained sensory panel clearly detected a reduction in flavour with increase of the product viscosity. It seems that only the release of the tastants to the receptors is delayed and that tastants rule the overall flavour perception (Koliandris et al., 2008).

Studies on the relation between mechanical properties of gelled systems and flavour perception (Bayarri et al., 2007; Koliandris et al., 2008) showed that the lower the strain at rupture the higher the flavour perception. The more brittle gels will break-up more easily on the mouth hence creating a higher surface area; it allowed easier tastant release, suggesting that this release to the receptors plays a major role in flavour perception.

These studies also revealed an effect of the hydrocolloid type on the perception and mouthfeel.

II.1.3 Differences induced by the type of hydrocolloid/thickener

Ferry et al. (2006) assessed the flavour perception of basil and salt in starch and hydroxypropylmethyl cellulose (HPMC) thickened products through sensory tests and tried to correlate the results with microstructural properties. The study demonstrated that starches showed less flavour inhibition than the HPMC. When a large magnitude of decrease in perception was observed with increasing HPMC concentration, the starches showed only a slight decrease. Moreover, differences occurred depending on the type of starch; waxy maize offered lower flavour perception than the cross-linked waxy maize. It was hypothesised that a higher flavour perception could be due to the way the thickened product mixes in the mouth and releases the volatile and non-volatile compounds to the receptors (Baines & Morris, 1987; Ferry et al., 2006; Mitchell et al., 2008). The ability of the thickeners to mix in the mouth is linked to their microstructure and their rheology. In hydrocolloid solutions, polymer entanglements could hamper mixing and thus tastant release and transportation to the taste buds (Baines & Morris, 1987). The studies mentioned above report a sharp decrease in flavour decrease above c* where the coils overlap, confirming the idea that polymer entanglement might be a key parameter (Baines & Morris, 1987; Cook et al., 2002; Cook et al., 2003). Ferry et al. (2006) showed that modified waxy maize starch pastes gave better perception and mouthfeel than the waxy maize ones. Visual observations indicated that a waxy maize paste was closer to a solution of random macromolecular coils with little residual granular structure whereas cross-linked waxy maize retained good granular form. Hence, the differences observed seemed to be due to the microstructure and could explain the differences in mixing behaviour. Suggested physical parameters related to flavour perception such as the degree of shear thinning (Mitchell, 1979) or Kokini oral stress do not directly relate to mixing (Cook et al., 2003). It was hypothesised that extensional behaviour would correlate better with mixing behaviour and thus with flavour perception and mouthfeel (Connelly & Kokini, 2004).

Part of this work is to study the extent of deformation of starch and HPMC thickened droplets; it is possible that the deformation and break-up of such droplets

correlate efficiently with mixing properties, an easy break-up suggesting a better mixing ability.

However, before reviewing the aspects of droplet deformation and the associated theories, it is necessary to understand starch, its structure and properties.

II.2 Starch: a complicated matter

Starch is a natural polymer that can be found in the plant world; botanical sources are abundant but the main ones are corn, potato and wheat. Starches can also be genetically, physically or chemically modified to improve their properties such as resistance to heating for example. Starch applications are numerous; among others are fillers and coatings in pharmaceutical products, as a material for building construction, in paper making and biodegradable packaging to name only those. However, its most common use is in the food industry.

Starch is consumed for its nutritional value but it also makes an important contribution to texture. Because of the ability of the starch to swell in excess water; it is and effective thickener and is used by the food industry to increase the viscosity of liquid products. The intake of water by the starch granule is possible thanks to its specific structure.

II.2.1. Starch structure

Starch is the plant energy reserve and is found in the form of granules in stems, roots and tubers. It is composed of a mixture of two polysaccharides: amylose and amylopectin. These carbohydrates differ in size and shape, due to different glycosidic bonds, but also in their proportions within the granule. The monomer unit of both molecules, a glucose molecule, is presented below.

II.2.1.1.The glucose unit

D-glucopyrannose exists in two anomeric forms referred to as “OH α-anomeric” when the hydroxyl group is in the axial position and “OH β-anomeric” when in the equatorial position (Figure 2.1).

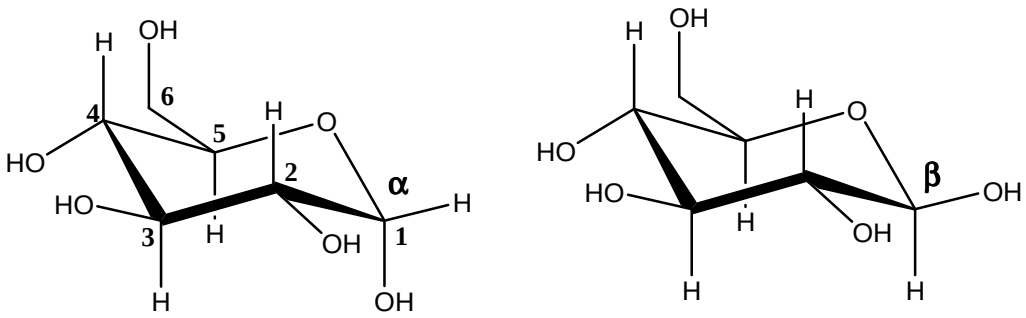

Figure 2.1: α-D-glucose and β-D-glucose

The carbons of the glucose molecule are numbered from 1 to 6 starting from the right of the oxygen atom; the 5th carbon is linked to the oxygen and a 6th atom is outside of the ring.

In the case of starch polymers, the monomer unit is the α-D-glucose; the other form β-D-glucose can be found for example in cellulose.

II.2.1.2.Amylose

Most starches consist of 15 to 30% of amylose (Zobel, 1988), this amount differs with botanical source or possible modification and can vary from 0 to 70%. The glucose units are linked in α (1-4), i.e. the first carbon of a glucose molecule is linked to the 4th carbon of another monomer unit (Figure 2.2). The polymer thus obtained is linear and can count 500 to 6000 monomer units.

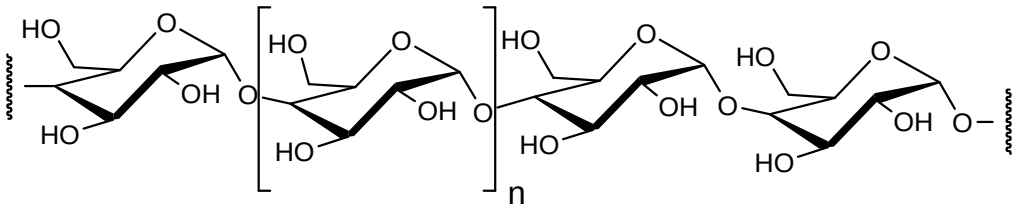

Figure 2.2: Representative partial structure of amylose.

Due to the conformation of glucose, the shape of the amylose chain is arranged most of the time in a stiff left handed helix. It is stabilized by hydrogen bonds, with 7 or 8 units per revolution (Oates, 1997). Amylose chains can sometimes form double helices (Shi et al., 1998; Tester et al., 1998). The inner surface of the helix is hydrophobic hence forming complexes with lipids and iodine I_2. The latter is used for the determination of amylose content.

II.2.1.3.Amylopectin

Amylopectin is the larger fraction (70-100%) of starch mainly because alone it can generate granules. Glucose units are linked in α (1-4) but five percent are linked in α (1-6) causing the amylopectin to be highly branched (Oates, 1997) (Figure 2.3).

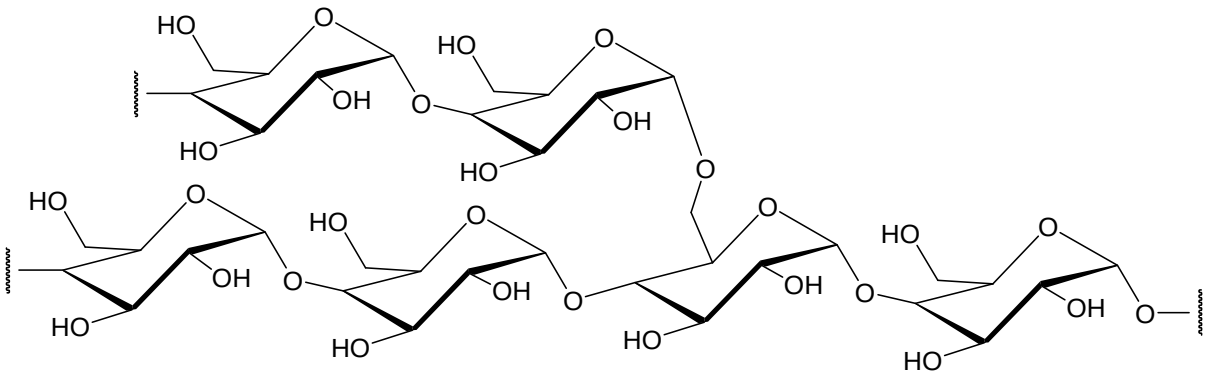

Figure 2.3: Representative partial structure of amylopectin.

The arrangement of amylopectin is therefore different from that of amylose; instead of a long linear chain, amylopectin is composed of many shorter chains organised in clusters. Current models for amylopectin fine structure suggest two populations of chains: A- and B-chains present in almost equal proportions. A-chains are “outer” unbranched chains, attached to the molecule by a single linkage while B-chains are linked to two or more chains (see Figure 2.4), the first being slightly more numerous than the “inner” branched chains. Amylopectin molecules will also possess one sinlge C-chain each with a reducing group. The size distribution of these chains can be separated into three groups (Han & Hamaker, 2001):

- Small chains (degree of polymerisation, DP, between 12 and 20 glucose units), mainly A-chains and small B-chains linking two clusters.
- Longer chains (30 < DP < 47) mainly long B-chains linking three or more clusters.
- Long chains (DP above 60 glucose units) comprised of B-chains that connect several clusters.

The cluster arrangement of amylopectin is responsible for the semi-crystalline organisation of the starch granule.

II.2.1.4.Semi-crystalline structure and location of amylose and amylopectin within the granule

Knowing the crystalline structure is of interest as it will give information on the swelling capacity of a granule. The location of the components within the granule will also give information on the global structure. However, location of amylose and amylopectin remains unsure and seems to depend on many parameters.

A starch granule observed under polarized light shows a Maltese cross, indicating through this birefringence phenomenon, a semi crystalline structure. Looking at acid hydrolysis treated starch (acid will cut the glucose bonds allowing water to penetrate the granule more easily) under light microscope it is possible to see concentric growth rings (mainly for large granule). The initial growth centre is called the hilum. These growth rings are a succession of alternated amorphous and crystalline zones (Figure 2.4a) thus suggesting that starch matures in a diurnal rhythm, and that newly synthesized material is deposited on the surface as the granule increases in size (Oates, 1997).

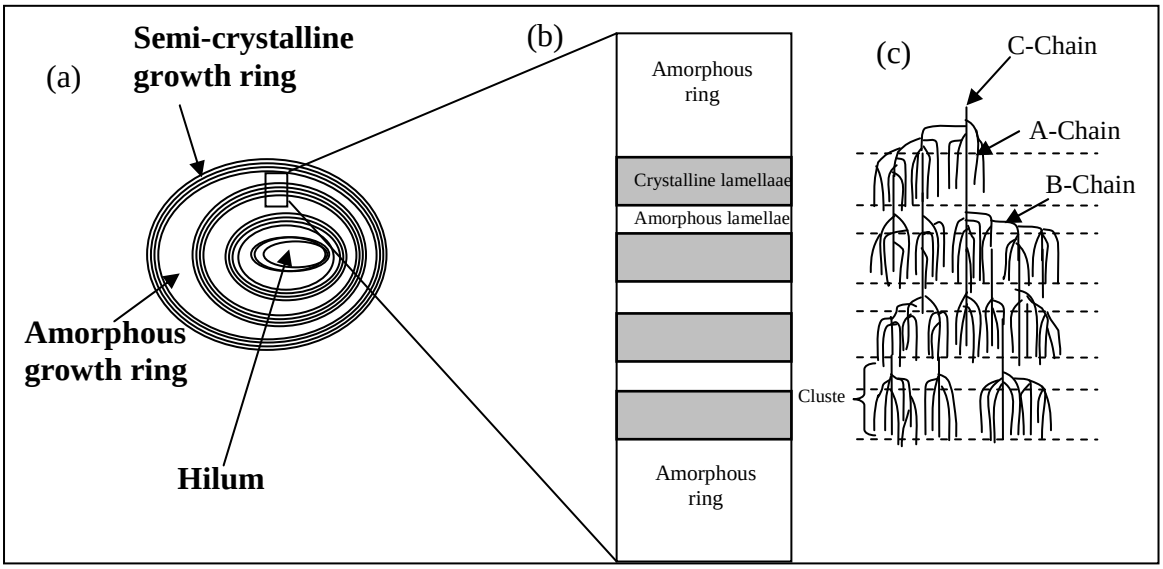

Figure 2.4: Schematic diagram of the structure of a starch granule. (a) Single granule comprising concentric rings, each containing stacks of amorphous and crystalline lamellae; (b) amorphous and crystalline lamellae; (c) chains of amylopectin arranged in a cluster structure (adapted from Jenkins & Donald, 1995)

Semi-crystalline growth rings (Figure 2.4b), mainly composed of amylopectin, are alternating amorphous and crystalline lamellae. The ordered regions (crystalline) are tightly packed glucose chains while the less ordered regions are predominantly composed of branching points. Gallant et al. (1997) described the structure as a "mozaic of hard and soft material", the soft material being a semi-crystalline shell (corresponding to the amorphous zone of Figure 2.4) and a crystalline hard shell. The latter is alternating amorphous and crystalline lamellae, in agreement with the description of Jenkins & Donald (1995). Visual observations of starch granules using various microscopy tools showed that the crystalline hard shells are composed of large blocklets of alternating crystalline and amorphous lamellae giving new insight on granular organisation. This alternation corresponds to what is described above, i.e. that the crystalline lamella is composed of amylopectin clusters in a double helical conformation and the amorphous part of branching points. The softer layer (semi-crystalline zone) also contains blocklets but smaller in size.

Native starch granules contain between 15 and 45% of crystalline material. X-ray diffraction gives two distinct patterns, A and B (Figure 2.5). A third pattern called C-type is a mixture of both A and B.

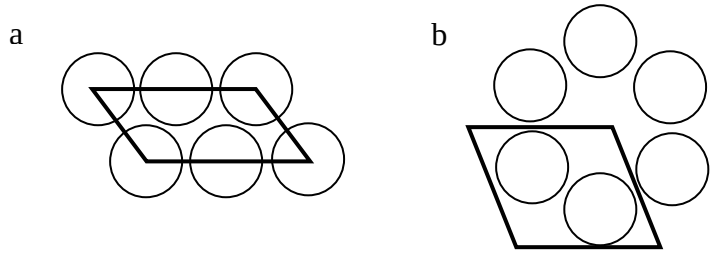

Figure 2.5: Crystalline patterns of starch. (a) A-Type; (b) B-Type (Zobel, 1988)

These two models for crystal polymorphs of starch, although they have the same helical structure, are based on the differences in the packing configuration of double helices and the water content (Gidley & Bociek, 1985; Imberty et al., 1991). Both crystalline structures are the result of double helices paired and stabilized by hydrogen and Van der Waals bonds.

The A-type pattern, seen mainly in cereal starches, is a face-centred monoclinic network composed of 12 glucose molecules, located in left-handed chains that contain four water molecules between the helices (Gidley & Bociek, 1985). The B-type crystallite (tuber starches mostly) is an hexagonal array formed by two left-handed parallel stranded double helices, where a unit cell contains 12 glucose residues and 36 water molecules. The A and B packing type depend on storage conditions (moisture, temperature); e.g. the B-type can become an A-type through heat moisture treatment allowing, in specific conditions, for the molecules to rearrange, hence leading to a denser packing making it more difficult for water to penetrate. This is one of the physical modifications that can be made to starch granules and is called annealing (Jayakody & Hoover, 2008).

The structure of the starch granule is pretty well understood regarding the location and conformation of amylopectin. However, where the amylose sits in the granule is still subject to debate. It is of importance to know the location of amylose and its relation to amylopectin as these parameters might influence the behaviour of starch in excess water. On one hand, several studies revealed that more amylose was located at the periphery of the granule (Gallant et al., 1997; Jane & Shen, 1993; Sevenou et al., 2002) and that it contributed to a high level of organisation at the surface leading to resistance to enzymic attack (Sevenou et al., 2002). On the other hand, Kuakpetoon & Wang (2007) showed that amylose was not at the periphery contradicting findings by Jane & Shen (1993). What can be said is that amylose

location depends on the starch type (Atkin et al., 1999). In any case, amylose is present in the whole granule and is thought to be in bundles among amylopectin clusters (Jane et al., 1992; Oates, 1997), causing disruption of the crystalline formation (Cheetham & Tao, 1998). However, Banks and Greenwood (1975) showed that amylose could contribute to crystallinity in high amylose starches by forming different crystal polymorphs. As it can be seen it is hard to determine the location of amylose and its influence on crystallinity; difficulties can arise from the variety of starches avalaible. Moreover, differences occur depending on the maturity of the starch, the storage and growing conditions. All of these differences will acount for gelatinization behaviour. Other small constituents, such as proteins and lipids, can also influence the swelling of the granule.

II.1.2.5.Small components in starch granules

Some starches, mainly cereal starches, may contain lipids such a lypophospholipids and free fatty acid or surface lipids. They are able to form complexes with amylose which melt at high temperature. Starch may also contain proteins and a small amount of minerals namely phosphorus (found mostly in potato starch). These small “contaminants” have been reviewed by Tester et al. (2004).

II.2.2. Starch in water: swelling and gelatinization process

Dry starch, when heated in excess water, starts swelling as the water is absorbed by the granules. Past a certain state the phenomenon is irreversible and is called gelatinization. This process is possible thanks to α-(1-4) linkage; the molecules can arange so as to allow water enter the structure. When the starch paste is cooled and ages the polysaccharide chains rearrange; this process is called retrogradation. Both gelatinization and retrogradation are presented below in Figure 2.5.

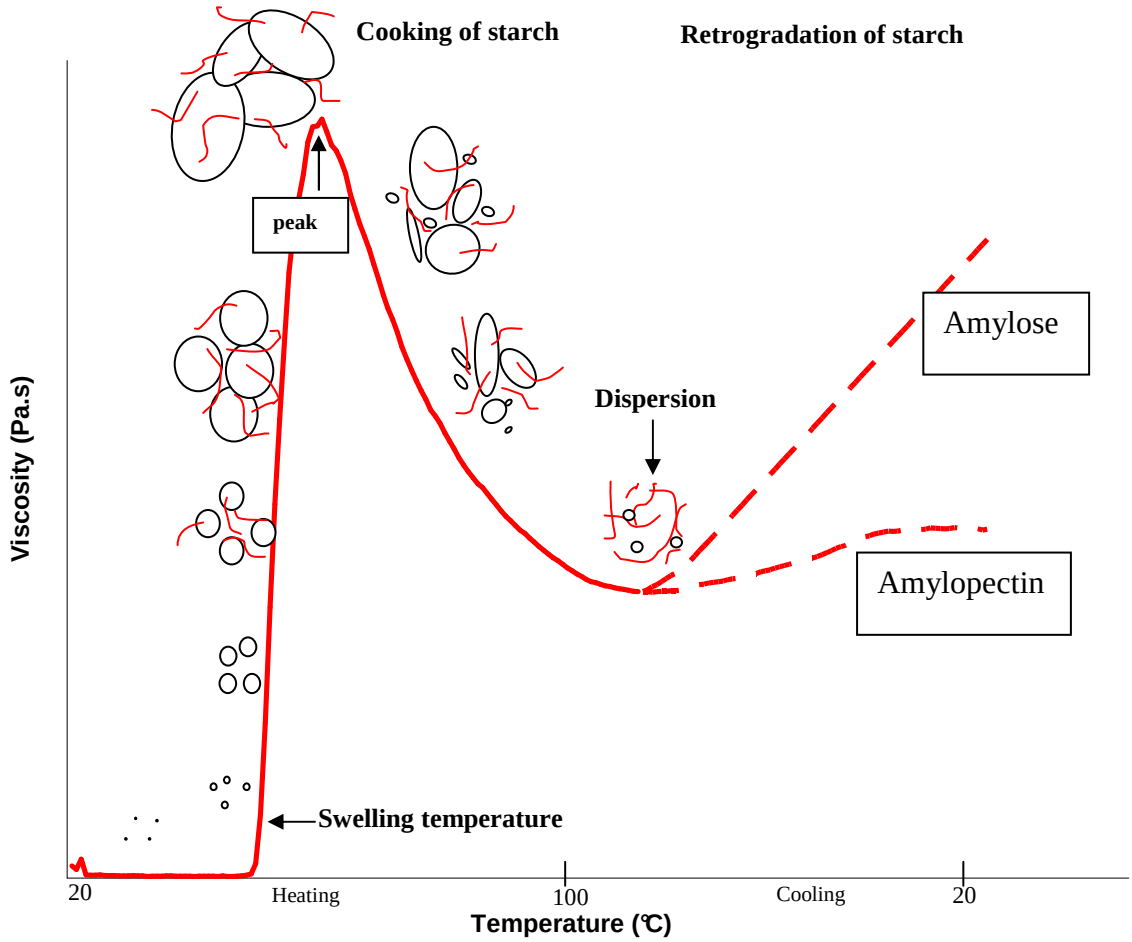

Figure 2.5: General behaviour of starch upon heating and cooling in excess water (from Boursier, Technique de l'ingénieur)

In Figure 2.5, the empirical rheology data obtained with a rapid visco-analyser is compared to the granular scale. The onset of temperature for which the granules starts swelling is shown in Figure 2.5. Once this temperature is reached the viscosity increases rapidly as the swelling reaches a maximum (viscosity peak). During this process the amylose molecules leach out of the granules creating a medium around the particles composed of solvent and amylose. The granules keep swelling until they have reached equilibrium. After maximum viscosity is reached, if the temperature continues to increase, the granules will burst and disperse completely. This explains the sharp decrease in viscosity called the viscosity breakdown of the paste. Upon cooling the starches will have different behaviours depending on the amylose/amylopectin ratio. Starch pastes with amylose content over 20% will see their viscosity increase at ambient temperature. This is due to re-association of aligned amylose chains, usually leading to a water release phenomenon called syneresis. The rather low increase in viscosity after cooling is

representative of “amylopectin behaviour”; the amylopectin re-crystallises at a slower rate than amylose and therefore a few days are necessary to observe a viscosity increase.

Most studies seem to agree on the fact that the swelling through hydration of the granule is due to polymer rearrangement (Atkin et al., 1998; Chiotelli et al., 2002; Gallant et al., 1997; Srichuwong et al., 2005; Tako & Hizukuri, 2002). However, whether it is due to dissociation of the crystallites favouring water/starch interactions (Chiotelli et al., 2002; Ratnayake & Jackson, 2007; Srichuwong et al., 2005) or to absorption of water by the amorphous regions (Gallant et al., 1997; Karapantsios et al., 2002) remains unclear. A kinetic study shows that 2 elementary reactions best describe the gelatinization process (Karapantsios et al., 2002) and it is most probable that both events occur simultaneously (Ratnayake & Jackson, 2007). Nevertheless the swelling of the granules will depend on the structure (crystallinity, molecular arrangement…). A less crystalline starch will absorb water more easily and hence allow polymer rearrangement (Srichuwong et al., 2005). The presence of pores at the surface and amorphous channels could also allow water to penetrate and diffuse through the granule (Gallant et al., 1997). The long chain to short chain ratio will also have an influence on swelling: a larger amount of long B-chains will increase the stability of crystalline packing and delay the swelling (Srichuwong et al., 2005). Finally, the presence of small components such as phospholipids on the surface of cereal starches will reduce the extent to which the granules expand (Padokhin et al., 2006; Srichuwong et al., 2005).

The rheology of starch pastes will depend on preparation conditions and the swelling of the granules. The rigidity of the granules depends on its swelling and is hence correlated to its rheological behaviour.

II.2.3. Starch under mechanical stress

This section will show the multiple aspects of starch rheology depending on starch origin and preparation conditions. The behaviour of a single swollen starch granule under mechanical stress would shed light on the bulk behaviour but only one publication on the subject was found in the literature.

II.2.3.1 Behaviour of a single swollen starch granule

The viscoselastic properties are thought to be governed by the swollen starch granules themselves (Evans & Lips, 1992). However, studies on the deformation of single swollen granules are scarce. Fischer et al. (1997) were able to make direct measurements of the deformation of a starch granule as a function of the applied force using two micropipettes, one holding the granule and the other, slightly modified, applying the force. Compression, indentation and hydrostatic manipulation revealed that the swollen granule acts like an elastic body and is highly deformable. Oates (1997) described rubbery regions (amorphous amylopectin) that protect the granules from compressive forces, thanks to a greater intramolecular mobility. Nevertheless, rubbery regions imply that some parts of the granule are less elastic or less resistant to mechanical stress; this heterogeneity of the granule deformation was demonstrated by Fischer et al. (1997). Rheological properties depend on the deformability of the swollen granules as it will be seen in the following section.

II.2.3.2 Rheological characterisation of starch pastes

Rheology of starch is a wide field of study as it is of interest for starch processing in food, or even to “correlate” to in mouth behaviour. However, regarding the numerous variations in starch types, structures and properties, it renders the matter difficult. Throughout literature, the influence of type of starch (Singh et al., 2006; Thebaudin et al., 1998), possible modification (Chamberlain & Rao, 2000; Eerlingen et al., 1996; Morikawa & Nishinari, 2000) and mostly pasting procedure for a same starch (heating temperature, shearing speed, choice of solvent)

was put into light (Doublier, 1986; Doublier et al., 1987; Meng & Rao, 2005; Nayouf et al., 2003; Rao & Tattiyakul, 1999; Tattiyakul & Rao, 2000; Velez-Ruiz et al., 2006; Youn & Rao, 2003). Nevertheless, some common conclusions can be drawn out of the rheological studies.

As it was said above, the rheology of the starch paste depends on the pasting procedure. If the conditions are severe such as high shear, high temperature or a specific solvent (acid for example), the starch paste will resemble a solution of macromolecular matter, a mixture of amylose and amylopectin. In mild conditions or if using physically or chemically modified starch, the granular integrity can be maintained; a general overview of the behaviour of such starch suspension will be given in the following paragraphs. In this case, starch pastes are considered as a suspension of swollen particles dispersed in a macromolecular medium; the continuous phase would correspond to the solubilized fraction which in most cases is amylose (Doublier, 1986).

As the system is considered as a suspension of swollen particles, the overall viscosity (η) can be estimated knowing the volume fraction (Φ) of the dispersed phase and the viscosity of the macromolecular solution around the granules (η_s) (Eq 2.1).

$$\eta = \eta_s f(\phi) \qquad 2.1$$

The viscosity of the continuous phase is proportional to the amount of leached out macromolecules. The term $f(\Phi)$ is a function of the quantity of the granules themselves and depends on their swelling degree and their deformability. Bagley & Christianson (1982) and Meng & Rao (2005) proposed that the volume fraction of a suspension with no solubilized material can be estimated from the product of the starch concentration c (%w/w) and the swelling capacity of the granules (Q in g/g), i.e. Φ = cxQ. In the case of a polymeric fraction dissolved in the media, the volume fraction can be obtained through the following expression (Eq 2.2) (Doublier et al., 1987):

$$\phi = \left(\frac{1-S}{100}\right) \times c \times Q \qquad 2.2$$

where S is the solubility index (%). The equation assumes that the sediment of a centrifuged suspension is fully filled by swollen granules and that no solvent remains around them (Bagley & Christianson, 1982).

It is obvious that above a certain volume fraction, the swollen granules occupying a certain volume will be in contact, creating a "network"; this concentration is referred to as the close packing fraction or critical concentration c* (Evans & Haisman, 1980). The rheological properties of the system will strongly depend on the suspension concentration whether it is above or below the close packing fraction. Two different regimes, comparable to those determined for random coil overlap in polymer solutions, depending on the volume fraction and thus on the concentration were defined (Doublier et al., 1987; Eerlingen et al., 1996):

- Dilute or semi dilute regime ($c<c^*$): no contact of the granules, no network created. The rheology of the system depends on the volume fraction occupied by the granules. At an identical concentration more swollen granule will yield higher viscosities.
- Concentrated regime (above close-packing fraction, c*): the overall rheology is governed by the granule, i.e. its ability to deform. The concentrated regime is detected as the onset of a measured yield stress. Highly swollen granules will be more deformable and more fragile and lead to a more important shear thinning behaviour.

As highly swollen starch granules are deformable and polydisperse all the space can be taken up by the granules and maximum packing fraction values of 1 can be obtained. This is specific to this type of material. Nevertheless, considering that a small or large amount of polymeric material is released, it is not possible to attain such a concentration even for cross-linked starches since even in the latter case a very small portion is solubilised in the continuous phase.The voulme fraction of 1 is a theoretical value that can be approached but not obtained.

The rheological properties of starch will depend on whether the system is diluted or concentrated (above or below c*) and also on the swelling ability of the granules. In the following part a description of the rheological behaviour observed for starch suspensions (=swollen granules in continuous medium) will be given.

- Flow behaviour:

The viscosity of a gelatinised starch suspension is attributed to frictional dissipation of energy between the granules (Schoch, 1969). Starch rheology depends on many factors listed above; hence, difficulties in summarising global findings can arise. Shear rate dependency, thixotropic behaviour and viscoelasticity are more or less constantly discussed throughout the literature. Current findings will be summarised in the following part.

Dilatancy or shear thickening behaviour of starch suspensions was reported by some authors (Bagley & Christianson, 1982; Frith & Lips, 1995; Jacquier et al., 2006; Rao et al., 1997; Rao & Tattiyakul, 1999). Frith & Lips (1995) suggested that it is due to the particles trying to occupy a greater volume than the overall volume, forming a close packed structure. Moreover, they thought that the particle deformability could play a dominant role. However, in all cases, this phenomenon occurs in specific conditions: high volume fractions of poorly swollen granules. High shear during the measurement was also suggested as a condition for observation of the dilantancy (Rao & Tattiyakul, 1999), though if the granules were further heated only shear thinning was observed. The shear thickening behaviour is thus dependent on the swelling degree of the granules. Shear thickening was reported in specific cases where the granules were poorly swollen, however, many studies also observe a **shear thinning behaviour** sometimes prior to shear thickening. Nguyen et al. (1998) studied the flow properties of maize and waxy maize starch and observed shear thinning of both suspensions. However, the concentration and swelling degree were not available so it is hard to determine whether it is expected behaviour or not. Nevertheless the absence of yield stress suggests that the suspension is below close packing fraction; this explains the absence of dilatant behaviour. A higher viscosity was reported for waxy maize starch due to its higher swelling degree. In that case, a higher volume is occupied by the granules leading to higher viscosities. Effect of starch origin was investigated using wheat, maize, waxy rice and modified waxy maize starches (Thebaudin et al., 1998). All starch pastes exhibited shear thinning but different behaviours between the non waxy and the waxy starches were detected; the first ones displayed low viscosities and thixotropic behaviours while the waxy starches showed high viscosities and antithixotropic behaviour. Thebaudin et al. (1998) attributed these

differences to the swelling-solubility of the starch. Waxy maize starches do not contain any amylose, hence less material is solubilised from the granule, explaining the distinction between the normal starches and the waxy starches.

Another important point to consider is the impact of the pasting procedure on the rheology of starch (Doublier, 1986; Doublier et al., 1987). It seems that starch pastes submitted to higher temperatures exhibit higher viscosities but also more evident shear thinning behaviour. It was hypothesised that highly swollen granules (swollen to their maximum) were more deformable making them sensitive to mechanical stress. Further investigation showed that low temperature combined with high shear led to a higher viscosity of the paste, while high temperature and high shear resulted in fragile granules and thus lower viscosities (Nayouf et al., 2003).
The influence of physical treatment such as annealing was also studied (Eerlingen et al., 1996). Starches submitted to this type of modification swell less due to molecule rearrangement; hence in the diluted regime the non treated starches had a higher viscosity than the treated starches whereas the opposite was true in the concentrated regime. It was inferred that in the first case, i.e. diluted regime, the rheological properties were determined by the volume fraction mostly and the soluble fraction (to a lesser extent) while in the second case the system was fully filled and the properties were governed by particle rigidity. What causes shear thinning in the concentrated regime? It is thought to be due to granule reorientation in the flow, reducing their resistance to flow (Jacquier et al., 2006). Ellis & Ring (1985) determined the concentration for coil overlap for amylose to be of 0.015g/g; accordingly a solubility of amylose of 0.02g/g will greatly influence the overall rheology (Doublier et al., 1987). On the contrary, according to Genovese & Rao (2003), the continuous phase does not play a major role on the rheology of the suspension. However, it is hard to determine when the solubility of amylose or amylopectin will influence the rheology as it depends on the amount and type of polymeric material released in the continuous phase and consequently on the heating conditions and the granules themselves.

Another important matter considered in the study of flow properties of starch suspensions is **thixotropic/antithixotropic behaviour**. Thixotropic behaviour at high shears and antithixotropic at low shears were both reported for a same measurement in several studies (Genovese & Rao, 2003; Meng & Rao, 2005; Nayouf et al., 2003; Rao et al., 1997; Tattiyakul & Rao, 2000; Tecante & Doublier,

1999; Thebaudin et al., 1998; Velez-Ruiz et al., 2006). Again, this type of behaviour can differ with starch origin and thus the characteristics of the dispersed phase (Genovese & Rao, 2003; Thebaudin et al., 1998). It was suggested that thixotropic/antithixotropic behaviour depended on the swelling conditions and hence on the deformability of the granules (Doublier *et al*., 1987; Nayouf *et al*., 2003), but also on the starch concentration (Nayouf *et al*., 2003).

- Viscoelastic behaviour:

In most studies, G' and G'' were seen to be both independent on the frequency; in addition G' was higher than G'' often by at least one decade (Abdulmola et al., 1996; Eerlingen et al., 1996; Evans & Haisman, 1980; Morikawa & Nishinari, 2000; Nguyen et al., 1998; Rao et al., 1997; Rodriguez-Hernandez et al., 2006; Singh et al., 2006; Tattiyakul & Rao, 2000; Thebaudin et al., 1998). Deviation from the Cox-Merz rule confirmed the gel-like behaviour of starch suspensions above the close packing fraction (Rao et al., 1997; Tattiyakul & Rao, 2000). Above the close packing fraction, viscoelastic and gel-like properties are governed by the rigidity and deformability of the granules (Doublier et al., 1987; Thebaudin et al., 1998). Below the close packing fraction the volume fraction occupied by the granules will play a major role. It was suggested that a way to access the rigidity of a single swollen granule would be to consider the elastic modulus of a suspension with a volume fraction of 1; in these conditions, it is thought that the measured modulus would be that of the single swollen granule (Steeneken, 1989; Nayouf et al, 2003). Nevertheless, achieving a volume fraction of 1 would be quite difficult due to the solubility of starch molecules in the continuous media (Doublier et al., 1987).

Other studies suggested that the origin of gel-like behaviour is granular interactions (Evans & Haisman, 1980; Abdulmola *et al.*, 1996; Nguyen *et al.*, 1998; Singh *et al*., 2006; Rodriguez-Hernandez *et al.*, 2006): indeed, a close network of granules could allow interactions between the outer amylopectin chains of the starch particle (Nguyen *et al.*, 1998). It was later reported that starches containing a higher amount of short side chains (outer A-chains) had lower breakdown in moduli (Singh et al., 2006), confirming previous assumptions of interactions between outer chains. The influence of the amylopectin chains on granular interactions could be of importance; indeed a study on acid hydrolysed amioca starch (amylopectin chains

were debranched by acid hydrolysis) revealed a liquid-like behaviour, the moduli increasing with increasing frequency and G''>G' (Chamberlain & Rao, 2000). The interactions occurring between granules are not limited to close packing cases: network behaviour has been seen in diluted regimes. This network can be created through attractive interaction such as cohesive association giving that stringy aspect to some starch pastes (Abdulmola et al., 1996). The latter study confirmed that granule association was possible at any volume fraction level, but that these interactions remained obscure (Evans & Haisman, 1980). Again, these are general observation as it was shown that, depending on the starch origin, the viscoelastic properties as a function of the volume fraction could be slightly different (Evans & Lips, 1992). The behaviour could be separated following 3 groups: cereal starches, tuber starches (e.g. potato) and modified/cross-linked starches.

To summarize, the rheological properties of starch suspensions depend on:

- starch type,
- shear rate applied (Jacquier et al., 2006),
- granule volume fraction (Doublier et al., 1987; Jacquier et al., 2006; Rodriguez-Hernandez et al., 2006),
- pasting procedure (Doublier et al., 1987),
- starch concentration (Doublier et al., 1987),
- deformability/rigidity (swelling degree) (Doublier et al., 1987),
- size distribution of the granules (Nayouf et al., 2003),
- rheology of the continuous phase (Doublier et al., 1987),
- entanglement between adjacent granules (Abdulmola et al., 1996; Evans & Haisman, 1980; Nguyen et al., 1998).

All of these parameters are to be considered when studying starch suspension rheology.

As the rheology depends on starch origin, specific attention will be given to modified/cross-linked waxy maize starch in the following section.

II.2.3.3 The rheology of modified/cross-linked waxy maize (CLWM)

Cross-linked waxy maize starch will normally retain a granular form. Moreover, as it is a waxy variety it does not contain amylose; hence little of polysaccharide is released from the granule. However, even in cross-linked starch a small polymeric fraction can be released into the continuous medium (Tecante & Doublier, 1999).

Dilatancy of the cross-linked waxy maize starch paste was observed (Rao *et al.*, 1997; Tattyakul & Rao, 2000) but this tendency decreased with increasing granule swelling (Rao *et al.*, 1997). Tattyakul & Rao (2000) suggested that dilatancy was due to large amounts of amylopectin in the continuous phase forming shear induced networks.

Studies on cross-linked waxy maize also reported thixotropic behaviour at high shear rates and antithixotropic behaviour at low shear (Genovese & Rao, 2003; Nayouf *et al.*, 2003; Rao *et al.*, 1997; Tattyakul & Rao, 2000; Tecante & Doublier, 1999; Velez-Ruiz *et al.*, 2006). It was suggested that antithixotropy was either due to rearrangement of starch granules enhanced by shearing (Nayouf et al., 2003; Velez-Ruiz et al., 2006) or to leached out amylopectin from ruptured granules creating a more structured shear induced paste than the initial one (Tattiyakul & Rao, 2000). However, the latter hypothesis seems quite unlikely as the starch is modified to maintain granule integrity when submitted to severe pasting treatments (high shear, high temperature); consequently, no granule rupture should occur. Finally, the viscoelastic properties indicate a gel like behaviour (G'>G'' and independent of the frequency) although it is not a gel (Abdulmola *et al.*, 1996; Rao *et al.*, 1997; Tecante & Doublier, 1999). It was reported that for a specific frequency, a sharp increase of tan δ (= G''/G') could be observed (Tecante & Doublier, 1999). It was thought that it could be the boundary between the elastic response given by the granule and the viscous response of the aqueous phase. These observations found in literature can also be seen for other starches but differ slightly in as much as conditions such as close-packing fraction, swelling and granule deformability will be different for other starches (Evans & Lips, 1992).

II.2.4. Conclusions

The amount of published information on starch is enormous. Throughout this review, the multiple aspects and infinite possibilities offered by starch have been outlined. Although many advances were made in the starch domain (the granule itself, starch rheology), some questions remained unanswered, such as the location of amylose in the starch granule and granular interactions for example. The structure of this versatile biopolymer depends on the starch type and on the maturation conditions. Subsequently, the gelatinisation process will be different from one starch to another. As the rheology is a function of granule deformability and hence the pasting procedure, it is necessary to know the characteristics of the starch studied to understand its behaviour under flow and to study droplet break-up.

II.3 Droplet deformation

When a droplet is submitted to shear it either deforms until it reaches a state where it no longer evolves (steady state) or it breaks up if the shear applied is higher than a critical value. The droplet may break-up into two or more droplets and the mechanisms are different (end-pinching, Rayleigh instabilities, etc). The study of multiphase systems, such as an isolated droplet in an immiscible matrix has been the subject of numerous experimental, theoretical and numerical publications. Many papers have tackled the issue and the theories that have been developed were successfully verified experimentally and numericaly.

Different cases can be found, depending on the rheological characteristics of the dispersed and continuous phases. The most studied one is the fully Newtonian system where both the dispersed phase and the suspending fluid are Newtonian. However, in many practical cases, at least one phase, if not both, is non-Newtonian (shear thinning, viscoelastic). In these reported cases the droplet is a solution but it is possible to imagine similar situations when the droplet is a suspension in a fluid matrix. In the following literature review, the theories and models developed for Newtonian and non-Newtonian systems will be presented. Attention will be given to the droplet deformation depending on its rheological behaviour and that of the matrix. An overview of the publication on a system where the dropolet is a suspension of particles will also be given (Smith & Van de Ven, 1985).

II.3.1 A few definitions and models

Research on the flow behaviour of two-phase systems (dispersed droplets in continuous phase) has led to the observation of droplet behaviour under shear flow. When a droplet is immersed in an immiscible liquid it adopts a spherical shape; when a flow is applied the droplet will deform. The drop in the suspending matrix will be submitted to a force balance between the viscous forces that deform the droplet and the interfacial forces that will tend to keep the droplet spherical. If the interfacial forces are overcome, the droplet will break up.

In the following case simple shear flow will be considered.

Simple shear flow is defined as a rotational flow with:

$u = \dot{\gamma} y$; $v = 0$; $w = 0$;

where u, v, w are the velocity components along the X, Y and Z axes respectively (Figure 2.6) and $\dot{\gamma}$ the shear rate.

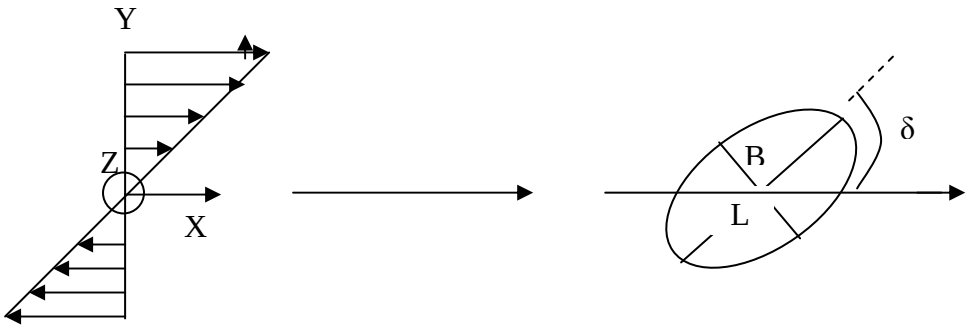

Figure 2.6: Rotational shear flow applied to a droplet (from Rumscheidt & Mason, 1961). Where L is the length of the droplet (large axis of the ellipsoid), B the breadth of the droplet (first small ellipsoid axis) and δ the orientation angle of the drop. W, which can not be seen here, is the second small axis in the vorticity direction (Z axis).

The first to tackle the issue of droplet deformation in an emulsion was Taylor (1932; 1934). He defined two dimensionless numbers for Newtonian systems, i.e. when both the droplet and the continuous phase are Newtonian: the viscosity ratio p and the Capillary number Ca. The value p is the ratio of the viscosity of the droplet (η_d) to the viscosity of the matrix (η_m) and is shown Equation 2.3.

$$p = \frac{\eta_d}{\eta_m} \qquad 2.3$$

The Capillary number (Equation 2.4) represents the ratio of the viscous forces (that tend to deform the droplet) to the forces that maintain the droplet spherical (minimise droplet surface).

$$Ca = \frac{\eta_m \dot{\gamma}}{\Gamma / R_0} \qquad 2.4$$

where $\dot{\gamma}$ the applied shear rate, Γ the interfacial tension and R_0 the radius of the undeformed droplet.

Taylor also defined the deformation of the droplet as (Equation 2.5):

$$D_{Taylor}=\frac{L-B}{L+B} \qquad 2.5$$

where L is the length of the droplet and B is the small axis in the flow gradient gradient direction. This relation is applicable for all deformed droplets, although at large deformations all D_{Taylor} values asymptotically approach unity 1 (Bentley & Leal, 1986). Taylor's model (2.6) states that the deformation of an isolated droplet in the small deformation limit (D_{Taylor} <0.2) is equal to the Capillary number.

$$D_{Taylor}=D=Ca \qquad 2.6$$

When the Ca = 0 the resulting deformation is D= 0 and the droplet is spherical. Deformation occurs (D_{Taylor} increases) when the shear rate increases and hence the Capillary number.

Further work on droplet deformation and conditions for break-up will be summarized in the following section.

II.3.2 Newtonian systems

Cox (1969) developed a model for a Newtonian droplet in a Newtonian matrix that describes the deformation by relating the dimensionless terms p (viscosity ratio) and Ca (Capillary number)(Equation 2.7).

$$\frac{L-B}{L+B}=\frac{5(19p+16)}{4(1+p)\sqrt{(20/Ca)^2+(19p)^2}} \qquad 2.7$$

Equation 2.7 is valid only if the resulting deformation is small (D<0.2); in this case p needs to be very large or Ca very small or both conditions fulfilled. Cox's model meets Taylor's theory if p tends towards 0. Equation 2.7 was verified experimentally by Torza et al. (1972), and was found to well describe deformation.

Later, Maffettone & Minale (1998) developed a phenomenological model (referred to as the MM model) for a fully Newtonian system. For small deformations it is assumed that the droplet is ellipsoidal at all times and that the interfacial drag forces are additive. The steady-state values of the three ellipsoid dimensions are presented below (Equations 2.8 and 2.9); W is the length of the second ellipsoid axis in the vorticity direction:

$$L^2 = \frac{f_1{}^2 + Ca^2 + f_2 Ca\sqrt{f_1{}^2 + Ca^2}}{(f_1{}^2 + Ca^2)^{1/3}(f_1{}^2 + Ca^2 - f_2{}^2 Ca^2)^{2/3}}$$

$$B^2 = \frac{f_1{}^2 + Ca^2 - f_2 Ca\sqrt{f_1{}^2 + Ca^2}}{(f_1{}^2 + Ca^2)^{1/3}(f_1{}^2 + Ca^2 - f_2{}^2 Ca^2)^{2/3}} \qquad 2.8$$

$$W^2 = \frac{f_1{}^2 + Ca^2 - f_2{}^2 Ca^2}{(f_1{}^2 + Ca^2)^{1/3}(f_1{}^2 + Ca^2 - f_2{}^2 Ca^2)^{2/3}}$$

with

$$f_1 = \frac{40(p+1)}{(2p+3)(19p+16)}$$

2.9

$$f_2 = \frac{5}{2p+3} + \left(\frac{3Ca^2}{2+6Ca^2}\right)$$

The term in f_2 between brackets in the equation 2.9 was added to improve the predictions at high viscosity ratios and high capillary numbers. The model is no longer valid if the deformation is too large and the droplet no longer ellipsoidal.

At first the droplet is spherical; it then deforms following the models described above. However, if a higher shear is applied, the drop continues to stretch and is no longer ellipsoidal. The droplet deforms above its steady-state value and finally breaks up. The critical value for which break-up occurs is called the critical capillary number (Ca*). It is determined by finding a critical shear rate at which an observed drop deforms until rupture occurs, in the case of a time-dependent increase of the shear rate. Rumscheidt & Mason (1961) determined four categories of deformation and break-up depending on the viscosity ratio p (Figure 2.7).

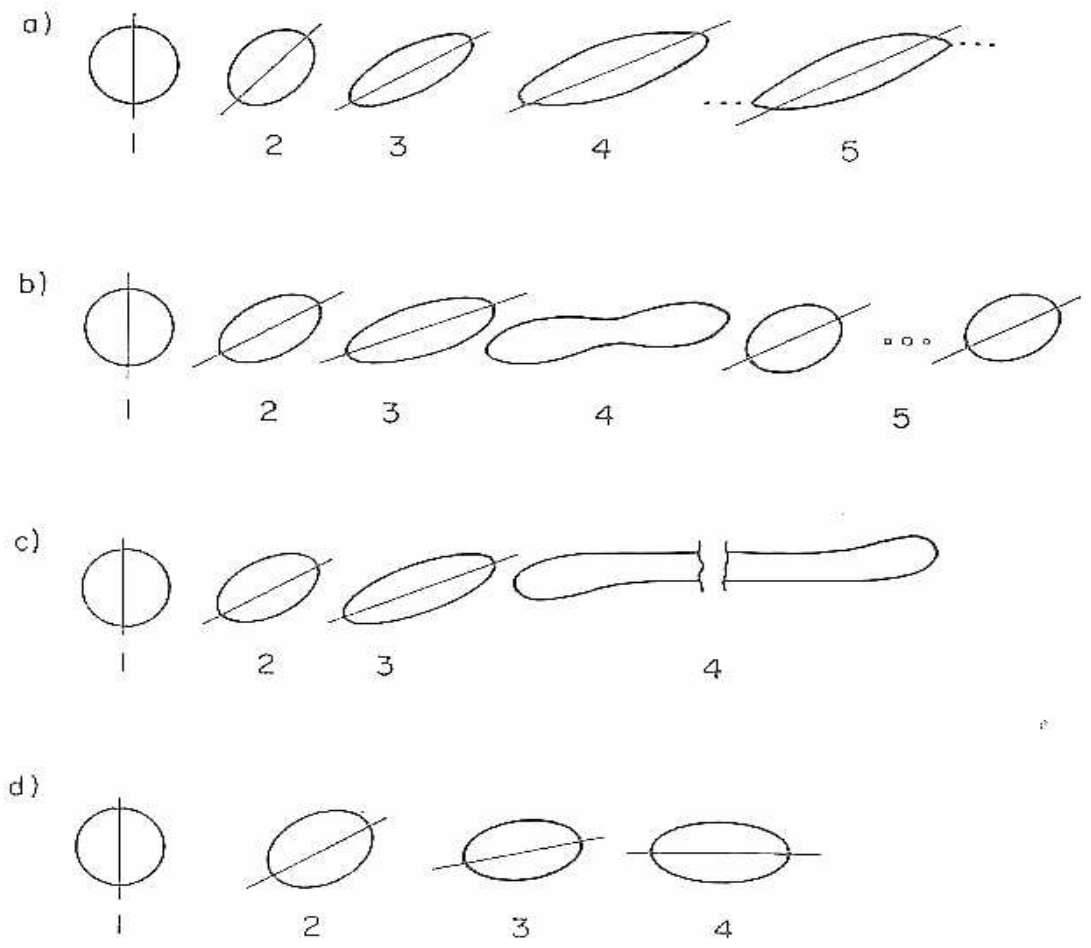

Figure 2.7: Main deformation modes of a droplet submitted to a simple shear flow (Rumscheidt & Mason, 1961, copied with authorisation of Elsevier). (a) p = 2*10^-4; (b) p = 1; (c) p = 0.7; (d) p = 6

Figure 2.7 shows the four classes of deformation and break-up. In all cases when no shear is applied the droplet is spherical. Upon shear the droplet deforms in an ellipsoidal shape when the deformation is small; as the shear rate is increased, differences in break-up can be observed:

(a) Deformation class-A, low p: for a shear rate>critical shear rate the droplet adopts a sigmoidal shape with pointed ends, from which small droplets are detached. This phenomenon is called tip-streaming.

(b) Deformation class-B1, p = 1: above the critical capillary number, the droplet forms a neck that disintegrates in three satellite droplet while the initial drop breaks up into two daughter droplets.

(c) Deformation class-B2, p = 0.7: Ca>Ca*, the drop is drawn into a cylindrical thread which breaks-up into many smaller droplets.

(d) Deformation class-C, p > 4: no rupture is observed.

When the drop is deformed it adopts an orientation in the shear flow gradient axis with a certain angle δ (Figure 2.7). This angle depends on the shear rate and the viscosity ratio p (Table 2.1). The angle formed between the major axis of the ellipse and the flow direction (X axis) at the start of the shear rate is 45°. It has been shown that the higher the shear rate, the smaller the orientation angle i.e. the droplet tends to orient in the flow direction (Rumscheidt & Mason, 1961).

Table 2.1: Effect of deformation on orientation angle (Adapted from Rumscheidt & Mason, 1961)

	p	D_{Taylor}	δ (°)
Class A	2.10^{-4}	0.01-0.4 0.54	45-30 25
Class B (B_1 & B_2)	1	0.1 0.2-0.58	45 30-15
Class C	17	0.29	0

The orientation angle can be calculated using Cerf's (1951) equation (2.10) later corrected by Rumscheidt and Mason (1961), knowing the deformation

parameter and p. Good agreement was found between measurements at small viscosity ratios and the equation of Cerf (see, e.g. Rumscheidt & Mason, 1961).

$$\delta = \frac{\pi}{4} - D_{Taylor}\left(\frac{2p+3}{5}\right) \qquad 2.10$$

In his study on immiscible fluid systems, Grace (1982) found through experimental data that the critical Capillary number Ca* is a function of p (Figure 2.7), giving further information on the break-up conditions. This curve, determined for Newtonian systems was later fitted by De Bruijn (1989). It can be seen from Figure 2.7 that Ca* varies with the viscosity ratio, i.e. the drop will break up more or less easily depending on p if keeping constant all the other parameters (interfacial tension and droplet initial radius).

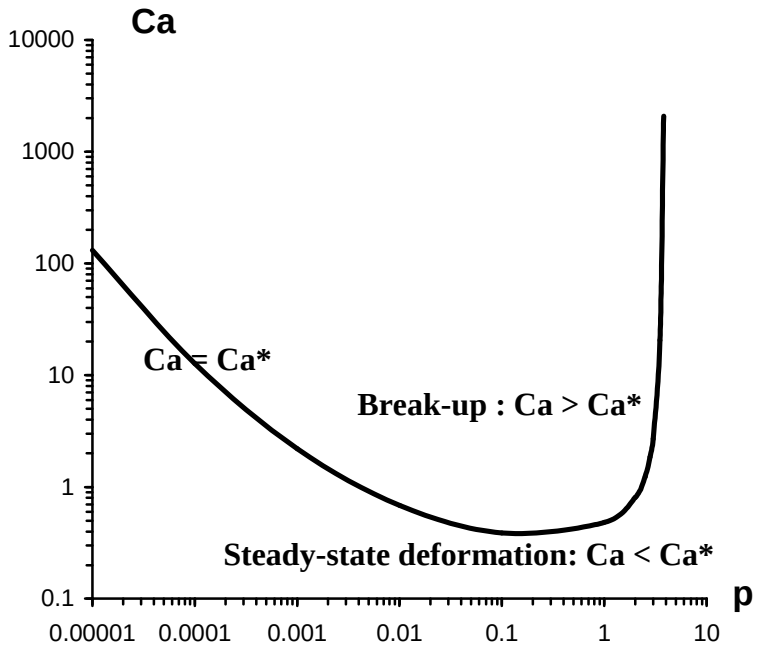

Figure 2.8: Effect of viscosity ratio on Ca* as determined by Grace (1982) and fitted by De Bruijn (1989).

For very low values of p, it is hard to break-up the droplet and it is most likely that it will undergo deformation. For example, at p = 1.10^{-5}, a capillary number of a 100 would have to be reached to induce break-up. Figure 2.8 also shows that it is easier to break up the droplet if p values are between 0.1 and 1: Ca*

≈ 0.5. Above a p value of 3.5-4 it is impossible to break-up the droplet; it confirms the findings by Rumscheidt and Mason (1961) who did not report rupture for high viscosity ratios. This type of curve can be obtained by increasing the shear rate stepwise, after reaching steady state for the previous step. The break-up mentioned above corresponds to the fracture of the main drop into two or more droplets. However, another break-up mechanism of the drop may occur, when p is low (<0.1) and Ca* ≈ 0.5, and is called tip streaming (Taylor, 1934; Rumscheidt & Mason, 1961; Grace, 1982; De Bruijn, 1989). The drop adopts a sigmoidal shape and a stream of very small droplets are detached from the tips (See Figure 2.7a). It was suggested that tip streaming was due to interfacial tension gradients at the surface of the droplet, resulting in lower interfacial tension at the tips (De Bruijn, 1993). Later studies on the effect of surfactant on drop deformation showed that the latter was enhanced by the presence of surfactants for values of viscosity ratio between 0.3 and 3.3. For high p values (p =30), the effect was much less pronounced. In both cases the droplet aligned in the flow direction, inducing smaller orientation angles (Bazhekov et al., 2006; Feigl et al., 2007).

Bentley & Leal (1986) and Stone & Leal (1989) worked on the effect of step changes in flow; they put into light a different break-up mechanism upon cessation of flow. When a droplet is extended above a critical deformation and the flow is abruptly stopped, it starts retracting to its initial state but then starts to fragment into smaller droplets. What can be visualised is that the ends of the drop become rounded and pinch off. This end-pinching is due to interfacial tension driving the drop to return to a spherical shape.

Cristini et al. (2003) have been interested in the size distribution of the drop fragments after break-up. The primary break-up produces two daughter droplets, similar in size to the critical size drop (where no more break-up of the droplet can occur) and independent of the initial droplet size. The secondary break-up occurs by end-pinching or capillary instabilities forming satellite drops. Their size is determined by the width of the neck after primary break-up. They concluded that for a given system the size distribution in diluted emulsions depends only on the average initial droplet size and the shear rate. On the other hand, a study by Lin & Guo (2007) showed that the diameter of daughter drops was linearly correlated to the inverse of the shear rate but was independent of the initial drop size. They also demonstrated that three break-up mechanisms could occur depending on the

capillary number. If Ca~Ca*, break-up mechanism is necking, thus producing daughter droplets of equal size, separated by satellite drops. For Ca* < Ca< 2Ca* end pinching preferentially occurs while the dominant break-up for Ca > 2 Ca* is capillary instabilities. Similar results were found by Zhao (2007) who studied the break-up mechanism and the final drop size distribution, the latter depending on the capillary number and the viscosity ratio; his results are summarized Figure 2.9.

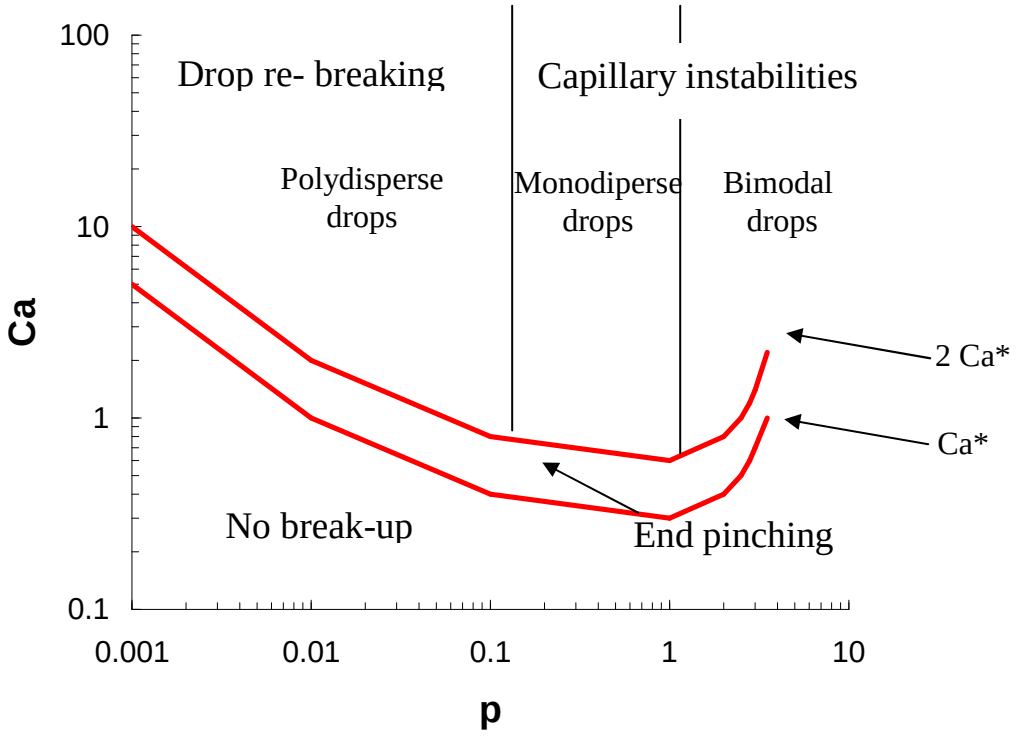

Figure 2.9: Drop break-up mechanism as a function of p and Ca (From Zhao, 2007).

This study unravels new evidence on droplet break-up, however these results should be considered with care as the droplets might have been submitted to wall effects promoting deformation (the ratio of the droplet diameter to the gap varies from 0.1 to 0.7, to prevent wall effects it should be 0.1). Recent studies (Cristini et al., 2003; Vananroye et al., 2006a; Vananroye et al., 2006b) have shown that confinement enhanced deformation and orientation in the flow direction; interestingly, it was possible to break-up droplets with high viscosity ratios (p>3.5). Confinement for p>1 decreased critical capillary number values, and hence eased break-up whereas for p< 1 Ca* increased. Sibillo et al. (2006) found similar results for p = 1; they showed that confinement, although it enhanced deformation, hampered break-up due to the closing of streamlines.

Deformation and break-up mechanism is a complicated issue and many models have been developed. These numerous studies have been extensively reviewed by Rallison (1984), Stone (1994) and Tucker & Moldenaers (2002).
The studies on deformation and break-up of Newtonian droplets in a Newtonian matrix have led to models that have proven efficient in predicting the drop behaviour. Nevertheless, in reality, most systems are not Newtonian; the dispersed or the continuous phase or both can be viscoelastic. The results obtained for these types of systems will be discussed in the section below.

II.3.3 Non- Newtonian systems

The very first attempt to study the behaviour of a Newtonian drop in a **viscoselastic matrix** in a Poiseuille flow was carried out by Gauthier et al., (1971) but they did not conclude on droplet deformation.
Flumerfelt (1972) measured deformation and break-up for a Newtonian droplet in a viscoselastic matrix. He found that the stresses required to break-up a drop in a viscoselastic fluid were lower than those necessary for a fully Newtonian system under similar conditions (same viscosity ratio, same stresses applied). Deformation of the droplets seemed to be enhanced by matrix elasticity (Elmendorp & Maalcke, 1985; Mighri et al., 1998). In fact, Elmendorp & Maalcke (1985) showed that a shear thinning matrix led to a more stable drop than Newtonian ones but when normal stress values increased the droplet was destabilised, leading to earlier break-up when compared to fully Newtonian systems. Although this study gave new insight on the influence of matrix elasticity, it did not allow a full understanding of the effect of elasticity and shear thinning of the matrix on the deformation of a Newtonian drop.

A further study by Sibillo et al. (2005) determined that elasticity of the matrix inhibits the drop deformation as compared to a similar Newtonian system (same p). The droplet is also reported to orient more in the flow direction than in Newtonian systems, i.e. smaller orientation angles result (Guido et al., 2003; Sibillo et al., 2006). It is thought that droplet orientation is directly linked to the normal stresses of the matrix fluid.

De Bruijn (1989) studied extensively the behaviour of **viscoelastic droplets** under shear, taking care of separating the contribution of shear thinning fluids, with no measured elasticity, as opposed to purely elastic fluids(Boger fluids). He showed that in the case of shear thinning drops, for $p<0.1$, the critical capillary number could be correlated to the break-up criterion determined for Newtonian fluids. Critical capillary numbers started deviating from those repoted for Newtonian systems for $p \geq 1$, and continued to increase with increasing viscosity ratio.

To study the effect of elasticity in droplet behaviour, De Bruijn (1989) used Boger fluids, i.e. fluids for which the viscosity does not depend on the shear rate but normal stresses can be measured. Many following studies used the same type of fluid (Lerdwijitjarud et al., 2004; Mighri et al., 1998; Milliken & Leal, 1991; Sibillo et al., 2005; Tsakalos et al., 1998; Varanasi et al., 1994). De Bruijn (1989) reported that drop elasticity resulted in higher critical capillary numbers, namely that it is harder to break up an elastic drop in a Newtonian matrix than a Newtonian drop in similar conditions. Most studies agree with the inhibition of the drop deformation and resistance to break-up caused by the droplet elasticity when compared to fully Newtonian systems (Mighri et al., 1998; Sibillo et al., 2005; Tsakalos et al., 1998; Varanasi et al., 1994). These studies concluded that the steady state Capillary number increases with the first normal stress difference of the dispersed phase. Sibillo et al. (2005) showed that no deviation from Newtonian droplet behaviour could be observed for small deformation and therefore the small deformation limit can be used to derive interfacial tension independently of the viscoelasticity of one or the other phase. For higher Capillary numbers, the droplets display a less deformed aspect and a smaller orientation angle than for the case of Newtonian droplets, confirming mathematical predictions (Greco, 2002). Sibillo et al. (2005) also reported an overshoot of the deformation before reaching its steady state.
In some cases, break-up in the vorticity axis was reported for Boger fluid drops (Li and Sundararaj, 2008). This type of behaviour is more often reported when both phases are viscoelastic.

Deformation and break-up when **both phases are viscoelastic** have been studied mainly to understand the morphology of polymer blends. It was reported that the deformation of a drop in such systems depends mainly on the elasticity

ratio, i.e. the ratio of the elasticity of the droplet to the elasticity of the matrix which correponds to the ratio of the first normal stress differences (Mighri et al., 1998). When this ratio is low (<0.37) and consequently the elasticity of the matrix is high, the droplet deformation is higher than that observed for Newtonian systems. On the other hand, when the droplet is highly elastic (elastic ratio >0.37) deformation is inhibited. This result is to be expected considering the observations mentioned in the previous sections. A more unusual deformation mechanism was observed consisting of a widening of the drop perpendicular to the flow, in the vorticity axis (Levitt & Macosko, 1996; Tanpaiboonkul et al., 2007). Levitt & Macosko (1996) were the first ones to report this phenomenon; they found an analytical relation between the second normal stress difference of the phases and the degree of widening. Tanpaiboonkul et al. (2007) divided the evolution in time of droplet deformation into three distinct sections. The first consists in an elongation of the droplet in the flow direction followed by a contraction, a secondary flow elongation and finally a widening along the vorticity direction. It seems that a strong enough elasticity of the droplet and/or matrix can hinder the break-up along the flow direction leading to break-up along the vorticity axis. The latter can be deferred to much higher capillary numbers than those observed in the flow axis. Finally a later study showed that this type of behaviour depended on the droplet size (Li and Sundararaj, 2008). The primary break-up occurred in the flow direction but the obtained daughter droplet broke up in the vorticity direction following an erosion break-up mechanism.

Ghodgaonkar & Sundararaj (1996) developed a model of the dispersed drop diameter in polymer blends, based on the balance between the viscous forces that deform the drop and the forces that resist deformation when the droplet is at equilibrium (Equation 2.11). Equation 2.11 is based on the capillary number. In this case, two new parameters, matrix and droplet elasticity were added. The first which is part of the forces that induce deformation (viscous forces) whereas the latter is added to the interfacial forces.

$$\eta_m \dot{\gamma} + 2G'_m \propto 2\Gamma/D + 2G'_d \qquad 2.11$$

where G' is the elastic modulus. Here G' can be used, as at low shear rates ($<10s^{-1}$) the first normal stress difference can be approximated by 2G'. Above $10s^{-1}$ the first normal stress difference is higher than 2G' but the quantities are proportional to each other.

In the case of swollen polyelectrolyte particles, a widening and release of solvent in the vorticity direction was observed when the complex modulus of the matrix became larger than the shear modulus of the swollen gel (Vervoort & Budtova, 2005).

Finally, break-up for viscosity ratios higher than 3.5 was observed in polymer blends (Lin et al., 2003). The droplet first formed a sheet along the flow direction which then ruptured into smaller daughter droplets along the flow direction; it was referred to as the "parallel break-up".

II.3.4 When the dispersed droplet is a suspension

Whereas literature is abundant on systems where both phases are liquid, what happens in systems where the droplet is a suspension in a continuous liquid phase has been rarely studied. To our best knowledge, only one paper treats this subject and does so in a qualitative way (Smith & Vandeven, 1985). They studied droplets of polystyrene beads dispersed in water; the particulate system was then suspended in silicon oil. The influence of the volume fraction of the beads on deformation and break-up was evaluated using a Couette counter rotating apparatus. When the drop contained only a few spheres, the deformation at low shear rates remained quasi unchanged compared to that of water. The spheres circulated within the drop as the shear rate increased disturbing the flow patterns, and finally concentrated at the two ends of the drop. After a while, spheres were detached from the main droplet taking along with them a small amount of surrounding water; rupture occurred through an "end-pinching" mechanism. When the shear rate was increased, all the spheres ultimately came out of the drop leaving only the dispersing media, in this case the water, which did not break up under these conditions. Smith and Van de Ven (1985) also observed droplets with higher sphere volume fractions (10% to 50%). At a volume fraction of 10% they saw that there was significant rearrangement of the

spheres leading to break-up resembling the B1 classification described by Rumscheidt & Mason (1961). A further increase of the volume fraction (20%) led the droplet to deform into a thread following a B2 classification mode. For a 50% volume fraction the system no longer resembled a droplet at zero-shear but appeared as an aggregate. Individual spheres or small aggregates could be detached under shear. To summarize, Smith and Van de Ven (1985) found that an increase in volume fraction showed similarities with an increase in viscosity for fluid droplets when considering their behaviour under flow. The authors in this paper did not quantify break-up, only observations were made as they noticed that this phenomenon was triggered by random particle rearrangements. They also noted that the capillary number required to break up systems with a relatively high volume fraction were below the ones observed for fluid droplets; at high volume fraction the particles are in close contact leading to smaller liquid bridge volumes. Nevertheless, it is important to note that the rheology of the dispersed phase (water+spheres) was not considered.

II.3.5. Conclusions on droplet deformation and break-up

Droplet deformation and break-up in Newtonian/Newtonian systems have been extensively studied and various models have been found to determine droplet shape and behaviour. Many of those can be applied to viscoelastic systems through various modifications and adjustments. Nonetheless, deformation and break-up of a droplet remain a complicated matter as they depend on the type of system (Newtonian or viscoelastic), the presence of surfactants, confinement and the shear rate. This literature review on droplet deformation and break-up also emphasises the lack of studies for systems where the drop is a suspension rather than a liquid or a solution.

II.4. Conclusions for Chapter 2

The literature review covered a wide range of notions from flavour perception to droplet deformation, showing the multiple aspects of this study.

General notions on flavour perception and the latest research that led to this project were given in the first part. Understanding of flavour perception has many aspects; one that can be considered is the relation between viscosity and tastant release in the mouth. The latter was suggested to be correlated to the microstructure of the product, suspension thickened products leading to better in-mouth properties as opposed to polymer solution thickeners.

Suspensions leading to better flavour perception and mouthfeel can be obtained with some starches and thus, this biopolymer was the focus of the second part. A general review on starch revealed its numerous origins and subsequently the multiple properties of each starch. A general picture with common features was drawn, showing the complex structure of alternating rings of crystalline and amorphous zones. The specificity of starch is its ability to swell in heated water, increasing the viscosity and is therefore used in the food industry as thickening agents. Swelling was seen to depend on the starch structure, on heating and shearing process, leading once again to multiple paste properties. The variation in starch suspensions and their rheology can be considered as a wide field of study and many questions such as the influence of granular interactions remain obscure. Preparation conditions of the starch suspension need to be known to understand the flow behaviour.

Rheological characterisation is an important feature to study the deformation and break-up of droplets in a suspending matrix. The third part of this literature review was focused on the theories developed and the observation made for such systems. Fully Newtonian systems are quite well understood and good advances have been made for cases where both phases are fluids but one or both are viscoelastic. However, the lack of information concerning systems where one phase is a suspension is highlighted.

In this PhD work, droplets of starch suspension in an immiscible fluid were studied to determine if conditions found for Newtonian and viscoelastic systems apply. The break-up was quantified using models determined for fluid droplets.

Prior to the study of droplet break-up behaviour, the starch granules and suspension was characterised.

Reference List

Abdulmola, N. A., Hember, M. W. N., Richardson, R. K., and Morris, E. R. (1996). Effect of xanthan on the small-deformation rheology of crosslinked and uncrosslinked waxy maize starch. *Carbohydrate Polymers*, 31, 65-78.

Atkin, N. J., Abeysekera, R. M., Cheng, S. L., and Robards, A. W. (1998). An experimentally-based predictive model for the separation of amylopectin subunits during starch gelatinization. *Carbohydrate Polymers*, 36, 173-192.

Atkin, N. J., Cheng, S. L., Abeysekera, R. M., and Robards, A. W. (1999). Localisation of amylose and amylopectin in starch granules using enzyme-gold labelling. *Starch-Starke*, 51, 163-172.

Bagley, E. B. and Christianson, D. D. (1982). Swelling capacity of starch and its relationship to suspension viscosity effect of cooking time, temperature and concentration. *Journal of Texture Studies*, 13, 115-126.

Baines, Z. V. and Morris E.R. (1988). effects of polysaccharide thickeners on organoleptic attributes., 4, 192-201.

Baines, Z. V. and Morris, E. R. (1987). Flavour/Taste<perception in thickened systems: the effect of guar gum above and below C*. *Food Hydrocolloids*, 3, 197-205.

Banks, W., Greenwood, C.T. In 'Starch and its components', Edinburgh University Press, Edinburgh, 1975, p 67-112.

Bayarri, S., Rivas, L., and Izquierdo, L. C. E. (2007). Influence of texture on the temporal perception of sweetness of gelled systems. *Food Research International*, 40, 900-908.

Bazhekov, I. B., Anderson, P. D., and Meijer, H. E. H. (2006). Numerical investigation of the effect of insoluble surfactants on drop deformation and breakup in simple shear flow. *Journal of Colloid and Interface Science*, 298, 369-394.

Bentley, B. J. and Leal, L. G. (1986). An Experimental Investigation of Drop Deformation and Breakup in Steady, Two-Dimensional Linear Flows. *Journal of Fluid Mechanics*, 167, 241-283.

Blanshard, J. M. V. (1987). Granule Structure and Function., 13, 16-54.

Cerf-Duscastel, B. and Murphy, C. (2001). fMRI Activation in Response to Odorants Orally Delivered in Aqueous. *Chemical Senses*, 26, 625-637.

Chamberlain, E. K. and Rao, M. A. (2000). Effect of concentraiton on rheological properties of acid-hydrolyzed amylopectin solutions. *Food Hydrocolloids*, 14, 163-171.

Cheetham, N. W. H. and Tao, L. (1998). Solide state NMR studies on the structural and conformational properties of natural maize starches. *Carbohydrate Polymers*, 36, 285-292.

Chiotelli, E., Pilosio, G., and Le Meste, M. (2002). Effect of sodium chloride on the gelatinization of starch: A multi measurement study. *Biopolymers*, 63, 41-58.

Connelly, R. K. and Kokini, J. L. (2004). The effect of shear thinning and differential viscoelasticity on mixing ina model 2D as determined using FEM with particle tracking. *Journal of Non-Newtonian Fluid Mechanics*, 123, 1-17.

Cook, D. J., Hollowood, T. A., Linforth, R. S. T., and Taylor, A. J. (2002). Perception of taste intensity in solutions of random-coil polysaccharides above and below c. *Food Quality and Preference*, 13, 473-480.

Cook, D. J., Hollowood, T. A., Linforth, R. S. T., and Taylor, A. J. (2003). Oral shear stress predicts flavour perception in viscous solutions. *Chemical Senses*, 28, 11-23.

Cox, R. G. (1969). Deformation of A Drop in A General Time-Dependent Fluid Flow. *Journal of Fluid Mechanics*, 37, 601.

Cristini, V., Guido, S., Alfani, A., Blawzdziewicz, J., and Loewenberg, M. (2003). Drop breakup and fragment size distribution in shear flow. *Journal of Rheology*, 47, 1283-1298.

De Bruijn R.A. (1989). Deformation and Breakup of drops in simple shear flow. Ph.D. thesis, Wagenigen, University.

De Bruijn, R. A. (1993). Tipstreaming of Drops in Simple Shear Flows. *Chemical Engineering Science*, 48, 277-284.

De Roos, K. B. (2003). Effect of texture and microstructure flavour retention and release. *International Dairy Journal*, 13, 593-605.

Doublier, J. L. (1986). A rheological comparison of Wheat, Maize, Faba bean and smooth pea starches. *Journal of Cereal Science*, 5, 247-262.

Doublier, J. L., Llamas, G., and Lemeur, M. (1987). A Rheological Investigation of Cereal Starch Pastes and Gels - Effect of Pasting Procedures. *Carbohydrate Polymers*, 7, 251-275.

Eerlingen R.C, Jacabs H., Block K., and Delcour J.A (1996). Effect of hydrothermal treatments on the rheological properties of potato starch. *Carbohydrate Research*, 297, 347-356.

Ellis, H. S. and Ring, S. G. (1985). A study of some factors influencing Amylose gelation. *Carbohydrate Polymers*, 53, 201-213.

Elmendorp, J. J. and Maalcke, R. J. (1985). A Study on Polymer Blending Microrheology .1. *Polymer Engineering and Science*, 25, 1041-1047.

Evans, I. D. and Haisman, D. R. (1980). Rheology of Gelatinized Starch Suspensions. *Journal of Texture Studies*, 10, 347-370.

Evans, I. D. and Lips, A. (1992). Viscoelasticity of Gelatinized Starch Dispersions. *Journal of Texture Studies*, 23, 69-86.

Feigl, K., Megias-Alguacil, D., Fischer, P., and Windhab, E. J. (2007). Simulation and experiments of droplet deformation and orientation in simple shear flow with surfactants. *Chemical Engineering Science*, 62, 3242-3258.

Ferry, A. L., Hort, J., Mitchell, J. R., Cook, D. J., Lagarrigue, S., and Pamies, B. V. (2006). Viscosity and flavour perception: Why is starch different from hydrocolloids? *Food Hydrocolloids*, 20, 855-862.

Fischer L.R, Carrington S.P, and Odell J.A (1997). Deformation Mechanics of individual swollen starch granules., 105-114.

Flumerfelt, R. W. (1972). Drop Breakup in Simple Shear Fields of Viscoelastic Fluids. *Ind.Eng.Chem.Fundam.*, 11, 312-318.

Frith, W. J. and Lips, A. (1995). The Rheology of Concentrated Suspensions of Deformable Particles. *Advances in Colloid and Interface Science*, 61, 161-189.

Gallant, D. J., Bouchet, B., and Baldwin, P. M. (1997). Microscopy of starch: evidence of a new level of granule organization. *Carbohydrate Polymers*, 32, 177-191.

Gauthier F, Goldsmith H., and Mason S.G (1971). Particle Motions in non-newtonian media. II. Poiseuille flow. *Transactions of the society of rheology*, 15, 297-330.

Genovese, D. B. and Rao, M. A. (2003). Role of starch granule characteristics (volume fraction, rigidity, and fractal dimension) on rheology of starch dispersions with and without amylose. *Cereal Chemistry*, 80, 350-355.

Ghodgaonkar, P. G. and Sundararaj, U. (1996). Prediction of dispersed phase drop diameter in polymer blends: The effect of elasticity. *Polymer Engineering and Science*, 36, 1656-1665.

Gidley, M. J. and Bociek, S. M. (1985). Molecular orgainization in Starches: A ^{13}C CP/MAS NMR study. *Journal of American Chem.Soc.*, 107, 7040-7044.

Grace, H. P. (1982). Dispersion Phenomena in High-Viscosity Immiscible Fluid Systems and Application of Static Mixers As Dispersion Devices in Such Systems. *Chemical Engineering Communications*, 14, 225-277.

Greco, F. (2002). Drop deformation for non-Newtonian fluids in slow flows. *Journal of Non-Newtonian Fluid Mechanics*, 107, 111-131.

Guido, S., Simeone, M., and Greco, F. (2003). Effects of matrix viscoelasticity on drop deformation in dilute polymer blends under slow shear flow. *Polymer*, 44, 467-471.

Han, X. Z. and Hamaker, B. R. (2001). Amylopectin fine structure and rice starch paste breakdown. *Journal of Cereal Science*, 34, 279-284.

Imberty, A., Buleon, A., Tran, V., and Perez, S. (1991). Recent advances in knowledge of starch structure. *Starch/Stärke*, 43, 375-384.

Jacquier, J. C., Kar, A., Lyng, J. G., Morgan, D. J., and McKenna, B. M. (2006). Influence of granule size on the flow behaviour of heated rice starch dispersions in excess water. *Carbohydrate Polymers*, 66, 425-434.

Jane, J., Xu, A., Radosavljevic, M., and Seib, P. A. (1992). Location of Amylose in Normal Starch Granules .1. Susceptibility of Amylose and Amylopectin to Cross-Linking Reagents. *Cereal Chemistry*, 69, 405-409.

Jane, J. L. and Shen, J. J. (1993). Internal Structure of the Potato Starch Granule Revealed by Chemical Gelatinization. *Carbohydrate Research*, 247, 279-290.

Jenkins, P. J. and Donald, A. M. (1995). The influence of amylose on starch granule structure. *International Journal of Biological Macromolecules*, 17, 315-321.

Jouquand, C., Ducruet, V., and Giampaoli, P. (2004). Partition coefficient of aroma compounds in polysaccharide solutions by the phase ratio variation method. *Food Chemistry*, 85, 467-474.

Jouquand, C., Ducruet, V., and Le Bail, P. (2006). Formation of amylose complexes with C6-aroma compounds in starch dispersions and its impact on retention. *Food Chemistry*, 96, 461-470.

Karapantsios, T. D., Sakonidou, E. P., and Raphaelides, S. N. (2002). Water dispersion kinetics during starch gelatinization. *Carbohydrate Polymers*, 49, 479-490.

Koliandris, A., Lee, A., Ferry, A. L., Hill S.E., and Mitchell, J. R. (2008). Relationship between structure of hydrocolloid gels and solutions and flavour release. *Food Hydrocolloids*, 22, 623-630.

Kuakpetoon, D. and Wang, Y. J. (2007). Internal structure and physicochemical properties of corn starches as revealed by chemical surface gelatinization. *Carbohydrate Research*, 342, 2253-2263.

Le Guen, S. and Vreeker, R. *Interactions between flavour compounds and milk proteins under static and dynamic conditions.* In: Flavour Research at the dawn of the twenty first century. Proceedings of the 10th Weurman Flavour research symposium, Beaune (France), 24-28th June 2003. p182-187.

Lerdwijitjarud, W., Sirivat, A., and Larson, R. G. (2004). Influence of dispersed-phase elasticity on steady-state deformation and breakup of droplets in simple shearing flow of immiscible polymer blends. *Journal of Rheology*, 48, 843-862.

Levitt, L. and Macosko, C. W. (1996). Influence of Normal Stress Differences on Polymer Drop Deformation. *Polymer Engineering and Science*, 36, 1647-1655.

Li, H. and Sundararaj, U. *Does drop size affect the viscoelastic drop breakup mechanism?* Proceedings of the 24th Annual meeting of the Polymer Processing Society, Salerno, 15-19 June 2008.

Lin, B., Mighri, F., Huneault, M. A., and Sundararaj, U. (2003). Parallel breakup of polymer drops under simple shear. *Macromolecular Rapid Communications*, 24, 783-788.
Lin, C. and Guo, L. (2007). Experimental Study of Drop Deformation and Breakup in Simple Shear Flows. *Chin.J.Chem.Eng.*, 15, 1-5.

Maffettone, P. L. and Minale, M. (1998). Equation of change for ellipsoidal drops in viscous flow. *Journal of Non-Newtonian Fluid Mechanics*, 78, 227-241.

Meng, Y. Z. and Rao, M. A. (2005). Rheological and structural properties of cold-water-swelling and heated cross-linked waxy maize starch dispersions prepared in apple juice and water. *Carbohydrate Polymers*, 60, 291-300.

Mighri, F., Carreau, P. J., and Ajji, A. (1998). Influence of elastic properties on drop deformation and breakup in shear flow. *Journal of Rheology*, 42, 1477-1490.

Milliken, W. J. and Leal, L. G. (1991). Deformation and breakup of viscoelastic drops in planar extensional flows. *Journal of Non-Newtonian Fluid Mechanics*, 40, 355-379.

Mitchell, J. R. (1979). Rheology of polysaccharide solutions and gels. 51-72.

Mitchell, J.R., Ferry, A.L., Desse, M., Hill, S.E., Hort, J., Marciani, L., Wolf, B. *Mixing hydrocolloids and water: polymers vs. particles.* In: P.A. Williams and G.O Phillips ed. Proceedings of Gums and Stabilisers for the Food Industry 14, Wrexham, 2008. BSC Publishing, 2008, 29-39.

Morikawa, K. and Nishinari, K. (2000). Rheological and DSC studies of gelatinization of chemically modified starch heated at various temperatures. *Carbohydrate Polymers*, 43, 241-247.

Nayouf, M., Loisel, C., and Doublier, J. L. (2003). Effect of thermomechanical treatment on the rheological properties of crosslinked waxy corn starch. *Journal of Food Engineering*, 59, 209-219.

Nguyen, Q. D., Jensen, C. T. B., and Kristensen, P. G. (1998). Experiment and modelling studies of the flow propertes of maize and waxy maize starch pastes. *Chemical Engineering Journal*, 70, 165-171.

Oates, C. G. (1997). Towards an understanding of starch granule structure and hydrolysis. *Trends in Food Science & Technology*, 8, 375-382.

Padokhin, V. A., Ganiev, R. F., Kochkina, N. E., and Anikin, Y. A. (2006). Effect of mechanical activation on starch swelling in an aqueous medium. *Doklady Chemistry*, 409, 142-144.

Rallison, J. M. (1984). The deformation of small viscous drops and bubbles in shear flows. *Annual Review of Fluid Mechanics*, 16, 45-66.

Rao, M. A., Okechukwu, P. E., Da Silva, P. M. S., and Oliveira, J. C. (1997). Rheological behavior of heated starch dispersions in excess water: role of starch granule. *Carbohydrate Polymers*, 33, 273-283.

Rao, M. A. and Tattiyakul, J. (1999). Granule size and rheological behavior of heated tapioca starch dispersions. *Carbohydrate Polymers*, 38, 123-132.

Ratnayake, W. S. and Jackson, D. S. (2007). A new insight into the gelatinization process of native starches. *Carbohydrate Polymers*, 67, 511-529.

Rodriguez-Hernandez, A. I., Durand, S., Garnier, C., Tecante, A., and Doublier, J. L. (2006). Rheology-structure properties of waxy maize starch-gellan mixtures. *Food Hydrocolloids*, 20, 1223-1230.

Rumscheidt F.D and Mason S.G (1961). Particle motions in sheared suspensions XII. Deformation and burst of fluid drops in shear and hyperbolic flow. *Journal of Colloid Science*, 16, 238-261.

Rutschmann and Solms (1989). Formation of inclusion complexes of starch with different organic compounds. I. Method of evaluation of binding profiles with menthone as an example. *Journal lebensmittel-Wissenschaft-und-Technologie*, 22, 240-244.

Schoch, T. J. (1969). Mechano-chemistry of starch. *Wallerstein Lab.Commun.*, 32, 149-166.

Sevenou, O., Hill, S. E., Farhat, I. A., and Mitchell, J. R. (2002). Organisation of the external region of the starch granule as determined by infrared spectroscopy. *International Journal of Biological Macromolecules*, 31, 79-85.

Shi, Y. C., Capitani, T., Trzasko, P., and Jeffcoat, R. (1998). Molecular Structure of a Low-Amylopectin Starch and Other High-Amylose Maize Starches. *Journal of Cereal Science*, 27, 289-299.

Sibillo, V., Guido, S., Greco, F., and Maffettone, P. L. (2005). Single drop dynamics under shearing flow in systems with a viscoelastic phase. *Macromolecular Symposia*, 228, 31-39.

Sibillo, V., Pasquariello, G., Simeone, M., Cristini, V., and Guido, S. (2006). Drop deformation in microconfined shear flow. *Physical Review Letters*, 97.

Singh, N., Inouchi, N., and Nishinari, K. (2006). Structural, thermal and viscoelastic characteristics of starches separated from normal, sugary and waxy maize. *Food Hydrocolloids*, 20, 923-935.

Smith, P. G. and Vandeven, T. G. M. (1985). Shear-Induced Deformation and Rupture of Suspended Solid Liquid Clusters. *Colloids and Surfaces*, 15, 191-210.

Srichuwong, S., Sunarti, T. C., Mishima, T., Isono, N., and Hisamatsu, M. (2005). Starches from different botanical sources II: Contribution of starch structure to swelling and pasting properties. *Carbohydrate Polymers*, 62, 25-34.

Stone, H. A. (1994). Dynamics of Drop Deformation and Breakup in Viscous Fluids. *Annual Review of Fluid Mechanics*, 26, 65-102.

Stone, H. A. and Leal, L. G. (1989). The Influence of Initial Deformation on Drop Breakup in Subcritical Time-Dependent Flows at Low Reynolds-Numbers. *Journal of Fluid Mechanics*, 206, 223-263.

Tako, M. and Hizukuri, S. (2002). Gelatinization mechanism of potato starch. *Carbohydrate Polymers*, 48, 397-401.

Tanpaiboonkul, P., Lerdwijitjarud, W., Sirivat, A., and Larson, R. G. (2007). Transient and steady-state deformation and breakup of dispersed-phase droplets of immiscible polymer blends in steady shear flow. *Polymer*, 48, 3822-3835.

Tattiyakul, J. and Rao, M. A. (2000). Rheological behavior of cross-linked waxy maize starch dispersions during and after heating. *Carbohydrate Polymers*, 43, 215-222.

Taylor, A. J. and Linforth, R. S. T. (1996). Flavour release in the mouth. *Trends in Food Science & Technology*, 7, 444-448.

Taylor, G. I. (1934). The formation of emulsions in definable fields of flow. *Proceedings of the Royal Society of London Series A-Mathematical and Physical Sciences*, 146, 0501-0523.

Taylor, G. I. (1932). The viscosity of a fluid containing small drops of another fluid. *Proceedings of the Royal Society of London Series A-Containing Papers of A Mathematical and Physical Character*, 138, 41-48.

Tecante, A. and Doublier, J. L. (1999). Steady flow and viscoelastic behavior of crosslinked waxy corn starch-k-carrageenan and gels. *Carbohydrate Polymers*, 40, 221-231.

Tester R.F., Karkalas J., and Qi X. (2004). Starch-composition, fine structure and architecture. *Journal of Cereal Science*, 39, 151-165.

Tester, R. F., Debon, S. J. J., and Karkalas J. (1998). Annealing of Wheat Starch. *Journal of Cereal Science*, 28, 259-272.

Thebaudin, J. Y., Lefebvre, A. C., and Doublier, J. L. (1998). Rheology of starch pastes from starches of different origins: Applications to starch-based sauces. *Food Science and Technology-Lebensmittel-Wissenschaft & Technologie*, 31, 354-360.

Torza, S., Cox, R. G., and Mason, S. G. (1972). Particle Motions in Sheared Suspensions XXVII; Transient and Steady Deformation and Burst of Liquid Drops. *Journal of Colloid Interface Science*, 38, 395-411.

Tsakalos, V. T., Navard, P., and Peuvrel-Disdier, E. (1998). Deformation and breakup mechanisms of single drops during shear. *Journal of Rheology*, 42, 1403-1417.

Tucker, C. L. and Moldenaers, P. (2002). Microstructural evolution in polymer blends. *Annual Review of Fluid Mechanics*, 34, 177-210.

Vananroye, A., Van Puyvelde, P., and Moldenaers, P. (2006b). Structure development in confined polymer blends: Steady-state shear flow and relaxation. *Langmuir*, 22, 2273-2280.

Vananroye, A., Van Puyvelde, P., and Moldenaers, P. (2006a). Effect of confinement on droplet breakup in sheared emulsions. *Langmuir*, 22, 3972-3974.

Varanasi, P. P., Ryan, M. E., and Stroeve, P. (1994). Experimental-Study on the Breakup of Model Viscoelastic Drops in Uniform Shear-Flow. *Industrial & Engineering Chemistry Research*, 33, 1858-1866.

Velez-Ruiz, J., Hernando, I., Gonzalez-Tomas, L., Perez-Munuera, I., Quiles, A., Tarrega, A., Lluch, M. A., and Costell, E. (2006). Rheology and microstructure of custard model systems with cross-linked waxy maize starch. *Flavour and Fragrance Journal*, 21, 30-36.

Weel, K. G. C., Boelrijk, A. E. M., Alting, A. C., Van Mil, P. J. J. M., Burger, J. J., Gruppen, H., Voragen, A. G. J., and Smith, G. (2002). Flavor release and perception of flavored whey protein gels: perception is determined by texture rather than by release. *Journal of Agricultural and Food Chemistry*, 50, 5149-5155.

Youn, K. S. and Rao, M. A. (2003). Rheology and relationship among rheological parameters of cross-linked waxy maize starch dispersions heated in fructose solutions. *Journal of Food Science*, 68, 187-194.

Zhao, X. (2007). Drop breakup in dilute Newtonian emulsions in simple shear flows: New drop breakup mechanisms. *Journal of Rheology*, 51, 367-392.
Zobel, H. F. (1988). Molecules to granules: A comprehensive review. *Starch/Stärke*, 40, 1-7.

Internet sources:

Definition of the dictionary of cell and molecular biology <URL: http://cancerweb.ncl.ac.uk/cgi-bin/omd?trigeminal+system>, (consulted July, 30th 2008)

Résumé du chapitre III

Matériaux et méthodes expérimentales

Ce chapitre recense les produits utilisés pour notre étude ainsi que les méthodes utilisées pour les caractériser. L'étude porte sur le comportement de l'amidon sous cisaillement et plus particulièrement sur l'amidon de maïs cireux modifié (Novation 2600, National Starch, UK). Néanmoins à titre comparatif, l'amidon de pomme de terre (Potato starch, National starch, UK) et l'hydroxypropylmethyl cellulose (HPMC K4M, Dow Chemical, UK) sont également utilisés. L'amidon est étudié sous trois formes différentes :

- Le granule d'amidon plongé dans l'huile de silicone est soumis à un cisaillement (comparaison avec grain isolé de pomme de terre),
- L'amidon sous forme de suspension (granules gonflés dans un solvant),
- L'amidon en tant que gouttelette de suspension immergé dans un liquide immiscible, l'huile de silicone (comparaison avec gouttelette d'HPMC)

Les deux tests principalement utilisés sont la rhéologie et la rhéo-optique contra-rotative. Cette dernière méthode combine l'essai mécanique et l'observation visuelle grâce au montage de deux plateaux parallèles transparents tournant en sens opposé sur un microscope optique. Il est donc possible d'observer la déformation d'une gouttelette ou d'un grain d'amidon gonflé sous cisaillement, en temps réel. La gouttelette ou le grain d'amidon sont plongé dans un fluide Newtonien, l'huile de silicone, afin de soumettre le système étudié à une contrainte suffisamment importante pour engendrer une déformation.

La rhéologie sert à la caractérisation de la viscosité et de l'élasticité de la suspension d'amidon, de la solution d'HPMC et de l'huile de silicone; elle est nécessaire pour interpréter les résultats obtenus avec l'outil rhéo-optique. La tension interfaciale entre l'huile et la goutte doit également être déterminée pour l'analyse de données. A cette fin, des mesures de tensions interfaciales ont été effectuées en utilisant la méthode de la goutte pendante. Par soucis de mise en œuvre, la phase

continue de la suspension d'amidon a été recueillie et utilisée pour les mesures. Afin de définir ce qui est mesuré et de quantifier les composants présents dans la phase continue, cette dernière a été caractérisée via diverses méthodes (spectrophotométrie, Differential Scanning Calorimetry, Ultracentrifugation, Chromatographie d'exclusion stérique couplé à la diffusion de la lumière).

La forme des granules ainsi que de leur topographie de surface sont observés à l'aide du microscope électronique à balayage et de la microscopie à force atomique.

Chapter III: Materials and methods

This chapter is dedicated to the materials and the experimental methods used for this study. In the first part (Materials), the main characteristics of the different materials used in this work are presented. Three main materials were studied: modified waxy maize starch, hydroxypropylmethyl cellulose and silicon oils. The sample preparation is described in detail. In the Methods section, the techniques and devices used for the study are explained with special attention being paid to sample loading and different sources of experimental error for rheo-optic experiments. Flow behaviour of the materials was characterized using a rotational rheometer and the rheo-optical counter rotating device and the interfacial tension between the fluids was assessed with a tensiometer. Greater attention was paid to the starch itself through an in-depth characterisation: the analysis of the continuous phase and its constituents was carried out using analytical techniques such as Differential Scanning Calorimetry, Analytical Ultracentrifugation, Size Exclusion chromatography and iodine staining. Finally, the starch granule itself was examined using microscopy techniques to evaluate granular shape (Scanning Electron Microscopy), surface roughness and topography (Atomic Force Microscopy) and behaviour under flow (counter rotating shear cell).

III.1. Materials: Their characterisation and sample preparation

III.1.1. Starch

The starch used was a commercial sample of modified waxy maize (Novation 2600, provided by National starch, UK) which is physically modified through a heat moisture treatment which induces an inhibited swelling, thus

mimicking a chemical cross-linking. As the swelling properties depend on the botanical sources of the starch as well as its physical or chemical modifications, it was important to determine the swelling conditions precisely in order to prepare reproducible suspensions, i.e. homogeneous with similar viscosities. Another starch, native potato starch (National Starch, UK) was used, to a lesser extent, in a few experiments on the behaviour of single granules under flow. *As the study was mainly carried out on the modified waxy maize starch, the latter will simply be referred to as starch. If potato starch is used, in that case it will be specified.*

III.1.1.1. Starch characterisation

- Gelatinisation temperature

The gelatinisation temperature depends on the intrinsic properties of the starch and needs careful determination. In fact, each granule gelatinizes at a specific temperature that can differ from granule to granule. This variation is thus generally referred to as a gelatinisation temperature range. However, we generally talk about a gelatinisation temperature rather than a range and it is considered as the temperature for which most granules are gelatinised.

The gelatinization temperature was determined using an optical microscope Metallux 3 (Leitz, Germany) fitted with a heating stage (Linkam TMS 91 hot plate, Linkam Scientific Instruments, UK) in polarised light. Starch granules were dispersed in excess of water at 20°C followed by heating to 95°C at a rate of 3°C/min. The gelatinisation temperature was defined as the moment where 90% of the observed granules had lost their birefringence, i.e. Maltese crosses were no longer visible under polarized light illumination. For modified waxy maize starch used in this study a gelatinisation temperature of around 73±1°C was found (this value was the mean of 3 replicates); using the same method, the gelatinisation temperature of potato starch was determined to be around 69±1°C.

At a given temperature, granules, depending on starch origin, can continue to swell. In a second set of measurements the effect of heating time on granule swelling was evaluated by heating a sample in excess water to the gelatinization temperature (73°C or 69°C) and holding it for 30min at this temperature. The swelling of the granules was evaluated every 5min, but no further increase of

granule size was observed for waxy maize starch. Thus, it can be concluded that most of the granules were swollen to their maximum at 73°C, with no further heating needed. For potato starch further swelling of the granules was observed; after 10min the maximum swelling at 69°C was attained (and no bursting was observed).

- Swelling degree and maximum concentration C_{max} ($\Phi = 1$)

The lengths of the dry and the swollen granules were measured using optical microscopy and image analysis software Ellix (Microvision, France). Based on the data acquired, the swelling degree, Q, was calculated using the following Equation (3.1):

$$Q = (L_{\text{swollen granule}}/L_{\text{dry granule}})^3 \quad 3.1$$

where $L_{swollen}$ and L_{dry} are the lengths of swollen and dry granules, respectively.

Q is determined by weight considering that the density of the granules remains constant.

From the swelling degree it was possible to calculate the critical concentration, C_{max}, at which theoretically the suspension of swollen-in-water granules contained no free water, i.e., all water was taken up by the granules in the process of swelling. Thus, the theoretical volume fraction was 100%. C_{max} was calculated as follows:

$$C_{max} = \Phi / Q \quad 3.2$$

where Φ is the volume fraction of the suspension (Doublier et al., 1987).

Maximum concentration C_{max} was also determined experimentally following protocols previously published (Vandeputte et al., 2003). Specifically, a starch suspension (potato and modified waxy maize) was prepared at the gelatinization temperature and then centrifuged for 10min at 2700g and 20°C. The supernatant was removed and the sediment weighed. C_{max} was calculated following Equation (3.3).

C_{max}= (dry matter starch weight x 100) / (sediment weight) 3.3

This measurement was repeated in triplicate and yielded a similar value to the one calculated with the swelling degree (see Table 3.1).

Table 3.1: Swelling degree and critical concentration values. Values are to be considered with a 10% error.

	Q (g/g)	Calculated C_{max} (%w/w)	Measured C_{max} (%w/w)
Modified waxy maize starch	12.5	8	7.8
Potato starch	20	5	5.4

It is important to consider these values with care as they are average values. As evident below, there was great polydispersity in the granule sizes and their swelling ability. Swelling occurs at different rates and varies from one starch granule to another. Consequently, the maximum concentration might vary from one sample to another.

- Granule size distribution

To underline the polydispersity of the starch granules, the size distribution of dry and swollen starch particles was determined using the same optical microscopy image analysis set-up as for the swelling degree determination.

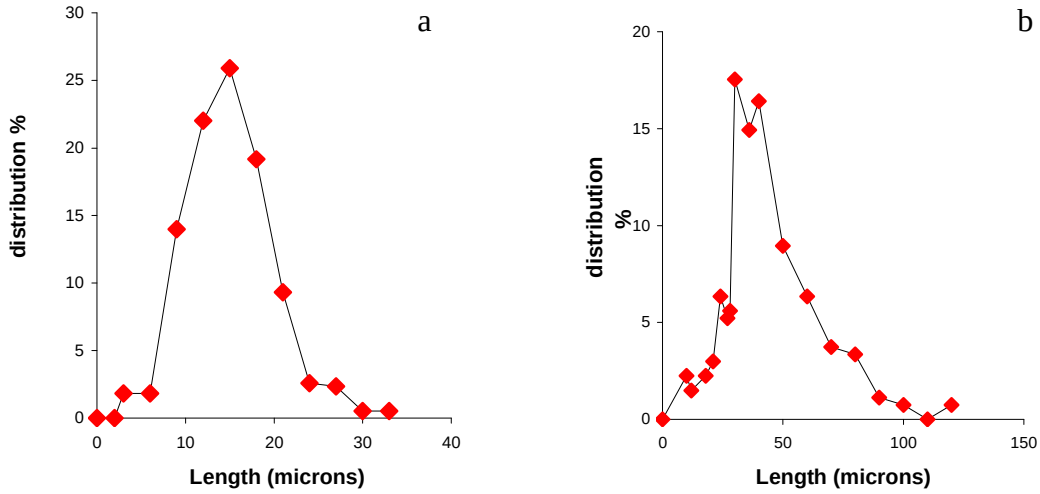

Figure 3.1: Modified waxy maize starch granule size distribution (a) in the dry state and (b) swollen-in-water. Lines are given to guide the eye.

Figure 3.1 shows a large polydispersity of the granules with a majority of granules measuring 15µm and 30µm in diameter in the dry and swollen states respectively. The size distribution of the swollen granules is wider than the size distribution of the dry granules suggesting different swelling rates and different swelling degrees; e.g. two granules of the same size will not reach the same final diameter. Hence, the values for the swelling degree and the critical concentration should be considered as an average value. The volume fraction is slightly overestimated and does not reach the theoretical value of 100%.

III.1.1.2. Preparation of starch suspensions

Modified waxy maize starch suspensions were prepared by adding starch to water while stirring vigorously for 10s to obtain proper dispersion, i.e. with no lumps. The mixtures (starch granules+water) were heated in a water bath and gently stirred (250rpm) until they reached gelatinisation temperature (73°C) and held at this temperature 1 min to ensure full swelling of the granules. Starch samples were prepared at various concentrations ranging from 1%w/w to 20%w/w. Concentrations provided are on a dry weight basis which required determination of the moisture content to the starch as received. Moisture content was determined by weighing the sample before and after oven drying at 50°C. The weight of the samples was measured regularly until no more weight loss was observed. Samples from 2 different batches and stored in different containers (glass bottle, plastic flask) were tested and results for the moisture content are presented in Table 3.2.

Table 3.2: Moisture content of starches. Results are the mean of triplicates

Type of container used for starch storage	Moisture content (%)
Plastic flask	9.1±0.5
Glass bottle	11.2±0.5

From Table 3.2 it can be seen that the starch granules contain naturally around 10% of water (Nguyen et al., 1998; Rao & Tattiyakul, 1999). The starch suspensions obtained give reproducible viscosities as evidenced in Chapter V.

For potato starch a similar method was used. When the gelatinisation temperature was reached, the suspension was held 10min at 69°C to allow the granules to reach maximum swelling. Suspensions were prepared only at the maximum concentration.

III.1.1.3. Preparation of the continuous phase

It is well-known that when starch is heated, the granules swell and amylose leaches out. If the slurry (starch+water) is futher heated the granules burst. Waxy starches contain amylopectin in a great majority (99.9%) and the inhibited swelling through physical modification prevents the granules from bursting as it mimics cross-linking of the amylopectin. Hence, the continuous phase of the suspensions used in this study should be composed of the solvent only, which is pure water. Nevertheless, a few preliminary measurements showed that polymeric material was dissolved in the continuous phase. The analysis of the continuous phase of the suspension in terms of type, concentration and molecular weight of the dissolved polymer is presented in Chapter IV.

A schematic representation of how the continuous phase is separated from the swollen granules is sketched in Figure 3.2. Initially, starch suspensions of different concentrations were prepared as described in 3.1.2 and centrifuged at varying times and speeds to determine the influence of centrifugation on the release of polymeric material in the solvent. The supernatant was removed from the centrifuge tube and set aside as the sediment was discarded. The supernatant was then centrifuged a second time for 20min at 2700g to ensure that there were no remaining starch granules. The 'final' supernatant was recovered for analysis.

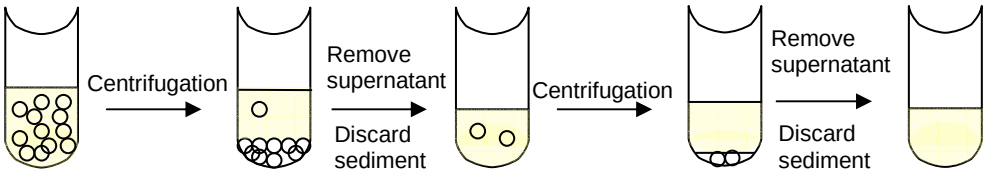

Figure 3.2: Schematic representation of the separation of granules from the continuous phase

However, centrifugation might enhance polymer release in the sample and increase the release of dissolved material in the supernatant. Based on experimental

design and statistical analysis the impact of centrifugation on the continuous phase properties was quantified. The experimental technique will be described in the Methods section.

III.1.2. Linear polymer solution: Hydroxypropylmethyl cellulose

One of the goals of the PhD work was to compare hydroxypropylmethyl cellulose (HPMC) solutions and modified waxy maize starch as thickening agents in terms of their droplet deformation and breakup mechanism. In this section a general overview of HPMC as a molecule and food thickener as well as a description of the preparation of HPMC samples is provided.

III.1.2.1. Molecular structure and general information

The HPMC chosen for this work was Methocel grade K4M provided by Dow Chemical (UK) with a zero shear viscosity of 4Pa.s for a 2%w/w solution (at 20.0°C), as given by the producer. The molecular weight of this HPMC is nominally 95 000g/mol (given by the provider). The degree of substitution is specific to this grade (K4M).

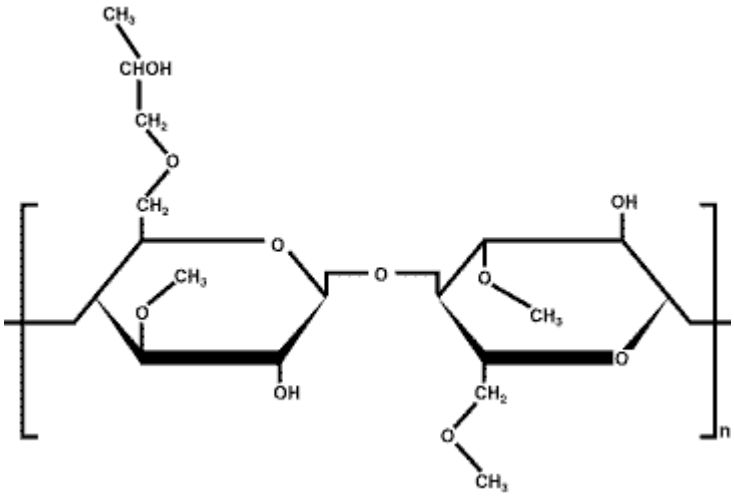

Figure 3.3: Theoretical structure of Hydroxypropylmethyl cellulose

Hydroxypropylmethyl cellulose is derived from cellulose to make it soluble in water; the modification leads to a product called cellulose ether. It is synthesised

by making an alkyl molecule react totally or partially with the hydroxyl groups of the glucose molecules forming ether functions (CH_x-O-CH_x), see Figure 3.3 for the molecular structure. Due to the alkyl chains the polymer is amphiphilic and hence lowers the interfacial tension between hydrophilic and hydrophobic media.

III.1.2.2. Sample preparation

HPMC solutions were prepared by dissolving the polymer powder in distilled water at 70˚C while vigorously mixing with an overhead stirrer (Eurostar Digital, IKA, Germany). The powder was slowly added into the vortex created by the overhead stirrer. When it was fully dispersed, the solution was removed from the heat and stirred until the viscosity increased abruptly. Finally, the samples were stored at 4˚C overnight to allow full hydration of the polymer chains. Measurements were performed on samples that were at room temperature. A range of concentrations was prepared from 1 to 3.75%w/w on a dry weight basis.

III.1.3. PolyDimethylSiloxane

III.1.3.1. Choice of suspending fluid

For rheo-optical study, carried out between two rotating plates combined with an optical microscope, the droplet under scrutiny is embedded in a matrix. For observation purposes this matrix needs to be transparent. It should also be liquid at ambient temperature as the study is conducted at 20°C. Moreover, it should be inert with respect to the studied system, i.e., there should not be any affinity between the droplet and the matrix, or physico chemical interactions and finally the infiltration of the matrix polymer chains in the droplet should be negligible. In the present case it means that the matrix phase should be hydrophobic. Densities have to be similar to prevent buoyancy. Finally, the viscosity should be sufficiently high to induce stresses capable of deforming the droplet.

Silicon oils (polydimethylsiloxane, PDMS) fit all these requirements and were therefore chosen. The silicon macromolecules are composed of carbon, silica and oxygen. Their general formula is shown Figure 3.4.

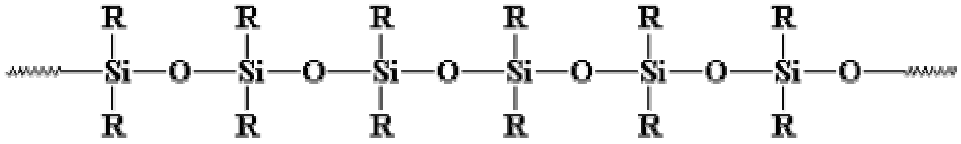

Figure 3.4: Chemical composition of silicon oil

Commercial oils of the type Rhodorsil (Rhône Poulenc, France) of three viscosity grades, 47 V 175 000, 47 V 200 000 and 47 V 1 000 000 referred to as PDMS 175, PDMS 200 and PDMS 1000, respectively, were used in this study. PDMS1M and PDMS 100 (Sigma Aldrich, UK) were also used. An overview of the silicon oils and their viscosity is presented in Table 3.3.

Table 3.3: Silicon oils and viscosity at 20°C

Name given by provider	Synonym used in this report	Viscosity given by provider (Pa.s)	Measured viscosity[a] (Pa.s)
47 V 175 000	PDMS 175	175	170
47 V 200 000	PDMS 200	200	220
47 V 1 000 000	PDMS 1000	1000	1100
PDMS 1M	PDMS 1M	1	1.15
PDMS 100	PDMS 100	0.1	n/a
	PDMS200/PDMS1M: 75/25		75
	PDMS200/PDMS1M: 50/50		21

[a] Values are the mean of three measurements. The standard deviation is less than 10% for all results

The flow curves acquired for the oils are provided in the following section with the exception of PDMS 100; as the latter is not used for the rheo-optical study, the viscosity is not needed.

III.1.3.2. Flow properties of PDMS

The oils were characterised using a rotational rheometer (Bohlin CVO-R, Malvern Instruments, UK) fitted with a cone-plate geometry. Measurements were carried out at 20°C and shear rates varied from 0.1 to 100s^{-1}. PDMS 200 was mixed with PDMS 1M in different proportions to obtain intermediate viscosities. Weight based mixing ratios were PDMS200/PDMS1M = 75/25 and 50/50. The flow curves of all oils used as continuous phase fluid in this study are reported in Figure 3.5.

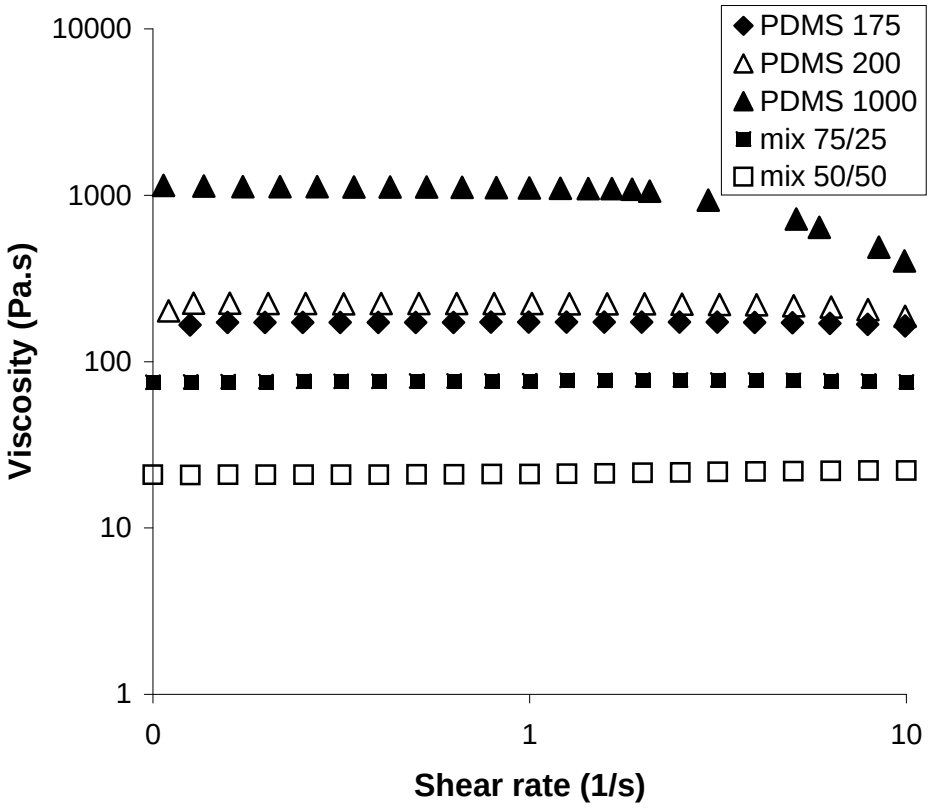

Figure 3.5: Viscosity of the silicon oils. Error bars are smaller than the points.

All measurements carried out on the rheo-optic device were conducted in the Newtonian region of each one of the silicon oils.

The first normal stress differences measured for the silicon oil were negligible and are consequently not presented.

III.2. Methods

III.2.1 Rheo-optics

Rheo-optical systems combine visual observation (microscopy, laser light scattering) with a flow field. It allows the visualisation of flow-induced structural changes. In this study a device developed at CEMEF that consists of a simple shear flow and an optical microscope was used. The two parallel plates creating the flow rotate in opposite directions, which is why it is being referred to as the counter rotating shear cell.

III.2.1.1. Description of the counter rotating shear cell

The counter rotating shear cell, see Figure 3.6 for a schematic representation, is composed of two transparent plates with individual control of rotational speed. Each plate has a diameter of 40mm and is driven by an independent motor. The velocities of the latter can be manually adjusted to turn in the same or in opposite directions. The sample composed of a matrix fluid (silicon oil) and a droplet of the studied system (see 2, Figure 3.6) is loaded between the two plates. The gap is set using the computer, in our case it was 1mm.

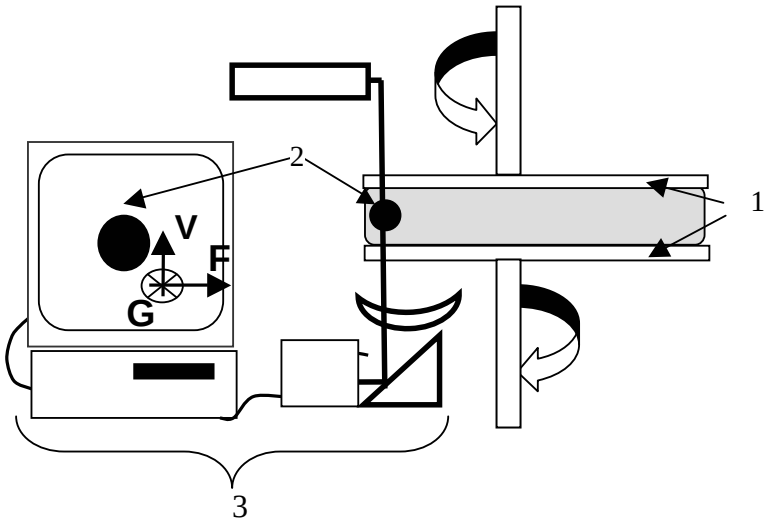

Figure 3.6: Schematic representation of the transparent counter rotating device (Vervoort , 2006). 1: glass plates; 2: sample; 3: Image acquisition unit.

For visual observation the device has been fitted onto a microscope (Metallux 3, Leitz) equipped with a camera (Sony DXC 107 AP). The camera is linked to a monitor and a DVD recorder acquiring and storing 25 images per second (component 3 in Figure 3.6). A time code is superimposed to each of the recorded images which allows accurate analysis of the evolution of flow-induced changes. The system is also linked to a computer with software registering the velocities of the plates, the radius at which the droplet sits in the observation window, and the gap. The software then calculates and records the applied shear rate from these parameters.

III.2.1.2. Principle

In the shear gap of the counter rotating plate-plate device simple shear flow is generated. For a Newtonian fluid, the resulting unperturbed flow velocity varies linearly with the height between ω_u and ω_l at the upper and lower plates respectively, see Figure 3.7. The advantage of using a counter rotating shear cell for the purpose of this study is demonstrated in Figure 3.7. In a system with only one rotating plate, see Figure 3.7a, the observed object moves with a certain speed which depends on the speed of the upper moving plate. Consequently, the changes an individual object may undergo as a result of the application of simple shear flow can not be monitored continuously since the object leaves the stagnant observation area. On the contrary, with the counter rotating plates the object is dynamically fixed, i.e., static in the laboratory reference and, thus, flow-induced structural changes can be observed throughout the measurement.

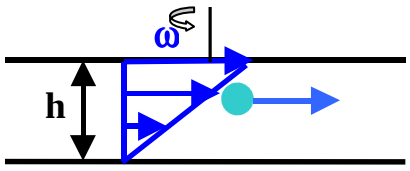

Figure 3.7a: Set-up with only 1 plate rotating

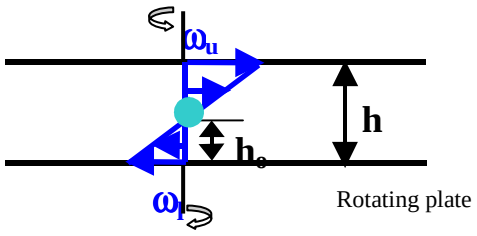

Figure 3.7b: Counter-rotating set-up (2 plates rotating)

ω_l and ω_u are a 2D representation the angular velocities of the lower and upper plates respectively.

The shear stress is calculated as follows:

$$\tau = \eta\dot{\gamma} = \eta\frac{(\omega_u - \omega_l)*r}{h} \qquad 3.4$$

where τ is the shear stress, η is the viscosity of the matrix fluid, $\dot{\gamma}$ the shear rate applied, h the gap between the 2 rotating plates, r the radial position of the droplet in the flow-vorticity direction and finally ω_u and ω_l are the angular velocities of the upper and lower plates, respectively.

At a certain height h_0 (see Figure 3.7b), a selected droplet (see 2 Figure 3.6) has a velocity of zero for an observer in the fixed laboratory reference. It can hence be kept in the field of view and its deformation can be monitored continuously throughout the experiment.

As much as possible, upper and lower velocities should be equal to ensure good experimental conditions. In that case, the plane of observation is in the middle of both plates and the droplet is not submitted to wall effects, if the drop size is sufficiently small (wall effects will be discussed in the next section). The experiments in this study were carried out for droplets at a radial position chosen between 5 and 12mm in order to obtain reasonable shear rate (the closer to the rotation centre the lower the shear rate) but also making sure we are not too close to the farther edge of the plate (plate radius is 20 mm). In the latter case, the shear rates induced are high, leading to a difficult stabilisation of the droplet.

III.2.1.3. Sample loading

A first layer of PDMS was placed on the lower plate. Small droplets of the studied sample were added using a spatula. The droplets were then covered by a second layer of PDMS. We are using here the term “droplet” in the general sense; it can be a droplet of a polymer solution, a droplet of suspension or even a single starch granule. When silicon oil viscosity is high, air is entrapped; hence, the system

was let to relax before lowering the upper plate onto the sample and starting the measurements. From the suspended droplets, one with a diameter between 40μm and 100μm was chosen. The droplet size was imposed to limit wall effects; it has been frequently reported, (De Bruijn, 1989; Bikard *et al.*, 2006) that shear gaps less than 10 times the size of the object under consideration affect its deformation behaviour, usually enhancing it (Vananroye et al., 2006; Vanaroye et al., 2007). In order to fulfil this criterion, it was ensured that the drops were located in the middle of the shear gap which was controlled by only analysing drops that were dynamically fixed at roughly equal angular velocity of the upper and the lower plate, respectively. Also, it was ensured that the volume fraction of droplets in the oil was such that the distance between the centres of neighbouring drops was at least three times the diameter of the largest drop in order to avoid flow perturbations that could influence deformation.

For the observation of single swollen-in water starch granules, the samples were loaded in similar way: first a layer of PDMS, then a droplet of starch suspension. This droplet was observed under the microscope and the granules were separated from one another. Finally, a second layer of PDMS was added. The same precautions were taken to ensure that the required conditions for proper data were fulfilled.

III.2.1.4. Experimental conditions

The experiments were conducted by stepping up the shear rate from zero to a fixed value; thus the system was directly submitted to the desired τ and no shear thinning of the droplet was involved. Shear rates were chosen from the region of the Newtonian flow behaviour of the PDMS. Droplet deformation was followed until either a break-up event or steady state deformation was observed. If the droplet did not break up the relaxation speed was then monitored by just stopping the shear flow.

For single swollen starch granules the experiments were carried out by increasing the shear rate stepwise from 0 to $10s^{-1}$. Each shear rate was held at least 30s to ensure that the steady state deformation of the granule was attained.

All experiments were conducted at 20±2°C, in a controlled temperature room.

III.2.1.5. Estimation of the error occurring during experimental settings

As the settings must be done manually, error on the gap, the radius and the velocities might occur for the calculation of the shear rate. The latter is calculated by the software as determined by equation 3.4. The error is thus the addition of the relative errors for each parameter entering the equation:

The relative speeds of the upper and lower plates are tested to see if there is a difference between the speed given by the software (and used to calculate the shear rate) and the actual speed of the plates. To determine the velocities of the plates, a pencil mark is done on the lower and upper plate. For a specific software speed, the number of rotations of the mark is counted as well as the time needed for the rotation. The real speed can then be calculated by dividing the number of rotations by the time necessary to do them. The relation between the velocities of the software and the measured velocities can be seen Figure 3.8 (a and b).

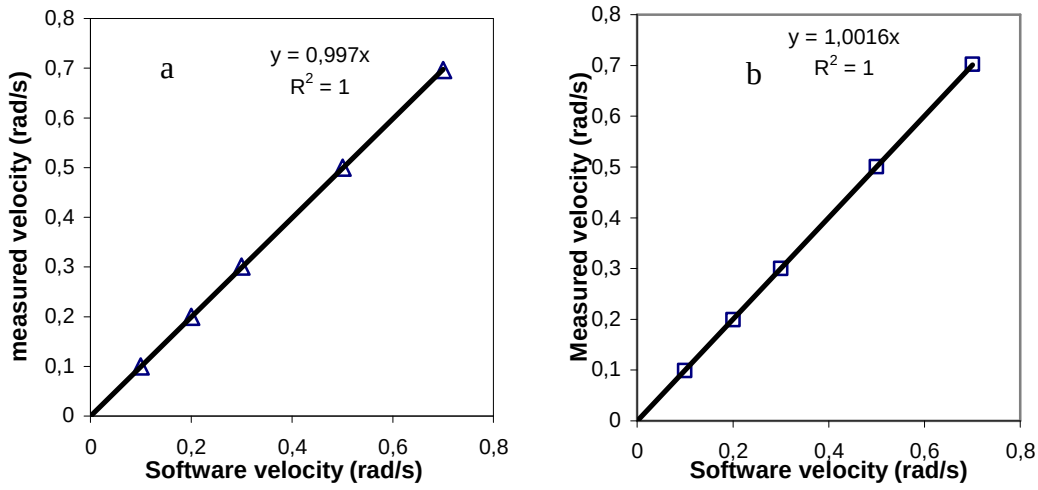

Figure 3.8: Correlation between the measured and calculated by software velocity; (a) lower plate, (b) upper plate.

Figure 3.8 shows an excellent correlation between the measured velocity and that given by the software. The estimated error for the lower plate is 0.2% and 0.1% for the upper plate.

The radial position of the particle is given by the software. It is varied using a micrometric screw, which in turn moves the part containing the two parallel plates, along a horizontal axis. Thus the observation window can be visualised from a zero radius to the maximum value possible. The zero radius value is entered in the software as the rotation centre of both plates; in the centre r =0 and consequently the shear rate is zero. The error on the radius may be due to an imperfection of the concentricity of the plates or any systematic shift. The rotation centres of the plates are 30µm apart thus inducing a 15µm error on the radius. It was determined by following a mark situated close to the rotation centers of the plates; when tracing the path of both marks (on the upper and the lower plate), it is possible to see the rotation centre of the plates. We consider that this small deviation from concentricity is not important.

The height between the two plates, referred to as the gap value, is given by the software. After setting the mechanical zero, namely when both plates are in contact (set manually) the zero gap value is set on the software. The desired gap, 1mm, is entered in the software. To check the accuracy of the software a comparator is used. The relation between the true gap and the software gap is presented Figure3.10.

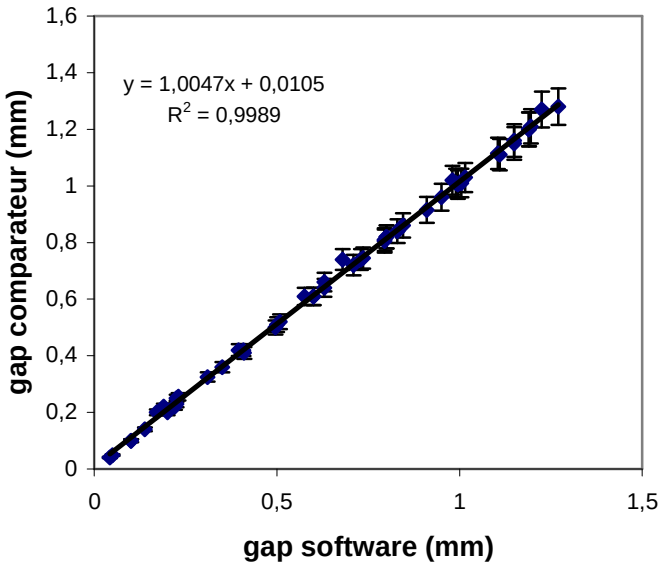

Figure 3.9: Correlation between the software gap and true gap

Figure 3.9 shows a good correlation between the gap given by the comparator ("true gap") and the gap given by the software. The overall estimated error is of 2.6% on average for all data points. For a gap of 1mm (which is what is used) this corresponds to a 26µm error.

The square of the relative error on the applied shear rate is calculated as the sum of the squared relative error on different factors (Vervoort, 2006):

$$(\delta\dot{\gamma})^2 = \left(\frac{\Delta\dot{\gamma}}{\dot{\gamma}}\right)^2 = \frac{(\Delta\omega_l)^2 + (\Delta\omega_u)^2}{(\omega_l + \omega_u)^2} + \left(\frac{\Delta r}{r}\right)^2 + \left(\frac{\Delta h}{h}\right)^2 \qquad 3.5$$

Bearing in mind other possible errors that cannot be estimated, we consider the global error to be around 5%.

As demonstrated above, the error on the machine is quite low. However, error on the shear rate might occur from other sources. A slip phenomenon of the silicon oil on the glass surface might induce a lower shear rate than that expected or calculated by the software. Slip depends on the wetting ability of the surface by the material; the higher the contact angle the lower the wetting ability and the higher the slip.

Slip was determined for PDMS oil by calculating the speed of a glass bead in the oil and comparing it to the rotation speed of the plates. The speed of the glass bead is determined by recording its trajectory on the monitor and determining the time it takes to cover that distance. It is then possible to calculate its speed. The value obtained is compared to the rotation value given by the software. Results showed a 5% difference between the rotation speed of the plate and the speed of the bead. It seems that slip occurs between the glass plates and the silicon oil.

III.2.1.6. Analysis of droplet deformation experiments and orientation angle

The dimensions of the initial and deformed droplet are determined using the image analysis software VISILOG® from Noesis. The measured dimensions are shown in Figure 3.10: the length L (flow axis) and the W the second minor axis of the drop (in the vorticity direction). The third dimension of the droplet, the breadth B, can not be seen with this set-up.

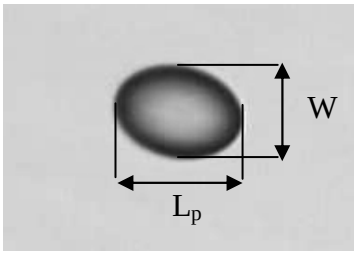

Figure 3.10: Definition of dimensions of deformed droplets in simple shear using the counter rotating shear cell.

Using the device developed in CEMEF the droplet is observed in the flow/vorticity axis. It is not possible to measure either the breadth B of the droplet (first minor axis, in the flow gradient direction) or the particle orientation in the flow gradient axis (see Figure 3.11). As a consequence, the droplet length measured on the image is a projected length L_p.

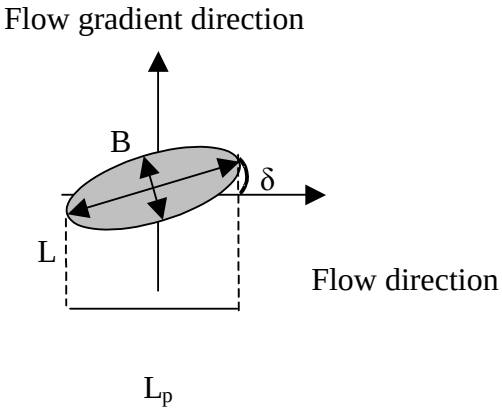

Figure 3.11: Droplet orientation under simple shear flow in a plane perpendicular to the vorticity axis

The orientation angle was determined using a counter rotating device developed in Le Mans University and described in detail by Assighaou et al., 2007. This set-up allowed observation of the droplet in both planes formed by the vorticity/flow and the flow/flow gradient axis, making it possible to determine the orientation of the droplet as a function of the shear rate. The real length was then calculated from the set of data obtained with the prior experiments using Equation 3.6. For large deformations (D>0.2), the droplet is no longer an ellipsoid and B ≠ W; the breadth in the flow gradient direction is hence calculated using the conservation volume Equation 3.7.

$$L = L_p / \cos\delta \qquad 3.6$$

$$B = \frac{V_0}{L * W}, \qquad 3.7$$

where V_0 is the initial volume of the droplet.

Deformation data for HPMC and starch suspension droplets will be presented chapter V.

III.2.2 Experimental procedures and devices used for rheological characterisation

The flow and elastic properties of starch suspensions, HPMC solutions and silicon oils were studied using rheological tools (the characterisation of the flow behaviour of silicon oils were presented in section III.1.3.2 above). A description of the different modes used (continuous, oscillatory) as well as the different devices will be provided in this paragraph. All measurements were carried out at constant temperature controlled by a Peltier-Plate system. As some experiments proved to be long, to avoid solvent evaporation and drying of the sample a thin layer of mineral oil was applied.

III.2.2.1. Flow properties

- Starch suspensions:

A first set of experiments was carried out on a rotational rheometer (C-VOR, Bohlin rheometer, Malvern Instruments, UK) to evaluate the influence of the geometry on the flow curve of an 8%w/w starch suspension. For these measurements different geometries were used:
- Cone-plate: stainless steel, 40mm, 2° cone angle
- Plate-plate: stainless steel, 40mm, gap varied from 400 to 1100µm
- Plate-plate: Cross-hatched, 40mm, gap varied from 400 to 1100µm
- Coaxial Cylinder (Couette), C14 cup and bob: cup dimensions (D = 15.4mm, H = 27.4mm), bob dimensions (D = 14mm, H = 21mm, angle 15°)
- Vane, C14 cup and vane: vane dimensions (‘D’=14mm, H = 21mm, 6 paddles)

The instrument is stress-controlled; moreover, suspensions of soft particles are known to be yield-stress fluids above a certain particle concentration and for these reasons, measurements will be carried out in stress-controlled mode (CS). The procedure used is as follows:

- Procedure for starch suspension, C-VOR rheometer:

Measurements were carried out in controlled stress mode at a constant temperature of 20°C; applied stresses are increased step wise from 1 to 1000Pa logarithmically. The shear stress is applied to the sample for 15s and left 30s for the sample to reach steady state before acquisition of the data point.

As it will be shown in section V.1, the results obtained with the different geometries were similar within 10% error; it can be concluded that slip does not seem to occur. Hence, for further measurements, the cone-and-plate geometry will be preferred, as it allows working at higher concentration than for the cylinder and Vane. Moreover, the shear rate is homogeneous throughout the gap and thus does not lead to agglomeration of granules in the low shear rate zones, unlike the plate-plate. Another reason to use the cone-plate system is that the first normal stress difference data can be obtained directly using this geometry.

Optimisation of the flow measurements of the suspension to determine yield stress and viscosity values as a function of applied stress and the starch concentration were performed on a different rheometer, (MCR-301, Anton Paar, Germany). The starch suspension is a structure system composed of more or less deformable granules. When the starch sample is loaded, the granules have not all been submitted to the same stresses; in order for the granules to have the "same history" a pre-shear above the yield-stress value is applied. Moreover, the granules, being deformable, need time to relax to their initial state (Cloitre, 2005), to obtain more reproducible results. Intrinsic relaxation time cannot be characterized as for conventional viscoelastic fluids (Cloitre, 2005); it seems that relaxation increases with time and that the measurements are carried out in an out-of equilibrium state. The pre-shear applied was slightly above the yield-stress value determined previously to allow rearrangement of the granules. The "relaxation time" was varied from 10min to 60min; above 20min no differences in the flow curve were observed.

- Procedure for starch suspension, MCR-301 rheometer

Pre-shear of 100Pa was applied for 60s to the sample. As the sample is concentrated, sedimentation is not a critical parameter here. The sample was then let

to relax for 20min as mentioned above. Finally, the shear stress was increased step wise from 1 to 1000Pa logarithmically. For each data point, an infinite time was left.

Yield stress was determined by applying a Herschel-Bulkley model. This method gave very reproducible results: the standard deviation for the yield-stress values (mean of 10 measurements) did not exceed 5%.

- HPMC solutions

The flow behaviour of HPMC solutions of various concentrations was studied using an ARG2 (TA instrument, UK) fitted with a 60mm stainless steel cone-plate geometry. The cone-plate geometry (60mm stainless steel cone-plate, 2°) was preferred as it offers a uniform shear rate within the gap; as HPMC is a solution, there is no problem of gap-size/particle size.

- Procedure for HPMC solution, ARG2 rheometer:

Measurements were carried out in controlled stress, following a step-wise logarithmic increase of the shear stress from 0.01 to 500Pa. Time dependence was tested by decreasing the stress from 500 to 0.01Pa, and at each stress the sample was left until steady state was reached.

- Note on first normal stress difference

First normal stress differences can be determined during a flow measurement when using a cone and plate geometry. For elastic fluids, a normal force F develops and acts on the plates in the direction of the rotation axis pushing the cone and plate apart. The force is measured with the rheometer. In the case of a cone-plate, a simple equation (3.8) relates the normal force to N_1 and is automatically calculated throughout the measurement. This relation is more complicated with a plate-plate geometry.

$$N_1=\frac{2F}{\pi a^2}$$ with a the plate radius 3.8

N_1 was determined from the flow measurements for starch suspensions and HPMC solutions; the methods for both samples are described above. Results presented in sections V.1.1.5 are to be taken with care as N_1 characterisation methods were not optimised. However, it is important to note that the results obtained for the first normal stress difference are not completely reproducible; a more rigorous procedure would be needed.

III.2.2.2 Oscillatory mode

The viscous, G'', and elastic, G', moduli were determined using the oscillatory mode (C-VOR Bohlin, Malvern Instruments, UK).

For HPMC solutions a cone-plate geometry was used. In the case of starch suspensions the oscillatory mode does not induce a gradient of shear rate along the radius of the geometry as very small deformations are applied; hence no agglomeration of granules in low shear rate regions can occur. For this reason a plate-plate geometry with a gap of 400μm is preferred hence freeing ourselves of the gap/size/particle size issue.

The first step in measuring G' and G'' is to determine the linear viscoelastic region (LVR). To determine the LVR, an amplitude sweep varying the stress amplitude from 0.1 to 100Pa was performed for all samples and for three different frequencies: 0.1Hz, 1Hz and 10Hz. These frequencies were chosen to make sure the applied stress during the frequency sweep was valid for the range of frequencies studied (0.1 to 10Hz).

- Procedure: for HPMC and starch suspension, linear viscoelastic region determination

Measurements were carried out in controlled stress, the latter varying from 0.1 to 100Pa. The measurements were performed at a constant frequency of 0.1, 1 or

10Hz. The shear stress was applied 15s to the sample and 15s were allowed for the sample to reach equilibrium before recording a data point.

Once a common LVR was determined for the samples, a stress value in the LVR was chosen. It will remain constant during the frequency sweep test. The frequency test procedure was slightly different for starch and HPMC as starch is a suspension of deformable particles and HPMC a polymer solution. As mentioned earlier, the granules need to be submitted to a pre-shear and given sufficient time to relax before performing the frequency sweep. .

- Procedure for HPMC suspension: frequency sweep

For all samples (various concentrations) a 1Pa stress was applied, which was a common value to all LVRs. The frequency varied from 0.1 to 10Hz.

It is slightly more complicated to measure G' and G'' for starch suspensions due to the deformability of the granule. As it was seen previously, the granules need to be submitted to the same history and also need time to relax to their equilibrium state. For this reason, the procedure was optimized similarly to viscosity measurement (see section III.2.2.1). Differences between viscoelastic curves, obtained for samples submitted to pre-shear and those that were not, were observed. Nevertheless, there was no noticeable difference detected between a pre-shear at 10Pa and one at 100Pa. We thus chose to pre-shear the samples at 10Pa. The influence of relaxing time was also assessed by varying relaxing time from 10 min to 60 min. The best results were obtained for a 60min relaxation time. The procedure used was the following.

- Procedure for starch suspension: frequency sweep

First the sample was pre-sheared for 60s at 10Pa and then let to relax for 60min. The frequency sweep from 0.1 to 10Hz was performed for a constant stress of 1Pa chosen in the LVR. The method gave reproducible results

Measurements were performed for various concentrations both with HPMC solutions and starch suspensions.

III.2.2.3 Low viscosity fluids: starch suspension supernatant

The viscosity of the starch suspension supernatant was determined with a rolling ball viscometer (AMVn, Anton Paar, UK) under precise temperature control (20.00°C ± 0.01). The relative, $\eta_{rel,}$ and specific viscosities, $\eta_{sp,}$ were calculated as follows (equations 3.9 and 3.10):

$$\eta_{rel} = \frac{\eta}{\eta_0} \qquad 3.9$$

$$\eta_{sp} = \eta_{rel} - 1 \qquad 3.10$$

where η is the dynamic viscosity (*i.e.* corrected for density) of a starch supernatant solution and η_0 is the dynamic viscosity of water (1.002 mPas), which was measured using the same method.

Measurements were made in triplicate for each supernatant solution taken from suspensions made at different starch concentrations, and intrinsic viscosities, [η], were estimated through calculation using the Solomon-Ciutâ approximation, Equation 3.11 (Solomon and Ciutâ, 1962):

$$[\eta] \approx \frac{\left(2\eta_{sp} - 2\ln(\eta_{rel})\right)^{1/2}}{c} \qquad 3.11$$

where c is the supernatant concentration determined separately from Size Exclusion chromatography coupled with light scattering (SEC-MALLS) and Analytical Ultracentrigation (AUC) data which are presented in section II.2.5 and III.2.6 respectively. The Solomon-Ciutâ equation allows for approximated values of the intrinsic viscosity without concentration extrapolation and can thus be used when the data is not sufficient.

The intrinsic viscosity of the starch supernatant was determined as it can give information on the shape, the flexibility, the degree of water-binding and it is also linked to the molar mass (for non spherical particles). This value can give a general idea of the conformation of the macromolecule.

III.2.3 Interfacial tension

The interfacial tension was determined using a tensiometer applying the pendant drop method (PAT-1, Sinterface, Germany). The set-up is equipped with a CCD camera and a recording system visualising the drop at all times; from the drop shape the interfacial tension can be calculated. Hence, the interfacial tension can vary depending on its volume; a computer controlled dosing system allows for reproducible results. By varying the amount of solution to form the drop, the volume range where no variation of the interfacial tension is observed can be determined. Using a capillary, the liquid of higher density forms a drop in the lower density fluid. The droplet is submitted to interfacial tension and gravity.
Measurements were carried out both in air and in silicon oil at room temperature.

- Measurements in air

A first set of experiments was carried out in air. The droplet was formed using a steel capillary in a quartz cell.

For water the droplet volume was fixed at 22mm^3, and the evolution of the interfacial tension was followed for 2min.

In the case of HPMC solution, its specific properties and concentration range used did not allow the control of the droplet size. When using the computer-controlled dosing, the droplet volume oscillated so the initial volume was set manually. However, the droplet size of the HPMC solution increased over time, probably due to gravity effects, or elasticity of the solution. Measurements were allowed to run for over 2h to allow stabilizing of the droplet. We considered the measurements correct when the values obtained were constant for 30min.

Starch suspension supernatant drops also showed oscillation when controlled with the computer. The volume was hence set manually; for each measurement a different volume was used to see if that influenced the results. Above 12mm^3, all the results obtained for the starch supernatant were consistent.

- Measurements in silicon oil

The interfacial tension between PDMS/(HPMC solution) and PDMS/(starch suspension supernatant) was measured in order to be used in the analysis of rheo-

optical experiments. PDMS/water was also measured as a reference. To obtain a proper drop shape a lower viscosity silicon oil than the ones used for droplet deformation experiments was chosen (PDMS oil viscosity = 100mPa.s). It has been demonstrated that the viscosity of the silicon oil does not influence the interfacial tension (Bergeron *et al.*, 1997). For measurements in oil, a plastic capillary was used to avoid a preferential affinity of the drop with the tube (not observed in air) which would change the drop shape and hence the result.

For water the drop volume was smaller in oil than in air to obtain reproducible results. For the two other systems the drop-forming method remained as described above.

The results obtained with the pendant drop method were compared to results obtained through drop deformation under shear. This method was tested for water only. It was performed using the rheo-optical equipment. According to Taylor and Cox approaches (Cox, 1969; Taylor, 1932; Taylor, 1934) for small Taylor deformations (Equation 2.5) $D_{Taylor} = (L - B)/(L + B) < 0.2$, where L represents the real length of the droplet (calculated with the orientation as described in section III.2.1.3) and B the width in the flow gradient direction, $D_{Taylor} = Ca$, where Ca is capillary number given by Equation 2.4 (Chapter II). By plotting D_{Taylor} (or Ca) values for the small deformation against $R_0 \dot{\gamma}$ and knowing PDMS viscosity, the interfacial tension can be obtained through the slope of the linear fit.

III.2.4 Differential Scanning Calorimetry

A standard power compensated Perkin Elmer DSC-7 (Perkin-Elmer, Ltd., Beaconsfield, UK) was used to investigate the presence of polysaccharides in the suspension supernatant. A portion of the dried, milled supernatant was weighed accurately in a high pressure, stainless steel pan and water was added to obtain a 1:3 ratio of dry sample to water. Finally, Lysophosphatidylcholine (LPC) was added at 5% concentration of the dry sample weight and the pan was hermetically sealed and left overnight on rotating rollers for moisture to equilibrate. For comparison purposes, the initial starch was prepared in the same manner. The occurrence of any

thermal event was studied by heating the previously mentioned sample in the DSC at a scanning rate of 40°C/min from 5 to 140°C. For each sample, three heating/cooling cycles were performed (cooling at 10°C/min) and the temperature was held for 5 min after each ramp. Only the heating scans are reported in the Results section. All measurements were performed in duplicate.

III.2.5 Size Exclusion Chromatography coupled to Multi-Angle Laser Light Scattering (SEC-MALLS)

Analytical fractionation was carried out using a series of SEC columns TSK G6000PW, TSK G5000PW and TSK G4000PW protected by a similarly packed guard column (Tosoh Bioscience, Tokyo, Japan) with on-line MALLS (Dawn DSP, Wyatt Technology, Santa Barbara, U.S.A.) and refractive index (Optilab rEX, Wyatt Technology, Santa Barbara, U.S.A.) detectors. The eluent (deionised distilled water at 25°C) was pumped at 0.80 ml/min (PU-1580, Jasco Corporation, Great Dunmow, U.K.) and the injected volume was 100 µl for each sample (in duplicate). Absolute molar masses, radii of gyration and concentrations were calculated for each sample using a Debye 1st order model (where the refractive index increment, *dn/dc* = 0.146 ml/g) incorporated into the ASTRA® (Version 5.1.9.1) software (Wyatt Technology, Santa Barbara, U.S.A.). The concentrations estimated were then used to prepare the samples to an appropriate concentration for sedimentation velocity experiments.

III.2.6 Analytical Ultracentrifugation AUC

Sedimentation velocity experiments were performed using a Beckman Instruments (Palo Alto, U.S.A.) Optima XLI Analytical Ultracentrifuge. Starch supernatant solutions (500 µl) and distilled water (510 µl) were injected into the solution and reference channels respectively of a double sector 20 mm optical path length cell. Samples were centrifuged at 20000 rpm at a temperature of 20.0 ºC. Concentration profiles and the movement of the sedimenting boundary in the

analytical ultracentrifuge cell were recorded using the Rayleigh interference optical system and converted to concentration (in units of fringe displacement relative to the meniscus, *j*) versus radial position, *r* (Harding, 2005). The data was then analysed using the ls-g*(s) model incorporated into the SEDFIT program (Schuck, 1998). This software, based on the numerical solutions to the Lamm equation, follows the changes in the concentration profiles with radial position and time and generates an apparent distribution of sedimentation coefficients in the form of *g*(s)* versus $s_{20,w}$, where the * indicates that the distribution of sedimentation coefficients has not been corrected for diffusion effects. Usually sedimentation coefficients $s_{20,w}$ are measured at a series of concentrations and extrapolated to infinite dilution ($s^0_{20,w}$) to account for non-ideality, however in this case as concentrations were very low, the weight average sedimentation coefficient was taken as equivalent to that at infinite dilution. The concentration of each sample after dilution in mg/ml was estimated from the area (A) under the *g*(s)* curve using the following relationship:

$$c\ (mg/ml) = 0.388A\ (fringes) \qquad 3.12$$

The concentration prior to dilution was then estimated by multiplying by 2, 6 and 20 for 10, 30 and 50mg/ml starch supernatant solutions respectively.

III.2.7 Design and statistical analysis of centrifugation influence on supernatant properties

A design was put into place to determine the influence of centrifugation speed and time of centrifugation on the release of dissolved material(s) using Design Expert software. The studied responses are the viscosity of the supernatant and the dry matter weight concentration; the results were obtained from the supernatant of a 3%w/w starch suspension. The design is of the factorial type, i.e. that the extreme points are represented: very low rotation speed/short time, low rotation speed/long time, high rotation speed/short time, high rotation speed/long time (see Table 3.4). Four centre points (intermediate rotation speed and time) were added for cross-checking and for statistical analysis. The samples were prepared in a random order

given by the software. Statistical significance of the results was assessed using factorial analysis of variance (ANOVA). All tests were conducted at a 5% significance ($p<0.05$).

Table 3.4: Factorial design to determine the influence of centrifugation on the release of polymeric material

Run	Centrifugation time, min	Centrifugation speed	
		rpm	g
1	**32**	**2300**	**1550**
2	**32**	**2300**	**1550**
3	5	4000	2700
4	60	500	340
5	**32**	**2300**	**1550**
6	**32**	**2300**	**1550**
7	5	500	340
8	60	4000	2700

The dry matter weight of the starch supernatant was obtained after drying the sample for one night in a vacuum oven at 70°C and its concentration in the supernatant was calculated as follows:

Dry matter weight concentration (%) = [Dry matter weight (g)/ supernatant weight (g)] * 100 3.13

III.2.8. Iodine staining: amylose/amylopectin determination

This method was used to determine the amount of amylose and amylopectin in the supernatant and the procedure was based on the ISO method (ISO, 1987). First, a reference system was prepared. Pure amylose (1mg) and pure amylopectin (1mg) were each dispersed in the mixture of 0.1mL of ethanol and 0.9mL of 1M

NaOH aqueous solution. For calibration purposes (amylose/amylopectin ratio) the samples were mixed together in a proportion of amylose ranging from 0 to 40%.
Once prepared, the mixtures were heated for 30min at 95°C and then let to cool. The samples were then diluted to 10mL with distilled water. A 1mL aliquot was pipetted and mixed with 5mL of distilled water, 0.1mL of a 1M acetic acid solution and 0.2mL of iodine solution (0.2% iodine in 2% potassium iodide). The volume was diluted to 10mL with distilled water and the solution well mixed. Finally, the flasks were left for 20min in a dark room for the colour to develop.

The supernatant to be analysed was prepared in the same manner (10mg of dry matter in 1mL of a mixture 0.1mL of ethanol and 0.9mL of M NaOH solution). The optical absorbance was recorded for wavelengths from 400nm to 800nm in spectrophotometer (DU-640, Beckam Instrument, Palo Alto, USA). A blank sample (distilled water) was taken as a reference.

III.2.9. Atomic Force Microscopy (AFM)

Atomic Force Microscopy was used to assess the surface of a starch granule, the topography and its roughness. This roughness could have a major influence on granular interactions and the behaviour of granules under flow.
AFM measurements were carried out on a Picoplus (Agilent Technologies, USA) in “tapping”/acoustic mode. It was used as the studied material is very soft and sticky; therefore the use of the contact mode would be inappropriate here. To determine the granule surface rugosity an untreated silicon cantilever with a principal frequency of 170 kHz is used. The scanned zone is 4µm x 4µm; the scan speed is 0.5l/s, i.e. it takes two seconds for the tip to scan 1 line of the observed zone.

Samples were prepared by spraying starch granules on a double face scotch tape glued to a transparent cell. The scotch was used to prevent the granules from moving when measuring with the AFM tip. To study swollen granules, water was heated to the gelatinisation temperature (determined previously); starch granules were sprayed on a glass slide and immersed in the heated water. The sample was immediately removed from water: this was sufficient to obtain swollen granules, as confirmed by optical observations, while ensuring that no molecules (amylose or

amylopectin) were leaching out. The glass slide was assembled with a cover to form the liquid cell. Then distilled water was added directly into it. The sample could then remain in water during the measurement to prevent dehydration. Images were analysed using the software Gwyddion, a free software used for Scanning Probe Microscopy such as AFM; the treatment of the AFM images is further described in Chapter IV, section IV.1.2.

III.2.10. Scanning Electron Microscopy (SEM)

The starch granules were characterized using environmental SEM (Philips XL-3000, NJ, USA). SEM offers greater resolution than optical microscopy and allows observations of irregular samples thanks to an important depth field. As starch is not conductive, measurements were done in Environmental mode and hence the sample does not require metallic coating or any other specific preparation. The temperature was fixed at 8°C and the chamber pressure at 0.7mBar. The voltage was fixed at 15Kv and GSE detector was used. Observation of the granule shape was carried out to understand the behaviour of a single dry granule submitted to shear.

III.2.11. Density measurements

Accurate values of density were needed for interfacial tension (pendant drop method) and supernatant viscosity measurements. A density meter (DMA 5000, by Anton Parr) was used to measure the density of starch suspension continuous phase, silicon oil, and HPMC solution at various concentrations. All measurements were performed at 20.00 ± 0.01°C in triplicate.

III.3. Conclusions for Chapter 3

Droplet deformation and break-up behaviour of solutions and suspensions in a silicon matrix were studied using a counter rotating shear cell. In order to analyse the data, rheological characterisation of the materials and values of interfacial tension between the suspended matrix and the droplets were needed. Special attention was given to starch and various methods were used to get a global idea of the starch particules studied and its specificities.

- Rheological characterisation with a rotational rheometer, i.e. flow and viscoelastic behaviour by optimizing measuring procedures
- Quantification and identification of the solubilised matter in the continuous phase, using analytical methods such as AUC and SEC-MALLS
- Shape and surface roughness of single granules, dry and swollen, using microscopy techniques (SEM and AFM).

Reference List

Assighaou, S., Pavy-Le Du, G., and Benyahia, L. (2007). Dispositif d'observation de gouttes sous déformation: développement et validation. *Rhéologie*, 11, 45-56.

Bergeron, V., Cooper, P., Fischer, C., Giermanska-Kahn, J., Langevin, D., Pouchelon, A. (1997). Polydimethylsiloxane (PDMS)-based antifoams. *Coilloids and Surfaces A: Physicochemical and Engineering Aspects*, 122, 103-120.

Cloitre, M. (2005). Tailoring the flow properties of soft colloidal dispersions. *Macromolecular Symposia*, 229, 99-106.

Cox, R. G. (1969). Deformation of A Drop in A General Time-Dependent Fluid Flow. *Journal of Fluid Mechanics*, 37, 601.

Doublier, J. L., Llamas, G., and Lemeur, M. (1987). A Rheological Investigation of Cereal Starch Pastes and Gels - Effect of Pasting Procedures. *Carbohydrate Polymers*, 7, 251-275.

Harding, S. E. (2005). Analysis of polysaccharides size, shape and interactions. In D. J. Scott, S. E. Harding, & A. J. Rowe (Eds.). *Analytical Ultracentrifugation Techniques and Methods* (pp. 231-252). Cambridge: Royal Society of Chemistry.

Harding, S.E. (2005). Challenges for the modern analytical ultracentrifuge analysis of polysaccharides. *Carbohydrate Research*, 340, 811–826.

International Organisation for Standardisation (1987). ISO 6647: 1987E. Rice - Determination of amylose content.

Nguyen, Q. D., Jensen, C. T. B., and Kristensen, P. G. (1998). Experiment and modelling studies of the flow propertes of maize and waxy maize starch pastes. *Chemical Engineering Journal*, 70, 165-171.

Rao, M. A. and Tattiyakul, J. (1999). Granule size and rheological behavior of heated tapioca starch dispersions. *Carbohydrate Polymers*, 38, 123-132.

Schuck, P. (1998). Sedimentation analysis of noninteracting and self-associating solutes using numerical solutions to the Lamm equation. *Biophysical Journal*, 75, 1503-1512.

Solomon, O. F. and Ciutâ, I, Z. (1962). Détermination de la viscosité intrinsèque de solutions de polymères par une simple détermination de la viscosité. *Journal of Applied Polymer Science*, **24**, 683-686.

Taylor, G. I. (1934). The formation of emulsions in definable fields of flow. *Proceedings of the Royal Society of London Series A-Mathematical and Physical Sciences*, 146, 0501-0523.

Taylor, G. I. (1932). The viscosity of a fluid containing small drops of another fluid. *Proceedings of the Royal Society of London Series A-Containing Papers of A Mathematical and Physical Character*, 138, 41-48.

Vananroye, A., Van Puyvelde, P., and Moldenaers, P. (2006). Effect of confinement on droplet breakup in sheared emulsions. *Langmuir*, 22, 3972-3974.

Vanaroye, A., Van Puyvelde, P., and Moldenaers, P. (2007). Effect of confinement on the steady-state behavior of single droplets during shear flow. *Journal of Rheology*, 51, 139-153.

Vandeputte, G. E., Derycke, V., Geeroms, J., and Delcour, J. A. (2003). Rice starches. II. Structural aspects provide insight into swelling and pasting properties. *Journal of Cereal Science*, 38, 53-59.

Vervoort S. (2006). Comportement d'hydrogels gonfles de solutions de polymères sous action mecanique, Ph.D, thesis, Ecole des Mines de Paris, Sophia-Antipolis.

Résumé du chapitre IV

Propriétés de surface d'un granule d'amidon et son comportement sous cisaillement

Une étude sur des granules d'amidon a été effectuée. Ce chapitre porte sur l'aspect des granules d'amidon, leurs propriétés de surface et leur comportement sous écoulement dans l'état sec ou gonflé, ceci afin de mieux comprendre le comportement des suspensions de ces mêmes granules. Deux amidons d'origine différente ont été comparés : le maïs cireux modifié, qui est au cœur de notre étude et l'amidon de pomme de terre. Ce dernier a été choisi à titre comparatif pour souligner les variations selon la source botanique et également car il possède des propriétés intéressantes, notamment celle d'être de grande taille et d'être hautement déformable. Dans ce chapitre, la forme des granules et la rugosité de surface ont été étudiés à l'aide de la microscopie électronique à balayage (MEB) et de la microscopie à force atomique (AFM) respectivement. Le comportement de granules sous cisaillement a été observé à l'aide du dispositif rhéo-optique contrarotatif.

Plusieurs observations sur la forme et les propriétés de surface des granules ont été faites. L'aspect des grains et la rugosité de surface sont très différents d'une variété à l'autre.

Les grains d'amidon de maïs cireux modifié ont une forme irrégulière, très angulaire avec de nombreuses faces, tel un silex taillé. Sur la surface de ces granules, des trous et des crevasses sont visibles, donnant une certaine rugosité. Ces aspérités sont probablement dues au traitement thermique subit par les granules lors de la modification.

Contrairement aux grains de maïs cireux modifié, les granules d'amidon de pomme de terre ont une forme régulière, de type patatoïde. La rugosité de surface est négligeable.

L'étude des particules sous cisaillement a permis de montrer plusieurs choses :

- Les granules secs agissent quasiment comme des sphères rigides.
- Les granules gonflés se déforment lorsqu'ils sont soumis à un cisaillement suffisant.
- Le grain déformé peut atteindre dans ce cas-ci jusqu'à deux fois sa taille initiale.

Pour l'amidon de pomme de terre, à des contraintes > 1500Pa, la déformation est maximale et il est possible d'observer des pointes au bout des granules. Cela correspond à un peu de solvant de l'intérieur des grains qui sort du granule sans se détacher.

Après cisaillement le granule a perdu un certain volume qui correspond au volume de solvant éjecté hors de la particule lors de l'expérience. Il y a donc éjection de solvant pour des cisaillements suffisamment grands appliqués pendant des temps suffisamment longs. Néanmoins, le cisaillement critique n'a pu être défini.

- Il existe des différences de quantité de solvant éjecté selon l'origine de l'amidon.
- L'amidon de maïs modifié perd plus de solvant que l'amidon de pomme de terre.

Les différences dans le comportement sous cisaillement sont expliquées par les différences entre les types d'amidon constatées par les études MEB et AFM. Il a été observé qu'une plus grande quantité de solvant été éjectée des grains d'amidon de maïs cireux que pour ceux de la pomme de terre. Cette différence pourrait être imputée aux trous et aux crevasses présentes à la surface de l'amidon de maïs et absent à la surface des grains de pomme de terre. Ces trous pourraient correspondre à des canaux par lesquels sort le solvant.

Chapter IV: Surface properties of starch granules and their behaviour under flow

The aim of this chapter was to study single granules in order to acquire a better understanding of their shape and surface properties as well as their behaviour when they are submitted to flow. The shape and the surface of potato and modified waxy maize starch granules were investigated using Scanning Electron Microscopy and Atomic Force Microscopy. The determination of these features will help understanding the behaviour of a single granule under flow but also could help building hypothesis for the suspension behaviour. In the first section the results obtained for starch granule shape and surface will be presented. The second part is dedicated to the behaviour of single granules submitted to simple shear in the dry and in the swollen state. In this latter state, the granules were prepared as described in section III.1.1.2, i.e. to their maximum swelling at the gelatinisation temperature. In this case, the swelling degrees of modified waxy maize and potato starch are 12.5g/g and 20g/g respectively.

The PhD work is focused on the behaviour of modified waxy maize. However, in this chapter comparison with potato is of interest:

- first to understand the implications of starch origin
- and also potato starch granules being quite large and highly deformable, their observation in the counter rotating shear cell is easier.

IV.1. Shape, size and surface properties of granules: modified waxy maize and potato

The aim of this section is to describe in more detail the shape and surface properties of starch granules depending on their origin. The first part will show the differences in size and shape between potato and modified waxy maize starch. The second part will deal with the description of the starch granule surface of both potato and modified waxy maize.

IV.1.1. Shape of the granules

Dry modified waxy maize and potato starch granules were observed using Scanning Electron Microscopy. Figure 4.1 a, b, c and d are different views of the same sample of starch (modified waxy maize) at increasing magnifications from a to d.

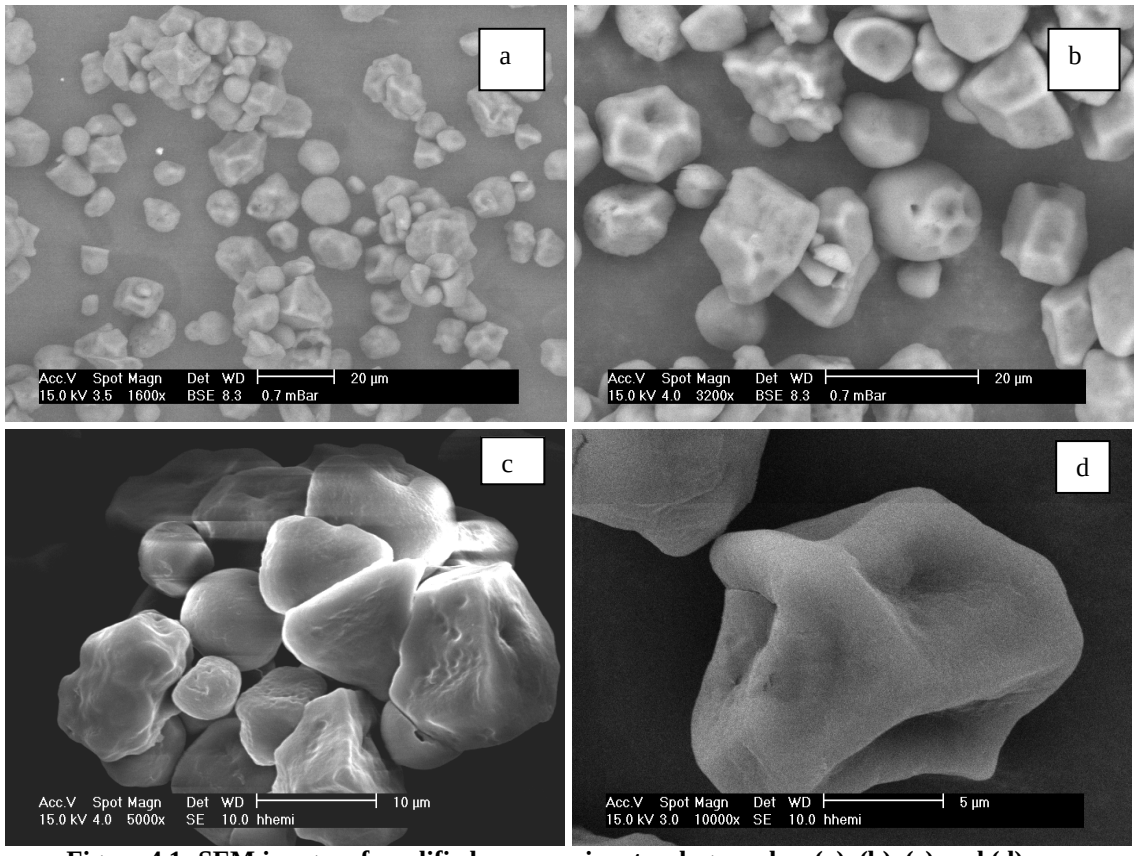

Figure 4.1: SEM images of modified waxy maize starch granules; (a), (b), (c) and (d). Magnification is increased for each picture from a to d, a being the smallest magnification and d the largest. Scale bars are shown for each micrographs.

Figures 4.1 (a) and (b) show the polydispersity of the dry starch granules as well as the variety of shapes. These figures are representative of the granular population. It can be seen that granules vary in size from ~4µm to ~16µm; some granules are spherical whereas most of them resemble a fragment of a flint with angular faces like octahedrons. The faces of the granules seem smooth and flat but when looking at higher magnifications (Figure 4.1 (c) and (d)), these surfaces show a more concave shape with a certain roughness (which will be quantified in the following section). Holes and cracks can also be observed, revealing a complex granular shape and surface.

Potato starch granules visualised with SEM are presented in Figure 4.2 a, b and c. It is obvious from Figure 4.2 (a) that the potato starch granules have an even greater polydispersity than the modified waxy maize starch with granules sizes ranging from ~8µm to ~60µm approximately which corresponds to what has been previsouly reported (Blaszczack et al., 2005).

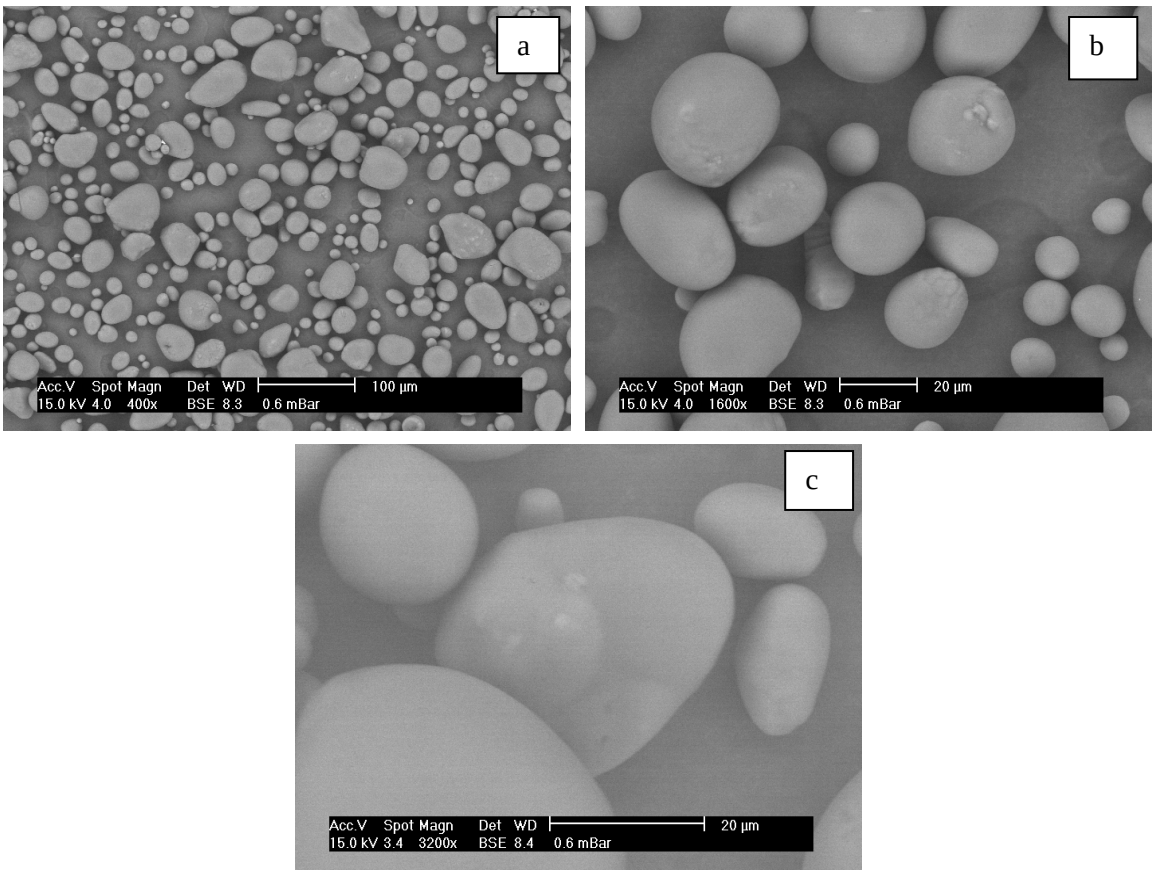

Figure 4.2: SEM images of potato starch granules. (a), (b) and (c).

Figure 4.2 (b) was obtained with the same sample but at a greater magnification. In addition to polydispersity, what can be seen in this figure is a quite homogeneous shape of the granules, most of them having an ellipsoidal shape, or even what could be called a “potato” shape. The overall surface seems rather smooth as shown by Figures 4.2 (b) and (c) despite a few asperities at the surface.

Surface roughness is too small to be observed (nanometer scale) with SEM measurements; an AFM study was carried out as it is best adapted for detecting submicronic roughness. Moreover, AFM allows measurements in liquid. The granules can thus also be observed swollen. In the next part, the relative roughness of both modified waxy maize and potato starch granules was determined.

IV.1.2. Surface roughness assessment using AFM

What is obtained from the AFM measurement is a raw signal of the topography of the granules (See Figure 4.3), which is difficult to interpret.

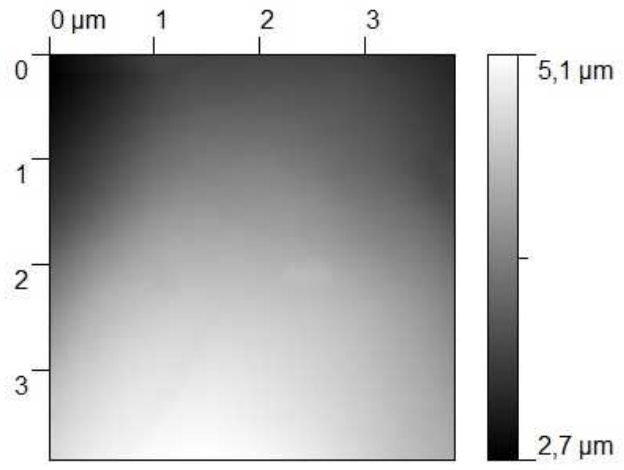

Figure 4.3: raw AFM signal obtained for modified waxy maize starch

In order to analyse these data, the signal is treated using a 2D-polynomial with a chosen degree to be optimized. Figure 4.4 is a schematic view of how the signal is treated.

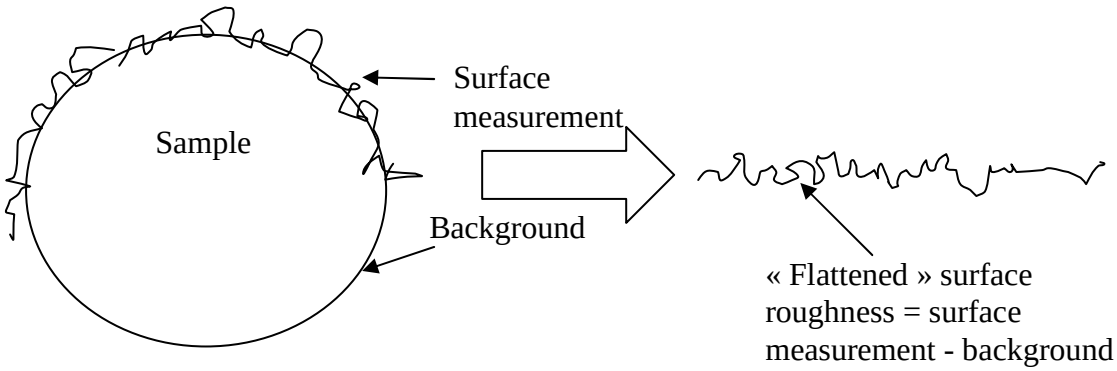

Figure 4.4: Schematic view of raw data treated for analysis.

If the sample is considered as being ellipsoidal (more or less like starch granules), the surface measurement of this sample will have a similar shape, i.e. ellipsoidal as well (see Figure 4.4). The raw data obtained is the surface measurement + backgroung and when not modified it will have a certain curvature which is that of the sample. To analyse the data, the idea is to smoothen the surface (take out its curvature) whilst conserving the surface roughness and removing the background thus easing the analysis and interpretation. The surface measurement is flattened using polynomials; however it is important to choose a polynomial with an intermediate degree in order to not biase the roughness. In the following cases, a second degree polynomial for both the y and x axis was used.

The surface topography of a dry modified waxy maize starch granule is shown Figure 4.5.

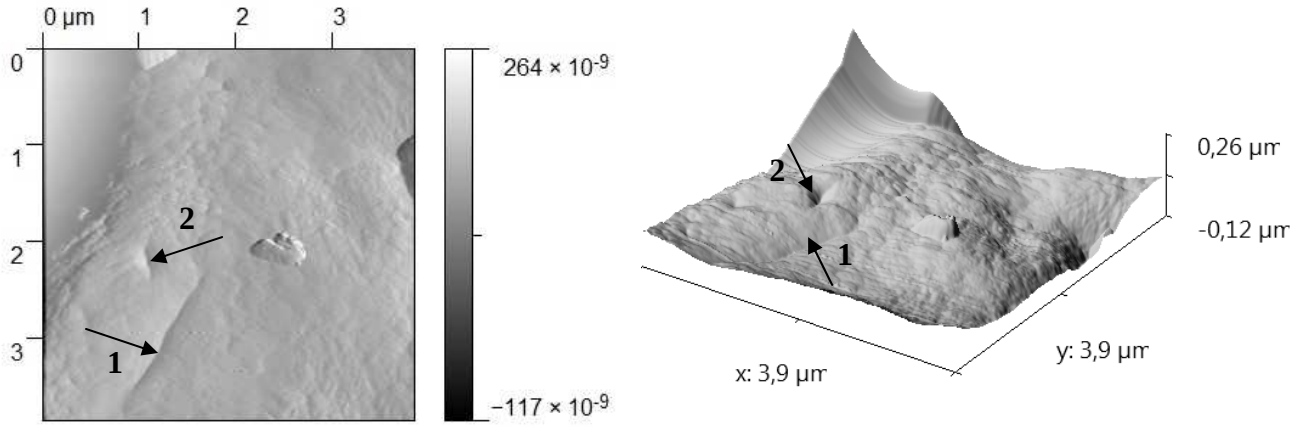

Figure 4.5: (a) AFM image of modified waxy maize starch granule. Scanned area 4µm x 4µm. (a) Topography, flattened signal. (b) 3-D Topography image.

Figure 4.5 is typical for the modified waxy maize starch surfaces observed using AFM. The presence of holes (See arrow 2 in Figure 4.5 a and b) and cracks (arrow 1 in Figure 4.5 a and b) was detected. These “defects” have been previously reported for the surface of rice starch granules, which showed large pits; these holes were attributed to the high heat treatment these granules had been submitted to (Dang & Copeland, 2003). It can thus be suggested that the imperfections on the granule surface are the results of the treatment used to modify the granules. The maximum depth measured at the surface was -54.1nm and the maximum height was observed at 38.6nm. The arithmetic mean roughness Ra, measured by the software, was 13.5nm. Roughness of the surface can cause particles interactions through mechanical anchoring (Kolli et al., 2002), impacting on the flow behaviour of a starch suspension where facets of the granules are in contact (above close packing fraction; the close packing concentration will be considered in chapter V).

However, this value of roughness could be accentuated by the accidental nature of the surface, i.e. the presence of large holes and cracks. The depth and wideness of these “imperfections” were determined and reported in Figure 4.6. Pits such as those imaged in Figure 4.5 and Figure 4.6 can attain a depth of 400nm and a width of 2µm (profile line 3 in Figure 4.6b). These holes can thus be considered as important and might have an impact on granule swelling (water can enter through the holes, easing the swelling); it is also possible to imagine ejection of solvent through the holes if a swollen granule is submitted to high stresses.

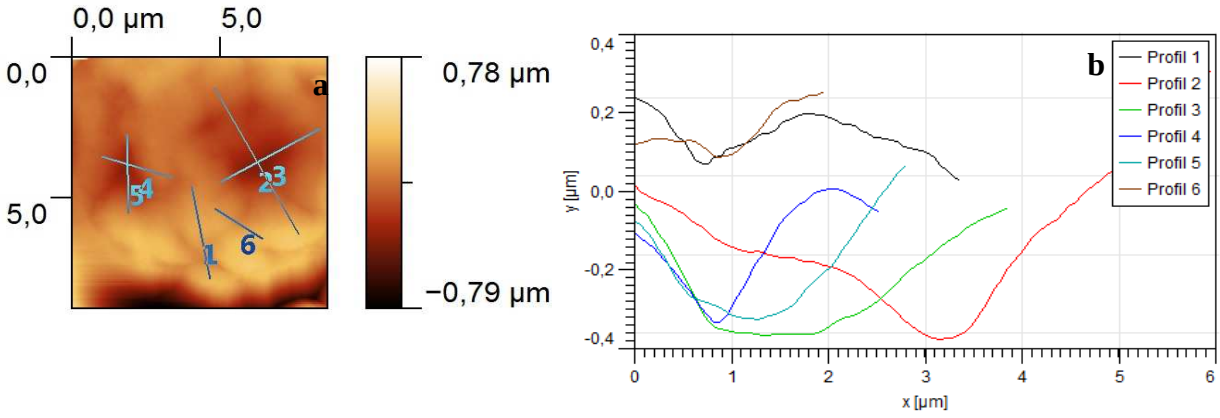

Figure 4.6: (a) AFM image of modified waxy maize granules, scanned area 10 µm x 10 µm. (b) Profile of surface holes

In part IV.1.1, it was shown that the modified waxy maize granules had a flint like aspect with multiple facets; the latter were also seen to be concave. The angle between two joining facets was determined using AFM imaging (Figure 4.7).

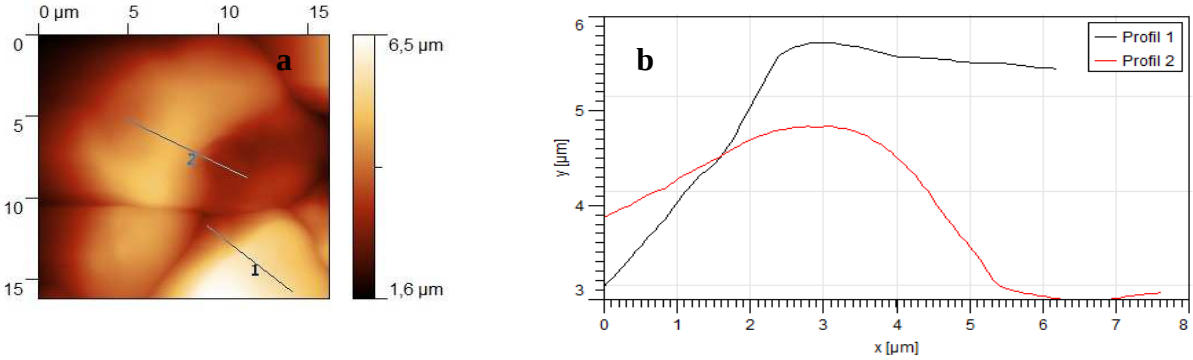

Figure 4.7: (a) AFM image of modified waxy maize granules, scanned area 15 µm x 15 µm. (b) Angle measure between two facets.

Angle determination must be done on the raw signal as the polynomial approach flattens the signal. For the first profile (profile line 1) the measured angle is 124° and 116° for the second one. More angles were measured and not presented here; the average value for these angles is around 120 ± 5°.

The observations of swollen-in-water modified waxy maize starch granules revealed that the cracks and holes do not disappear with the swelling, which was to be expected (results not shown). Nevertheless, these pits were slightly less deep (200 nm) than in the dry sample.

Data obtained for a dry potato starch granules is presented in Figure 4.8. Again, the results are representative of most potato starch granules.

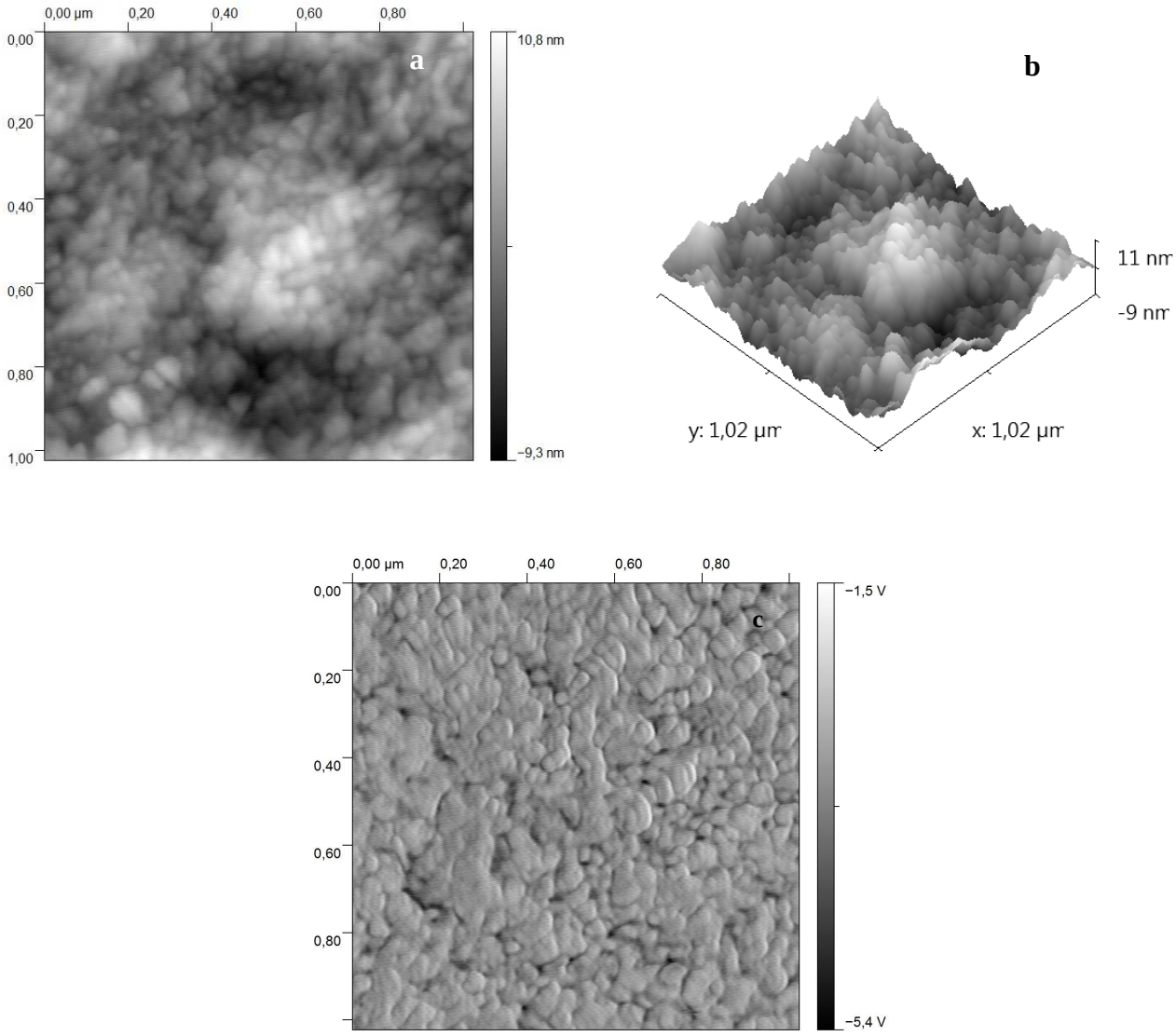

Figure 4.8: (a) AFM image of a dry potato starch granule. Scanned area 1µm x 1µm. (a) 2D-topography, flattened signal. (b) 3-D Topography image. (c) Phase signal

Unlike modified waxy maize starch granules, no holes or cracks could be detected. This potato starch has not been modified, supporting the previous hypothesis that treatment might be the origin of the uneven surface. Measured mean arithmetic roughness was quite low, around 2nm, which was less than the value reported for the modified waxy maize starch. However, looking closely at Figure 4.8 (a and b), a "lighter" zone (200nm large, 20nm high) can be seen; it could correspond to protruding amylopectin molecules arranged in a blocklet (Baldwin et al., 1998; Szymonska & Krok, 2003).

The phase signal (Figure 4.8c) does not give information on the topography but on the "viscoelasticity" of the observed object. A sinusoidal signal is sent to the

granule surface; the response can be in phase which would correspond to an elastic material or a phase angle lag can occur. The phase signal for the potato starch granule suggests a heterogeneous composition of the surface. It is possible to think that it corresponds to alternation between amorphous and crystalline zones conferring a “rubbery” quality to the granules. This heterogeneous state allows for great resistance of the potato starch granules (Oates, 1997).

The observation of potato starch granules swollen in water did not lead to topography images but displayed interesting behaviour; when the AFM tip was approached to the surface of the granule, it deformed and the AFM tip embedded itself in the granule. The potato starch granule had a very “elastic” behaviour: it deformed under the stress of the AFM tip but never burst and when the cantilever was removed the granule instantly took its initial swollen shape. This could be due to the specific structure of the potato starch granule; indeed, the latter has a large amount of amylose at the periphery of the granule giving a high level of organisation (Blaszczack et al., 2005) and strong resistance to enzymatic attack (Sevenou et al., 2002). It is thus possible to think that this “amylose layer” accounts for its specific behaviour when swollen. It was also suggested that potato starch had a sort of membrane which would be specific to this starch (Fisher et al, 1998).

IV.1.3. Conclusions

The microscopic observations of dry and swollen potato and modified waxy maize granules revealed differences from one starch to another. First the shape of the granules is radically different, one being a smooth ellipsoidal (potato) shape whereas the other one has a very irregular and angular cut shape with facets. Moreover, the observation of the surface showed that the overall surface roughness of the modified waxy maize starch was significant as compared to the smooth potato granule. The holes and cracks observed for the modified waxy maize can account for these differences. The phase signal for potato starch gave interesting results on the heterogeneity of the surface (alternating hard and soft zones) that were not

observed for modified waxy maize starch. These differences will probably lead to different behaviour under shear.

IV.2. Behaviour of a single granule under flow

Study of the deformation of dry and swollen granules under simple shear flow was carried out using a counter rotating shear cell. This type of study has never been done and could be of great interest for the understanding of starch suspension rheology. The study of swollen in water starch granules is of particular interest as the starch used in industry is mostly in the swollen state.

IV.2.1 Dry starch granules

IV.2.1.1. Rotation of a solid sphere: Jeffery's law

A solid sphere suspended in an immiscible fluid and submitted to a simple shear flow will rotate around the vorticity axis. The time (T) it takes for a solid sphere to complete one rotation at a given shear rate in a Newtonian matrix was first considered by Jeffery (1922). He determined the rotation of a spherical particle at low Reynolds' numbers and neglected object's inertia. The predicted rotation given by Jeffery for spherical particles, i.e. all the axis are equal, is as follows (Equation 2.1):

$$T = \frac{4\pi}{\dot{\gamma}} \qquad 2.1$$

where T is the time for one rotation (or period of rotation) and $\dot{\gamma}$ the applied shear rate.

The goal of this part was to study the behaviour of one granule under shear. To do this, starch granule (either dry or swollen, this will be specified) was placed in

a silicon oil of a known viscosity and granule behaviour was studied using rheo-optics. First, to verify that the results obtained with the counter rotating device are accurate, the rotation of a glass bead in silicon oil, PDMS 200 (i.e. with a viscosity of 220Pa.s) was determined and compared to Jeffery's law (Figure 4.9).

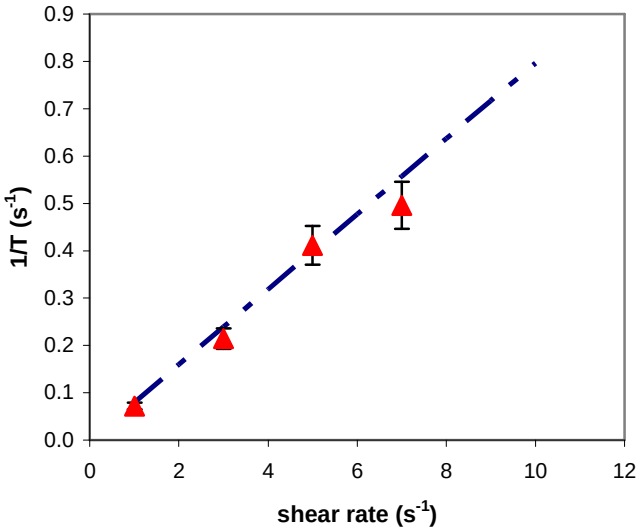

Figure 4.9: Period of rotation as a function of shear rate for solid glass beads in PDMS 200. Dotted line represents Jeffery's law; triangles are the data obtained for glass beads.

As can be seen in Figure 4.9, the results obtained for a glass bead are in good agreement with those predicted by Jeffery's law. It can thus be assumed that the data generated with the counter rotating shear cell is accurate.

IV.2.1.2. Rotation of starch granules submitted to simple shear

The dry granules, either potato or modified waxy maize, did not deform even at high stresses; they are solid objects when no swelling is involved. The rotation of dry starch granules was studied to determine if they obey Jeffery's law or if some deviation from the model occurs. Figures 4.10 and 4.11 show the rotation of the dry granules placed in PDMS 200 observed at shear rates of $2s^{-1}$. It can be seen that the potato starch granules are much larger than those of the modified waxy maize starch making it easier to look at (on the counter rotating cell) and easier to determine the period of rotation.

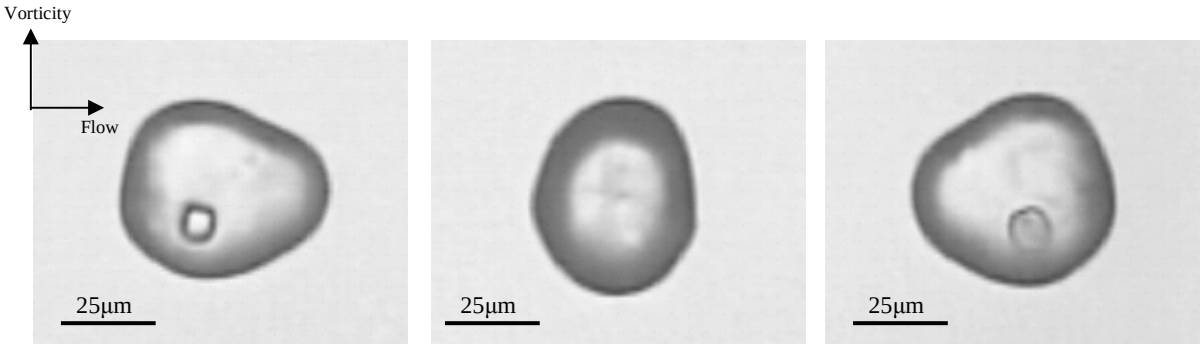

Figure 4.10: Rotation of a dry potato starch granule. L_0 = 70µm, PDMS 200, $\dot{\gamma} = 2s^{-1}$

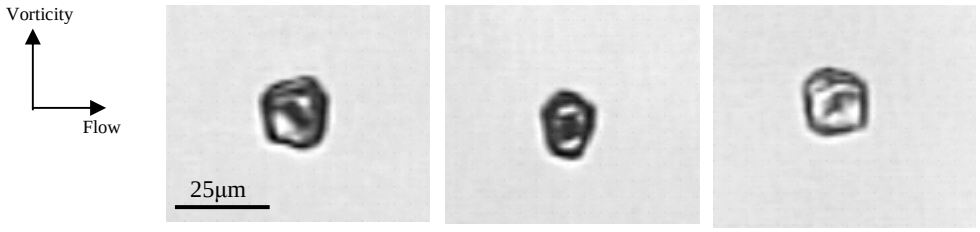

Figure 4.11: Rotation of a dry modified waxy maize starch granule. L_0 = 12µm, PDMS 200, $\dot{\gamma} = 2s^{-1}$

In Figure 4.10 the rotation of the granule can be observed using an imperfection on the particle. Half of a rotation is shown here; in the first picture the smaller 'end' of the granule is oriented to the left. In the second picture, the granule has done a quarter of a rotation around the vorticity axis. In the final picture, the smaller end of the granule is oriented to the right; the particle has completed half of a rotation.

Similar observations can be made for Figure 4.11, although it is less obvious due to the more 'spherical' shape of the granules.

The period of rotation determined for modified waxy maize and potato starch granules is shown Figure 4.12.

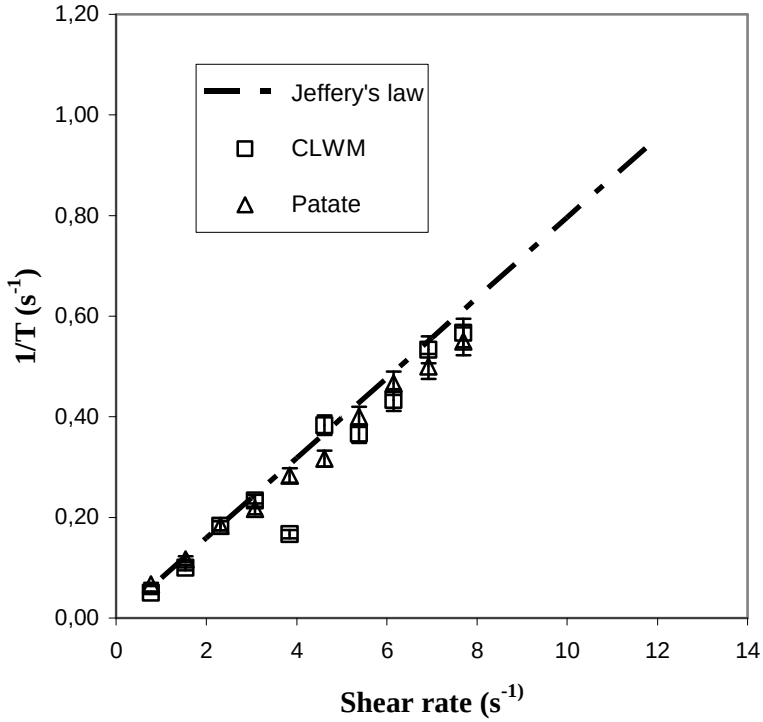

Figure 4.12: Period of rotation for dry starch granules compared to Jeffery's law, in PDMS 200

The rotation periods determined for modified waxy maize and potato starch are close to that determined by Jeffery. The deviation for both starch granules is within experimental error (less than 10%); it seems that both potato an modified waxy maize behave similarly to rigid spheres. It is thus difficult to conclude on the influence ant the surface properties and the shape of the granules on the period of rotation.

IV.2.2. Swollen in water starch granules

In this section evidence of granule deformation under shear, which was previously suggested (Doublier et al., 1987, Fischer et al., 1997), will be demonstrated. However, the results shown here are to be taken as qualitative data as variation in granule size and swelling ability render reproducibility difficult.

IV.2.2.1. Deformation of the granule and ejection of solvent

The deformation of a single modified waxy maize starch granule swollen to its maximum (12.5g/g) and placed in PDMS 200 with increasing shear stress is shown in Figure 4.13.

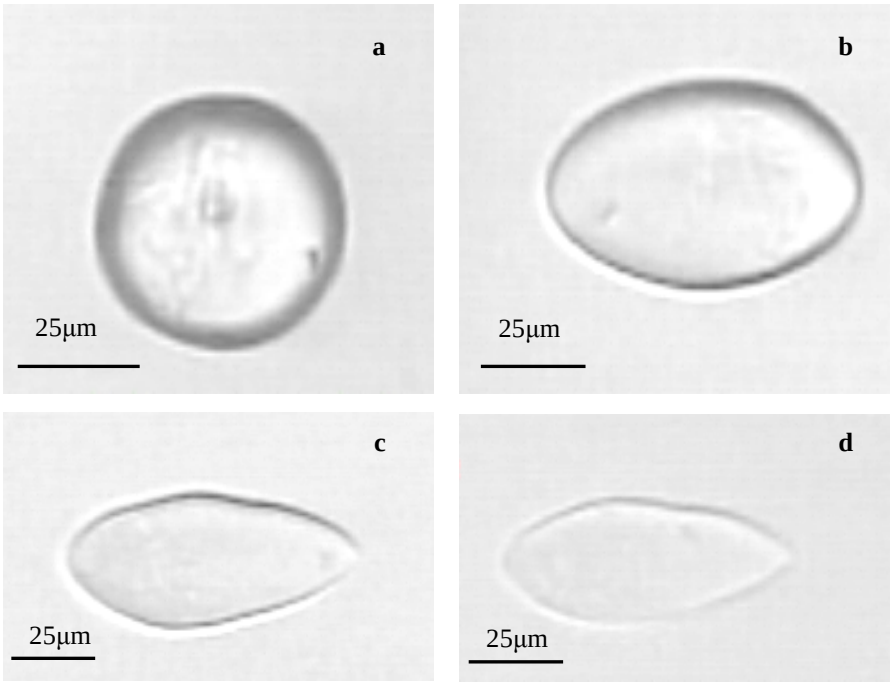

Figure 4.13: Single swollen-in-water modified waxy maize starch granule in silicon oil: (a) at rest; (b) shear stress = 800Pa; (c) shear stress = 1500Pa; (d) shear stress = 2000Pa. Initial granule size is 50µm.

At rest (Figure 4.13a) the observed granule was almost spherical. Its initial diameter was 50µm which is among the larger granules for the modified waxy maize. This can indicate either that the initial dry granule was large or that it was highly swollen (more than the others). In Figure 4.13b, at shear stress = 800Pa the granule is deformed (L/L_0~1.6); deformation started being observed for shear stresses around 300Pa. Around 1500Pa (Figure 4.13c) deformation reached a maximum value. As the shear stress increased, it became harder to see the particle (Figure 4.13d). Determination of the volume of the granule after the experiments indicated a volume loss of 29%.

Figure 4.14 shows the deformation of a modified waxy maize starch and potato starch granules as a function of strain.

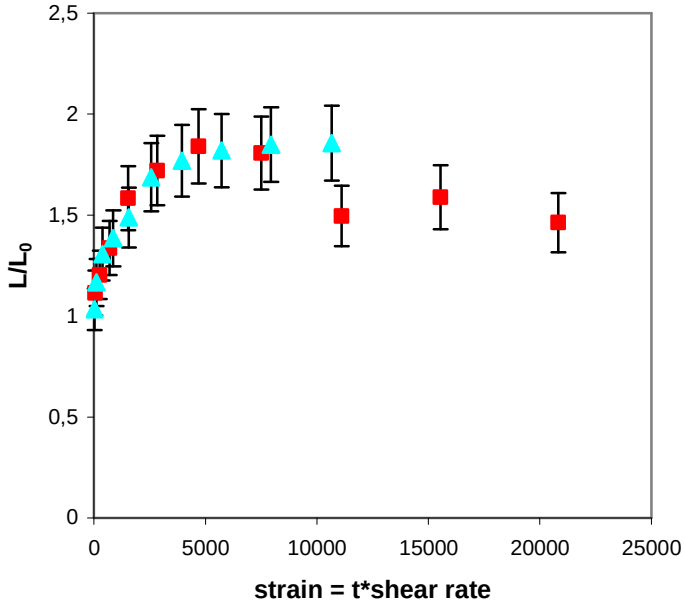

Figure 4.14: Evolution of granule deformation vs. strain. Squares represent modified waxy maize starch; triangles are for potato starch. 10% error bars are shown here.

It can be observed in Figure 4.14, that the modified waxy maize starch granule reaches a maximum deformation before decreasing. This confirms the loss of volume (noticed at the end of the experiment) occurring during the experiment, meaning that there is ejection of the solvent in the suspending medium. This phenomenon is further confirmed by the lack of visibility of the granule at the end of the experiment. The solvent ejection leads to an increase of the density of the granule and consequently changes its refractive index. As the experiment is carried out and solvent is ejected, the refractive index becomes closer to that of the silicon oil, explaining the loss of visibility of the granule. Solvent ejection is evidenced by the loss of volume and the change of refractive index of the granule; however, no tip-streaming was observed. It is possible that the resolution of the CCD camera is not sufficient to detect very small droplet coming out of the granule.

The deformation of a swollen at 20g/g (maximum swelling) potato starch granule was also studied for comparison (Figure 4.15). The granule was spherical at rest (Figure 4.15a) and its initial size was 72µm. This is rather a small size for swollen potato starch granules (probably initial dry granule was small or restricted swelling occured). When the shear stress increased, deformation of the potato

granule was observed (Figure 4.15b). This deformation occurred for shear stresses of 220Pa (i.e. shear rates as low as $1s^{-1}$).

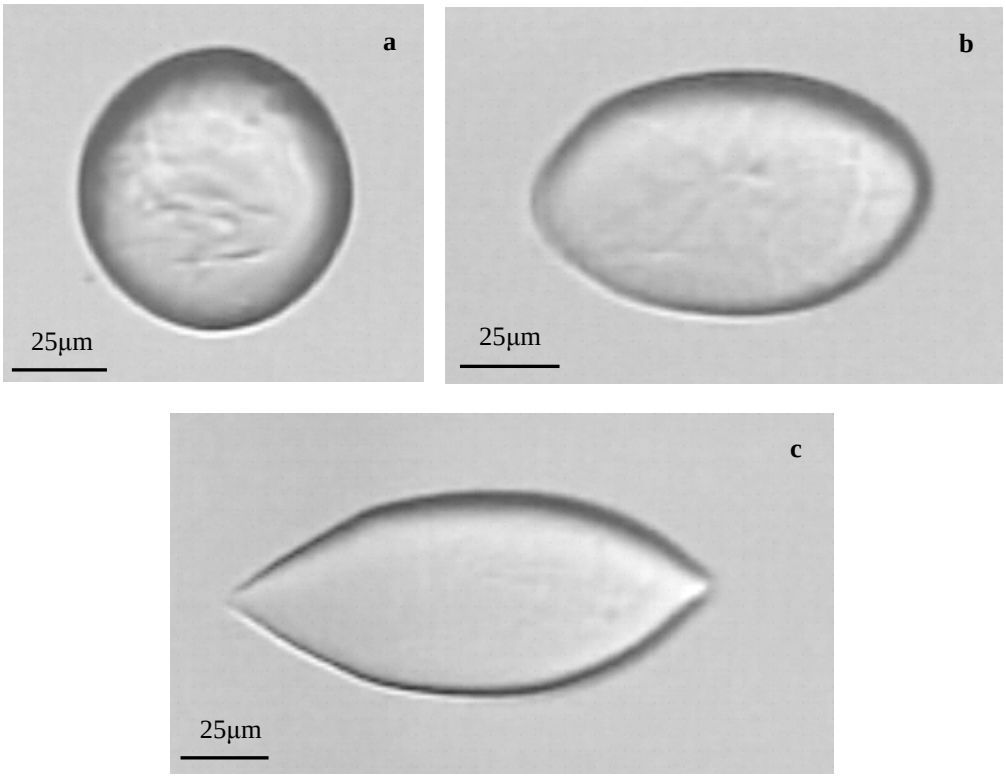

Figure 4.15: Single swollen-in-water potato starch granule in silicon oil: (a) at rest: initial granule diameter is L_0 = 72µm; (b) shear stress = 1500Pa; (c) shear stress = 2300Pa.

In figure 4.15b, a small "cap" at the left extremity of the granule can be observed. This could correspond to solvent that is released from the granules but still attached to the tips. This phenomenon was previously described for swollen microgel particles in aqueous solutions (Vervoort & Budtova, 2003). When the stress was further increased, pointed tips appeared (Figure 4.15c) confirming the probable presence of solvent at the extremities of the granules (i.e. solvent release). It can also be assumed that solvent was ejected from the granule for high shear stresses.

Figure 4.15 shows the evolution of the deformation of a swollen potato starch granule as a function of strain. The deformation is maximum ($L/L_0 \sim 1.8$) for strains around 5000. Contrary to the modified waxy maize starch granule, no decrease in deformation can be observed which can be attributed to a lack of data available for this type of experiment. However, the determination of the final granule volume,

after several experiments, showed that a decrease of 6% to 18 can occur, suggesting the ejection of solvent in the PDMS oil.

The observations shown here should be taken with caution as all granules even within one type of starch are different. The data given here is qualitative as it is difficult to compare starch granules due to their wide variety in shape, size, structure and ability to swell. It should be emphasised that in order to compare quantitatively the deformation of starch granules, the swelling degree should be the same which is not the case here. In this study, the granules were swollen to their maximum, hence they were in the same state but did not contain the same amount of solvent as the swelling degree is different. The granule with the highest swelling degree should have the highest volume loss (which is not the case here as the volume loss in potato starch granules is less important). The granules at the same swelling degree could be compared but in that case, the granules would not be in the same state: e.g. if the granules are swollen to 10g/g then the modified waxy maize starch would be close to its maximum swelling whereas for potato starch the swelling degree would be two time lower and hence the granule would be less deformable. Consequently, it is very difficult to study the deformation of starch granules in a quantitative way. Moreover variations can occur within one starch sample. Some starch granules are smaller than others and some granules will swell more than others although they have the same initial size. It is almost impossible to achieve a good comparison of two random starch granules from different origins. To quantify granule deformation many more experiments should be carried out and statistical analysis of the data should be done: it is not the aim of this PhD research.

In this paragraph a short qualitative comparison of both starches will be given. The observation of the data shown in Fig.4.15 obtained for potato starch suggested that the deformation asymptotically reaches a maximum value approximately twice its initial size at shear stresses of around 1500Pa (the decrease in size during the experiment was not monitored); this value is lower than those reported for microgel particles (Vervoort & Budtova, 2003). On the other hand, the deformation of the modified waxy maize starch granule did not stabilise but rather reached a maximum value of 1.8 at τ = 1300Pa before decreasing. This suggested that solvent release and ejection in the suspending medium occured, although it

could not be visualised during the experiment. On the other hand, solvent release (pointed tips) was visible for potato starch (Figure 4.15 b and c) at high shear stresses, approximately above 1500Pa, when the granules have reached their maximum deformation. Nevertheless, as for modified waxy maize starch, the ejection in the matrix was still not visible. The process of solvent ejection could not be visualised using the experimental set-up for both potato and modified waxy maize, therefore it was not possible to determine a critical stress for this occurrence. Solvent release and ejection has been previously reported for a swollen particle submitted to simple shear (Vervoort & Budtova, 2003; Zanina & Budtova, 2002; Zeo et al., 2005).

It was shown that modified waxy maize had a volume decrease of 29% whereas the values found for potato starch did not exceed 18%. Although the granules do not have the same swelling degree, it would be expected to have a greater volume loss for potato starch granules as they should be more swollen. The differences in the amount of solvent ejected between potato and modified waxy maize could be explained by different hypotheses. First, the initial size of the starch granule is small or it is poorly swollen. Another possibility to consider is the presence of holes and cracks in the modified waxy maize granules which could lead to higher solvent ejection than for potato starch as the latter has an undisrupted surface. Also, the high level of organisation of the periphery of the potato granule could delay solvent ejection (Blaszczack et al., 2005; Fisher et al., 1998; Sevenou et al., 2002). Finally, the interfacial tension between the released material and the suspending medium plays a major role: a high interfacial tension can prevent solvent ejection (Zeo et al., 2005). It should be considered when studying the solvent release. As will be shown in the next chapter, the released solvent can be a low molecular weight amylopectin solution. In any case, further investigation on the nature of the ejected solvent is needed as well as more systematic experiments on various granules (considering size and swelling degree) in order to carry out statistical analysis.

IV.2.3. Conclusions

The study of dry and swollen-in-water starch granules submitted to simple shear revealed interesting behaviour as well as differences between the granules depending on the botanical source. First, the rotation of the dry granules followed that of solid spheres considering the experimental error. The experiments in simple shear flow carried out on swollen-in-water granules showed that they could deform up to twice their initial size (or more depending on the swelling) which is interesting as it has always been suggested but never demonstrated in this type of flow. Even more interestingly, evidence of solvent ejection in the suspending matrix was found.

IV.3. Conclusions for Chapter 4

The microscopic study of single starch granules, dry and swollen, revealed differences in the shape, size and surface properties depending on the botanical source.

Their behaviour under simple shear flow showed that dry granules acted like solids, and that their behaviour is close to that of spheres within the experimental error. Swollen-in-water granules, deformed as expected but also ejected solvent in the suspending medium. This is an interesting result that has never been shown before. Again, differences occurred between the starches; they were explained by the properties specific to each starch revealed by the SEM and AFM study. Differences in composition (amylose and amylopectin) could also lead to variation in interfacial tension which might explain the differnces in solvent ejection. However, the composition of the released and ejected solvent is not known. Further investigation is needed to better determine what comes out and how it varies with the granule swelling. Whatever is ejected, it may have an influence on the suspension rheology In the second part of the following chapter, the supernantant of the starch suspension is under study; it could answer the questions on the polymeric components that are released from modified waxy maize starch and their amount.

Reference List

Baldwin, P. M., Adler, J., Davies, M. C., and Melia, C. D. (1998). High Resoltuion Imaging of Starch Granule Surfaces by Atomic Force Microscopy. *Journal of Cereal Science*, 27, 255-265.

Blaszczack, W., Valverde, S., Formal, J. (2005). Effect of high pressure on the structure of potato starch. *Carbohydrate Polymers*, 59, 377-383.

Dang, J. M. C. and Copeland, L. (2003). Imaging Rice Grains Using Atomic Force Microscopy. *Journal of Cereal Science*, 37, 165-170.

Doublier, J. L., Llamas, G., and Lemeur, M. (1987). A Rheological Investigation of Cereal Starch Pastes and Gels - Effect of Pasting Procedures. *Carbohydrate Polymers*, 7, 251-275.

Fischer L.R, Carrington S.P, and Odell J.A (1997). Deformation Mechanics of individual swollen starch granules., 105-114.

Jeffery, G. B. (1922). The motion of ellipsoidal particles in a viscous fluid. *Proceedings of the Royal Society of London Series A-Containing Papers of A Mathematical and Physical Character*, 102, 161-179.

Kolli, V. G., Pollauf, E. J., and Gadala-Maria, F. (2002). Transient normal stress response ina concentrated suspension of spherical particles. *Journal of Rheology*, 46, 321-334.

Oates, C. G. (1997). Towards an understanding of starch granule structure and hydrolysis. *Trends in Food Science & Technology*, 8, 375-382.

Sevenou, O., Hill, S. E., Farhat, I. A., and Mitchell, J. R. (2002). Organisation of the external region of the starch granule as determined by infrared spectroscopy. *International Journal of Biological Macromolecules*, 31, 79-85.

Szymonska, J. and Krok, F. (2003). Potato starch granule nanostructure studied by high resolution non-contact AFM. *International Journal of Biological Macromolecules*, 33, 1-7.

Vervoort, S. and Budtova, T. (2003). Evidence of shear-induced polymer release from a swollen gel particle. *Polymer International*, 52, 553-558.

Zanina, A. and Budtova, T. (2002). Hydrogel under shear: A rheo-optical study of the particle deformation and solvent release. *Macromolecules*, 35, 1973-1975.

Zeo, U., Tarabukina, E., and Budtova, T. (2005). Kinetics of shear-induced gel deswelling/solvent release. *Journal of Controlled Release*, 108, 73-83.

Résumé du chapitre V

Propriétés d'une suspension d'amidon

Ce chapitre a pour but la caractérisation de la suspension d'amidon sous écoulement mais aussi de sa phase continue. Lorsque l'amidon de maïs cireux modifié est ajouté sous agitation dans de l'eau et que ce mélange est chauffé, les grains d'amidon vont gonfler sous l'action thermique. Il en résulte une suspension de granules plus ou moins gonflés selon les conditions, suspendus dans un liquide qui est a priori de l'eau. Néanmoins, une certaine quantité de molécules peuvent sortir des granules et modifier les propriétés de la phase continue et par conséquent la rhéologie de la suspension.

Dans la première partie, les suspensions d'amidon ont été étudiées à l'aide d'un rhéomètre en mode écoulement et oscillatoire. Tout d'abord, un cas particulier où les granules sont gonflés au maximum et la fraction volumique théorique est 1 a été considéré. Dans le cas présent, la suspension est en régime dit concentré, c'est-à-dire au-delà de la fraction volumique critique où les granules sont en contact. Dans ce cas, il a été montré que:

- La suspension a un seuil d'écoulement.
- Au-delà de ce seuil, la suspension est rhéofluidifiante dû à la déformation et l'orientation des granules dans le sens de l'écoulement.
- Une première différence de force normale peut être mesurée pour des contraintes au-delà de 300Pa. Or, les granules d'amidon commencent à se déformer à ces contraintes. Dans ce cas, les granules stockent de l'énergie à l'origine de l'élasticité de la suspension.
- Les mesures de viscoélasticité en faible déformation indiquent que la suspension a un comportement de type gel.

Il existe une concentration minimale pour laquelle les granules sont en contact. Elle est définie comme étant la concentration à laquelle un seuil d'écoulement peut être déterminé. Dans le cas de l'amidon étudié et aux conditions

de préparation présentées dans le chapitre « Matériaux et méthodes », cette concentration est de 5% (défini rhéologiquement).

Au dessous de cette concentration, il a été montré que la rhéologie de la suspension est principalement gouvernée par la phase continue et la fraction volumique occupée par les granules. Des interactions entre granules suffisamment proches (fraction volumique = 0.4) ont été mises en évidence. Il semblerait que des molécules en surfaces des granules puissent interagir, permettant ainsi une augmentation de la viscosité.

Au dessus de la concentration critique, en régime concentré, la rhéologie est gouvernée par la rigidité des granules ; moins les granules sont déformables, plus la viscosité et le seuil d'écoulement sont élevés. De plus, un grand nombre de granules va multiplier les zones de contacts et par conséquent le nombre d'interactions mécaniques ce qui augmente d'autant plus le seuil d'écoulement.

L'étude de la tension de surface entre l'air et la phase continue de la suspension a révélé qu'une certaine quantité de polymère était solubilisée lors de la préparation des échantillons. Une analyse plus poussée a permis de déterminer la nature du composant relargué dans la phase continue ainsi que la quantité. La phase continue de suspensions de diverses concentrations ont été regardées (1%, 3% et 5% d'amidon dans la suspension initiale). Tout d'abord, le composant a été identifié à l'aide de la DSC et d'une méthode de complexation avec l'iode. Ces deux expériences ont montré que de l'amylopectine était présent dans la phase continue. Ensuite l'ultracentrifugation et la chromatographie d'exclusion stérique ont permis de déterminer la quantité relarguée et sa masse moléculaire. Il semblerait que de l'amylopectine de faible masse moléculaire soit présent dans la phase continue et que sa concentration augmente quand la concentration en amidon dans la suspension initiale augmente. La présence de l'amylopectine dans la phase continue peut être expliquée par :

- Les molécules d'amylopectine en surface sont arrachées par l'agitation mécanique lors de la préparation et se retrouvent donc dans le milieu aqueux.
- Certaines molécules d'amylopectine sont suffisamment petites pour sortir des granules d'amidon lors de la procédure de préparation

Ces deux hypothèses ensemble peuvent expliquer la présence de l'amylopectine dans la phase continue. La concentration en amylopecine est suffisamment faible pour avoir peu d'influence sur la rhéologie de la suspension.

Chapter V: Properties of the starch suspension

This chapter is dedicated to the properties of a starch suspension. The latter is composed of swollen-in-water starch granules immersed in the solvent, namely water and soluble matter. The interest of this chapter is to get a better understanding of the rheological behaviour of the suspensions, the influence of granular concentration and rigidity. The soluble fraction in the continuous media is also investigated. Determination of the polymer content in the solvent is important as it might have an impact on the overall rheology of the suspension. In a first part, the flow and viscoelastic behaviour of the suspension will be discussed. The 'ideal' case, where the starch granules are swollen to their maximum and the theoretical volume fraction is 1, is first examined; the influence of concentration on rheological behaviour is then presented. Finally, the purpose of the second part is to show the presence of polymeric material released in the solvent, to determine its nature and quantify its amount.

V.1. Rheological study of a starch suspension

In this section the rheological behaviour of the modified waxy maize starch suspension is studied. In a first part a specific case will be considered, where the starch granules are packed at the maximum fraction (i.e. $\Phi = 1$) but are nevertheless swollen to their maximum. This theoretical volume fraction of 1 is possible due to the specific properties of the starch granules: high deformability, polydispersity and irregular shape. The suspension is prepared at 8%w/w (see preparation in Chapter III.1.1.3); the suspension is concentrated and there is little or no solvent around the granules. In a second part, the influence of concentration will be studied. All rheological measurements were carried out at 20°C.

V.1.1. Suspension at maximum average swelling and at theoretical volume fraction of 1

V.1.1.1. Influence of geometry

The choice of geometry to measure the flow behaviour of a suspension is governed by several considerations. Different problems can arise depending on the geometry used. With a cone-plate, the size of the particles can be an issue; if they are too large, they can not fully relax (Cloitre, 2005). In the case of a plate-plate geometry, the shear rate is inhomogeneous within the gap as a gradient of shear rate develops along the radius with shear rates being higher at the edge of the plate and lower for small radii. The particles agglomerate in the low shear rate zones leading to a decrease in viscosity over time for a constant shear rate or shear stress. With a smooth surface like stainless steel (used here) slip can occur. This phenomenon is due to a depletion of particles at the surface of the plates. Under motion particles deform asymmetrically creating a force pushing the particles away from the wall (Cloitre, 2005). Bigger particles induce a thicker slip layer due to steric hindrance (Gulmus & Yilmazer, 2005). The vane is appropriate to measure systems that can have a yield stress, which is the case of this suspension as it is above close packing fraction.

Different geometries were tested to rule out the occurrence of slip by determining if there are any differences in yield stress depending on the used geometry. The most adequate geometry for the measurements carried out was determined. Results obtained with various geometries are presented Figure 5.1.

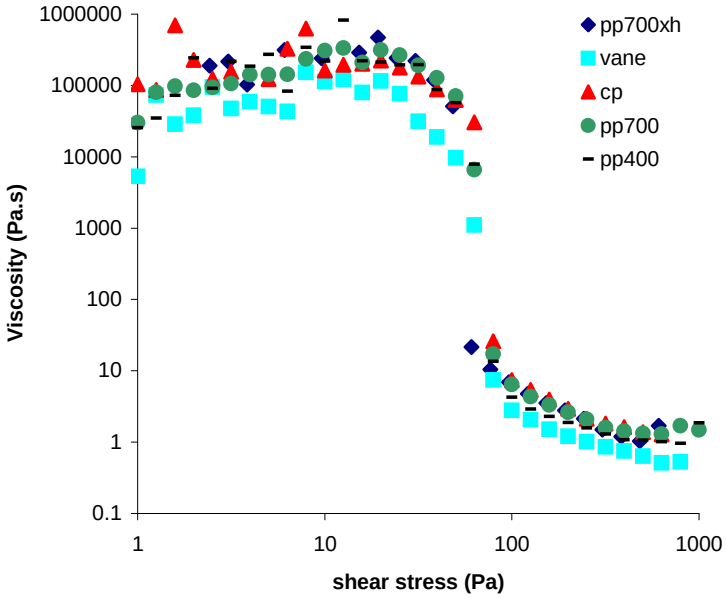

Figure 5.1: Comparison of geometries and gap settings. Influence of the geometry on starch suspension yield stress. Legend: pp is for parallel plates, the following number is the gap size, xh is for a cross-hatched parallel plate (e.g. pp700xh is cross-hatched parallel plate with a 400µm gap), cp is for cone-plate geometry.

As seen in Figure 5.1, yield stress did not vary with varying geometry or even with different gaps; slip does not seem to occur. Above the yield stress the starch paste is shear thinning. Below the yield stress the granules are trapped by the neighbouring granules; when the shear stress is high enough the granules can rearrange and order themselves under flow. This structuring is made easier by the deformability and softness of the particles (Adams et al., 2004; Jacquier et al., 2006). For further flow measurements the cone-plate geometry was used.

V.1.1.2. Optimization of the measurements

Performing rheological measurements on the starch suspensions can be difficult as the properties of soft concentrated suspensions may vary in time. Results could be altered by sample preparation and shear history. If no pre-shear is applied, the granules are not submitted to the same history and the results thus obtained are not completely reproducible (Figure 5.2).

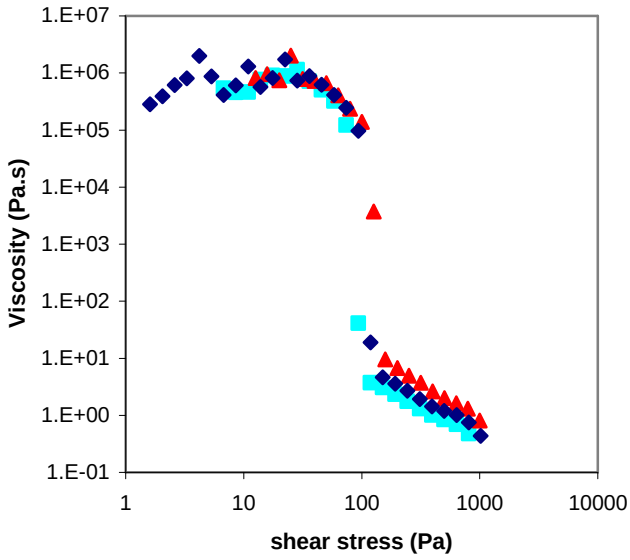

Figure 5.2: Same sample loaded three times; absence of pre-shear. Effect on reproducibility of results.

In order to obtain reproducible results the starch suspensions were submitted to a pre-shear slightly above the estimated yield stress and the sample was let to recover for 20min (Cloître, 2005; method described in Section III.2.2.1). Results obtained are shown Figure 5.3.

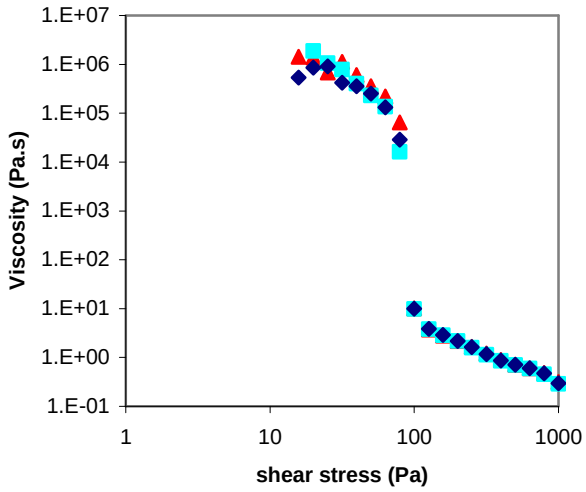

Figure 5.3: Same starch suspension loaded three times (3 different samples), presence of pre-shear followed by a rest time of 20min.

In this Figure the curves were obtained for the same starch suspension preparation. Three tests were conducted, each time loading a new sample of the same suspension. It can be seen here that the second parts of the curves coincide perfectly. It can be concluded that the method has proven satisfactory and the information obtained can be considered as valid.

Another issue that may occur when determining the rheological behaviour of a starch suspension is the sample preparation, as the latter might have an impact on the final properties. The method was described in section III.1.1.2 and the samples were always prepared in the same way. However, the starch suspension samples are only used for a few hours as they can retrograde (rearrangement of the polymer chains). Due to the aging of the starch sample, new suspensions were prepared every day. The polydispersity of the granules and their differences in swelling rate and final swelling degree might account for suspensions displaying slightly different flow curves from one sample to another. Figure 5.4 shows the results obtained with two samples prepared separately in the same conditions, using the same procedure.

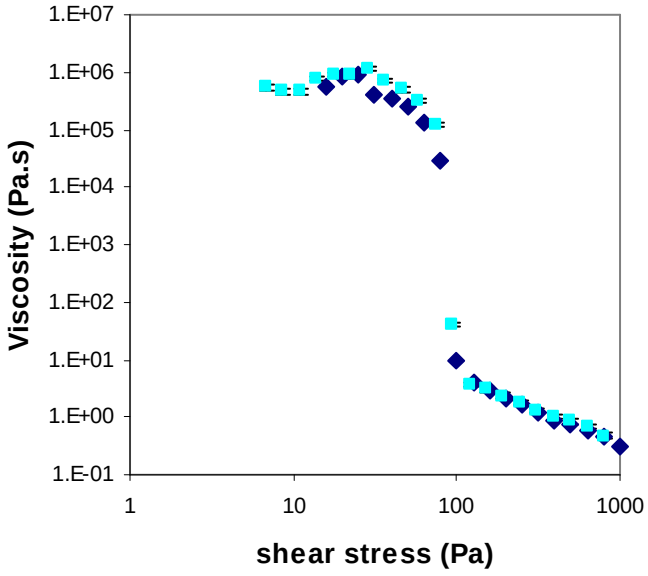

Figure 5.4: Results for two samples prepared separately using the same preparation procedure; Reproducibility of the sample preparation method

Through Figure 5.4, it can be seen that the method used for sample preparation is quite reproducible and that results obtained for starch suspensions prepared with the same method but separately can be compared.

Consequently, it is possible to say that the sample preparation and the measurement method were adequate. Assumptions can be made that all further measurements were correct and could be analysed.

V.1.1.3. Description of the flow curve

A yield stress can be measured in suspensions at concentration above the close packing concentration. The suspension acts like a solid below a certain stress applied; above that specific stress the suspensions starts to flow. Figure 5.5 (a) and (b) are representations of the same data set.

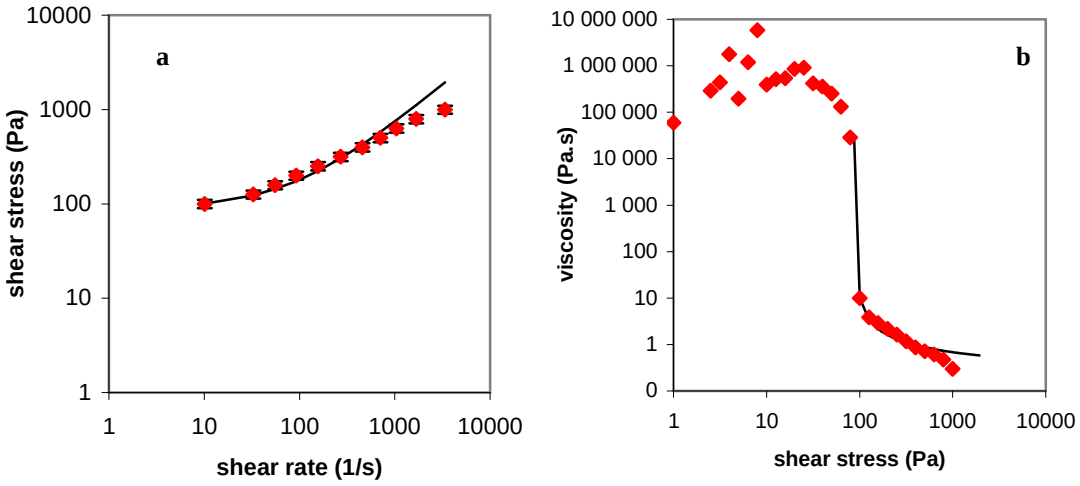

Figure 5.5: Different representation of the same data set. (a) Shear stress vs. shear rate; (b) Viscosity vs. shear stress. Squares is the measured data, the black line represents the Herschel Bulkley model.

Figure 5.5 (a) shows the presence of a yield stress which is not obvious when looking at Figure 5.5 (b). Indeed, on the flow curve (viscosity vs. shear stress) a 'pseudo' Newtonain plateau can be seen; this plateau could be an artefact as the rheometer is not measuring the flow of the suspension but that of a solid. Seeing that this starch suspension is a yield stress fluid, the data was fitted with the Herschel Bulkley model (Equation 5.1):

$$\tau = \tau_0 + k\dot{\gamma}^n \qquad 5.1$$

where τ is the shear stress, τ_0 the yield stress, $\dot{\gamma}$ the shear rate, k is the consistency coefficient and n the power index.

The value of yield stress hence obtained is 95 ± 3Pa which is the mean value of 8 measurements. The determination of the yield stress can be considered as accurate as the model fits the beginning of the curve: from the yield stress (determine around 95Pa) to around 300Pa (see Figure 5.5b). However, for shear stresses above 300Pa, the curve starts deviating from the model. This discrepancy has been reported in literature (Omari et al., 2006) and can be attributed to the deformability of the granules as the Herschel Bulkley model (HB model) was developed for rigid spheres. Moreover the population of granules is polydisperse and individual granules are of irregular shape (as seen in Chapter IV section IV.1)

also causing the flow behaviour to deviate from the HB model. Another possible reason for the deviation from the HB model is the appearance of a measured first normal stress difference (N_1 starts being measured for τ = 300Pa).

The yield stress can be explained by the fact that the granules are surrounded by other granules and considered to be entrapped in a "cage" with no possibility to move (Cloitre, 2005). When increasing the shear stress, energy barriers are overcome and the granules can reorganise themselves and exchange position, going from a disordered to an ordered state. Above the yield stress, granule orientation and deformation occur, reducing their resistance to flow (Evans & Haisman, 1980; Jacquier et al., 2006; Snabre & Mills, 1999).

V.1.1.4. Time dependence: thixotropic/antithixotropic behaviour

In this section the time dependence of the starch suspension viscosity was studied. It should be noted that in this case a pre-shear was <u>not</u> performed and the sample was not let to recover. This might influence the results. Indeed, the rest time (recovery) after pre-shear is usually conducted to erase possible thixotropic effects (Mahaut et al., 2008). Results in Figure 5.6 show the viscosity as a function of shear rate for the 8% starch suspension (theoretical voulme fraction is 1).

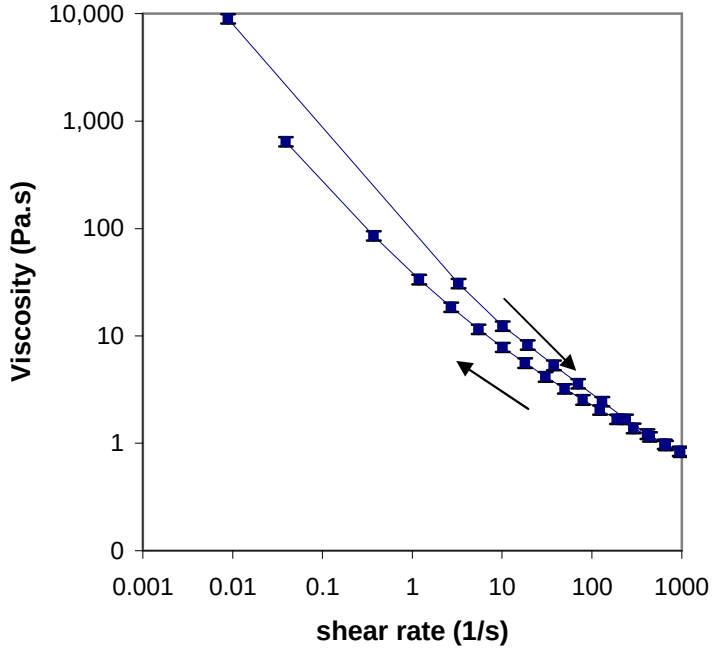

Figure 5.6: Viscosity vs. shear rate; up and down curve. Lines are given to guide the eye.

A thixotropic behaviour was observed for the starch suspension sample as it can be seen in Figure 5.6. This type of behaviour has been previously reported for different types of starch (Doublier, 1986; Doublier et al., 1987; Nguyen et al., 1998). Thixotropy depends on the type of starch, the preparation procedure and the swelling capacity (Doublier et al., 1987); the more the granules are swollen, the more "sensitive" the suspension is to shear, namely the granules are more deformable and the suspension is more shear thinning, inducing a more thixotropic behaviour. However, studies on modified (cross-linked) waxy maize starch revealed a tendency to thixotropy at high shear rates and antithixotropy at low shear rates and a much lower sensitivity to shearing (Tattiyakul & Rao, 2000; Thebaudin et al., 1998; Velez-Ruiz et al., 2006). Tattiyakul & Rao (2000) suggested that it was due to the rupture of granules which occurred under the effect of high shear and high temperature (130°C), thus releasing amylopectin. They interpreted the antithixotropy at low shear as being a result of a shear induced structure of these macromolecules.

V.1.1.5. First normal stress difference

First normal stress differences usually develop in a viscoelastic sample and are associated with non linear effects. It can be measured when the normal stresses are no longer equal (see figure 5.7). At low shear rates, the flow is slow enough for second order terms to be negligible; therefore the normal stresses are equal. However, when increasing the shear rate, normal stress differences appear as second order effects (Barnes et al., 1989).

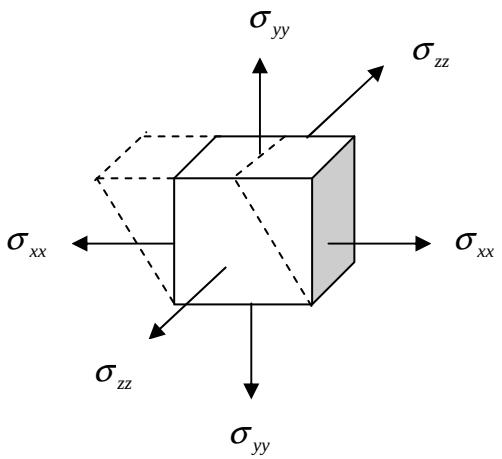

Figure 5.7: stress distribution in simple shear flow on a viscoelastic element (Harris, 1977)

In simple shear flow:

$$v_x = \dot{\gamma}\gamma \quad \text{and} \quad v_y = v_z = 0 \qquad 5.2$$

$$\sigma_{xy} = \sigma = \eta(\dot{\gamma})\dot{\gamma}, \qquad \sigma_{xz} = \sigma_{yz} = 0 \qquad 5.3$$

$$\sigma_{xx} - \sigma_{yy} = N_1(\dot{\gamma}), \qquad \sigma_{yy} - \sigma_{zz} = N_2(\dot{\gamma}) \qquad 5.4$$

with N_1 first normal stress difference and N_2 second normal stress difference. From a physical point of view, unequal normal stress components arise from the fact that in a flow process the microstructure of the liquid becomes anisotropic.

Results obtained for the 8% suspension are presented Figure 5.8. Three replicates are shown here which were reproducible. It can be seen that first normal stress differences can be measured during a flow measurement above 300Pa

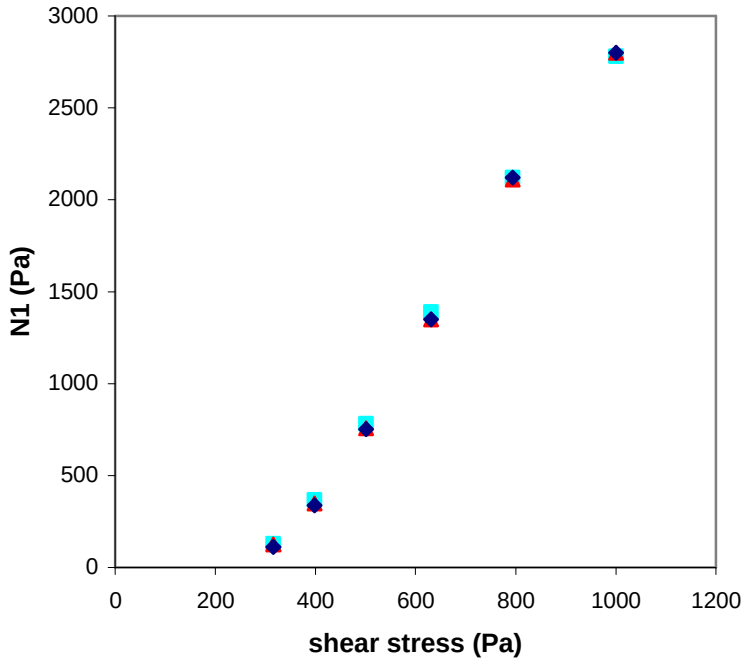

Figure 5.8: First Normal stress difference vs. shear stress. Results shown here are 3 replicates.

It was suggested that the origin of elasticity in an emulsion is due to an excess of interfacial energy stored when the emulsion droplet is deformed (Holmes et al., 2005; Seth et al., 2006). Here it is a suspension and not an emulsion; however, some parallels could be made. As seen in the previous Chapter, the starch granules start deforming when the stresses applied exceed 300Pa. It is possible to think that

measured first normal stress differences are correlated with deformation of the granules. Being deformed the granules store energy; this excess of energy then results in elasticity of the sample.

V.1.1.6. Viscoelasticity of the suspension

The viscoelastic behaviour measured at small deformations of the starch suspension is shown Figure 5.9. Measurements were carried out in the linear regime in the range of frequencies applied. Three samples of the suspension were loaded three different times, showing the reproducibility of the results. The main observation is that the elastic modulus G' is much higher than the viscous modulus G''. Moreover, both G' shows little or no frequency dependence, suggesting a gel-like behaviour. This is what was expected taking into account steady-state results: the suspension of closely packed particles is in a "solid-like" state, particles are not moving, they are slightly deforming under the stress applied and all energy is dissipated by the particles' elastic response.

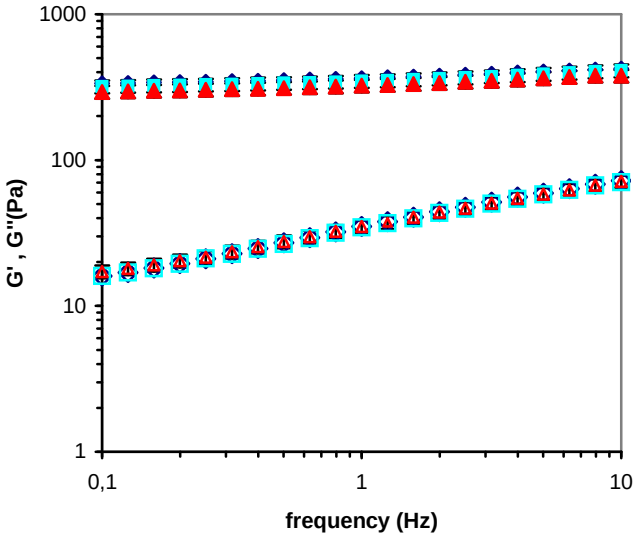

Figure 5.9: Viscoelastic properties of a starch suspension at a theoretical volume fraction of 1. Constant stress τ =1Pa. Close symbols G', open symbols G''.

This gel like behaviour was frequently reported for starch suspensions (Rao et al., 1997; Tattiyakul & Rao, 2000; Thebaudin et al., 1998). All of these studies also showed that starch suspension did not follow Cox-Merz rule, suggesting that it was due to its gel-like behaviour. For the 8% starch suspension the observation of Cox-Merz rule is pretty good for a complex system (Figure 5.10). However, the application of the Cox-Merz rule can be questioned as the response of granules to forces applied in both modes can be very different.

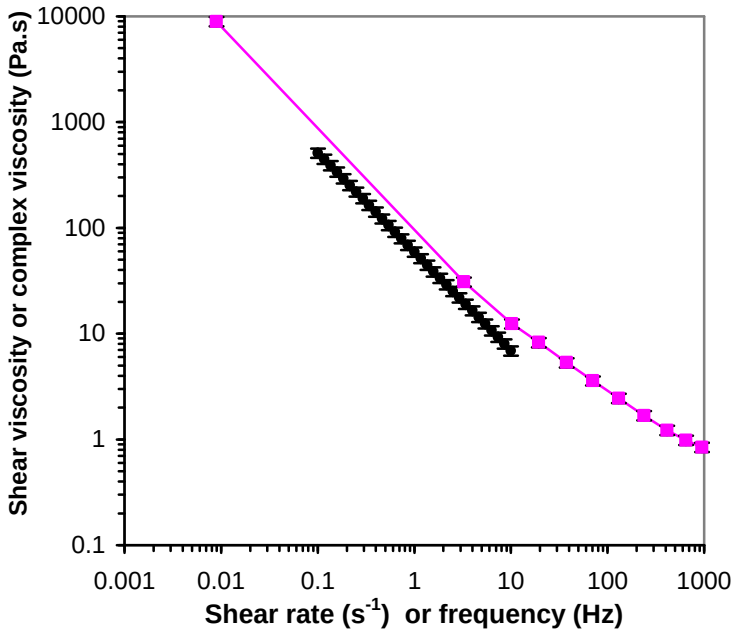

Figure 5.10: Representation of the Cox-Merz rule. x-axis: frequency or shear rate; y-axis: shear viscosity or complex viscosity. Dots are for the complex viscosity as a function of frequency, square are for the shear viscosity vs. shear rate.

V.1.2. Influence of starch concentration on suspension behaviour

In the following section, the starch concentration is varied; the concentrations, volume fractions and equivalent swelling degree at these volume fractions used in this section are given in Table 5.1.

Table 5.1: Values of concentration, volume fraction and swelling decree.

Concentration (%w/w)	Φ	Q (g/g)
1	0.125	12.5
3	0.375	12.5
5	0.615	12.5
7	0.875	12.5
8	1	12.5
9	1	11.1
10	1	10.0
12.5	1	8.0
15	1	6.7
20	1	5.0

V.1.2.1. Flow behaviour of suspensions with a volume fraction below 1

Measurements on starch suspensions with volume fractions below 1 were carried out. In these conditions sedimentation problems might occur and it is of importance to ensure that this does not happen during the measurements. Sedimentation rate was evaluated through calculation using Stokes equation (5.5):

$$\nu = \frac{2r^2 \Delta\rho g}{9\eta} \qquad 5.5$$

where v is the sedimentation rate, r the radius of the granule, Δρ the difference in density between the granules and the continuous media, g the acceleration due to gravity and η the dynamic viscosity of the continuous media. The mean radius of swollen granules was taken to be 20μm, η was taken to be that of the supernatant of the suspension (1.02Pa s for a 1% suspension and 1.07Pa.s for a 3%w/w suspension) and measured using the rolling ball viscometer, described in section III.2.2.3. Finally the density of the suspension was considered to be that of a swollen granule to its maximum (swelling degree 12.5g/g). The density was calculated by considering the density of the dry granule and the density of water (density of the swollen granule = (density of the dry granule + 11*density of the water)/12).

For starch suspensions of 1% and 3% polymer concentration (0.125 and 0.615 particle volume fraction considering that granules are at their maximal swelling degree which is 12.5 g/g) the approximate value of sedimentation is $0.1mm.h^{-1}$ which is slow enough to perform proper measurements (Evans & Haismann, 1980). Nevertheless, special care was taken to make sure the results obtained reflected that of a homogeneous suspension. Measurements were performed by starting at high shear stresses and decreasing to lower values. The flow behaviour of a 1% starch suspension (volume fraction = 0.125) is presented Figure 5.11.

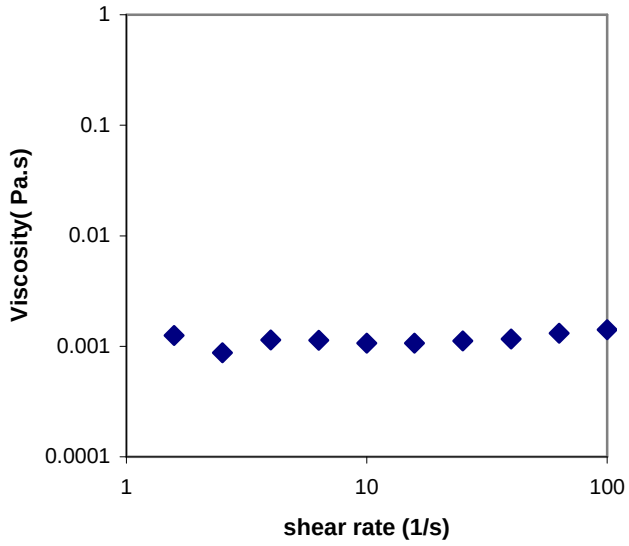

Figure 5.11: Flow behaviour of a 1% w/w starch suspension, Φ= 0.125

It can be seen in Figure 5.11 that a starch suspension at Φ=0.125 volume fraction (1%w/w) displays a Newtonian behaviour. Moreover the viscosity of the suspension is close to that of the continuous medium which in turn is very close to water. Hence, it is possible to think that in this case the continuous phase of the suspension plays a major role in the overall viscosity as the volume fraction occupied by the granule is low. Measurements were also carried out for suspensions of 3 and 5% w/w, which correspond to volume fractions of 0.375 and 0.615 respectively. The flow behaviour of both suspensions is presented Figure 5.12.

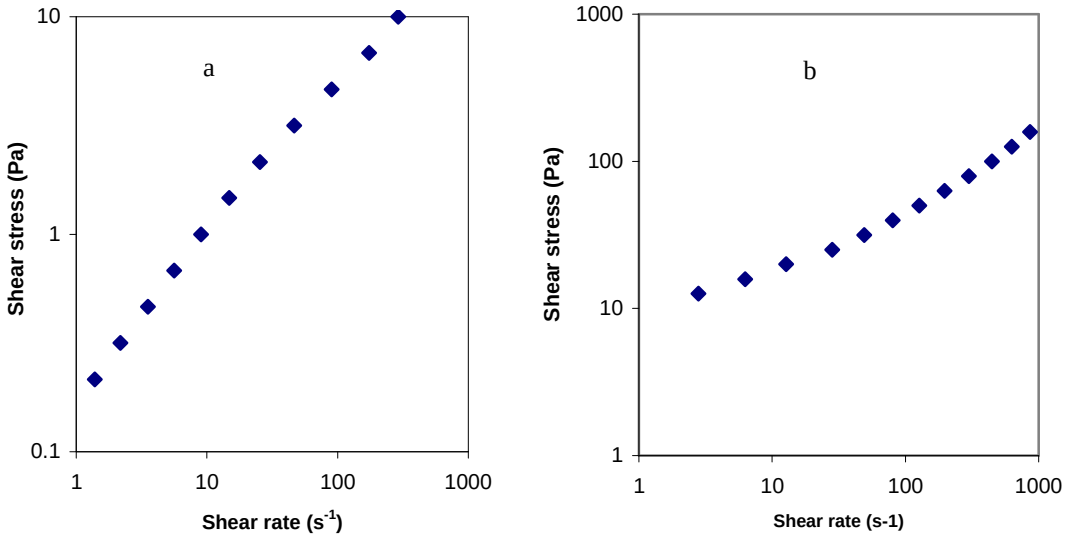

Figure 5.12: Flow behaviour of starch suspension; Shear rate vs. shear stress. (a) 3% w/w, Φ= 0.375. (b) 5% w/w, Φ= 0.615.

Both suspensions presented in Figure 5.12 display shear thinning behaviour. The 3% suspension displayed a Newtonian plateau followed by a slight shear thinning at high shear rates. The data shows that for the 3% suspension no yield stress can be measured whereas for 5% w/w a yield stress value of around 1Pa was found. It can thus be thought that at 5% (or 0.615 granule volume fraction) the suspension is at the close packing concentration or at least slightly above it. This value is close to the one reported for a close-packing fraction of emulsions (Saiki et al., 2007). However, many studies have shown that a polydisperse suspension should see its value of close packing fraction higher than 0.63 as small granules can be dispersed among larger ones (Seth et al., 2006). The fact that starch suspension demonstrates rather low close packing concentration suggested that other mechanisms, such as inter-particle interactions, occur when considering such granules.

The dependence of suspension viscosity on particle volume fraction is shown in Fig. 5.13. Viscosity data are taken from Newtonian region. If the granules were rigid spherical particles, such suspension viscosity could be estimated through the Krieger Dougherty model (Krieger & Dougherty, 1959) (KD model, see Equation 5.6), as shown in Figure 5.13.

$$\eta = \eta_0 \left(1 - \frac{\phi}{\phi_{max}}\right)^{-2.5\phi_{max}} \qquad 5.6$$

where η_0 is the viscosity of the suspending medium, ϕ is the volume fraction of the suspension, ϕ_{max} is the maximum volume fraction that can be obtained for a solid sphere suspension (in this case ϕ_{max} = 0.63). However, starch granules are deformable and the maximum packing fraction can be 1 which means that no correlation with KD should be expected.

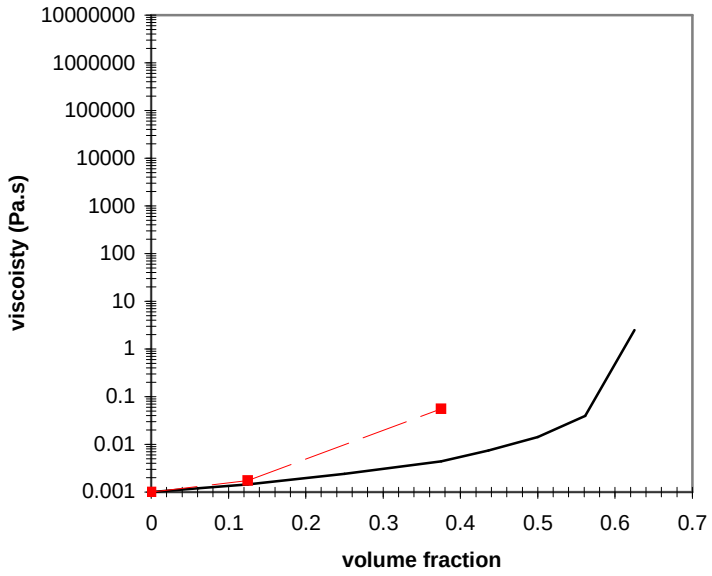

Figure 5.13: Viscosity vs. Volume fraction; solid line represents the KD model, dashed line is the viscosity of the paste determined at 1Pa (Newtonian plateau).

For low volume fraction (0.125, i.e. 1%w/w concentration) the estimated viscosity is in good agreement with the KD predictions. It may be speculated that at very low shear rates and at low concentrations the suspension of swollen granules can be considered as a solid sphere suspension, as long as the granules do not deform. The behaviour of the suspension starts to strongly deviate from the KD model for volume fractions higher than 0.3-0.4; similar values were also found by Saiki et al. (2007). At these volume fractions, the volume concentration of particles is high enough to induce perturbations of the flow streamlines, creating hydrodynamic interactions with the neighbouring granules and thus increasing the

suspension viscosity. The flow perturbation may also lead to the deformation of the granules. However, if the granules start deforming and orienting in the flow direction, the viscosity should be lower than that predicted for hard spheres. Hao (2008) suggested that the abrupt increase of viscosity for lower volume fraction was correlated to the particle shape; e.g. for fibre type shapes the increase in viscosity occurs for much lower volume fraction. In the studied case, modified waxy maize starch granules have a nearly spherical shape; therefore the influence of aspect ratio is negligible. The deviation occurred for volume fractions of 0.3-0.4 for which no yield stress was measured. This viscosity increase, compared to the hard sphere model, at low volume fraction strongly suggests the formation of a sort of a network before close packing occurs. The formation of the "network" would be the result of interparticle interactions between adjacent molecules at the surface of the starch granules (Abdulmola et al., 1996; Evans & Haisman, 1980; Hao, 2008).

V.1.2.2. Effect of starch concentration above close packing volume fraction on flow behaviour and yield stress

In this section, most of the studied suspensions had the same volume fraction (Φ = 1), except the 5% and 7%w/w suspensions (volume fractions are 0.615 and 0.872 respectively). Above 8% (volumes fractions are unity) only the granule "rigidity" changed as the swelling decreased (Table 5.1). By increasing starch concentration, the amount of water for each granule is reduced; the granules are poorly swollen and their deformability decreases.

At high starch concentrations, the rigidity of the granules is much higher than for low starch concentration (but equivalent volume fraction) where the granules are fully swollen. The behaviour of suspensions with concentrations varying from 5% to 20% is presented Figure 5.14. For all suspensions a yield stress was determined; it increased with increasing concentration (Figure 5.15). Above the yield stress, i.e. disruption of the "cage" structure, all suspensions were highly shear thinning. This type of behaviour was previously reported for agar microgel suspensions (Adams et al., 2004). The shear thinning behaviour can be attributed to the deformability of the granules allowing them to orient in the flow direction

(Jacquier et al., 2006; Saiki et al., 2007). Although the granule rigidity increased, no shear thickening behaviour was observed in the studied range of shear stresses. It is probably because even at these low swelling degrees the granules are still slightly deformable.

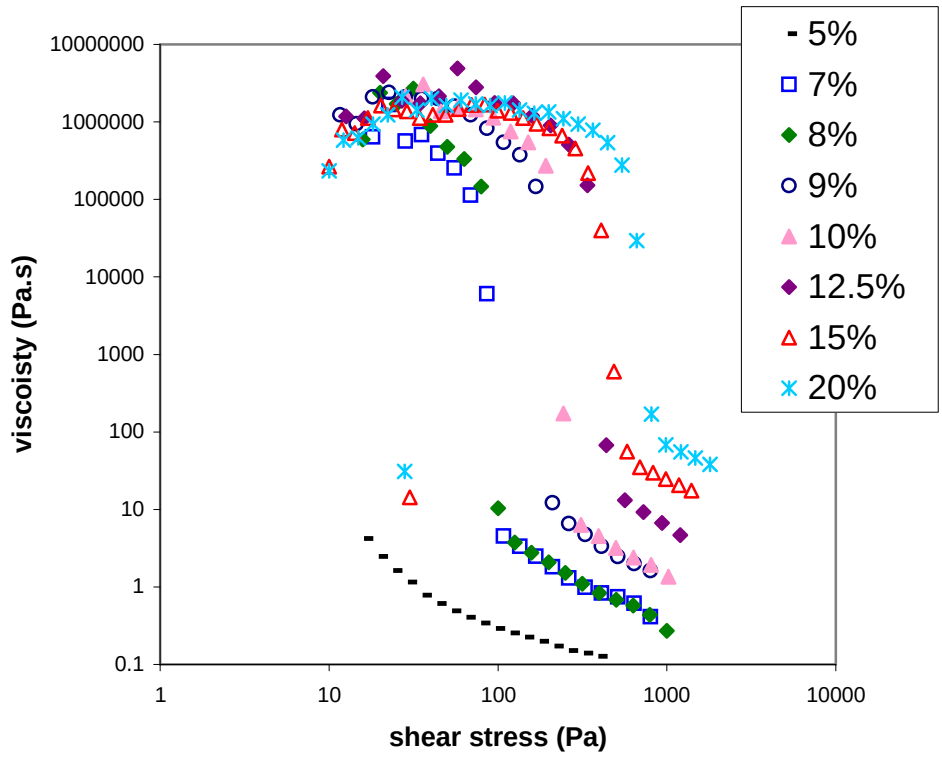

Figure 5.14: Flow of starch suspensions at various concentrations and granule swelling degrees.

Figure 5.15 shows the evolution of the yield stress value with starch concentration. It can be seen here that the yield stress increased linearly with increasing concentration; this behaviour was previously reported for magnetic particle suspensions (Evans & Haisman, 1980; Kwon et al., 1997), but for suspensions with volume fractions below 1. The yield stress value tended towards zero at a certain starch concentration which corresponds to the concentration for close packing onset (Evans & Haisman, 1980). Consequently, the close packing fraction can be determined as 0.625 corresponding to 5% w/w which is in good agreement with our previous observations (section V.1.2.1). As the concentration increase, the number of contact zones between the granules increase. Kolli et al. (2002) suggested that mechanical interactions could occur between particles with a certain surface

roughness, increasing their contact. As shown in the previous chapter, modified waxy maize starch granules possess a relative surface roughness. Mechanical interactions could explain the increase of viscosity and yield stress; when the number of granules increases, the mechanical interactions become more numerous.

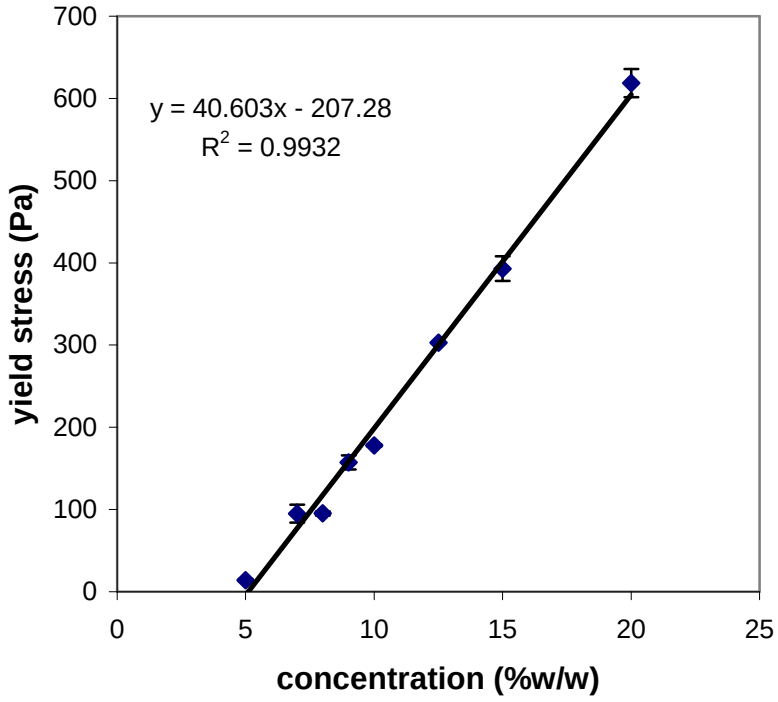

Figure 5.15: Evolution of yield stress as a function of the starch concentration

The behaviour of starch suspensions was studied for suspensions with a constant volume fraction of 1, but with increasing starch concentration. This is possible because the granule swelling degree can be varied and the volume fraction of 1 can be achieved due to granules deformability and highly convoluted shapes. As the concentration is increased, the rigidity of the granules will also increase as less water is available for the granules. This type of study has not yet been carried out to our best knowledge. A non-linear viscosity increase would be expected when granule rigidity increases (Nayouf et al., 2003). From the onset of the close packing fraction, i.e. the lowest concentration for which the granules are in contact (in our case, 5%w/w and $\Phi = 0.625$), to the highest presented concentration, the increase is linear (Figure 5.15) suggesting that above close packing fraction, the rigidity of the granules varies linearly with the concentration. Above the close packing fraction, the rigidity of the granules governs the overall viscosity as shown by Figure 5.15.

Results obtained for first normal stress difference as a function of concentration are not shown here as they were not very conclusive. A more systematic study is needed to obtain reproducible results. However, the qualitative results showed that N_1 increased with increasing concentration. The granule rigidity or deformability seems to be playing a major role as for viscosity measurements.

V.1.2.3. Evolution of viscoelastic properties with starch concentration

The evolution of the viscoelastic behaviour of starch suspensions of various concentrations is presented below, Figure 5.16 (elastic modulus as a function of frequency). For clarity the viscous modulus curves are not presented; G' values were two decades lower and showed slightly more frequency dependence.

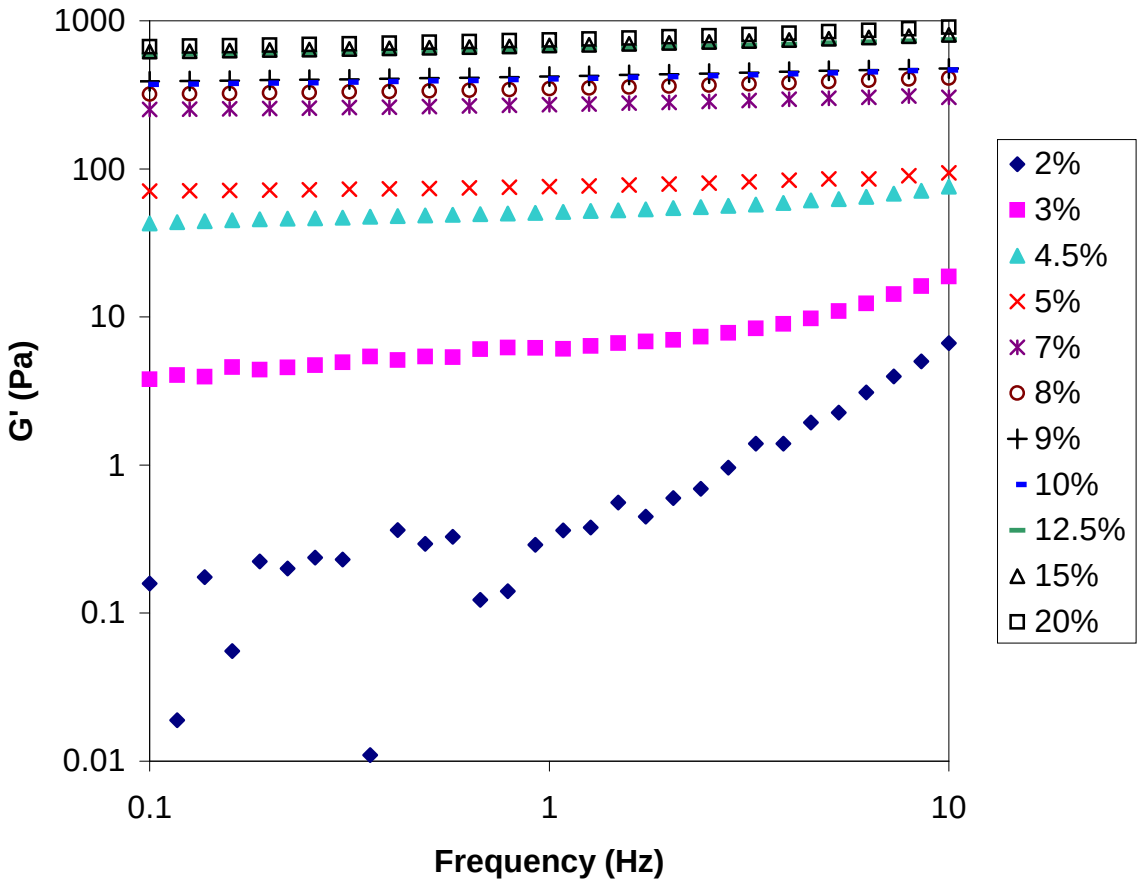

Figure 5.16: Evolution of elastic modulus G' vs. frequency for suspensions of different concentrations and volume fractions.

The data obtained for 2% suspension displays data scattering which is probably due to the sensitivity of the rheometer: similar results were obtained for agar microgel suspensions (Adams et al., 2004) for low concentrations. At this concentration, G' is frequency dependent and the values are low, reflecting a liquid-like behaviour. A much higher elastic modulus along with the disappearance of the frequency dependence can be observed for 4.5-5% suspension, corresponding to the close packing fraction concentration, in good agreement with the previous results. At the concentrations above close packing fraction, the overall rheology was governed by the granules only and no longer by the continuous phase and the volume fraction occupied (Adams et al., 2004). A further, but smaller increase of G' can be seen when the concentration increases but the volume fraction stays constant at 1 (for concentration of 8% and higher). Moreover, at these concentrations (Φ = 1) the elastic modulus increased slowly up to around 800Pa for suspensions of 20%w/w concentration. The evolution of G' and G'' as a function of concentration is presented in Figure 5.17.

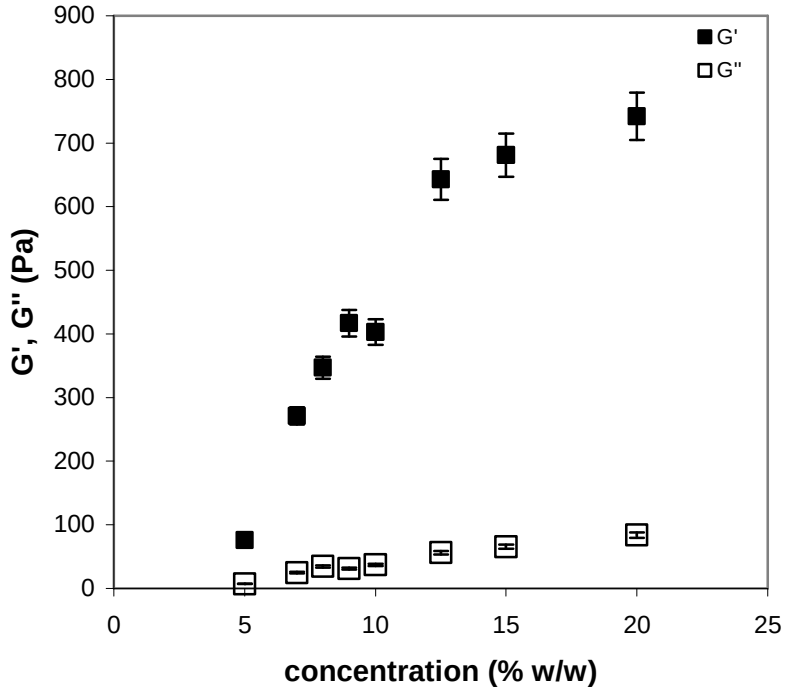

Figure 5.17: Evolution of G'(full squares) and G'' (Hollow squares) as a function of the starch concentration.

Data shows that the elastic modulus is much higher than the viscous modulus. The difference between G' and G'' increases with increasing concentration as the G' reaches higher values faster. In both cases, the increase slows down for value of 12.5% and above as the granules become more rigid.
At the maximum packing fraction ($\Phi = 1$), G' is a function of the modulus of the individual granule, more rigid particles leading to higher elastic moduli.

V.1.3. Conclusions

Throughout this first part of chapter 5, the importance of the procedure used to obtain reproducible results was demonstrated. Above a certain concentration, namely the close packing concentration (around 5%), a yield stress of the starch suspension was measured. Below this concentration, the flow and viscoelastic behaviour of the suspension is governed by the suspending medium and the volume fraction occupied by the granules; the suspensions behaved as fluids. Above the close packing fraction a first normal stress differences can be measured. When the stress was higher than the yield stress, the suspension displayed a highly shear thinning behaviour due the high deformability of the granules and their orientation in the flow direction (deviation from the HB model). Deformability of the granules also induced first normal stress difference (stored energy when the granules deform). The rheology of the starch suspension at $\Phi = 1$ mainly depended on the granule rigidity. This rheological study gave new evidence of interactions occurring between granules below the close packing fraction concentration (higher viscosity than that predicted by Krieger-Dougherty). It is thought that it is due to interactions between adjacent molecules at the surface of the granules. At high volume fractions, when the granules are in contact, mechanical interactions can take place thanks to the relative surface roughness of these particles.

It was suggested (Mewis, 1996) that in a concentrated suspension of large particles the viscosity was determined by particle geometry, viscosity of suspending medium, instantaneous microstructure and the flow field. According to Doublier et al. (1987), the continuous phase can greatly influence the overall viscosity

depending on the nature and amount of solubilised polymeric material. In the following section, the component solubilised in the continuous phase will be identified and quantified.

V.2. Analysis of the continuous phase of a starch suspension

This section is divided into several parts to progressively demonstrate how the substance dissolved in the continuous phase of the suspension was identified and characterised. The continuous phase was obtained through centrifugation of the suspension. The supernatant is recovered for analysis (see Chapter III.1.1.3 for more details). Analysis of the continuous phase is important not only to understand suspension rheology but also for the interpretation of the droplet deformation results. To analyse droplet deformation, it is necessary to know what is in contact with the hydrophobic medium to determine the interfacial tension. The continuous phase of three starch suspensions with initial concentration 1%, 3% and 5% were analysed. First, using surface tension measurements the presence of some dissolved material in the suspension continuous phase was demonstrated. Viscosity and dry matter concentration results coupled with statistical analysis approach will help understanding the influence of centrifugation time and speed on supernatant concentration; the concentration of the supernatant was estimated for 3%w/w starch suspension. Using DSC and iodine staining the type of the polysaccharide present in the supernatant was determined. Finally, using AUC and SEC-MALLS methods, the precise polymer concentration in the continuous phases of each three suspensions was obtained and the molecular weight was determined. In the final part all results together were considered to discuss and hypothesise about the possible reasons for the presence of the polysaccharide in the continuous phase of this swollen-in-water modified waxy maize starch suspension.

V.2.1. Surface tension

The values for (starch suspension supernatant)/air surface tension and (starch suspension supernatant)/oil interfacial tension are presented in Table 5.2 together with the values for water/air and water/oil as references. The results for the supernatant/air surface tension were obtained for a 6%w/w initial starch suspension concentration

Table 5.2: Surface tension values of water/air and starch supernatant/air and interfacial tension values between starch supernatant/oil and water/oil.

	Water	Starch supernatant
In air (surface tension in mN/m)	72 ± 2	68 ± 2
In oil (interfacial tension in mN/m)	36 ± 2	33 ± 2

The values of the water/air surface tension and water/oil interfacial tension are in good agreement with literature (Bergeron et al., 1997; Tice et al., 2003; Wolf & Windhab, 1995). Table 5.1 shows that the surface tension and the interfacial tension for the starch supernatant were lower than those measured for water thus indicating that the supernatant is not pure water. Although the starch studied was modified to mimic cross-linked starches, it seems that a slightly surface active component is leaching out from the granule into the continuous medium.

V.2.2. Statistical analysis

To rule out a possible effect of centrifugation on the release of matter into water from starch granules, an experimental factorial design was done (Table 5.3, see also section III.2.7 for more detail). This answered the question as to whether the release is due to swelling and gelatinisation of the granules or just due to high spinning of the sample. The experiments were performed on the 3%w/w (=30 mg/mL) initial starch suspension.

Table 5.3: Factorial design with 4 centre points (in bold): results were obtained from the supernatant of the initial 3%w/w starch suspension.

Run	Centrifugation time, min	Centrifugation speed		Viscosity, mPa.s	Dry matter concentration in the supernatant, mg/ml
		rpm	g		
1	**32**	**2300**	**1550**	**1.0811**	**2.57**
2	**32**	**2300**	**1550**	**1.0746**	**2.85**
3	5	4000	2700	1.0813	2.85
4	60	500	340	1.0747	2.85
5	**32**	**2300**	**1550**	**1.0530**	**2.35**
6	**32**	**2300**	**1550**	**1.0622**	**2.28**
7	5	500	340	1.1368	4.57
8	60	4000	2700	1.0707	2.42

Row 7 of Table 5.2, speed 500rpm and time 5min shows very different results; it was considered as an outlier and not used for statistical analysis. The statistical analysis of the results obtained confirmed that centrifugation time, rotation speed and the interaction of both parameters do not influence either viscosity or dry matter weight. This means that the results are not significantly different and that the parameters mentioned above do not influence the release of substance from the starch granule in the continuous media. Indeed, the viscosity mean value is 1.07 ± 0.009 mPa s and it is slightly higher than for water (1.002 mPa s). The same observations were made for the concentration of the dissolved matter in the supernatant: the mean value 2.6mg/mL is in good agreement with the results obtained with AUC and SEC MALLS, as will be shown later. This latter result indicated that about 10% of dry starch in a 3%w/w (30 mg/ml) suspension is released in the continuous phase.

V.2.3. Differential Scanning Calorimetry

The complexation of the initial modified waxy maize starch and of its supernatant with Lysophosphatidylcholine (LPC) was investigated using DSC. The dry fraction of the supernatant and the initial dry starch powder were both mixed with 5% LPC (see details in III.2.7) and the thermograms obtained were compared. DSC thermograms obtained for the initial dry starch and for the supernatant of a 5%w/w (50mg/ml) are presented Figure 5.18 a and b, respectively. In Figure 5.17a (initial starch + LPC) the first heating ramp (1) presents a wide and high peak at a temperature of 77°C which corresponds to the gelatinization of the Novation 2600 starch sample. The large peak at 56°C in Fig. 5.17b (supernatant + LPC) could be explained by the melting of a retrograded structure of the molecules released from starch and present in the supernatant, as the sample was left for five days at ambient temperature.

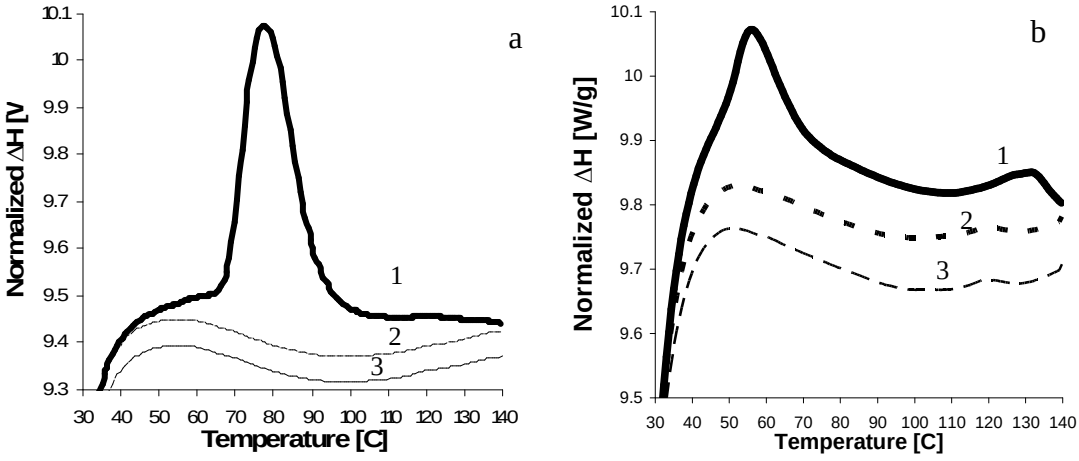

Figure 5.18: Thermograms obtained from DSC for (a) initial dry starch mixed with LPC (5%) and (b) supernatant from a 5%w/w (= 50mg/ml) starch suspension mixed with LPC (5%). First run (1), 2nd run (2), 3rd run (3).

Data presented in Figure 5.18a are speculated to be the result of an interaction between the initial starch and LPC (see peak at a temperature range of 112-127 ºC) evidenced as a slight endotherm in the three heating scans. Despite the fact that these endotherms were not considerable, the possibility that melting of a thermal event was detected cannot be ruled out. The detection of the melting of the (starch supernatant)-LPC complex was more evident as can be seen in Figure 5.18b.

Clear endotherms were observed in the three heating scans. These dissociation endotherms demonstrate the presence of a complex formed between the lipid and a linear chain (ΔH=0.126J/g for the second heating ramp, ΔH=0.117J/g for the 3rd heating ramp in Figure 5.18b). As waxy maize starch is supposed to be pure amylopectin, it can be hypothesised that the collected supernatant should be mainly composed of sufficiently linear amylopectin segments, able to complex LPC. However, it is also possible to think that some traces of amylose present in the sample could be at the origin of this complexation with LPC. A further study with an iodine staining method will confirm whether it is amylose or amylopectin.

V.2.4. Iodine staining

The spectrograms of the iodine stained samples are presented Figure 5.19. The pure amylopectin sample (line 2) has an absorbance peak around 555 nm which is consistent with literature (Banks and Greenwood, 1975). The supernatant sample from a 5%w/w initial starch suspension (line 1) has similar absorbance behaviour, i.e. the absorbance wavelength is nearly the same (around 540nm). The absorbance wavelength for the pure amylopectin is slightly higher than that of the supernatant (555nm vs.540nm) because of the difference of the origin of the starches: the amylopectin used is from potato whereas the supernatant is obtained from a modified waxy maize starch. The maximum absorbance peak position is dependent on the linear chain length (Santacruz et al., 2005): the higher the degree of polymerisation (DP), the higher the absorption wavelength. It can thus be assumed that the pure amylopectin from potato has a slightly higher DP than the amylopectin of the supernatant sample. The absorbance peak value of the supernatant is much higher than that of the pure amylopectin solution (0.44 for the supernatant vs. 0.12 for the pure amylopectin) due to a difference in polymer concentration (details on sample preparation can be found in section III.2.8).

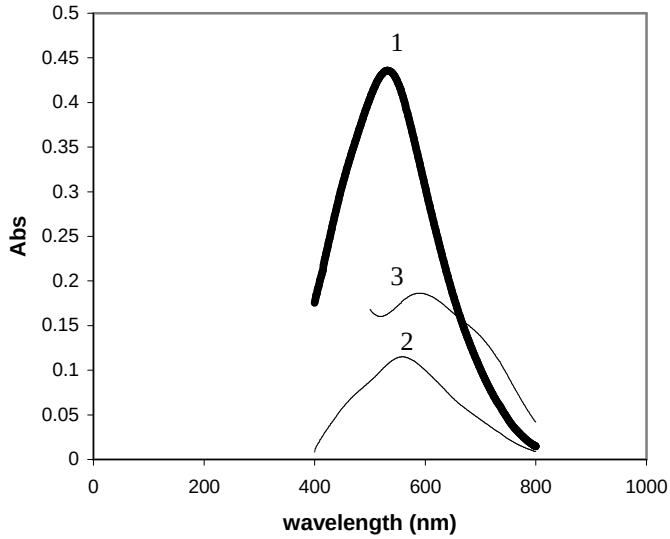

Figure 5.19: Spectrogram of iodine stained samples: supernatant (1), 100% amylopectin (2), 60% amylopectin/40% amylose (3).

A range of amylose/amylopectin mixtures, ranging from 5% to 40% amylose, were tested. For clarity only the sample with 40% amylose is shown here. The 60% amylopectin/40% amylose sample (line 3) shows a shift of the absorbance peak towards higher wavelengths. This is attributed to the presence of amylose in the sample: the amylose/iodine complex is known to absorb at 620nm (Santacruz et al., 2005). The mixture of amylose and amylopectin absorbs at an intermediate wavelength between amylose and amylopectin (595 nm). Pure amylopectin and the supernatant sample absorbed at very close wavelengths and showed similar brownish coloration of the sample typical of amylopectin/iodine complexation. Hence, the data demonstrates that the iodine staining method confirmed the presence of amylopectin dissolved in the continuous phase. The data also shows that there is no amylose in the supernatant sample.

V.2.5. Size Exclusion Chromatography coupled to Multi-Angle Laser Light Scattering and Analytical Ultracentrifugation

SEC chromatograms show a single wide peak for each supernatant solution collected from 10, 30 and 50 mg/mL initial starch suspensions (Figure 5.20). The

heights of the peaks (concentration detector) increase non-linearly with increasing initial starch concentration; also there is a slight increase in weight average molecular weight (Table 5.4).

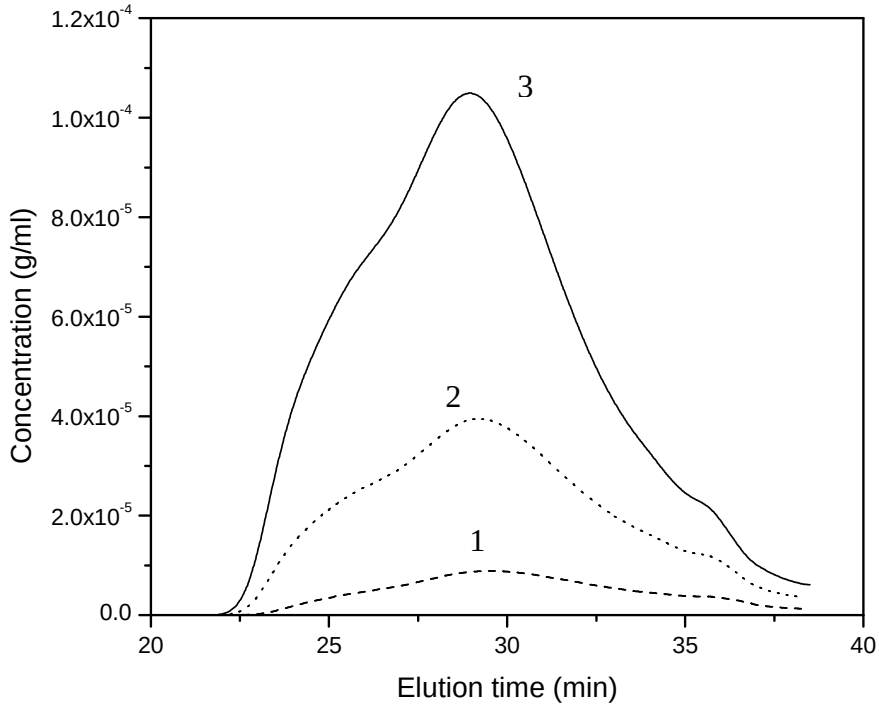

Figure 5.20: SEC-MALLS elution profile: concentration vs. time for supernatants collected from the initial 10mg/mL (1); 30mg/mL (2) and 50mg/mL (3) starch suspensions.

Results obtained with analytical centrifugation are presented in Figure 5.20 and summarised in Table 5.3 for the same three supernatants. The area under the curve gives an estimate of the concentration of amylopectin in the supernatant (after dilution); corrected (or recalculated) concentrations are given in Table 5.3 (Correction after dilution, see section III.2.6 for details).

Table 5.4: Summary of results from AUC, SEC-MALLS and intrinsic viscosity determination

Initial starch suspension concentration, mg/mL	Amylopectin concentration estimate in the supernatant, mg/mL		$M_w \cdot 10^6$, g/mol	$s_{20,w}$, S	[η], mL/g
	AUC	SEC-MALLS			
10	0.58 ± 0.01	0.63 ± 0.02	1.2 ± 0.025	15.9 ± 0.1	22 ± 1
30	2.49 ± 0.02	2.68 ± 0.01	1.54 ± 0.015	16.4 ± 0.1	21 ± 1
50	6.77 ± 0.05	6.67 ± 0.02	1.72 ± 0.017	19.0 ± 0.1	29.5 ± 0.3

From Figure 5.21 the evolution of the sedimentation coefficient of the supernatant with initial starch concentration can be observed; the values shown in Table 5.4 demonstrate that this evolution is not linear. The sedimentation coefficient values between 15.9 and 19 S (Table 5.4) allow an estimation of the molecular weight of around 10^6 g/mol, which slightly increases with initial starch concentration, in good agreement with estimates from SEC-MALLS. Moreover, the peaks are quite wide hence indicating a polydisperse population of macromolecules.

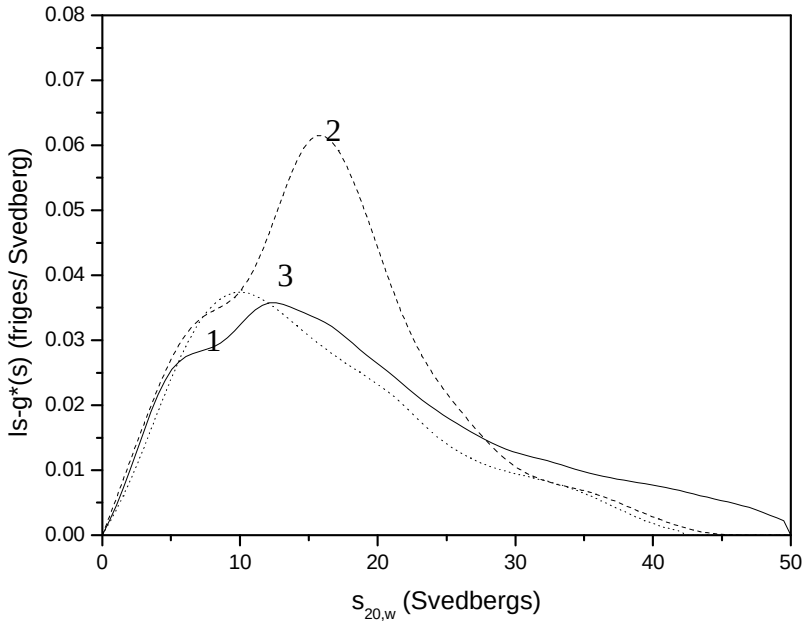

Figure 5.21: Sedimentation coefficient distribution, for starch supernatants, from the initial starch suspensions of 10mg/ml (1); 30mg/ml (2) and 50mg/ml (3) diluted 2, 6 and 20-fold respectively.

Figure 5.21 was obtained for (approximately) infinitely diluted supernatant. Although the area under the curve is greater for the supernatant obtained from the 30mg/mL starch suspension than from the 50mg/mL starch, this is an artefact resulting form the differing dilutions and has been corrected in Table 5.4. It is worth noting that supernatant concentrations obtained through dry matter weight, AUC and SEC-MALLS methods yielded the same values.

V.2.6. Discussion

It is known that when starch is heated, amylose leaches out of the granule. However, in the case of modified waxy maize used in the study amylose should only be present in traces if at all. Hence, no polymeric material should be dissolved in the water, which as it was demonstrated, was not the case. It has been reported (Tecante & Doublier, 1999) that a soluble fraction is present in the continuous phase of a chemically cross-linked waxy maize starch suspension, but it was not analysed. Our physico-chemical study revealed the presence of a slightly surface active component in the supernatant and starches have been shown to be surface active (Prochaska et al., 2007). Fast scan DSC measurements allowed detecting the presence of a small portion of linear chains (which could be amylopectin) and the iodine staining method confirmed the presence of amylopectin chains in the medium. Indeed, the brown-red colour obtained with the iodine staining is typical of linear polysaccharide chains with low DP ($12<DP<45$) (Santacruz et al., 2005) which would correspond to the small linear part of amylopectin. The results obtained with AUC and SEC-MALLS showed that it was in fact low molecular weight amylopectin of about 10^6 g/mol (usually amylopectin is above 10^7 g/mol) that was dissolved in the continuous phase with concentrations varying from 0.6 to 6.7 mg/ml for initial 10mg/mL and 50mg/mL starch suspensions, respectively.

The measured values of intrinsic viscosity (around 25 mL/g) seem quite low compared to those reported for the waxy maize amylopectin dissolved in water/dimethylsulfoxide mixtures which were measured to be around 200mL/g,

(molecular weight around $M_w = 10^7$ - 10^8 g/ mol) (Bello-Perez et al., 1998; Carrière, 1998; Chamberlain & Rao, 2000; Fiedorowicz & Rebilas, 2002; Fishman et al., 1996). Banks et al. (1972) reported values in the same range as ours (35 mL/g) when the starch was stirred and boiled in water. The wide variety for amylopectin intrinsic viscosity values given in the literature can arise from the starch origin, the solvent, the temperature, the preparation method and the time of storage (Bello-Perez et al., 1998; Millard et al., 1997). In our case the low intrinsic viscosity values could be also explained by a rapid depolymerization in the supernatant before the measurement (Bello-Perez et al., 1998) or the preparation conditions (Millard et al., 1997).

The "low" (when considering amylopectin molecules) intrinsic viscosity also suggests that the polymer present in the continuous phase is highly branched and has a random-coil conformation. Solution conformation can be estimated semi-quantitatively using the translational frictional ratio, f/f_0 (Tanford, 1961) in Equation 5.7. As a general approximation f/f_0 ~ 1 - 2; 2 - 5 and > 6 for compact spheres, random-coils and rigid rod type conformations, respectively.

$$\frac{f}{f_0} = \frac{M_w(1-\bar{v}\rho_{20,w})}{(N_A 6\pi\eta_{20,w} s^0_{20,w})}\left(\frac{4\pi N_A}{3\bar{v}M_w}\right)^{1/3} \qquad 5.7$$

where $\bar{v}$ is the partial specific volume of amylopectin (0.64 mL/g); N_A is Avogadro number and $\rho_{20,w}$ and $\eta_{20,w}$ are the densities and viscosities of water at 20.0 °C, respectively. For the starch supernatants, an average translational frictional ratio of 3.8 ± 0.3, consistent with a random-coil conformation was found. This value also depends on hydration of the macromolecule and on molecular weight and therefore more hydrated and/or higher molecular weight polymers may appear to have a less compact structure than is truly the case.

Different hypotheses can be proposed to explain the release of low molecular weight amylopectin from modified waxy maize starch into the continuous phase. The starch used in our experiments shows inhibited swelling but no evidence of

cross-linking (according to National Starch). The granules do not burst even with severe heating, so the possibility of the amylopectin being released through bursting is highly unlikely. The hypothesis is that low molecular weight amylopectin chains are able to leach out of the granules due to their small size. The small size can also be because of high branching, which is reflected by low intrinsic viscosity values. A second hypothesis is that clusters of amylopectin chains on the surface of the granule are "ripped" during stirring. This suggestion is based on the results reported in (Stark & Lynn, 1991) which stipulates that amylopectin clusters constitute the beginning of the next growth ring, and compares the granule to a hairy ball. The amylopectin clusters are linked to other amylopectin molecules via glucosidic bonds; the dissociation energy of the latter is of 77 kJ/mol (Jang et al., 2005) which is weak enough to be broken with mechanical energy and heat. If only "hairy particle" should be the reason of the presence of amylopectin in the continuous phase, amylopectin concentration in the supernatant should be roughly proportional to the initial starch concentration in power 2/3, which is not the case (it is proportional to the initial starch concentration in power 1.5). Thus it is thought that both hypotheses are valid for the case studied.

V.2.7. Conclusions

The study of the continuous phase of swollen-in-water Novation 2600 starch granules suspension revealed the presence of low molecular weight amylopectin. The first detection step showed the presence of a surface active compound. Viscosity measurements and estimation from the drying method demonstrated that a certain amount of matter is leaching out of the granules into the continuous phase. Further investigation using fast scan DSC and iodine staining allowed the identification of this released component as amylopectin. The latter result was to be expected as modified waxy maize starch is almost uniquely composed of amylopectin, the amylose fraction being only traces. Finally, two different quantification methods, AUC and SEC-MALLS, allowed the estimation of the molecular weight of the amylopectin molecules, $M_w \approx 10^6$, as well as its precise concentration in the continuous media: 0.6, 2.7 and 6.7 mg/mL for 10, 30 and 50

mg/mL initial suspensions, respectively. Both methods yielded similar results also in agreement with the results obtained for the concentration estimated from dry matter weight, thus showing the accuracy of the measurements. The molecular weight values obtained for the amylopectin molecules is quite low suggesting that only small and/or branched chains are released in the continuous phase. The presence of amylopectin in suspension continuous phase should be taken into account if preparing mixtures with other (bio)polymers.

V.3. Conclusions for Chapter 5

From the obtained results it can be concluded that at volume fraction $\Phi = 1$ the rheology of the suspension was governed by the rigidity of the granules. More rigid granules lead to higher viscosities. The shear thinning behaviour suggested that even at low swelling degrees (high starch concentration, less water available), the granules were still sufficiently deformable. At intermediate concentrations, evidence of granular interactions was put into light. These granular interactions led to higher viscosities than those that could be achieved with no interacting particles.

The study on the continuous phase showed that the latter was Newtonian, suggesting that the effect on the overall rheology of the suspension is minimal. Moreover, the amylopectin concentration in the supernatant at the highest initial starch concentration does not exceed the critical value of 0.02g/g suggested by Doublier et al. (1987). It was shown that the viscosity of a 1% starch suspension (10mg/mL) was Newtonian and not governed by the granules. Hence, it is possible to think that only for very low concentrations does the continuous phase influence significantly the overall flow behaviour.

Reference List

Abdulmola, N. A., Hember, M. W. N., Richardson, R. K., and Morris, E. R. (1996). Effect of xanthan on the small-deformation rheology of crosslinked and uncrosslinked waxy maize starch. *Carbohydrate Polymers*, 31, 65-78.

Adams, S., Frith, W. J., and Stokes, J. R. (2004). Influence of particle modulus on the rheological properties of agar microgel suspensions. *Journal of Rheology*, 48, 1195-1213.

Banks, W., Geddes, R., Greenwood, C. T., and Jones, I. G. (1972). Physicl-chemical studies on starches. *Starch/Stärke*, 24, 245-251.

Barnes H.A, Hutton J.F, and Walters K. (1989). An introduction to rheology. First edition.

Bello-Perez, L. A., Roger, P., Colonna, P., and Paredes-Lopez, O. (1998). Laser light scattering of high amylose and high amylopectin materials stability in water after microwave dispersion. *Carbohydrate Polymers*, 37, 383-394.

Bergeron, V., Cooper, P., Fischer, C., Giermanska Kahn, J., Langevin, D., Pouchelon A. (1997). Polydimethylsiloxane (PDMS)-based foams. *Colloids and Surfaces A: Physicochemical and Engineering Aspects*, 122, 103-120.

Carrière, C. J. (1998). Network development during shear-thickening in semidilute solutions of gently solubilized starches. *Journal of Polymer Science*, 36, 2085-2093.

Chamberlain, E. K. and Rao, M. A. (2000). Effect of concentraiton on rheological properties of acid-hydrolyzed amylopectin solutions. *Food Hydrocolloids*, 14, 163-171.

Cloitre, M. (2005). Tailoring the flow properties of soft colloidal dispersions. *Macromolecular Symposia*, 229, 99-106.

Doublier, J. L. (1986). A rheological comparison of Wheat, Maize, Faba bean and smooth pea starches. *Journal of Cereal Science*, 5, 247-262.

Doublier, J. L., Llamas, G., and Lemeur, M. (1987). A Rheological Investigation of Cereal Starch Pastes and Gels - Effect of Pasting Procedures. *Carbohydrate Polymers*, 7, 251-275.

Evans, I. D. and Haisman, D. R. (1980). Rheology of Gelatinized Starch Suspensions. *Journal of Texture Studies*, 10, 347-370.

Fiedorowicz, M. and Rebilas, K. (2002). Physicochemical properties of waxy corn starch and corn amylopectin illuminated with linearly polarised visible light. *Carbohydrate Polymers*, 50, 315-319.

Fishman, M. L., Rodriguez, L., and Chau, H. K. (1996). Molar masses and sizes of starches by high-performance size-exclusion chromatography with on-line multi-angle laser light scattering detection. *Journal of Agriculture and Food Chemistry*, 44, 3182-3186.

Gulmus, S. A. and Yilmazer, U. (2005). Effect of volume fraction and particle size on wall slip in flow of polymeric suspensions. *Journal of Applied Polymer Science*, 98, 439-448.

Hao, T. (2008). Viscosities of liquids, colloidal suspensions, and polymeric systems under zero or non-zero electric field. *Advances in Colloid and Interface Science*, 142, 1-19.

Harris J. (1977). Rheology and Non-Newtonian flow. First edition.

Holmes, C. B., Cates, M. E., Fuchs, M., and Sollich, P. (2005). Glass transition and shear thickening suspension rheology. *Journal of Rheology*, 49, 237-269.

Jacquier, J. C., Kar, A., Lyng, J. G., Morgan, D. J., and McKenna, B. M. (2006). Influence of granule size on the flow behaviour of heated rice starch dispersions in excess water. *Carbohydrate Polymers*, 66, 425-434.

Jang, J. H., Hui Ching, H., Ike, M., Inoue, C., Fujita, M., and Yoshida, T. (2005). Acid Hydrolysis and quantitative determination of total hexosamines of an exopolysaccharide produced by Citrobacter sp. *Biotechnology letters*, 27, 13-18.

Kolli, V. G., Pollauf, E. J., and Gadala-Maria, F. (2002). Transient normal stress response ina concentrated suspension of spherical particles. *Journal of Rheology*, 46, 321-334.

Krieger, I.M., Dougherty T.J. (1959). A mechanism for non-Newtonian flow in suspensions of rigid spheres. *Trans. Society of Rheology*, 3, 137-152.

Kwon, T. M., Jhon, M. S., and Choi, H. J. (1997). Rheological study of magnetic particle suspensions. *Materials Chemistry and Physics*, 49, 225-228.

Mahaut, F., Chateau, X., Coussot, P., and Ovarlez, G. (2008). Yield stress and elastic modulus of suspensions of noncolloid particles in yield stress fluids. *Journal of Rheology*, 52, 287-313.

Mewis, J. (1996). Flow behaviour of concentrated suspensions: predictions and measurements. *International Journal of Mineral Pocessing*, 44-45, 17-27.

Millard, M. M., Dintzis, F. R., Willet, J. L., and Klavons, J. A. (1997). Light-scattering molecular weights and intrinsic viscosities of processed waxy maize starches in 90% dimethyl sulfoxide and H_20. *Cereal Chemistry*, 74, 687-691.

Nayouf, M., Loisel, C., and Doublier, J. L. (2003). Effect of thermomechanical treatment on the rheological properties of crosslinked waxy corn starch. *Journal of Food Engineering*, 59, 209-219.

Nguyen, Q. D., Jensen, C. T. B., and Kristensen, P. G. (1998). Experiment and modelling studies of the flow propertes of maize and waxy maize starch pastes. *Chemical Engineering Journal*, 70, 165-171.

Omari, A., Tabary, R., Rousseau, D., Calderon, F. L., Monteil, J., and Chauveteau, G. (2006). Soft water-soluble microgel dispersions: Structure and rheology. *Journal of Colloid and Interface Science*, 302, 537-546.

Prochaska, K., Kedziora, P., Le Thanh, J., and Lewandowicz, G. (2007). Surface activity of commercial food grade modified starches. *Colloids and Surfaces B: Biointerfaces*, 60, 187-194.

Rao, M. A., Okechukwu, P. E., Da Silva, P. M. S., and Oliveira, J. C. (1997). Rheological behavior of heated starch dispersions in excess water: role of starch granule. *Carbohydrate Polymers*, 33, 273-283.

Saiki, Y., Prestidge, C. A., and Horn, R. G. (2007). Effects of droplet deformability on emulsion rheology. *Colloids and Surfaces A-Physicochemical and Engineering Aspects*, 299, 65-72.

Santacruz, S., Anderson, P. D., and Aman, P. (2005). Characterisation of potato leaf starch with iodine-staining. *Carbohydrate Polymers*, 59, 397-400.

Seth, J., Cloitre, M., and Bonnecaze, R. T. (2006). Elastic properties of soft particle pastes. *Journal of Rheology*, 50, 353-376.

Snabre, P. and Mills, P. (1999). Rheology of concentrated suspensions of viscoelastic particles. *Colloids and Surfaces A-Physicochemical and Engineering Aspects*, 152, 79-88.

Stark, J.R., Lynn, A. *Biochemistry of plant polysaccharides*. In: CATLEY B.J. ed. Proceedings of the 640th Meeting on Biochemistry of Plant Polysaccharide, Edinburgh, 4-6 September1991. Edinburgh: Biochemical Society Transactions, 1991, p. 7-12.

Tattiyakul, J. and Rao, M. A. (2000). Rheological behavior of cross-linked waxy maize starch dispersions during and after heating. *Carbohydrate Polymers*, 43, 215-222.

Tecante, A. and Doublier, J. L. (1999). Steady flow and viscoelastic behavior of crosslinked waxy corn starch-k-carrageenan and gels. *Carbohydrate Polymers*, 40, 221-231.

Thebaudin, J. Y., Lefebvre, A. C., and Doublier, J. L. (1998). Rheology of starch pastes from starches of different origins: Applications to starch-based sauces. *Food Science and Technology-Lebensmittel-Wissenschaft & Technologie*, 31, 354-360.

Tice, J. D., Song, H., Lyon, A. D., and Ismagilov, R. F. (2003). Formation of droplets and mixing in multiphase microfluidics at low values of the Reynolds and the capillary numbers. *Langmuir*, 19, 9127-9133.

Velez-Ruiz, J., Hernando, I., Gonzalez-Tomas, L., Perez-Munuera, I., Quiles, A., Tarrega, A., Lluch, M. A., and Costell, E. (2006). Rheology and microstructure of custard model systems with cross-linked waxy maize starch. *Flavour and Fragrance Journal*, 21, 30-36.

Wolf B., Windhab E. (1995). Interfacial rheology of deformable droplets in viscometric flows. *Rheology*, 5 (4), 182-189.

Résumé du chapitre VI

Déformation et rupture sous cisaillement d'une goutte de suspension d'amidon : comparaison avec une goutte de solution de polymère

L'étude de la déformation et la rupture de gouttelettes est d'une grande importance pour comprendre le comportement sous écoulement des émulsions ou encore la morphologie des mélanges de polymères. Dans ce chapitre, nous allons considérer la déformation et la rupture de gouttelette de suspensions d'amidon dans une matrice immiscible et comparer son comportement à un système modèle, une goutte de solution d'hydrocolloïde (Hydroxypropylmethyl Cellulose, HPMC). Ces deux systèmes sont des épaississants utilisés dans l'industrie agroalimentaire et offrent des différences de perception du gout. Il semblerait que cette perception soit liée à la capacité du produit à se mélanger en bouche : plus le produit se mélange bien, plus le transport des agents de flaveurs vers les récepteurs sensoriels est favorisé et donc meilleur est la perception. L'objectif ici est de trouver un paramètre physique qui puisse permettre de déterminer la capacité d'un système à se mélanger et ainsi de le corréler avec la perception en bouche.

Pour analyser le comportement des gouttelettes suspendues dans une matrice immiscible il est nécessaire de connaître les caractéristiques physico-chimiques des deux systèmes étudiés. Ainsi, une étude rhéologique de la solution d'HPMC ainsi que la détermination de ses propriétés de surface a été menée. Une étude comparative des propriétés physico-chimique des deux systèmes a également été faite en regroupant les données obtenues pour la suspension d'amidon et éparpillées dans le manuscrit.

Comme les deux systèmes sont rhéofluidifiants, les expériences sont conduites à cisaillement constant afin d'éviter une variation du rapport de viscosité. La gouttelette de la solution d'HPMC se conduit bien comme une goutte viscoélastique, tandis que dans le cas de la gouttelette de suspension d'amidon, elle

aussi viscoélastique, se comporte plus comme une goutte newtonienne. De plus lorsque les deux systèmes sont comparés dans des conditions de contraintes, de temps et de tailles similaires mais des rapports de viscosité différents, la goutte de suspension se rompt plus facilement bien que le contraire soit attendu. Pour ces raisons, une étude plus approfondie des conditions de rupture d'une goutte de suspension d'amidon a été effectuée.

L'étude de la rupture de goutte de suspension d'amidon a montré que le mécanisme était différent de celui des fluides. La rupture se produit lorsque la circulation interne permet un réarrangement des granule, créant ainsi des zones de déplétions ou la rupture peut se produire. En ce sens, le seuil d'écoulement de la suspension joue un rôle majeur. En dessous du seuil d'écoulement, il n'y a pas de circulation interne et la goutte se conduit comme un solide. Si la contrainte appliquée à l'extérieur de la goutte est légèrement au dessus du seuil d'écoulement, une perte d'énergie due à la friction des granules engendre une diminution de la contrainte à l'intérieure et la circulation interne n'est plus assez forte pour permettre la rupture ; on passe d'un système fluide à un système liquide. Lorsque la contrainte appliquée est très forte, les granules à l'intérieur se déforment et facilitent la circulation du liquide à l'intérieur de la goutte, provoquant une rupture plus rapide que celle observée pour les systèmes Newtoniens.

Chapter VI: Shear induced deformation and break-up of a starch suspension droplet: comparison with a polymer solution

The deformation and break-up of droplets suspended in an immiscible fluid is a wide field of research. To this day, the major interest of this type of study is the understanding of multiphase system behaviour (e.g. emulsion rheology) or morphology (polymer blends). Another suggested application would be to link droplet break-up to flavour perception. Differences in mouthfeel and flavour perception between starch and polymer thickened products have been demonstrated (Ferry et al., 2006). It is thought that good mixing of the product in the mouth favours the release of tastants to the receptors, hence leading to enhanced flavour perception. Mixing ability could be linked to the microstructure of the systems; however, to this day no physical parameter directly correlates the properties of the thickening agent and flavour perception. A possible parameter to consider is the break-up of a hydrocolloid or starch thickened droplet: an easy break-up suggesting a better ability of the product to mix in the mouth.

In the following study, the differences in deformation and break-up behaviour between a starch thickened droplet and a hydrocolloid solution droplet will be shown. Hydroxypropylmethyl cellulose (HPMC) was chosen as a viscoelastic model droplet as it is widely used in the food industry and because the behaviour of such systems has previously been investigated; the results obtained can thus be compared to literature. Nevertheless, prior to studying the shear induced behaviour of a droplet, the physico-chemical parameters of the HPMC solutions need to be determined. The first part of this chapter will be on the characterisation of

an HPMC aqueous solution, i.e. rheological behaviour and interfacial properties both being necessary for the analysis of droplet behaviour under simple shear. The second section will focus on the deformation and break-up of two types of droplets: HMPC solution and starch suspension, both immersed in silicon oil as a model matrix. Visual observations of the systems depending on polymer concentration will be shown and droplet orientation, deformation and relaxation will be studied. Finally, special attention will be given to the starch suspension droplet as it unravels new break-up mechanisms.

VI.1. Characterisation of the rheological behaviour and surface activity of Hydroxypropylmethyl Cellulose aqueous solution

VI.1.1. Flow and viscoelastic properties of HPMC solutions

An example of a flow curve obtained for a 3.75%w/w HPMC solution is shown Figure 6.1. A low-shear Newtonian plateau can be observed, at higher shear stresses the sample is shear thinning; this is a typical behaviour for a hydrocolloid solution. Shear thinning is caused by orientation of the polymer coils in the directions of the flow (Clasen & Kulicke, 2001).

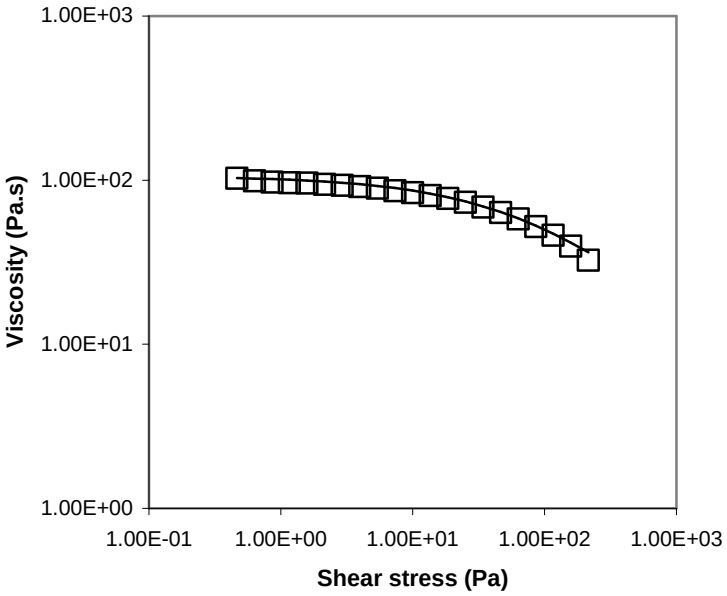

Figure 6.1: Flow curve of a 3.75%w/w HPMC solution; viscosity vs. shear stress. Hollow squares represent experimental data. The line is for the Ellis model.

The data was fitted with the Ellis model (Equation 6.1) as can be seen in Figure 6.1.

$$\frac{\eta_0}{\eta(\tau)} = 1 + \left(\frac{\tau}{\tau_{1/2}} \right)^{\alpha-1} \qquad 6.1$$

where is the zero shear viscosity (η_0= 105Pa.s), $\tau_{1/2}$ the shear stress at which the viscosity is 50% of the Newtonian limit and α-1 the slope of the viscoity in the power law regime.

HPMC solutions were prepared in a wide range of concentrations and viscosity-shear stress dependences were measured (Figure 6.2a): the goal was to see if this HPMC (K4M) behaves as a hydrocolloid solution in good agreement with the literature but mostly to obtain a wide range of viscosities to choose from for the future droplet deformation experiments. All the HPMC flow curves were fitted with the Ellis model except for 0.5% which was fitted with the Newtonian model. Zero shear viscosity was then plotted against HPMC concentration (Figure 6.2b).

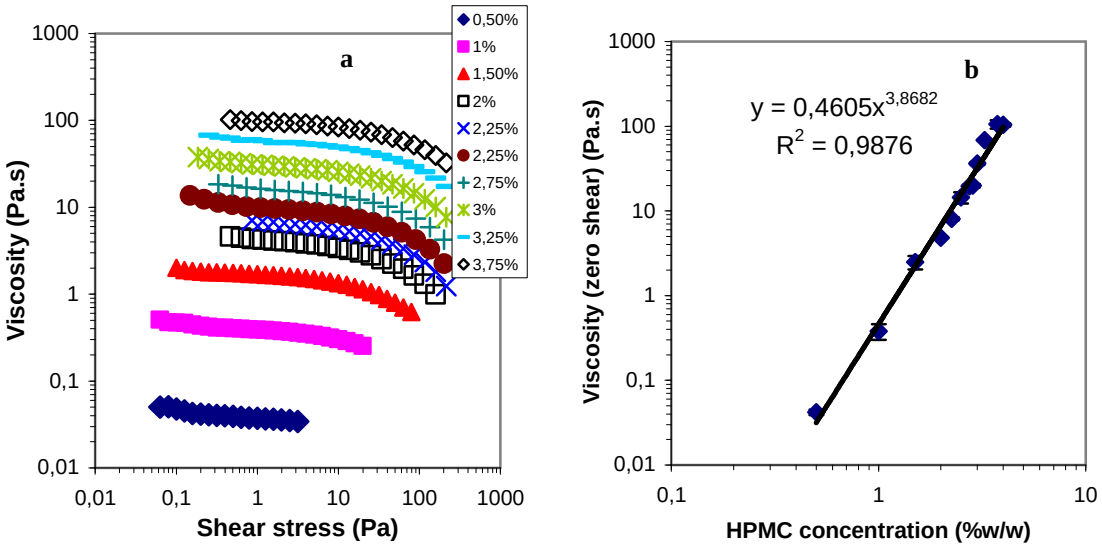

Figure 6.2: Flow behaviour of HPMC solutions. Evolution with concentration. (a) Viscosity vs. shear stress; (b) Zero shear viscosity vs. HPMC concentration.

Figure 6.2a shows that the viscosity of HPMC increased with increasing concentration, as expected. Figure 6.2b shows that the HPMC as a function of hydrocolloid concentration follows a power law (Equation 6.2):

$$\eta = KC^n \qquad 6.2$$

where K is a constant coefficient (here K = 0.4605) and n the power law index. The value of this latter parameter is usually reported to be between 3.5 and 4 (Kavanagh & Ross-Murphy, 1998) for a polymer solution in the semi-dilute regime, i.e. when the coils overlap but are not entangled. It is clear by looking at Figure 6.2b that all concentrations are above c* (coil overlap concentration, from diluted to semi-diluted regime) as there is no sharp change in the slope. The value of the critical concentration c* for the studied HPMC samples (K4M) was determined to be around 0.1% (Cook et al., 2002; Ferry et al., 2006). In our case n=3.8, confirming that HPMC behaves as a polymer solution in semi-dilute regime. The HPMC solutions were not completely transparent. It is due to unsubstituted cellulose backbone that is only partly dissolved and aggregated in bundles, when the sample is below the gelation temperature (Desbrieres et al., 2000; Haque et al., 1993; Hirrien et al., 1998). If the temperature is increased, the bundles come apart leading to association of hydrophobic zones and exposing the hydrophilic groups to the

aqueous environment (Haque et al., 1993). The results obtained were reproducible, with a standard deviation of less than 3%, indicated that the measurements were carried out on a homogeneous solution.

The thixotropic behaviour of HPMC solutions was also investigated (Figure 6.3). In the shear induced droplet deformation experiment, the droplet might be submitted to shear prior to the experiment in order to obtain smaller droplets. Hence, it is of importance to see whether pre-shear will affect the sample or not.

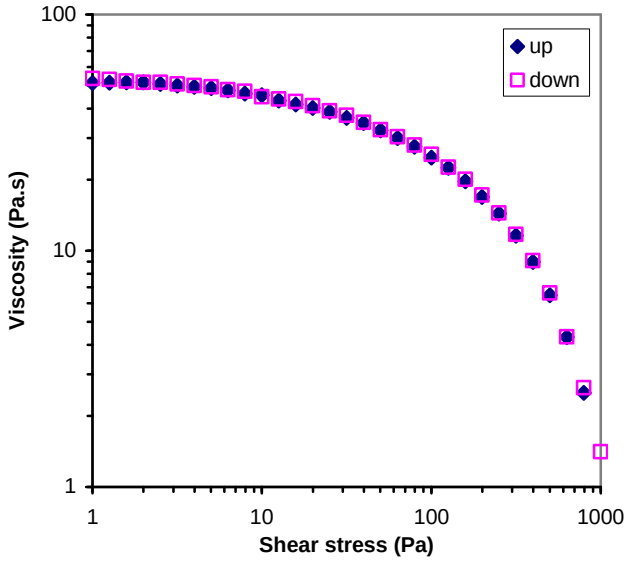

Figure 6.3: Non thixotropic behaviour of HPMC at 3.25%w/w. Viscosity vs. shear stress, up and down curve.

No hysterisis loop can be seen for the HPMC, i.e. the “up” and the “down” curves fully coincide (Figure 6.3) indicating a non-thixotropic behaviour.

During the flow measurement, a first normal stress difference developed (Figure 6.4). Only the results for solutions with concentrations ranging from 3 to 3.75%w/w are presented in this figure as they were later used for the droplet deformation and break-up study.

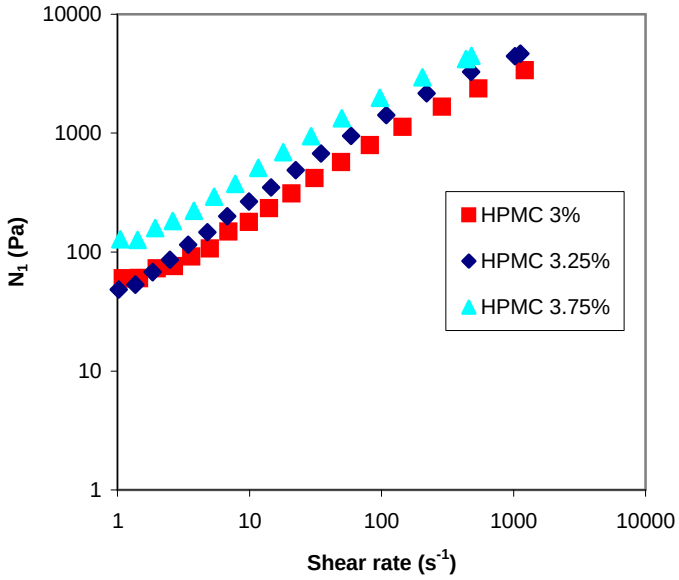

Figure 6.4: Evolution of first normal stress difference with HPMC concentration.

It can be observed that for all 3 studied concentrations that the first normal stress difference increases with increasing shear rate. Moreover, Figure 6.4 shows that the higher the HPMC concentration, the higher the N_1 value. The origin of the rise in first normal stress difference with increasing shear rate is interpenetration of the coils; this leads to a build-up of the entanglement points of intertwined polymer chains and thus the appearance of elastic behaviour (Clasen & Kulicke, 2001). When the concentration is increased, the number of entanglement points increase as well leading to high N_1 values.

The viscoelasticity at small deformation amplitude of HPMC solutions was studied using oscillatory measurements. It is well-known that HPMC solutions have the specific property that when the temperature is increased they form reversible gels. However, the measurements here were conducted at temperatures below the gelation point, at 20°C. The gelation of HPMC solutions occurs in two steps; the first one is thought to be a phase separation occurring (leading to a decrease in G'

and G'') and the second step, the gelation of the polymer rich phase(Hussain et al., 2002). These two steps were reported to occur for this type of HPMC (K4M) around 55°C and 70°C respectively for concentrations ranging from 2 to 5%w/w (Hussain et al., 2002). The elastic and viscous moduli of HPMC solutions, G' and G'', obtained for different concentrations varying from 1% to 3.75%w/w are presented in Figures 6.5 and 6.6 as a function of frequency. It can be noticed that the viscous modulus is higher in value than the elastic modulus for low frequencies but asymptotically become closer in value at higher frequencies and eventually cross, with elastic behaviour becoming dominant due to insufficient time for the polymer chains to relax. This behaviour is usually observed for liquids. Only the 3.75% sample shows a cross-over of G' and G'' in the frequency range investigated; it occurs around 7Hz.

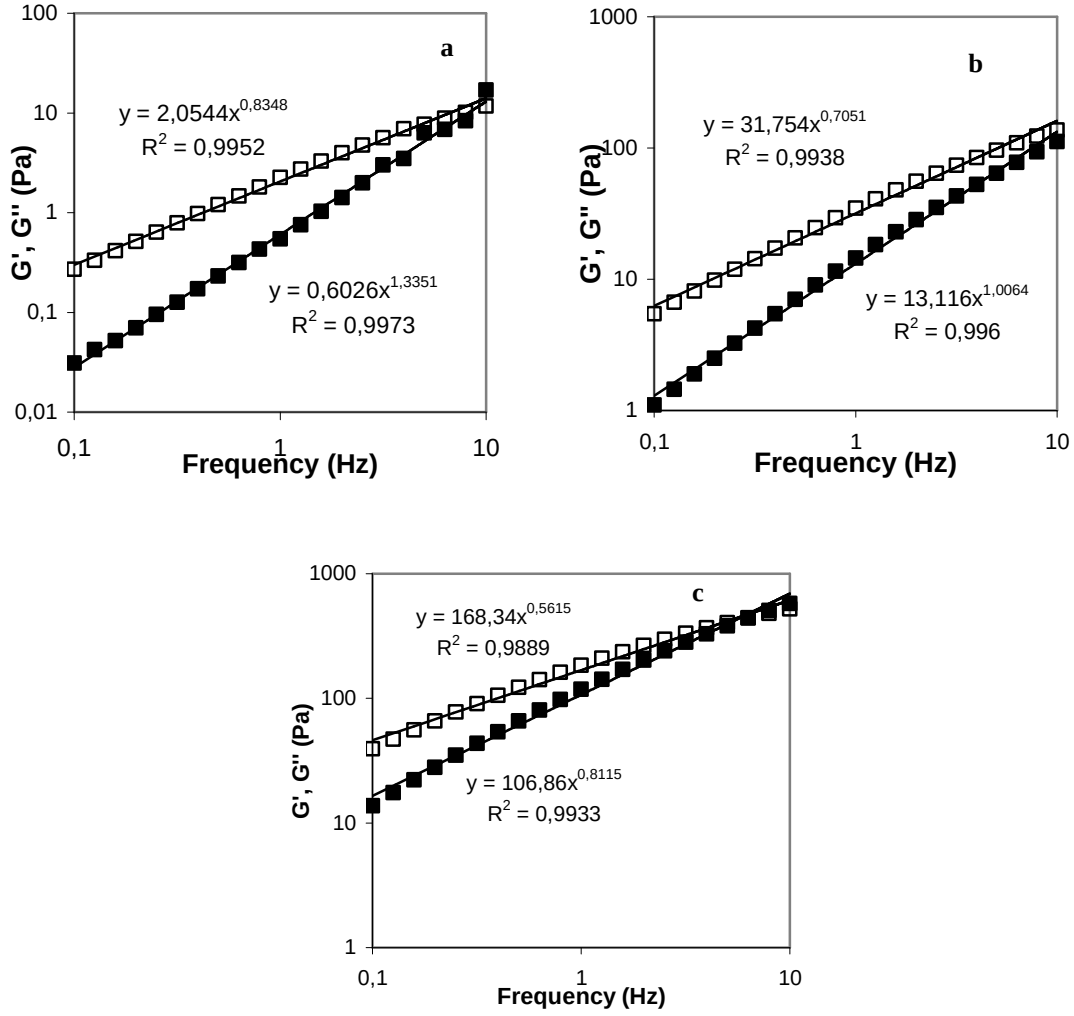

Figure 6.5: Evolution of G' and G'' as a function of frequency at 20°C. Filled squares represent G' and hollow squares G''. (a) 1% w/w HPMC solution; (b) 2.5% w/w HPMC solution. (c) 3.75% w/w HPMC solution. Lines are power law fits.

For liquids, the dependence of G' and G'' at low frequencies should follow: G'' = f(ω^1) and G' = f (ω^2), ω being the frequency (Kavanagh & Ross-Murphy, 1998). The curves obtained in Figure 6.5 a, b and c were all fitted with a power law equation. None of the values obtained for the power index fit the liquid-like behaviour, which is probably due to the rather high frequency interval at which the samples were studied. Moreover, as it can be seen, the slope decreased with increasing concentration. It can be suggested that the HPMC solutions have an intermediate behaviour between a liquid and a gel. As polymer concentration is increased, the amount of HPMC chain interactions increases leading to the creation of more hydrophobic zones. Slope values reported in literature (Choi et al., 2006) are slightly lower than those obtained here: for example, for 1% HPMC solution, the

slope values obtained by Choi et al. (2006) are 0.66 for G' and 0.55 for G'' versus 1.3 for G' and 0.8 for G'' in our case. This difference can be explained by the fact that in the case reported by Choi et al., (2006) the measurements were carried out at 25°C and that the higher the temperature, the more the sample acts like a gel (less frequency dependence) as there is more interactions between the hydrophobic zones.

The evolution of G' as a function of the hydrocolloid concentration is shown in Figure 6.6.

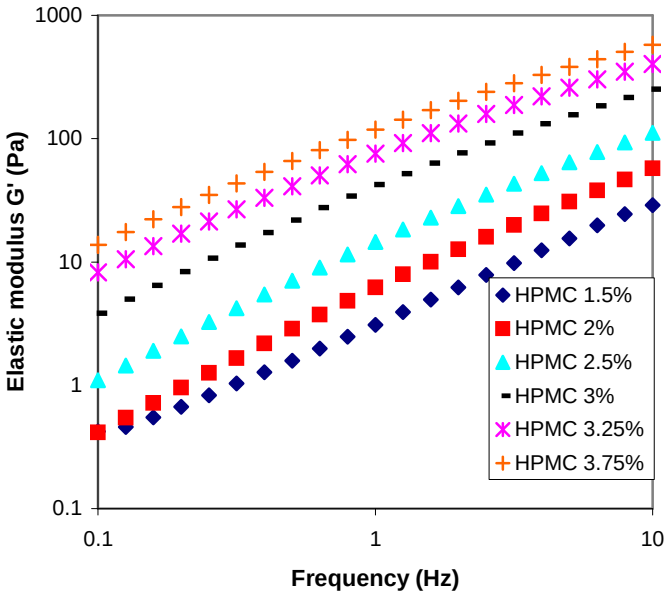

Figure 6.6: Evolution of the elastic modulus vs. frequency. Effect of hydrocolloid concentration.

Elastic modulus increased with increasing concentration. In all cases, G' was frequency- dependent and lower than G''.

The study of the rheological behaviour of HPMC solutions has shown that they were shear thinning and displayed elastic behaviour (measured N_1). At the studied temperature (20.0°C), their behaviour was close to that of liquids.

VI.1.2. Surface and interfacial tension

The density as a function of HPMC concentration is given in Figure 6.7. The values are the means of triplicates. It can be seen that density increases linearly with HPMC concentration.

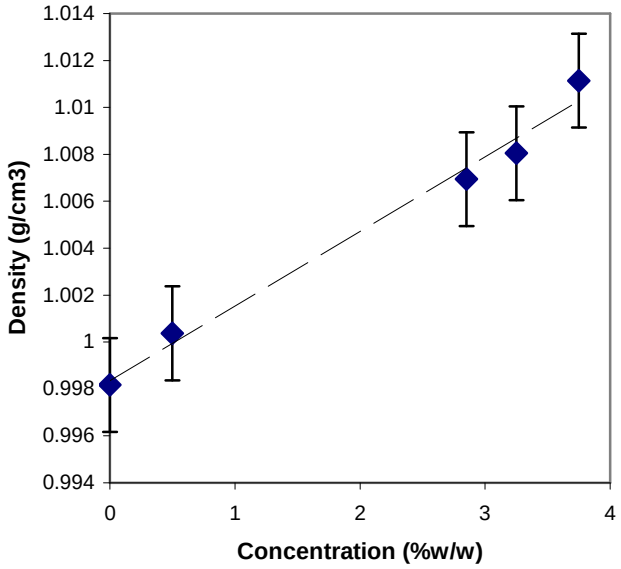

Figure 6.7: Density of HPMC depending on concentration

These values were determined as they are required for the analysis of the measured surface tension between air and the HPMC solutions and the interfacial tension at the oil/HPMC interface.

The evolution with time and the values as a function of concentration for the surface tension and interfacial tension are shown in Figure 6.8a-6.9a and Figure 6.8b-6.9b, respectively. In order to compare the data and check that the measurements are valid, the surface tension of water/ air and the interfacial tension between water and oil was studied. The values obtained are 72.8mN/m and 36.5mN/m respectively. These values are in good agreement with literature (Bergeron et al., 1997; Tice et al., 2003; Wolf & Windhab, 1995). Moreover, the value for water in silicon oil was cross-checked using the small deformation method (III.2.3); results were in good agreement with those found using the pendent drop method.

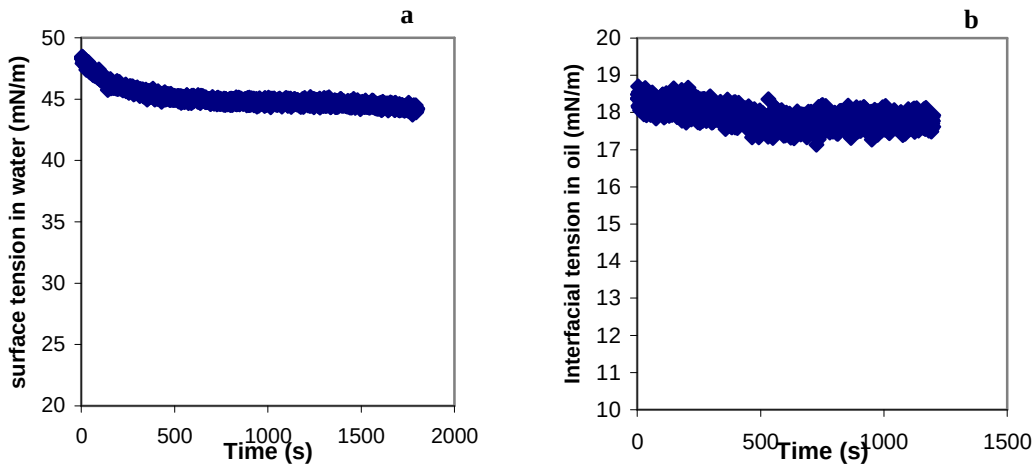

Figure 6.8: Evolution of tension properties as a function of time. (a) surface tension 3.75%HPMC/air. (b) interfacial tension 3.75%HPMC/silicon oil.

Figure 6.8 shows the data obtained for HPMC solution both in air (a) and in oil (b). The experiments were carried out over a period of time of 20-30min to make sure that the sample had reached equilibrium. As it can be seen, a stable value is reached after ~500s. The interfacial tension values obtained are lower than those seen for water in air and in silicon oil. Indeed, HPMC has hydrophobic groups (methyl) and hydrophilic groups (hydroxypropyl); it is thus surface active (amphiphilic) leading to a decrease in interfacial tension. The time to reach equilibrium depends on the time taken by the polymer chains to rearrange at the interface.

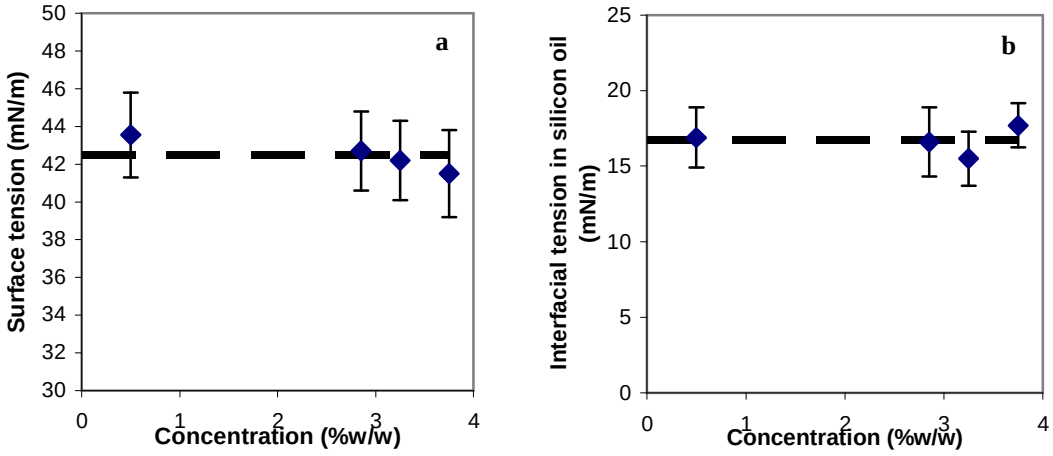

Figure 6.9: Surface and interfacial tension properties of HPMC solutions at various concentrations (a) in air; (b) in silicon oil. Lines are given to guide the eye.

Each value obtained for Figure 6.9 (a) and (b) are the mean of 10 experiments. Figure 6.9 a and b shows that the surface tension or the interfacial tension of HPMC in air and in oil respectively do not vary with the concentration within the studied range: around 42.5mN/m in air and 16.5mN/m in oil. It could be thought that the value of HPMC in air decrease with increasing concentration; however, considering the error bars this decrease is not significant. The constant values obtained can be explained by the high concentration of the solutions (above C*), the surface is thus saturated with polymer chains and no further decrease in the surface tension can be observed. Moreover, the values measured are within the range determined by Dow Chemical for this type of product.

Characterisation of HPMC solutions revealed that they displayed shear thinning behaviour and elasticity. These two parameters are important to know when considering droplet deformation experiments. The shear thinning behaviour will be counteracted by doing step-up shear stress experiments and the elasticity will be considered when interpreting the results. Finally, having quantified the interfacial tension between oil and HPMC, the Capillary number (defined in Equation 2.4) can be calculated.

VI.2. Shear induced droplet deformation and break-up

VI.2.1. Deformation of solution and suspension droplets

VI.2.1.1Visual observation of droplets at different concentrations

The observation of droplets immersed in silicon oil under shear using the counter rotating shear cell gives interesting results as the evolution of the droplet can be monitored during the entire duration of the experiment. In the following section, a description of what was observed will be given. It was chosen to compare the behaviour of an HPMC solution and a starch suspension for two different cases of sample concentration: diluted and concentrated. Both types of droplets were placed in PDMS 200 (silicon oil).

Figure 6.10 is composed of 5 pictures a, b, c, d and e which are representations of the diluted starch suspension droplet at different shear stresses. In this case, the shear stress was gradually increased from 0 to 500Pa. At rest (Figure 6.10a) the amount of solvent around the granules (water + amylopectin, see V.2 for details) was sufficient for the droplet to be spherical. Moreover, the granules inside the droplet could be distinguished. When a small shear stress was applied, the droplet deformed and aligned in the flow direction; the granules inside were seen to circulate along closed streamlines (Figure 6.10b). In Figure 6.10c, the shape of the droplet, after the shear stress was further increased to 170Pa, is shown and the first detachment of small droplets concentrated in starch granules through an end-pinching mechanism was observed. In that case, the circulation of the granules within the droplets had started decreasing slightly because some granules remained at the tips of the deformed droplet; further end-pinching occurred. At even higher stresses, no more internal circulation could be seen: all the granules are confined to the tips (Figure 6.10d). A close inspection of Figure 6.10d indicates that the droplet is at a critical state where more end-pinching will occur. This phenomenon will take

place until no more granules remain and the final droplet contains only solvent. In Figure 6.10e, that state is nearly reached; end-pinching occurs at one end and only a few granules remain at the other end.

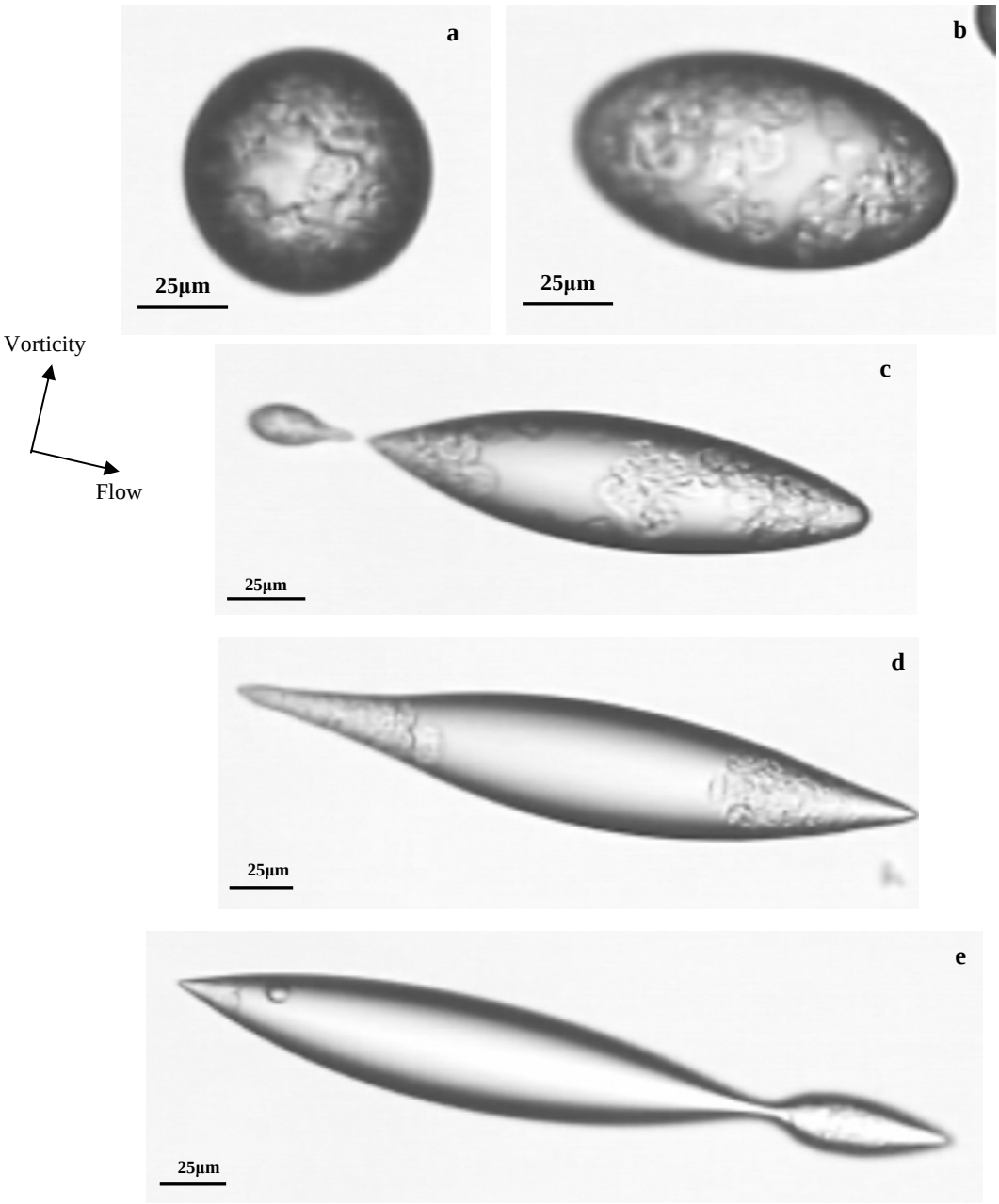

Figure 6.10: Deformation of a diluted (0.8%w/w) starch suspension droplet (initial diameter 70µm) with increasing shear stress: at rest (a), τ = 110Pa (b); τ = 170Pa (c); τ = 320 (d); τ = 485(e).

This type of behaviour has previously been reported for diluted suspension droplets of polystyrene beads in water (Smith & Vandeven, 1985).

Diluted HPMC droplets showed a very different break-up mechanism (Figure 6.11). The droplet was spherical at rest as expected (Figure 6.11a). When shear stress was applied, the droplet deformed into an ellipsoid aligned in the flow direction as can be seen in Figure 6.11b. At this point, steady state deformation, i.e. when at a constant stress no further deformation can be observed, has not yet been reached. This is demonstrated by Figure 6.11c, which was obtained for the same shear stress but not the same strain (shear rate*time). In Figure 6.11c, higher deformation than for Figure 6.11b can be seen. In this case the deformation is no longer in the small deformation limit as defined by Taylor, i.e. D > >0.2 (see II.3.1).

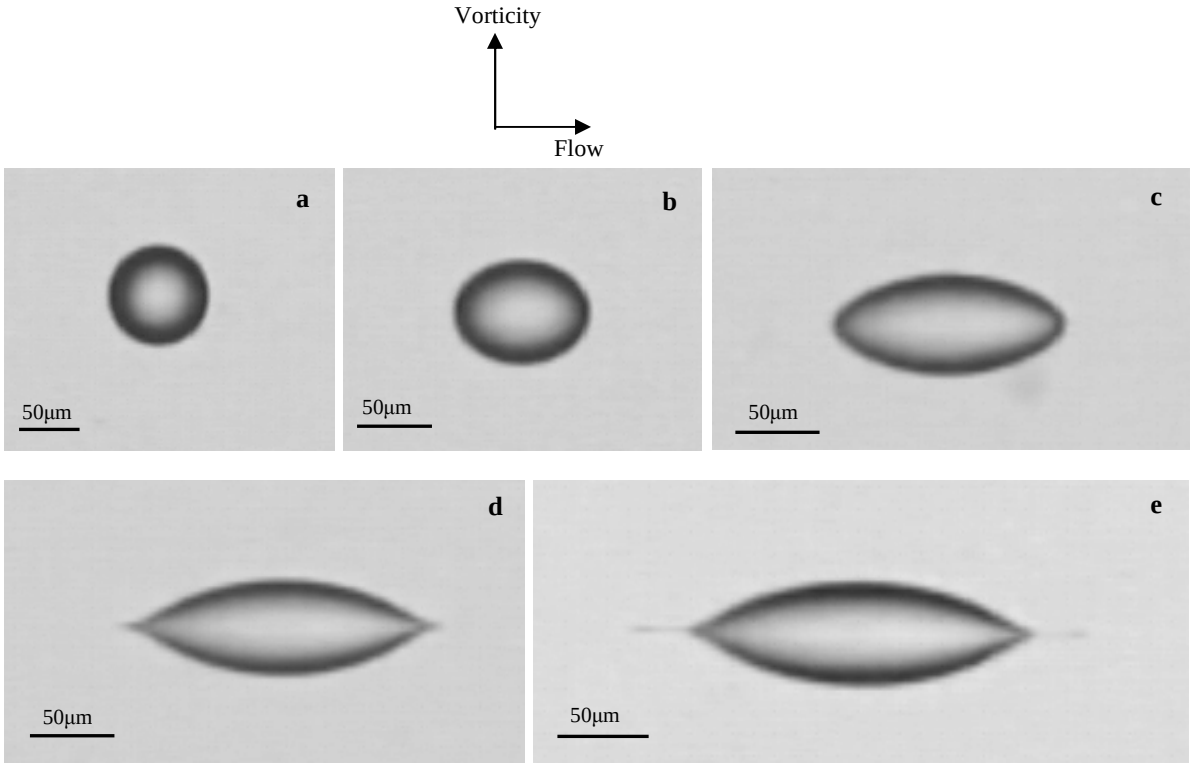

Figure 6.11: Deformation of a diluted (0.1%w/w) HPMC solution droplet (initial diameter 70µm) with increasing shear: at rest (a), τ = 310Pa (b); τ = 310Pa (c); τ = 490 (d); τ = 640 (e).

When the shear stress was further increased, pointed tips appeared (Figure 6.11d) which corresponded to the onset of break-up through a tip-streaming mechanism. This occurrence is evident from Figure 6.11e, where a thin stream of liquid coming out of the droplet can be seen. Tip-streaming has previously been reported in various studies (De Bruijn, 1989; Grace, 1982; Taylor, 1932; Taylor, 1934). De Bruijn

(1993) suggested that this phenomenon occurred when a gradient of interfacial tension developed at the surface of the droplet. It can hence be observed when a droplet containing a small amount of surfactant is submitted to shear. As it was shown above (VI.1.2), HPMC is amphiphilic and has thus surface active properties, explaining the observation of the tip-streaming phenomenon.

Figure 6.12 shows typical images of the deformation and break-up of a 100% volume fraction swollen-in-water starch suspension droplet (starch concentration is 8%w/w) placed in an immiscible matrix (PDMS).

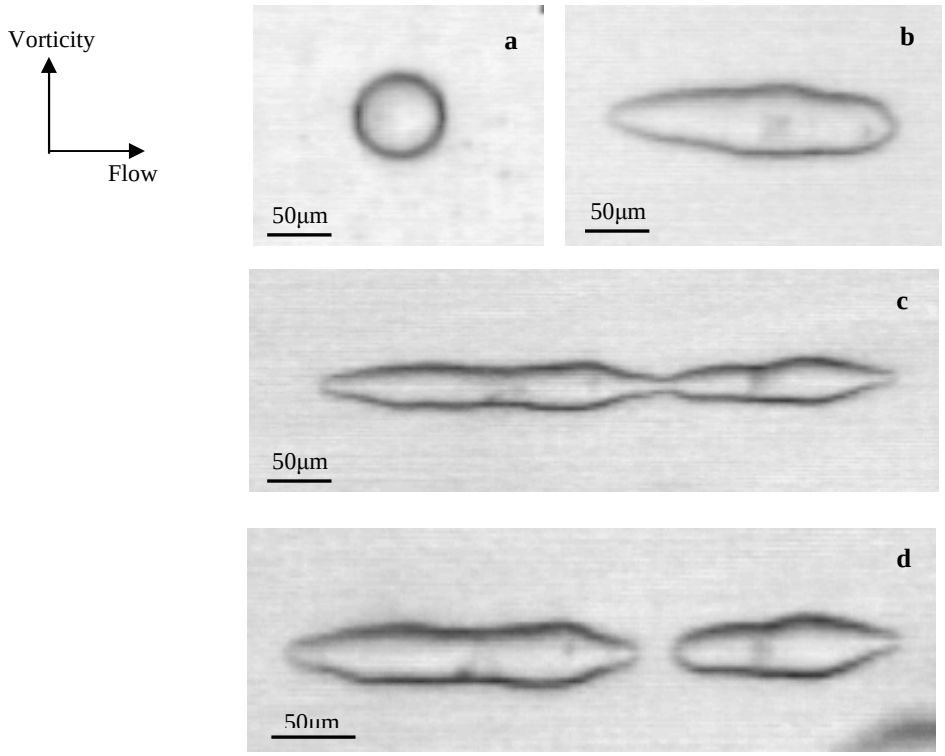

Figure 6.12: Time dependent deformation concluding in break-up of a concentrated starch suspension droplet (initial diameter 70µm) upon shear stress step-up from rest to 640Pa: at rest (a), t = 10s (b); t = 40s (c); t = 53s (d).

In Figure 6.12a it is demonstrated that the droplet is spherical at rest; this means that although the suspension is at a theoretical volume fraction of 1 there is still a small amount of solvent around the granules. Upon application of shear stress (here: stepped-up from rest), the droplet starts deforming (Figure 6.12b). The shape of the droplet is irregular which is in stark contrast to the perfect ellipsoidal shape of deforming fluid droplets. This is a result of the presence of swollen granules irregular in shape and size which, albeit fully occupying the volume of the droplet,

were observed to move on closed streamlines inside the droplet (the size of individual granules is not resolved in the micrographs presented). As the granules move around, there is a constant change of the aspect of the drop. Internal shear in fluid droplets undergoing shear deformation is a well-known phenomenon, see, e.g., Rumscheidt & Mason (1961). Figure 6.12c shows further elongation of the droplet in time and shape irregularities prevail. By maintaining the shear stress, the droplet can either stabilise and reach its steady state deformation, in which case rearrangement of granules continues to be observed, or break-up. For the shear stress applied in the experiment discussed, break-up with the formation of two daughter droplets of similar size is evident from Figure 6.12d. In this case, the deformation pictured in Figure 6.12c is already critical, and its shape resembles the shape the droplet assumes to break-up. The break-up pattern observed for the droplet system under investigation is not dissimilar to what has been reported previously for fluid droplets (Rumscheidt & Mason, 1961); however, there are several discrepancies which are discussed in detail in section VI.2.3.

The time dependent behaviour of a concentrated HPMC droplet (3.25%w/w) submitted to the same shear stress as the concentrated starch suspension droplet is presented Figure 6.13.

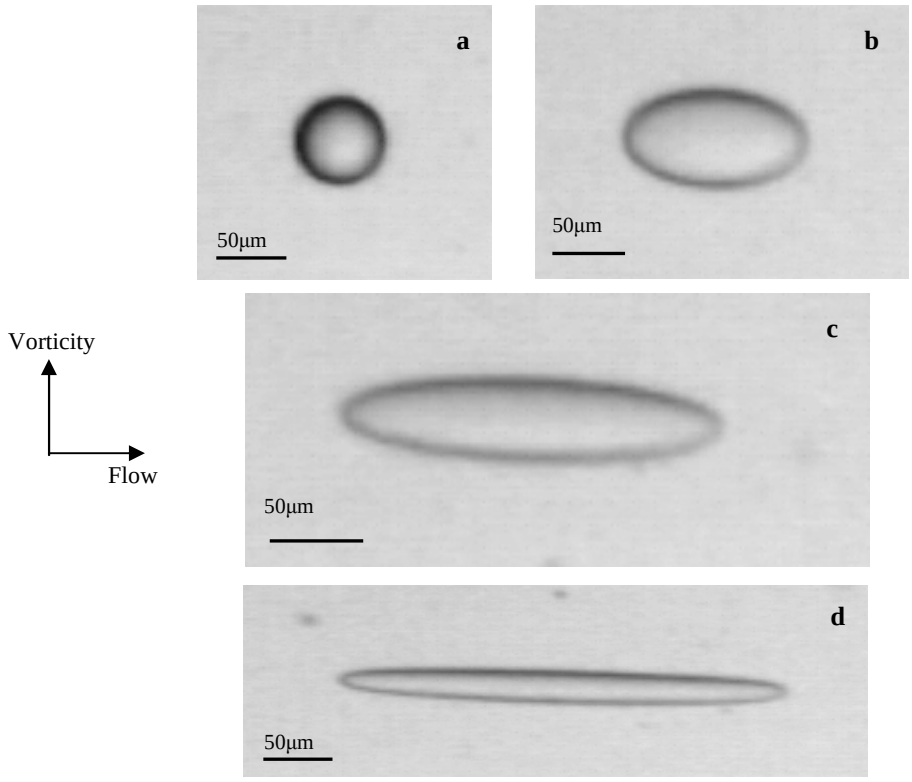

Figure 6.13: Time dependent deformation of a concentrated HPMC solution droplet (initial diameter 80µm) upon shear stress step-up from rest to 640Pa: at rest (a), t = 4s (b); t = 6s (c); t = 50s (d). No break-up was observed.

The droplet was spherical at rest (Figure 6.13a) but started deforming once the desired shear stress was applied (Figure 6.13b). At first, the deformation was small but it increased with time and the drop assumed the shape of a flattened ellipsoid (Figure 6.13c). Between Figure 6.13b and c the small axis of the ellipsoid (the width W defined in Chapter II.3.1) decreased and the other small axis in the velocity gradient direction (the breadth, B), which is not visible here, also contracted. An increase in strain leads to even higher deformation until the droplet has reached a steady state deformation (Figure 6.13d) or break-up. In the cases that will be presented, break-up was never observed for the concentrated HPMC droplets. In its steady state deformation the shape of the droplet is that of a thin thread with pointed tips (Figure 6.13d). If the stress is stopped, the droplet will relax to its initial spherical shape.

The observation of diluted and concentrated (or smi-diluted regime for HPMC) droplets of different thickening agents revealed interesting differences depending on concentration, the break-up mechanism being the main one. For diluted systems, tip streaming (HPMC droplet) or end-pinching (starch droplet) were the break-up mechanisms. However, the study of diluted systems can only be qualitative, at least for starch suspension droplets, as it is not possible to control the concentration of granules within the drop. **Therefore, the following studies have been carried out in a specific case where all the space is taken by the granules i.e. when the volume fraction is close to 1 (starch concentration 8%w/w)**. In this case, all starch suspension droplets will have the same concentration and a quantification of deformation and break-up can be done.

This study also revealed differences between two types of concentrated droplets, the suspension and the solution: rupture occurs for one (starch) but not the other in the conditions applied in this experimental work.

VI.2.2.2.Comparison between the physico-chemical aspects of a starch suspension and an HPMC solution

In this paragraph, a brief summary of the physico-chemical properties of both the starch suspension and the HPMC solution in the concentrated state will be given. As the behaviour of a starch droplet will be compared to an HPMC thickened droplet, a description of the general features of both systems will be given gathering the data put forth throughout the thesis.

- Rheological behaviour

The major differences in rheological behaviour observed between starch and HPMC are presented in the table below (Table 6.1).

Table 6.1: Rheological properties of the starch suspensions and HPMC solution.

8% swollen starch (modified waxy maize)	**HPMC**
Suspension	Solution
Presence of a yield stress then shear thinning	Low shear Newtonian plateau then shear thinning
Fitted with Herschel-Bulkley model	Fitted with the Cross model
Gel-like behaviour	Liquid-like behaviour

Table 6.1 shows that the studied systems are quite difficult to compare: one is a solution with a low shear Newtonian plateau and the other a suspension with a yield stress. Nevertheless, they are both shear thinning. Due to this non-Newtonian behaviour the experiments were carried out at constant shear rate (by stepping-up to the required stress), hence avoiding any variation of the viscosity ratio during the measurement. At first, the samples were compared at equal shear rates; the HPMC concentrations were adjusted to have equivalent viscosities with the starch suspension (8%w/w). At shear rates $1.8s^{-1}$, $2.9s^{-1}$, the samples had the same viscosity if the HPMC solutions were prepared respectively at the following concentrations: 3.75%, 3.25%, see Figure 6.14. The droplet deformation and break-up experiments were thus conducted at these shear rates.

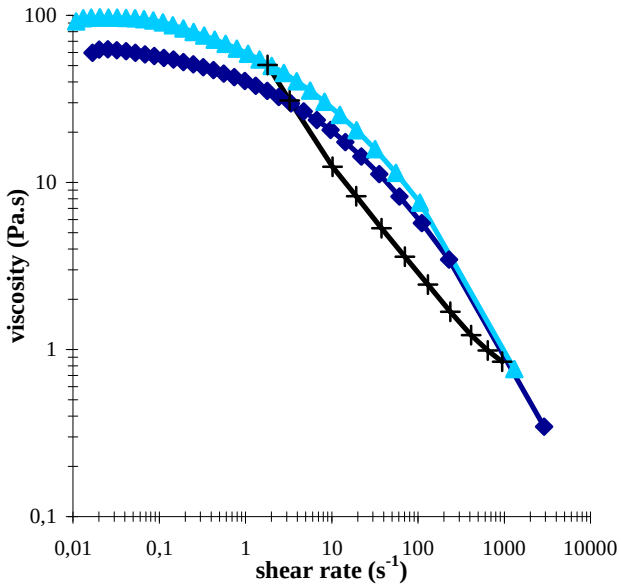

Figure 6.14: Viscosity of studied systems vs. shear rate. Diamonds: 3.25% HPMC; Triangles: 3.75% HPMC; Crosses: starch suspension 8%. Lines are given to guide the eye.

However, in the counter rotating shear cell, the droplets are immersed in silicon oil. It makes more sense to consider the shear stress applied to the droplet rather than the shear rate, as in the shear stress the viscosity of the oil (which is part of the viscous forces deforming the droplet) is taken into account. The resulting shear stress for the applied shear rates are the product of the viscosity of the silicon oil (220Pa) and the shear rate, i.e. 400Pa and 640Pa. Using the data obtained with rheology measurements, viscosity and viscosity ratios were determined for the given shear stresses as shown in Tables 6.2 and 6.3.

Table 6.2: Viscosity and *p* values for HPMC solutions of different concentrations

	η (Pa.s)	p
τ= 400Pa (HPMC 3.75% w/w)	20.5	$9.3*10^{-2}$
τ=640Pa (HPMC 3.25% w/w)	5.7	$2.59*10^{-2}$

Table 6.3: Viscosity and *p* values for the modified waxy maize starch suspension of 8%

	η (Pa.s)	p
τ= 400Pa	1.68	$7.63*10^{-3}$
τ=640Pa	0.98	$4.45*10^{-3}$

It can be noticed that the values of viscosity for the given shear stresses are not equivalent in this case for starch suspensions and HPMC solutions. The systems were not prepared to be equivalent at shear stresses as at first, the viscosity of the samples were considered alone and not immersed in the oil.

The elasticity of the studied systems is also important to consider as it will have an impact on the deformation and break-up conditions. It has been reported in literature (see Chapter II.3.2) that elasticity will hamper the deformation and increase the Capillary number at which break-up will occur. The measured first normal stress differences for all three samples are presented in Figure 6.15. It can be observed that the elasticity of the starch suspension develops at higher shear stresses but for shear stresses above 500Pa it is equal to those measured for the HPMC

solutions. However, it is important to point out that the origin of the elasticity is very different. For HPMC solutions, elasticity arises from interpenetration of the polymer chains (see VI.1.1), whereas for starch suspension the origin of the first normal stress difference is the deformation of the granules (see V.1.1.5).

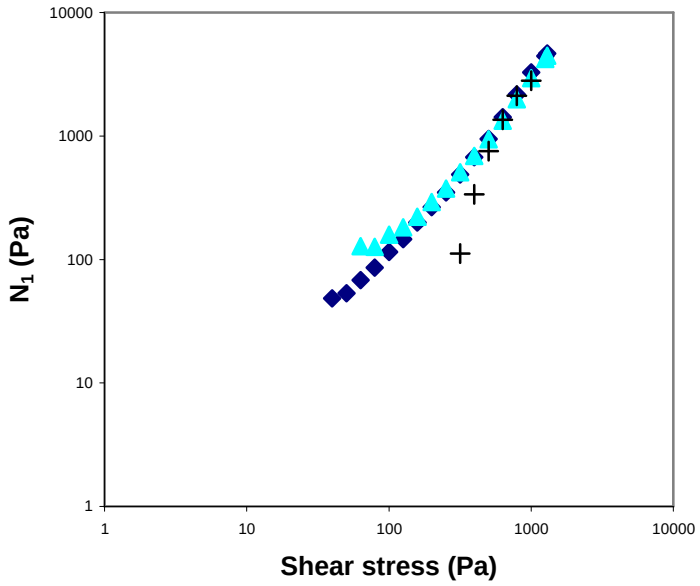

Figure 6.15: First normal stress differences vs. shear stress. Diamonds: 3.25% HPMC; Triangles: 3.75% HPMC; Crosses: starch suspension 8%.

The rheological properties of the starch suspension and the HPMC solutions are very different. The origin of these differences is the microstructure of the samples. This makes it difficult to actually compare these two systems appropriately. In the following, the results of experiments, their deformation and break-up conditions will be compared when they were submitted to the same shear stress. However, it should be considered that the resulting viscosity ratios and elasticities of the two systems were slightly different.

- Interfacial tension:

The interfacial tension between the silicon oil and the studied system also play a major role as it tends to keep the droplet spherical. A high interfacial tension will lead to higher break-up conditions, i.e. that higher capillary numbers are needed to rupture the droplet. The values obtained for all the systems are summarised in Table 6.4.

Table 6.4: Interfacial tension in oil, measured using the pendent drop method.

Studied system	Γ (mN/m)
Water	36
Modified waxy maize supernatant	33
HPMC 3.25%	16.5
HPMC 3.75%	16.5

As expected, water has the highest interfacial tension; the value obtained with the pendent drop method and the small deformation method (rheo-optical measurement) yielded similar results. The value for the starch supernatant/oil interfacial tension is slightly lower than that obtained for water, due to the presence of small amounts of amylopectin chains (see Chapter V.2). Finally both HPMC solutions have the same interfacial tension value and also the lowest of all systems. This is to be expected as HPMC is known to be surface active thanks to its hydrophilic and hydrophobic substituents. When considering only interfacial tension values, HPMC should be easier to break up than water or starch suspension. However, as it will be shown later, different parameters such as elasticity for example, are involved in the deformation and break-up mechanisms.

This section showed that it is difficult to compare the starch suspension droplet and the HPMC solution droplet in similar conditions. Not only are their rheological behaviours very different but their interfacial tension with oil as well. Even if the viscosity ratios were equivalent (equivalent viscosity at a given shear stress), the capillary numbers would be different as the interfacial tensions are different.

VI.2.2.3. Droplet orientation

A deformed droplet under flow adopts a certain orientation following the velocity gradient axis. This angle usually depends on the applied shear rate (or Capillary number) and the viscosity ratio (Rumscheidt & Mason, 1961). The angle

was determined by carrying out a set of measurements on a different counter rotating cell developed in Le Mans (see description in Section III.2.1.6) which allowed visualisation in the flow/(velocity gradient) plane.

To check that the data obtained is reliable, experiments were carried out on a known system, i.e. a Newtonian system: water in silicon oil. The measured angle for a water droplet in PDMS 200 at low capillary numbers (Ca = 0.1) was around 40° which is in good agreement with literature (Caserta et al., 2007; Greco, 2002; Rumscheidt & Mason, 1961).

The values obtained for the orientation angles of HPMC and starch droplets at Ca= 0.35 (considering the experimental conditions that were applied in the counter rotating shear cell) are presented below in Table 6.5.

Table 6.5: Orientation angle of the droplets at Ca = 0.35

	p	Angle φ (°)
HPMC 3.25%	0.2	25
HPMC 3.75%	0.3	20
Starch	0.017	15

At the start of an experiment, droplets have an orientation angle of 45° which decreases rapidly as they align in the flow direction and finally reach a steady orientation. The values determined here were taken when the droplet had reached steady state deformation. Results obtained for the HPMC solution droplets are in good agreement with literature (Assighaou, 2006; Maffettone et al., 2005). It would be expected that the starch suspension droplet adopts a similar orientation to that of the HPMC droplet or a higher angle closer to those reported for Newtonian droplets (at low stresses elasticity has not yet developed in starch suspensions). Further experimentation is required to find an explanation for the low orientation angle (15°) observed.

The higher the Capillary number (increasing shear rate), the more the droplet orients in the flow direction: the angle decreases. When the Ca>0.5, the orientation angle is around 5° (Guido et al., 2004; Maffetone & Minale, 1998). At 5° the effect of the angle on the projected length is minor; it can thus be considered as the real

length. In the following experiments, the orientation angle was taken into account to calculate the value for D when the Capillary number was below 0.5.

VI.2.2.4. Droplet deformation

The experiments were carried out by stepping up the shear from zero to the desired value; during the experiments the shear rate was kept constant to avoid any shear thinning of the droplet (see section III.2.4). Consequently, the viscosity ratio (reported Tables 6.2 and 6.3) within the experiment did not vary. Both systems displayed evident elasticity as shown in Figure 6.14.

Results obtained for the deformation of starch and HPMC droplets are presented in Figures 6.16 and 6.17. The elongation of the droplet along the flow direction is determined as a function of strain (Shear rate*time). The data shown here are representative of the behaviour of all the droplets whatever the shear stress applied. In Figure 6.16 and 6.17, the deformation of the droplet is considered as the extension of the droplet, i.e. the length divided by the initial diameter.

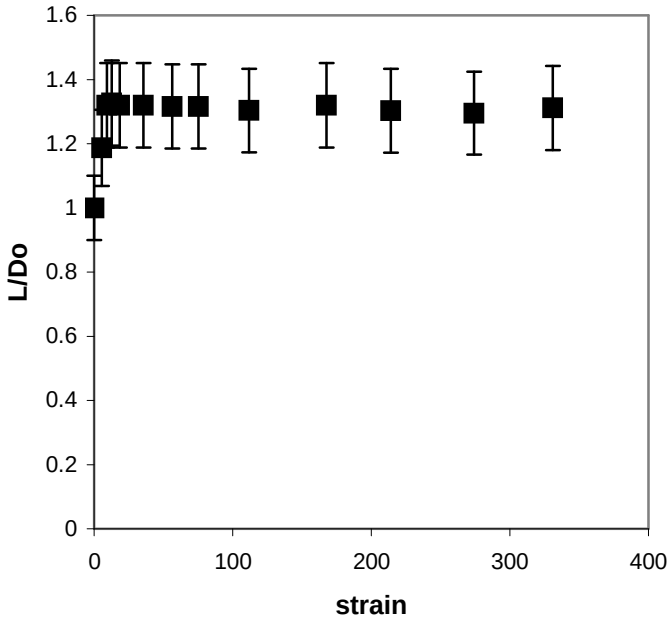

Figure 6.16: Deformation of a starch suspension droplet as a function of strain. Initial droplet size = 70µm. Shear stress 400Pa.

When comparing Figure 6.16 and 6.17, HPMC and starch display different behaviours before reaching steady state deformation. In Figure 6.16, it can be noticed that the droplet reached its steady state deformation quasi instantly whereas in the case of the HPMC droplet the steady state was reached much later (see Figure 6.17). It seems that starch acts like a Newtonian droplet when submitted to stepped-up shear. For the HPMC droplet, an overshoot can be noticed occurring prior to the steady state. This phenomenon has been previously reported (Maffettone et al., 2005; Sibillo et al., 2005) and appears to be a typical behaviour of viscoelastic droplets.

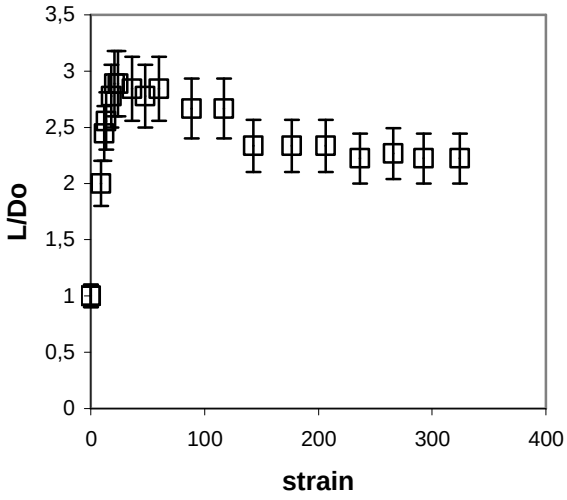

Figure 6.17: Deformation of an HPMC droplet (3.25%w/w) as a function of strain. Initial droplet size = 50µm. Shear stress 640Pa.

Figure 6.18 (a) and (b) shows Taylor's deformation D (Equation 2.5) for starch suspension and HPMC droplets as a function of the Capillary number. The data obtained was compared to the predictions from Cox's model (Equation 2.7; Cox, 1969).

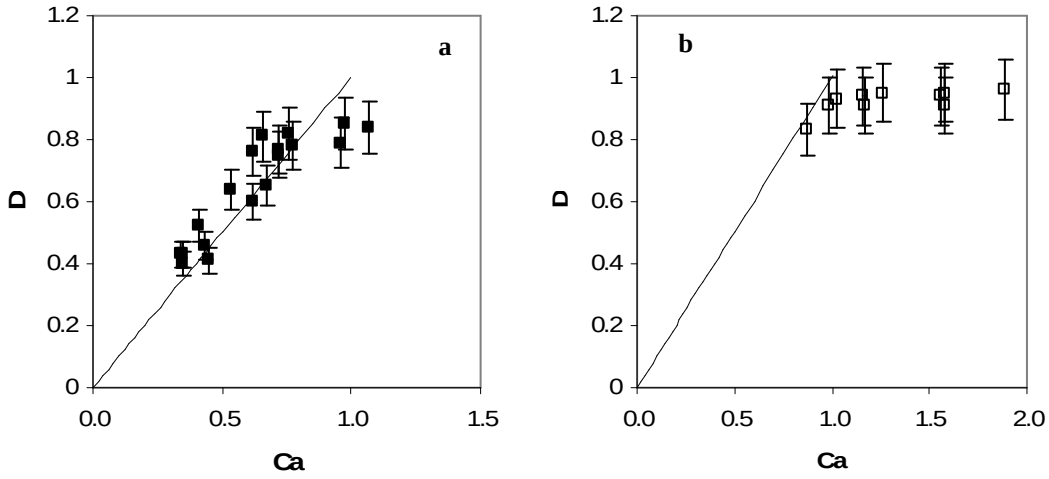

Figure 6.18: D as a function of the Capillary number. (a) Starch suspension droplets (8%w/w); (b) HPMC droplets (3.25% and 3.75%w/w). Solid black line is the model developed by Cox (Cox, 1969).

The deformation D of starch suspension droplets seems to be similar to that determined for Newtonian droplets. For values of Ca around 1 and above, the deformation is lower than what is predicted from the model. This deviation could be explained by the fact that at large stresses the elasticity of the starch suspension is increased leading to lower deformations. It could also be that Taylor's deformation is not sufficient to describe large deformation as all values tend towards one. This later hypothesis is evidenced when looking at Figure 6.18b. The capillary numbers applied are high leading to high deformations. No conclusions can be drawn using D as all droplets seem to have the same value. Hence, to study the deformation of the HPMC, the ratio of the long droplet axis to its initial size will be plotted against the Capillary number. The results obtained for HPMC are compared to those of the starch suspension droplet (Figure 6.19). In this figure each point corresponds to one experiment. The deformation of each droplet reported in this figure is defined as the moment when no more evolution of the droplet is observed, i.e. the steady state.

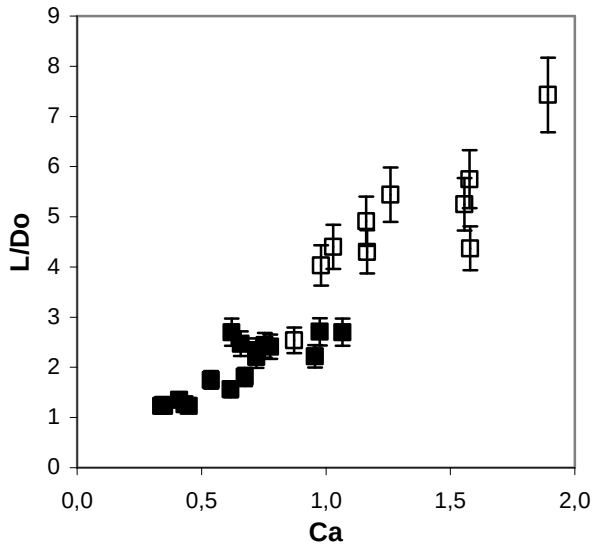

Figure 6.19: Deformation vs. Capillary number. Full squares: starch suspension droplets; Hollow squares: HPMC droplets (3.25% and 3.75%w/w). Error bars are for the error of the experimental set-up

It can be seen in Figure 6.19 that the deformation for starch droplets are lower than those for HPMC droplets. However, it seems that a straight line from the origin of the graph could fit both sets of data. Deformation increases linearly with increasing Capillary numbers for HPMC as observed for the behaviour of starch. The deformation is linear for low Capillary numbers (0.7). It is possible to think from the data in Figure 6.19 that the deformation of HPMC would be similar to that of starch at low capillary numbers. Figure 6.20 represents the deformation (L/D_0) as a function of the applied strain and the behaviour shown here was observed in all cases where the droplets were compared at the same stress and for the same size. The droplets of both types investigated had the same initial size and the applied stress was the same. Both the starch suspension and the HPMC solution are viscoelastic at the applied stress.

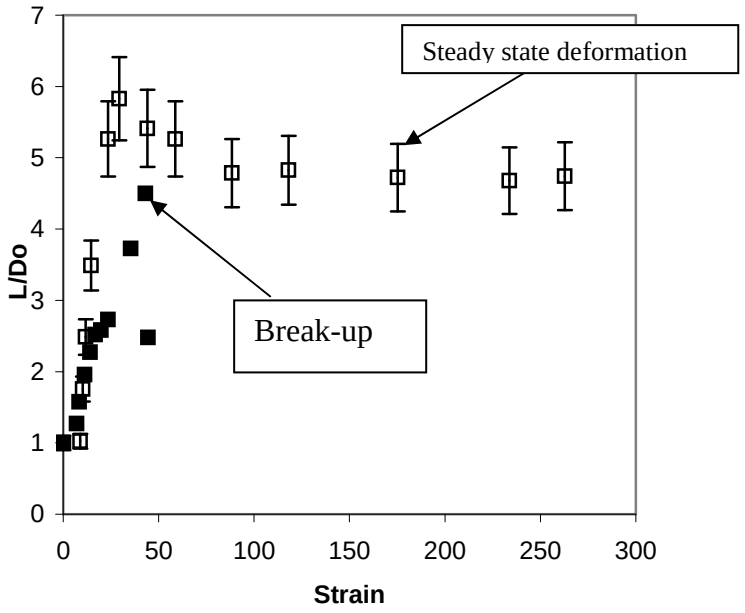

Figure 6.20: Deformation vs. Strain for a starch suspension droplet (dark points) and a 3.25%HPMC solution droplet (open points). Applied shear stress = 640Pa; $D_{0HPMC}=D_{0Starch}=80\mu m$

Figure 6.20 shows that the starch suspension droplet breaks up more readily than the HPMC solution droplet. It would be expected to see the droplet of HPMC break up at lower capillary numbers than that of starch one as the viscosity ratio is higher and the interfacial tension is lower (Ca are 0.75 and 1.55 and p values are $4.45*10^{-3}$ and $2.59*10^{-2}$ for the starch suspension droplet and the HPMC solution droplet respectively). Interpretation of this phenomenon is explained further when discussing the break-up of starch suspension droplets (section VI.2.2). It seems, however, that starch suspension droplet in this case act more like a Newtonian fluid droplet than a droplets of a viscoelastic system. The behaviour of the HPMC droplet is in good agreement with literature which states that higher Capillary numbers are required to break up viscoelastic droplets than Newtonian ones (Lerdwijitjarud et al., 2004; Mighri et al., 1998; Milliken & Leal, 1991; Sibillo et al., 2005; Tsakalos et al., 1998; Varanasi et al., 1994).

VI.2.2.5. Droplet relaxation

When the shear flow is stopped the drop relaxes; when doing so it can either break-up into smaller droplets through end-pinching or Rayleigh instabilities or retract to its intial spherical shape (Tucker & Moldenaers, 2002). These phenomena are driven by the interfacial tension. The behaviour of the droplet depends on the aspect ratio of the filament. Carrière et al. (1989) defined the deformed drop as being a cylinder capped with two semispherical ends. If the aspect ratio of a deformed drop, i.e. length of the cylinder (L) to the radius of the cross section (r) does not exceed a critical value which depends on the viscosity ratio (Tjahjadi et al., 1994) then the droplet will retract to its initial shape; above a critical value of L/r, end-pinching occurs (Tjahjadi et al., 1994). Droplet rupture through Rayleigh instabilities can be seen only when L/r >>60 (Stone et al., 1986).

Figure 6.21 shows the relaxation of a starch droplet submitted to a shear stress of 400Pa for 3min, which means that the droplet is at its steady state deformation; its value is $L/D_0 = 2$ prior to relaxation. The droplet has reached its steady state deformation and has adopted the shape of an ellipsoid. Once the shear stress is stopped, the droplet starts retracting into an ellipsoid (Figure 6.21 c and d). Finally, after just a few seconds, the droplet is back to its initial shape.

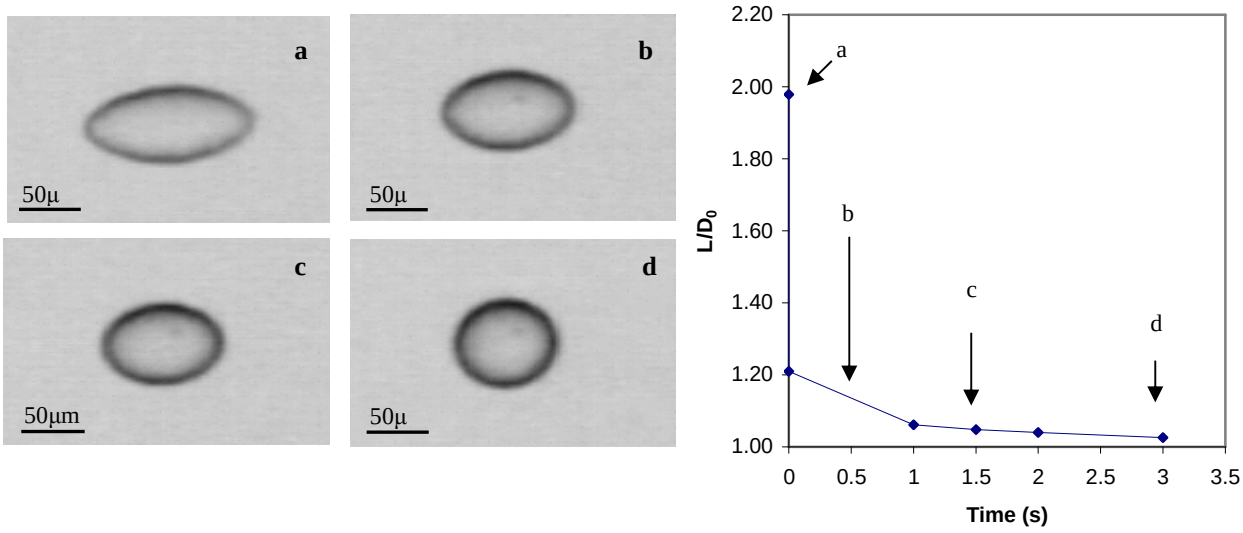

Figure 6.21: Relaxation of a starch suspension droplet (8%w/w). (a) t =0s; (b) t = 0.5s; (c) = 1.5s; (d) t = 4s. L_0 = 75µm. Line is given to guide the eye.

Figure 6.21 also shows the evolution of the major axis of the droplet as a function of time. It can be seen that the droplet retracts to its initial state in 2-3 seconds. The decrease in the size of the long axis is exponential which is to be expected (Tucker & Moldenaers, 2002).

The relaxation of a 3.75% HPMC droplet is shown in Figure 6.22. The droplet in Figure 6.22a has a cylindrical shape with pointed caps; this droplet shape corresponds to its steady state deformation. Once the shear stress has been stopped and the droplet has started to relax, deformation decreases and the shape is that of a cylinder with semi-spherical caps as described above (Figure 6.22b and c). This type of behaviour has previously been reported for hydrocolloid (Hydroxypropyl cellulose) solution droplets (Takahashi et al., 2007). After 10s the droplet adopts an ellipsoidal shape (Figure 6.22d) before becoming spherical (Figure 6.22e).

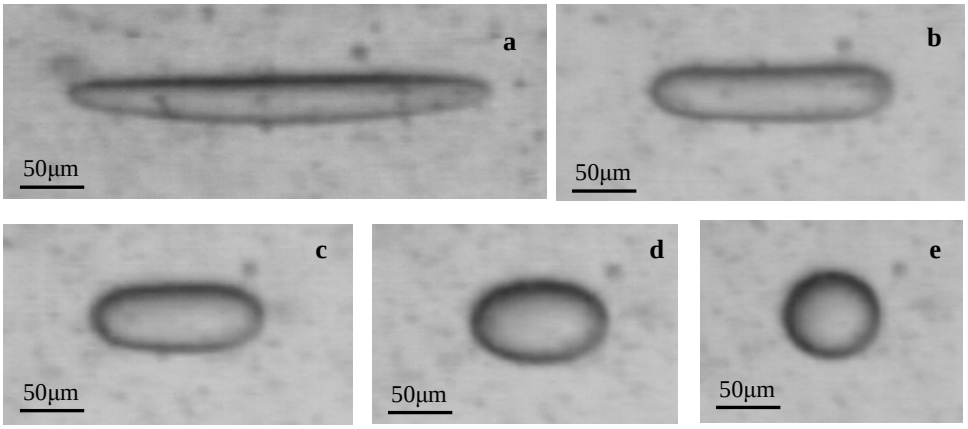

Figure 6.22: Relaxation of a 3.75%HPMC solution droplet. (a) t =0s; (b) t = 3.5s; (c) = 7.5s; (d) t = 10s, (e) = 14s. $D_0 = D_{final}$ = 79µm.

The aspect ratio of the deformed droplet is L/r =12. Upon relaxation no rupture is observed, thus the critical value of the aspect ratio had not been reached. The aspect ratio is expected to be higher with viscoelastic drops than for Newtonian ones as elasticity of the droplet tends to resist deformation and rupture.

Effect of initial droplet size and viscosity ratio on relaxation time can be seen in Figures 6.23 and 6.24.

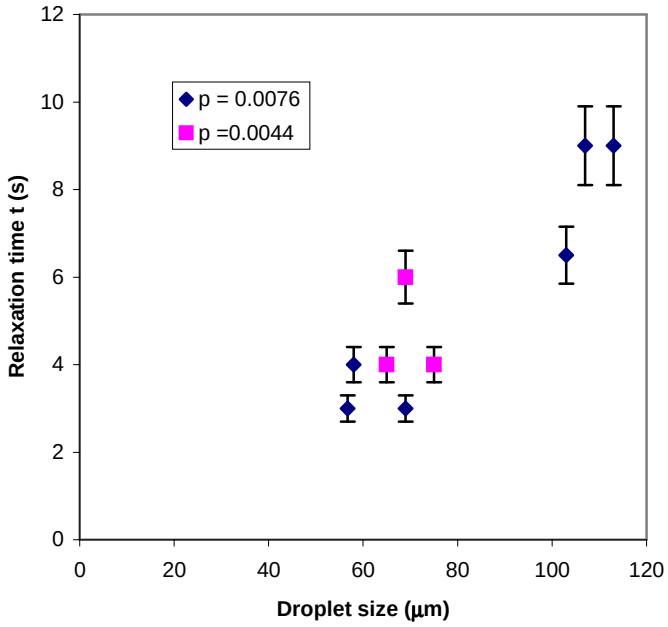

Figure 6.23: Relaxation time vs. initial starch suspension droplet size. Diamonds are for p = 0.0076 and squares are for p = 0.0044.

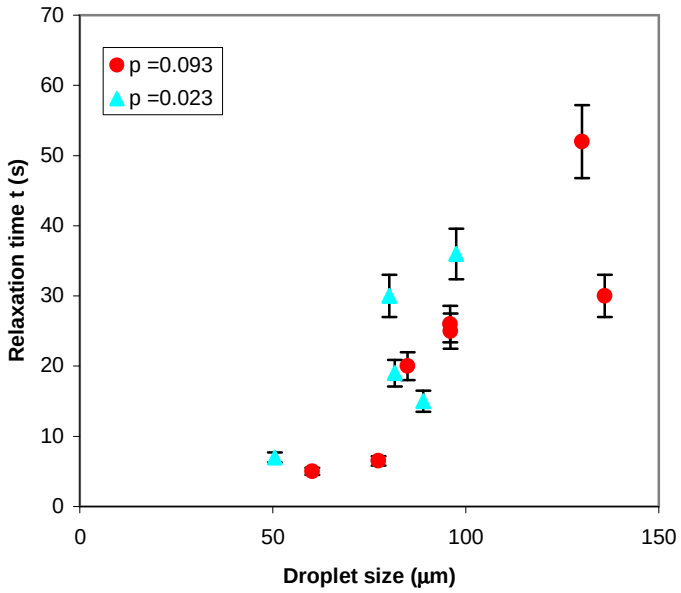

Figure 6.24: Relaxation time vs. initial HPMC droplet size. Diamonds are for p = 0.0076 and squares are for p = 0.0044.

Relaxation time increases with increasing initial droplets size, but there is no or little effect of the viscosity ratio. Droplet relaxation time is known to increase with initial steady state deformation (Tucker & Moldenaers, 2002). As deformation

increases with droplet size, it is normal to observe an increase of relaxation time as a function of the initial droplet. However, it was shown previously that relaxation time depended on the viscosity ratio between the droplet and the suspending fluid (Moran et al., 2003). This difference from earlier observations can be explained by the fact that the variation between the viscosity ratios is small. Indeed, differences in relaxation time were seen when one of the viscosity ratio is 10 times bigger than the other.

Differences occurring between the relaxation of starch suspension droplets and HPMC solution droplets can be seen Figure 6.25. In this case, they were compared when the initial deformation is equivalent.

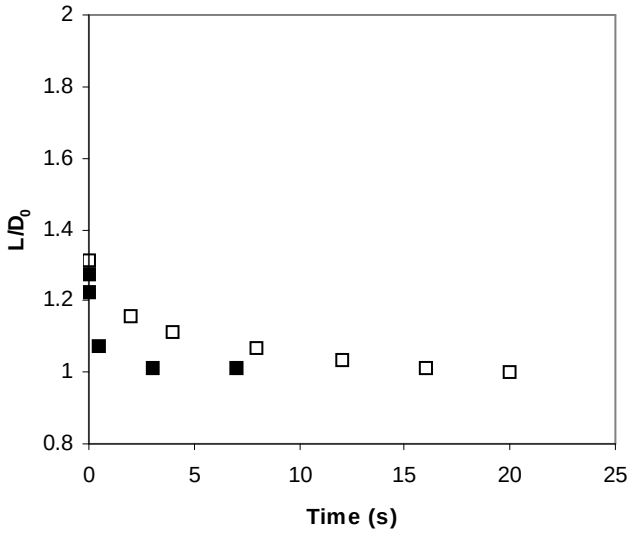

Figure 6.25: Comparison between relaxation time for starch suspension droplet (full squares) and 3.25% HPMC solution droplet, with the same initial deformation.

The HPMC droplet takes nearly 15s to retract to its spherical shape. On the other hand, the starch suspension droplet reaches its initial state in approximately 7s. The origins of this difference can be various. First, the interfacial tension between the starch suspension droplet and the suspending matrix (silicon oil, PDMS 200) is twice as high as that of the HPMC/oil interface. Another reason for this occurrence is the viscosity ratio of the droplet: for starch p = 0.0044 whereas for HPMC p= 0.023 which is nearly 10 times the viscosity ratio between starch and oil. This result is in good agreement with literature (Moran et al., 2003); they showed that the

relaxation time was increased when the viscosity ratio varied from 0.01 to 0.1. Finally, the different microstructure of these two systems could also explain these differences: the intrinsic relaxation time of a polymer chain would be higher than that of a single starch granule.

The primary interest for the PhD study was to correlate mixing properties with droplet break-up. The idea behind this hypothesis was to find a parameter to help understanding and predicting the variation of in-mouth flavour perception depending on the type of thickener. As mixing ability was suggested as a key issue in the release of flavour to the taste buds (Ferry et al., 2006), droplet break-up was hypothesised to provide new insights on this matter. This section has underlined the differences existing between HPMC solution droplets and starch suspension droplets. It has been demonstrated here that modified waxy maize starch, which offers better flavour release and better mixing ability in thickened products than HPMC, breaks up more easily although physico-chemical parameters (viscosity ratio, interfacial tension) suggest the opposite. It is thus possible to think that the study of droplet break-up can give good information on the mixing ability. However, further and more extensive studies, using a variety of thickeners, should be carried out to fully conclude on this matter.

The observation of the break-up of starch suspension droplets raised questions on this phenomenon. What happens within the droplet when it is submitted to stress? How do the granules influence the droplet behaviour? An attempt in answering these questions is made in the following section.

VI.2.2. Break-up condition of a droplet of starch suspension

In this section, a detailed study of starch suspension droplet break-up is presented and rupture mechanisms are discussed. Critical capillary numbers for droplet rupture, $Ca^* = \frac{\eta_{PDMS}\,\dot{\gamma}}{\Gamma / R}$ where Γ is the (starch supernatant)/PDMS interfacial tension and R the droplet initial radius, were calculated for droplets of different sizes

immersed in silicon oils of different viscosities and sheared at various shear rates. A reminder is that within one experiment, the applied shear rate (and thus the shear stress) is kept constant to avoid shear thinning phenomenon and thus to keep constant the viscosity ratio $p = \eta_{droplet}/\eta_{PDMS}$. To calculate the critical Capillary number, a critical droplet radius R_{crit} is determined as all other parameters remain constant throughout the experiments. Figure 6.26 represents the way R_{crit} is determined; the x-axis is for the droplet size. On the Y axis, y = 0 corresponds to the cases when the droplet does not break up while y = 1 indicates that break up occurred.

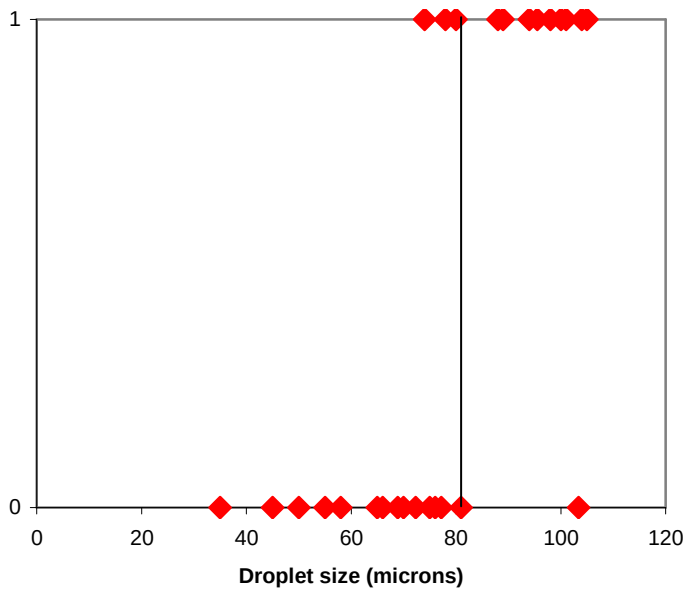

Figure 6.26: Determination of the critical droplet radius. The line corresponds to determined critical radius.

The critical droplet radius for break-up was defined as the radius at which the droplet has more than 80% of a chance to break-up. For example, at $p = 2.73*10^{-3}$, a droplet with a diameter between 35 and 80µm sheared at τ = 640 Pa has a 87% chance not to break up. For a diameter above 80µm, the droplet has a 91% chance to break in these conditions.

Figure 6.27 shows Ca* plotted versus the viscosity ratio $p = \eta_{droplet}/\eta_{PDMS}$, often referred to as the 'Grace' curve (Grace, 1982), where η_{PDMS} is the viscosity of the silicon oil used in the corresponding experiment and $\eta_{droplet}$ was taken at the

deforming shear stress applied ($\eta_{PDMS}\,\dot{\gamma}$). The different oil viscosities (for details see section III.1.3) and the shear stresses applied for each point are presented Table 6.6.

Table 6.6: Viscosity of the different oils, shear rates applied and equivalent shear stresses.

Viscosity of the silicon oil (Pas.s)	Shear rate (s^{-1})	Shear stress (Pa)
25	6.4	160
75	1.5	110
170	1.25	200
170	1.6	280
220	1.8	400
220	2.9	640
220	6	1320
1000	1	1000

It should be recalled that each data point is based on an average result of the analysis of at least 25 droplets, as shown in Figure 6.26, which leads to a high experimental error in the critical radius determination (15-20%) but excludes other non-systematic errors. Moreover, in all studied cases the internal shear stress of the droplet is lower than those reported for solvent release or ejection.

At $p \geq 0.1$ droplet break-up was not observed - at least under the maximum shear stress conditions applied here; the value of Ca* = 10 000 at p = 0.1 is arbitrary just to demonstrate the absence of break-up. The overall behaviour is characteristic for the break-up of Newtonian droplets albeit the critical p value is around 4. For comparison with the data on starch suspension droplets the Grace curve for purely Newtonian systems calculated using the De Bruijn approach (De Bruijn, 1989) has been added in Figure 6.27 (dashed line).

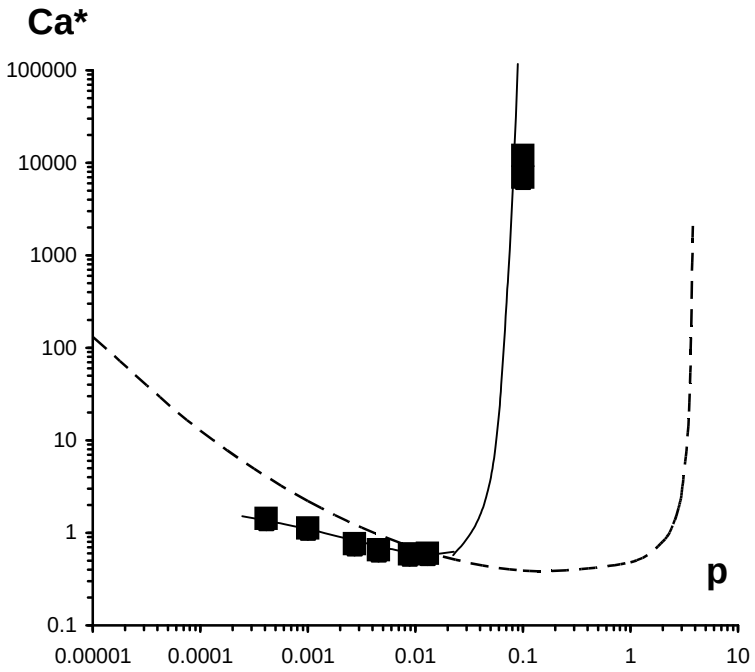

Figure 6.27: Critical Capillary numbers as a function of viscosity ratio for starch suspension droplets (points) and for a Newtonian fluid based on the De Bruijn approach (dashed line). The solid line is given to guide the eye. The points at p = 0.1 demonstrate the absence of droplet break-up. Error bars are smaller than the size of the points.

A first observation is that the shape of the starch suspension droplet break-up curve is the same as for fluid droplets. This is explained by the overall liquid-like behaviour of the suspension studied which, despite the presence of granules that are theoretically occupying 100% of the droplet volume, can deform and break-up as illustrated (see section VI.2.2.1).

Droplet break-up was not observed when the applied stress was below the yield stress, since then the droplet viscosity was about two orders of magnitude higher than the viscosity of the matrix fluid (PDMS). This was, for example, observed when a suspension droplet was immersed in a mixture of silicon oils with a viscosity 75 Pa.s and sheared at $1.12s^{-1}$. The corresponding average shear rate is 110 ± 4 Pa which is slightly higher than the yield stress found to be 90-100 Pa (Chapter V.2). The internal shear is however thought to be lower than the applied shear stress, and thus below the yield stress of the starch suspension. With $\eta_{droplet}$ being around

60 000 Pa.s, the droplet/matrix viscosity ratio is thus about 800. Not only was break-up absent under these conditions, deformations recorded in the rheo-optical experiment were within the experimental errors, i.e., suspension droplets sheared at stresses around the yield stress practically did not deform. It should be noted that a liquid-like behaviour of starch suspension droplet can be observed when starch is highly swollen and granules are soft and deformable. The lower the starch swelling degree, the more the suspension "droplet" behaves like an agglomerate of solid particles in which case it is far from being spherical at rest. Under shear deformation such agglomerates were reported not to break up and practically not to deform. Instead, rotation akin to solid particles was observed (Huijbrechts et al., 2008).

The mechanism of suspension droplet rupture is very different compared to mechanism of a fluid droplet, despite the similarity of the curve shape observed at break-up. The first aspect to be taken into account is that droplet rupture occurs between two granules. It has been demonstrated (Section 3.3) that individual granules remain intact even at high stresses which defines the interstitial "path" of rupture. Secondly, the break-up of a suspension droplet is thought to be due to the rearrangement of the granules under shear (Smith & Vandeven, 1985). Indeed, above the yield stress, an internal shear together with the droplet deformation induces a rearrangement of the granules thus creating 'zones' depleted in granules enabling break-up.

Three domains on the suspension droplet break-up curve can be distinguished with regard to Newtonian drop behaviour (see Figure 6.27):

a) The right-hand side. The limiting break-up viscosity ratio, above which droplet rupture is not possible, is 0.08-0.1 for a suspension droplet compared to 3.5-4 for a fluid droplet. This shift may be explained by the fact that the shear stress inducing droplet deformation and ultimately droplet break-up (calculated by multiplying the shear rate applied in the rheo-optical experiment with the viscosity of the matrix fluid) is dissipated inside the droplet due to intergranular friction (Schoch, 1969), and hence an internal characteristic shear stress is decreased. This decrease can be critical when the shear stress applied is just slightly higher than the

yield stress of the suspension as it may lead to a transition of the suspension from behaving as a low viscosity fluid to a high viscosity fluid. For example, absence of rupture was observed at "150 Pa" applied based on a 25 Pa.s viscosity matrix fluid for which the suspension viscosity is 2.5 Pa.s giving p = 0.1 At this stress the suspension is shear-thinning but not very far from the yield stress state (Chapter V.1.2, Figure 5.5). If the internal stress of the droplet is decreased by 50 Pa, the suspension is in the yield stress state with the consequence that the viscosity ratio is increased by several orders of magnitude. Thus, the droplet does not break-up.

b) Middle part. The Ca* values obtained for suspension droplets at p between $6.8*10^{-3}$ and $1.3*10^{-2}$ are close to those observed for Newtonian droplets although the rupture mechanism is different due to the nature of the droplet (suspension versus single phase fluid). Nevertheless, the overall behaviour of the suspension is similar to the behaviour of a shear-thinning fluid which in turn is akin to the behaviour of a Newtonian droplet when for the calculation of Ca* the droplet viscosity at the shear stress applied is considered (De Bruijn R.A., 1989).

c) Left-hand side. The third part concerns the critical capillary numbers at $p < 6.8* 10^{-3}$, where the Ca* data measured for suspension droplet break-up lay beneath the break-up conditions found for Newtonian droplets. The point obtained for $p = 6.8*10^{-3}$ starts to diverge slightly from the Newtonian curve. In this case, the shear stress applied is 400 Pa which is slightly above the stress for which suspension elasticity can be detected (Chapter V, Figure 5.8) and for which it is possible to observe granule deformation. At lower p values the shear stresses applied to induce break-up ranged from 640 to 1300Pa. At these stresses, the suspension shows increasingly significant levels of viscoelasticity as demonstrated by the detection of a first normal stress difference in the rheological characterisation of the suspension (see Chapter V, Figure 5.8). Based on the single granule deformation data it can be postulated that the first normal stress difference originates from granule deformation. It is thought that the deformation of the granules induced by the stress facilitates their rearrangement leading to the formation of granule "depleted zones" and, thus, droplet break-up. The paradox is that in comparison to a viscoelastic fluid (Lerdwijitjarud et al., 2004; Mighri et al., 1998; Milliken & Leal,

1991; Sibillo et al., 2005; Tsakalos et al., 1998; Varanasi et al., 1994) the critical capillary numbers of a viscoelastic suspension are lower than the ones for Newtonian droplets (Figure 6.24). This result could be explained by the origin of the viscoelasticity that is different in the fluid and in the suspension. As argued above, the elastic properties of the suspension are governed by the deformability of the starch granules (Doublier et al., 1987) and not by the elastic response of macromolecules in solution. The ease with which droplets of suspensions of starch granules break-up under stresses in excess of the yield stress could explain the very efficient mixing with saliva of starch thickened fluids compared with viscoelastic solutions of other hydrocolloid thickeners (Ferry et al., 2006; Mitchell et al. 2008).

All factors mentioned above show that the mechanisms of suspension droplet rupture are quite different compared to liquid droplets and other criteria should be taken into account. What should also be taken into account (but not done here) is that the break-up of a suspension droplet not only depends on the parameters of the Capillary number and viscosity ratio, but also on the internal shear, particle interactions, their deformability, orientation and reorganization in the flow, and also their size, shape, number and polydispersity.

VI.3. Conclusion for Chapter VI

It was demonstrated in this chapter that HPMC solutions and starch suspensions behaved differently when submitted to shear. First the differences in the bulk rheology of both systems was presented; HPMC solution had a low shear Newtonian plateau and a more liquid like behaviour whereas starch suspensions showed a yield stress and gel like behaviour. However, both solution and suspension were shear thinning and elastic at large deformation scales. Their surface activity differed greatly due to their difference in chemical composition; HPMC has hydrophobic and hydrophilic groups unlike released-from-starch amylopectin molecules which only has hydrophilic groups.

The study of the deformation and break-up of such systems immersed in a suspending fluid yielded interesting results. Starch suspension droplets broke up more easily than HPMC droplets when submitted to the same shear stress. This

result could be of interest when considering the mixing ability of food thickeners. However, more studies should be carried out to give quantitative explanation of the effects observed.

The in-depth study of starch suspension droplets in a simple shear flow revealed a different break-up mechanism and conditions. It was shown that starch suspension droplets:

- Could not break-up for p values above 0.1.
- Acted like Newtonian fluids for intermediate p values.
- Broke up more easily for low p values and high shear stresses, when the deformation of the starch granules was large.

It was hypothesised that the yield stress and the internal circulation played a major role in the break-up conditions. Indeed, below the yield stress the droplet acted like a solid where deformation is small and no internal circulation could occur. When the applied stress was slightly above the yield stress energy dissipation led to a decrease in shear stress and hence internal circulation was too low to induce depleted zones that caused rupture of the droplet. For high apparent shear stress, the deformation of the granule was thought to induce easier break-up thanks to higher circulation of the small amount of solvent in the droplet. A study on other types of suspension might be of interest to better understand the break-up mechanism.

Reference List

Assighaou, S. (2006). Comportement sous grandes déformations de gouttelettes de polymères dans une matrice newtonienne. Ph.D.Thesis, Université du Maine, Le Mans.

Bergeron, V., Cooper, P., Fischer, C., Giermanska Kahn, J., Langevin, D., Pouchelon A. (1997). Polydimethylsiloxane (PDMS)-based foams. *Colloids and Surfaces A: Physicochemical and Engineering Aspects*, 122, 103-120.

Caserta, S., Reynaud, S., Simeone, M., Guido, S. (2007). Drop deformation in sheared polymer blends. *Journal of Rheology*, 51 (4), 761-774.

Clasen, C. and Kulicke, W. M. (2001). Determination of viscoelastic and rheo-optical material functions of water-soluble cellulose derivatives. *Progress in Polymer Science*, 26, 1839-1919.

Cook, D. J., Hollowood, T. A., Linforth, R. S. T., and Taylor, A. J. (2002). Perception of taste intensity in solutions of random-coil polysaccharides above and below c. *Food Quality and Preference*, 13, 473-480.

Cox, R. G. (1969). Deformation of A Drop in A General Time-Dependent Fluid Flow. *Journal of Fluid Mechanics*, 37, 601.

De Bruijn R.A. (1989). Deformation and Breakup of drops in simple shear flow. Ph.D. Thesis, Wagnigen University, Wagenigen.

De Bruijn, R. A. (1993). Tipstreaming of Drops in Simple Shear Flows. *Chemical Engineering Science*, 48, 277-284.

Desbrieres, J., Hirrien, M., and Ross-Murphy, S. B. (2000). Thermogelation of methylcellulose: rheological considerations. *Polymer*, 41, 2451-2461.

Doublier, J. L., Llamas, G., and Lemeur, M. (1987). A Rheological Investigation of Cereal Starch Pastes and Gels - Effect of Pasting Procedures. *Carbohydrate Polymers*, 7, 251-275.

Ferry, A. L., Hort, J., Mitchell, J. R., Cook, D. J., Lagarrigue, S., and Pamies, B. V. (2006). Viscosity and flavour perception: Why is starch different from hydrocolloids? *Food Hydrocolloids*, 20, 855-862.

Grace, H. P. (1982). Dispersion Phenomena in High-Viscosity Immiscible Fluid Systems and Application of Static Mixers As Dispersion Devices in Such Systems. *Chemical Engineering Communications*, 14, 225-277.

Greco, F. (2002). Drop deformation for non-Newtonian fluids in slow flows. *Journal of Non-Newtonian Fluid Mechanics*, 107, 111-131.

Guido, S., Grosso, M., Maffetone, P.L. (2004). Newtonian drop in a Newtonian matrix subjected to large amplitude oscillatory shear flows. *Rheologica Acta*, 43, 575-583.

Haque, A., Richardson, R. K., Morris, E. R., Gidley, M. J., and Caswell, D. C. (1993). Thermogelation of Methylcellulose .2. Effect of Hydroxypropyl Substituents. *Carbohydrate Polymers*, 22, 175-186.

Hirrien, M., Chevillard, C., Desbrieres, J., Axelos, M. A. V., and Rinaudo, M. (1998). Thermogelation of methylcelluloses: new evidence for understanding the gelation mechanism. *Polymer*, 39, 6251-6259.

Hussain, S., Keary, C., and Craig, D. Q. M. (2002). A thermorheological investigation into the gelation and phase separation of hydroxypropyl methylcellulose aqueous systems. *Polymer*, 43, 5623-5628.

Kavanagh, G. M. and Ross-Murphy, S. B. (1998). Rheological characterisation of polymer gels. *Progress in Polymer Science*, 23, 533-562.

Lerdwijitjarud, W., Sirivat, A., and Larson, R. G. (2004). Influence of dispersed-phase elasticity on steady-state deformation and breakup of droplets in simple shearing flow of immiscible polymer blends. *Journal of Rheology*, 48, 843-862.

Maffettone, P. L. and Minale, M. (1998). Equation of change for ellipsoidal drops in viscous flow. *Journal of Non-Newtonian Fluid Mechanics*, 78, 227-241.

Maffettone, P. L., Greco, F., Simeone, M., and Guido, S. (2005). Analysis of start-up dynamics of a single drop through an ellipsoidal drop model for non-Newtonian fluids. *Journal of Non-Newtonian Fluid Mechanics*, 126, 145-151.

Mighri, F., Carreau, P. J., and Ajji, A. (1998). Influence of elastic properties on drop deformation and breakup in shear flow. *Journal of Rheology*, 42, 1477-1490.

Milliken, W. J. and Leal, L. G. (1991). Deformation and breakup of viscoelastic drops in planar extensional flows. *Journal of Non-Newtonian Fluid Mechanics*, 40, 355-379.

Moran, K., Yeung, A., Masliyah, J. (2003). Shape relaxation of an elongated viscous dop. *Journal of Colloid and Interface Science*, 267, 483-493.

Rumscheidt F.D and Mason S.G (1961). Particle motions in sheared suspensions XII. Deformation and burst of fluid drops in shear and hyperbolic flow. *Journal of Colloid Science*, 16, 238-261.

Schoch, T. J. (1969). Mechano-chemistry of starch. *Wallerstein Lab.Commun.*, 32, 149-166.

Sibillo, V., Guido, S., Greco, F., and Maffettone, P. L. (2005). Single drop dynamics under shearing flow in systems with a viscoelastic phase. *Macromolecular Symposia*, 228, 31-39.

Smith, P. G. and Vandeven, T. G. M. (1985). Shear-Induced Deformation and Rupture of Suspended Solid Liquid Clusters. *Colloids and Surfaces*, 15, 191-210.

Takahashi, M., Macaubas, P.H.P., Okamoto, K., Jinnai, H., Nishikawa, Y. Stress prediction for polymer blends with various shapes of droplet phase. *Polymer*, 48, 2371-2379.

Taylor, G. I. (1932). The viscosity of a fluid containing small drops of another fluid. *Proceedings of the Royal Society of London Series A-Containing Papers of A Mathematical and Physical Character*, 138, 41-48.

Taylor, G. I. (1934). The formation of emulsions in definable fields of flow. *Proceedings of the Royal Society of London Series A-Mathematical and Physical Sciences*, 146, 0501-0523.

Tice, J. D., Song, H., Lyon, A. D., and Ismagilov, R. F. (2003). Formation of droplets and mixing in multiphase microfluidics at low values of the Reynolds and the capillary numbers. *Langmuir*, 19, 9127-9133.

Tsakalos, V. T., Navard, P., and Peuvrel-Disdier, E. (1998). Deformation and breakup mechanisms of single drops during shear. *Journal of Rheology*, 42, 1403-1417.

Tucker, C. L. and Moldenaers, P. (2002). Microstructural evolution in polymer blends. *Annual Review of Fluid Mechanics*, 34, 177-210.

Varanasi, P. P., Ryan, M. E., and Stroeve, P. (1994). Experimental-Study on the Breakup of Model Viscoelastic Drops in Uniform Shear-Flow. *Industrial & Engineering Chemistry Research*, 33, 1858-1866.

Wolf B., Windhab E. (1995). Interfacial rheology of deformable droplets in viscometric flows. *Rheology*, 5 (4), 182-189.

Chapter VII: Conclusions & Future work

In view of obtaining better in-mouth flavour perception in thickened products, starch has been put forward as it was previously shown (Ferry et al., 2006) to offer better results than hydrocolloids and more specifically starches that remain in their granular form. Mixing ability was suggested as a key feature for flavour perception: good mixing properties offer better mouth feel and enhanced transportation of flavour components to the receptors. In this way the research on droplet deformation and break-up was thought to correlate well with in-mouth mixing of food thickeners.

The purpose of this research was to investigate the behaviour of a modified waxy maize starch submitted to flow, at different scales. First, the surface properties and shape of a single granule were characterised and its deformation under shear was analysed in a counter rotating shear cell. The determination of the rheological properties of a starch suspension (granules in a continuous media) was then carried out and the results were interpreted using the information obtained from the single granule deformation data. To understand the starch suspension behaviour and characteristics, the continuous medium was analysed to determine whether or not polymeric material was released during sample preparation. Once the sample was fully characterised, the behaviour of droplets of starch suspensions in silicon oil was investigated and compared to a model system, aqueous solution of hydroxypropyl cellulose, also used as a food thickener. Finally, the differences in behaviour were interpreted based on a microstructure of the two systems

VII.1.Results and Interpretation

The complex aspect of the starch granule was revealed through SEM and AFM observations:

- Modified waxy maize starch granules were seen to be polydisperse and very irregular in shape with angular facets.
- The modified waxy maize granule surface was rough due to the presence of larges pits and cracks which helped solvent to enter and swell the granules. The presence of these pits is thought to be due to the treatment used to modify the granules. The arithmetic mean roughness was determined to be 13.5nm.
- Potato starch has a smooth surface and a potato-like shape. The arithmetic mean roughness was determined to be 2nm, which in comparison with modified waxy maize starch is not significant. The AFM study revealed alternating hard and “rubbery” zones in potato starch corresponding to amorphous and crystalline zones. This specific structure allows for good resistance of the granules to disruption and enzymatic attacks.

The shape and surface of starch granules differed from one starch type to another. These specificities have an influence on their behaviour under flow as well as their degree of swelling when considering swollen granules. Dry granules under flow acted similarly to rigid spheres.

The study of swollen starch granules in simple shear flow not only revealed that the granules could deform up to twice their initial size without rupturing but also that solvent was released at a critical shear stress determined to be around 1500Pa. The solvent ejection in the suspending medium was evidenced through a loss of volume of the granule at the end of the experiment. This ejection occurred between 1500Pa and 2200Pa. A larger amount of solvent was ejected from modified waxy maize as compared to potato starch. However, quantificative comparison between the two types of granules is flawed as they do not have the same swelling degree when fully swollen. Potato starch is theoretically the most swollen as its maximum swelling degree is higher; hence it should eject more solvent than modified waxy maize starch. An easier solvent ejection from the waxy maize starch

was interpreted to be due to the presence of the holes and cracks at the surface of the granule, absent on the surface of potato starch granules. Another explanation put forward was that the surface of the potato starch has a more structured surface due to the large amount of amylose at the periphery which slows down the solvent ejection.

Flow and viscoelastic properties of a suspension of modified waxy maize starch were investigated at stresses below the onset of solvent release from the granules. The observations of the rheological behaviour were explained by the surface properties, the shape and the ability to deform of the starch granules.

- Because of the polydispersity, irregular shapes and deformability of the granules, starch suspensions can achieve theoretical volume fraction of 1.
- Suspensions of swollen granules have a shear thinning behaviour due to the deformability of the granules. A more swollen granule will be more deformable and hence more shear thinning. Moreover, the viscosity of suspensions with highly swollen granules will be lower than those with more rigid granules.
- Elasticity (N_1) of the suspension was measured for shear stresses above 300Pa. This value corresponds to the shear stress for which deformation of the starch granules was observed. It is interpreted that the deformation of the granules is at the origin of the measured elasticity for the suspension.
- Above the close packing concentration(c* =5%, i.e. Φ = 0.625), the starch suspension needs to be submitted to a certain shear stress to start flowing, indicating that it is a yield stress fluid. The interpretation for this occurrence is that each granule is trapped by the surrounding granules and that a certain energy barrier needs to be overcome to allow the granules to flow freely. It was thought that due to the high surface roughness of the starch granules and their irregular shape, granule-granule interactions could occur, such as mechanical anchoring, making it even harder for them to flow.
- Below the close packing concentration (c* =5%, i.e. Φ = 0.625), the flow behaviour of the suspension is governed by the volume fraction occupied by the granules and the continuous medium. However, a higher viscosity than predicted for rigid spheres gave evidence of granular interaction through the amylopectin chains present at the surface of the granules.

- The analysis of the continuous phase of the suspension revealed that low molecular weight amylopectin was released during the preparation of the sample. The continuous phase can also have an influence on the overall rheological behaviour of the suspension although it was minor because of low amylopectin concentration.

In the final chapter, experiments on the deformation and break-up of a starch suspension droplet in an immiscible fluid (silicon oil) were carried out. The information obtained on the single granules and on the suspension (rheological behaviour and continuous phase analysis), allowed to analyse and interpret the results obtained on suspension droplet behaviour. All experiments were performed in the region of shear stresses where no solvent release (solvent comes out of the granule but is not detached) and ejection (solvent is detached from the granule into the suspending matrix) from a granule was observed. The behaviour of the starch droplet was also compared to that of a droplet of hydrocolloid solution (HPMC) which was previously characterised in terms of its rheology and interfacial tension in oil. The comparison of the two systems showed that:

- In similar conditions, starch suspension droplets break up more easily than the HPMC droplet. At the same shear stress and the same droplet size, the capillary number applied to HPMC is higher than that for starch as the interfacial tension of HPMC in oil is 2 times lower. Moreover, the p value of HPMC (2.9*10-2) is higher than the p value of starch (4.45*10-3). At the p values for HPMC the required Ca to break up the droplet is lower. It would be expected to see the HPMC droplet rupture rather than the starch droplet. The interpretation for this result is that the microstructure of starch allows for easier break-up. Indeed, the HPMC droplet is a solution of entangled polymers whereas starch is a droplet of granules with no entanglement involved.
- The break-up mechanism of a starch suspension droplet is different from that of a solution droplet. For a suspension droplet, granules circulate within the drop under the action of internal stress. This leads to a rearrangement of the granules and the droplets break up in zones that are depleted of granules.

The easier break-up of the starch suspension droplet leads us to think that this physical parameter can correlate with the mixing ability of food thickeners.

Thus, an easier break-up allows for better mixing and consequently for better mouth feel and flavour perception. An in-depth study of the break-up of the starch suspension droplet as a function of the viscosity ratio p, unravelled interesting results for this type of system:

- For viscosity ratios above 0.1 and low shear stresses applied, it is not possible to observe rupture of the droplet.
- For intermediate p values and shear stresses, the suspension follows the behaviour of a Newtonian fluid at a fixed shear stress.
- For high shear stresses and low viscosity ratios, the critical capillary number at which break-up occurs is lower than for Newtonian fluids.

It was hypothesised that the yield stress is a key parameter in the break-up of the starch granule. Indeed, rupture occurs when internal circulation is strong enough to induce rearrangement of the granules which creates thin “zones” between them. In this case, the droplet breaks up where there is a depletion of granules. If the stress applied is close to the yield stress of the suspension, the internal stress is lower than the yield stress due to energy dissipation through granule friction. This would greatly reduce the internal circulation and the suspension becomes “solid-like” with a very high viscosity. Deformability of the granules is also important when considering the break-up of starch suspension droplets. At high stresses the granules are greatly deformed allowing better internal circulation of the surrounding fluid. This would lead to earlier break-up when compared to Newtonian fluids, explaining the lower values of the critical capillary number observed at high stresses.

VII.2. Suggestions for further research

The study of the starch granules whether they are observed alone or in a suspension, in bulk rheology or in the shape of a droplet in a suspending matrix, has led to new information on the flow behaviour of starch suspension under shear. However, further research is needed to get a better understanding of the mechanisms involved.

From a fundamental point a view, the following subjects should be looked at:

- A logic continuation of this study would be work on a droplet of a model suspension of soft particles. Work in that direction has been started and revealed that the size and the number of particles would play a role in the break-up mechanism. Furthermore, the presence of liquid bridges between two particles was seen to be important in the break-up of a droplet of such a suspension under flow. However, more work on these types of systems would be of great help in understanding the influence of yield stress, particle elasticity/rigidity, size and number of particles. Ideally, a system where the size and the deformation could be varied independently should be used. Moreover, the particles should not show any preferential interactions.
- Due to the wide variety of starches, their polydispersity and their ability to swell, systematic experiments should be conducted to understand granule deformation. In further studies, it would also be interesting to consider granule surface and the influence of rigidity by reducing their swelling degree. This last parameter is thought to have an influence on solvent release and ejection as the granules would contain smaller amounts of liquid. This also raises the question of the ejection: what exactly is released (probably water+polymeric material)? In what quantity? It would also be interesting to determine a critical shear stress for which solvent ejection occurs. It is thought that it varies with starch origin.

From an industrial application point of view, it would be interesting to study a wide variety of food thickeners to obtain systematic data which would allow choosing the best one depending on the food application. For example, a study on

starches that do not retain granular form and that could be considered as a solution of macromolecules would be of great interest.

VII.3. Suggestion for possible industrial applications

It was shown that starch granules when submitted to high shear could release and even eject solvent. A possible application of starch granules as a vector for drug delivery in pharmaceutical products, active compounds in cosmetic can be imagined. It would allow the replacement of synthetic carriers by a natural product.

Reference list:

Ferry, A. L., Hort, J., Mitchell, J. R., Cook, D. J., Lagarrigue, S., and Pamies, B. V. (2006). Viscosity and flavour perception: Why is starch different from hydrocolloids? *Food Hydrocolloids*, 20, 855-862.

Résumé de thèse :

L'amidon utilisé comme épaississant alimentaire présente tout d'abord un intérêt nutritif mais offre également une meilleure perception du goût comparé à d'autres épaississants de type hydrocolloide. Cette propriété semble liée à la capacité des produits à se mélanger en bouche et donc à la diffusion des agents de flaveurs aux récepteurs. Un paramètre physique qui pourrait refléter la capacité à se mélanger serait la facilité d'une goutte de cet épaississant à rompre lorsque celle-ci est soumise à un cisaillement. Le but de cette étude est de comprendre le comportement d'une goutte de suspension de granules d'amidon, gonflés dans l'eau, sous écoulement et de le comparer à une goutte d'un autre épaississant connu, la solution aqueuse de hydoxyproplmethyl cellulose (HPMC). Les gouttes, placées dans l'huile de silicone, sont étudiées sous cisaillement à l'aide d'un rhéo-optique contra-rotatif. Les conditions de rupture d'une goutte de suspension d'amidon sont étudiées en détails et comparées à celle d'une goutte d'HPMC. Le mécanisme de rupture d'une goutte de suspension est différent comparé à une goutte de solution d'HPMC. La déformation d'une goutte de suspension a été liée au comportement rhéologique de la suspension et à la déformation d'un granule seule gonflé sous cisaillement.
Mots-clefs : amidon, rhéologie, goutte de suspension, rheo-optique

Abstract :

Starch used as a food thickener is interesting for its nutritional value but also because it offers better flavour perception when compared to other food thickeners such as hydrocolloids. This latter property seems to be linked to the ability of the product to mix in the mouth and thus to the diffusion of the tastants to the receptors. A suggested parameter that could reflect the ability to mix in the mouth and allow differentiating food thickeners is the break-up of a droplet submitted to simple shear. The aim of this study is to understand the behaviour of a swollen-in-water starch suspension droplet and compare it to the behaviour of a known fluid droplet, an aqueous solution of hydroxypropylmethyl cellulose (HPMC). The droplets placed in an immiscible fluid (silicon oil) are submitted to a simple shear flow using a counter rotating shear cell. The break-up conditions of a starch suspension droplet are studied in detail and compared to the HPMC solution droplet. The break-up mechanism of the suspension droplet is different from that of the HPMC solution droplet. The deformation of the suspension droplet was explained by the rheological behaviour of the suspension and the deformation of a single swollen starch granule submitted to shear.
Key-words: starch, rheology, suspension droplet, rheo-optics